

For New Technology Network

**NTN**®

# TECHNICAL REVIEW

No.  
**85**

Special issue on  
"Automotive Products and Electric Module Products"

October 2017



**Osaka University forms  
"NTN Next Generation Research Alliance Laboratories."**

NTN Corp (hereafter, NTN) formed the "NTN Next Generation Research Alliance Laboratory" within the Graduate School of Engineering at the National University Corporation Osaka University (Headquartered in Suita-City, Osaka Prefecture, under the presidency of Dr. Shojiro Nishio; hereafter Osaka University) on September 1, for creating new business and accelerating technical innovation.

NTN, which commemorates its 100th anniversary in March of 2018, is working on enhancing platform technologies toward the next 100 years and creating new business by introducing new products into the new fields. NTN has formed the "NTN Next Generation Research Alliance Laboratory" (hereafter, Laboratory) at the University by leveraging the Research Alliance Laboratory system of Osaka University\*. The specially-appointed professor, Yoshinobu Akamatsu, of the Graduate School of Engineering at Osaka University (former NTN executive officer) will become the general manager and the Dean of the Graduate School of Engineering at Osaka University, Prof. Toshihiro Tanaka, will become the deputy general manager of the Laboratory.

Together with Osaka University, NTN is conducting research and development of an innovative, artificial 3D cellular tissue. Using cell laminating technology with iPS-derived cells, in conjunction with NTN's own technology, a microscopic coating applicator, the creation of new medicines and applications to regenerative medicine is possible. In addition, the Laboratory plans to initiate development of residual bearing life prediction by estimating damage to the bearings for automobiles, rolling stock, machine tools, etc. Also the degradation of grease leveraging artificial intelligence (AI), as well as achieving bearing operational trend management and failure prevention by applying multi-functional sensors is being studied. NTN is also working on lightweight and compact product development by applying advanced simulation technology toward energy saving and fuel efficiency for the automotive industry, as well as research for shorter development intervals.

Through activities in this Laboratory, NTN will enhance our partnership with Osaka University which possesses state-of-art technology, work on research and development for strengthening platform technology, and create next-generation businesses by incorporating the newest technology.

\* A System aimed at the promotion of transferring research results into industries, advanced research activities and development of human resources for both industry and academia by mutual use of information, technology and facilities between businesses and Osaka University in common fields.



**[Overview of NTN Next Generation Research Alliance Laboratory]**

Name	NTN Next Generation Research Alliance Laboratory
Location	Graduate School of Engineering at Osaka University (2-1 Yamadaoka, Suita, Osaka 565-0871 Japan)
Open	September 1, 2017
General Manager	Yoshinobu Akamatsu



# TECHNICAL REVIEW

**No.85**

**Special Issue;**

**Automotive Products and  
Electric Module Products**

# NTN TECHNICAL REVIEW No.85

## CONTENTS

<b>Preface</b>	For Automotive Products and Electric Module Products Yoshinori TERASAKA	1
<b>Contribution</b>	Issues on Electrification and Autonomous Driving for Automobiles Tetsusei KURASHIKI Dr. Eng. Associate Professor Management of Industry Technology, Graduate School of Engineering, OSAKA UNIVERSITY	2
<b>Perspective</b>	NTN Approach toward the Electrification and Autonomous Driving Koji KAMETAKA	14
<b>● Special Issue for Electric Module Products</b>		
	Development of Electric Motor, Actuator Series Kimihito USHIDA and Masashi NISHIMURA	18
	Hub Module with Motor and Generator Function Kentaro NISHIKAWA, Yuuji YADA, Yasuyuki FUJITA, Mitsuo KAWAMURA and Hiroki YABUTA	26
	Influence of Vehicle Body Motion on the Effects of G-Vectoring Control Yuta SUZUKI, Shuichi KOSAKA and Weipeng CHENG	33
<b>● Technical Articles and New Products</b>		
	History of Constant Velocity Joints Shinichi TAKABE	40
	History of Axle Unit Bearings for Automobile Daisuke NAKA	46
	ULTAGE Tapered Roller Bearing for Automotive Application Yasuhito FUJIKAKE, Takanori ISHIKAWA and Susumu MIYAIRI	51
	High Speed Rotation Ball Bearing for Pulley Hayato KAWAGUCHI, Shouhei FUKAMA and Masaharu INOUE	56
	Ultra Low Friction Sealed Ball Bearing for Transmission Katsuaki SASAKI, Takahiro WAKUDA and Tomohiro SUGAI	62
	Low Friction Hub Bearing Makoto SEKI	67
	Chain Tensioner for Motorcycle Engine Kouichi ONIMARU	72
	Light Weight Drive Shaft for FR vehicle "R series" Tomoshige KOBAYASHI	78
	Effects of Lubricant on Hydrogen-Related Rolling Contact Fatigue Life Improvement Takayuki KAWAMURA	84
	Relationship between Cage Stress and Degree of Freedom of Motion in Dynamic Analysis for Needle Roller Bearings Naoto SHIBUTANI and Tomoya SAKAGUCHI	90
	Proposal of Low Fuel Consumption and High Functionality of Composite Material Products for Automobile Kayo SAKAI, Tomonori YAMASHITA, Hajime ASADA and Takuya ISHII	97
<b>● Award Winning Products</b>		
	Japan Powder Metallurgy Association Awards 2016 in the New Products Category (New Design) Hybrid Magnetic Material Reactor Core for Booster Hajime KATSUURA, Toshihiro TAKAKUSU, Shinya AMANO and Shouhei SUZUKI	103
	Japan Powder Metallurgy Association Awards 2016 in the New Products Category (New Design) Multi Layer BEARPHITE® Takashi YAMAGUCHI, Toshihiko MOURI and Kazuki TAKAI	104
	2016 "Cho" MONODZUKURI Innovative Parts and Components Award, Environmental Components Award Low Torque Seal Ring Kouzou KAKEHI, Takuya ISHII, Takumi KONDOU, Yuuki YAMAZOE and Souichirou YAMAMOTO	105
	<b>Our Line of New Technology</b>	106
	<b>Our Line of New Product</b>	107

*A message for the special topic of  
"Automotive Products and Electric Module Products"*



**Yoshinori TERASAKA**  
Managing Director

It has been a long time since the realization of a low-carbon society was called to address global warming, environmental pollution, etc. and there is a strong demand for reduction of CO<sub>2</sub> emissions. The governments of France and UK both made an announcement "banning of fossil fuel automobiles after 2040" indicating a clear shift to EVs. The largest automotive market, China, has also shown similar moves, accelerating electrification of vehicles and their various components, marking a major turning point in automotive components.

Furthermore, a separate, recent trend of the development of autonomous driving has made great strides toward implementation by improving vehicle safety. With "level 2," partial implementation already introduced into the market, it is assumed that "levels 3-5" will also be achieved very rapidly, requiring control units with higher precision and faster responsiveness for various automotive components.

As the shift from engine vehicles to EVs accelerates, higher functionality will be required for NTN's core products, such as bearings, hub bearings and constant velocity joints. Additionally, lower torque/higher efficiency, as well as drastic weight reduction will be needed.

NTN has now developed "electric motors and actuators" with high precision and fast responsiveness, as an alternative to conventional pneumatic and hydraulic products, taking advantage of NTN's core competence in tribology, high-precision processing and analysis, and has launched them into the market as a standard catalog products. These are modular products achieving unprecedented improvements in size and weight, which, coupled with supporting electric systems that integrate transmissions, in-vehicle pumps, various valves as well as other components, contribute to the shift towards EVs and electrification.

As a new approach for accelerating the development of technology and creating new business, on September 1<sup>st</sup> of this year, NTN established the "NTN Next Generation Research Alliance Laboratory" within the Graduate School of Engineering at the National University Corporation Osaka University, making it a research and development center for next generation technology. This Laboratory will combine and integrate NTN's technology/engineering competency with the university's knowledge and intellectual base. By leveraging artificial intelligence (AI), the Laboratory will work on the development of residual bearing life prediction technology through the monitoring of the operational status of the rolling bearings applied to automobiles, rolling stock, machine tools, etc. as well as establishing bearing operational trend management and failure prevention technology by incorporating multi-functional sensors into bearings with the aim of creating new added value in bearings.

NTN will mark its 100th anniversary in March 2018. It is also the final year of the mid-term management plan of "NTN 100" which NTN has been working on since 2015. While advancing the "Transformation and Building Foundation for the Next 100 Years" that NTN is currently conducting alongside "NTN 100," NTN strives to contribute to the sustainable development of society through new product development continuing "security and safety" toward the next 100 years under NTN's philosophy that "We shall contribute to international society through creating new technology and developing new products (For New Technology Network: Networking the World with New Technology)."

# Issues on Electrification and Autonomous Driving for Automobiles



**Tetsusei KURASHIKI**

Associate Professor, Business Engineering,  
Graduate School of Engineering at Osaka University

An overview of large-scale R&D projects of our country in the manufacturing industry field on automobiles was described. Technical issues and market forecast on next generation-automobiles, special issues on electrification/autonomous driving, and the roadmap in the transportation field were also described with public information of each ministry in our country. It is important to develop additional value with cooperation of industry/academia/government aimed to solution-oriented "connected industries" based on Japan's high technologies and faculties in the manufacturing filed.

## 1. Introduction

As the mid-long term socio-economic challenges, such as, declining population and global competition that Japan faces toughen, creation of new added value by innovation will become one of the driving forces to overcome these challenges.

The automotive industry, in particular, is one of the leading industries in Japan with strong international competitiveness that earns foreign currencies, boasting vast support industries and significant employment and is one of the principal pillars supporting regional economies. It is also a national industry consistently promoting an attitude of exploring quality, reliability and productivity which has provided its workers with opportunities to grow as human beings in its history for over 100 years.

In this paper, an overview of Japan's large projects on technology development in manufacturing, center on the automotive industry, and challenges in vehicle electrification and autonomous driving is provided, based upon public information from various governmental organizations and NEDO. In addition, policy concerns and the future direction of the mobility area (autonomous driving, etc.) in "New Industrial Structure Vision" published in May 2017 by the Ministry of Economy, Trade and Industry, is also presented.

## 2. Technology development projects in manufacturing industry in Japan

As an example of the overall R&D projects, [Fig. 1](#) shows an overview of the initiatives taken by the ministries regarding technology development in the

manufacturing industry in FY2017. It is organized in such a way that manufacturing technology is categorized into "resources," "material development," "component processing (manufacturing process)" and "finished product" The projects in those areas are plotted based on the development phases (basic research, R&D, implementation/demonstration). The size of the circles reflects the budget in FY2017 and color coded by sponsor ministry, such as Ministry of Education, Culture, Sports, Science and Technology (MEXT), Cabinet Office and Ministry of Economy, and Trade and Industry (METI). The projects with a budget size of over 1 billion yen are depicted; therefore, the chart can be considered as a representative summary of manufacturing industry technology in Japan.

These projects span several years and include elements of cooperation that are difficult to conduct by a single company. An example of large projects in the automotive industry is "Innovative Structural Materials Technology Development" promoted by the Cabinet Office and METI. This is to support technology development for drastic weight reduction of transportation equipment (automobile, rolling stock, etc.) which has a significant impact on energy consumption and CO<sub>2</sub> emissions reduction, specifically, development of light materials for achieving both high-functionality and cost competitiveness such as innovative steel sheets/non-ferrous metal/CFRP, development of high-function magnets that allow higher efficiency motors, bonding technology, and development of optimal methodology for multi-material design, etc. The project spans 9 years from FY2014 to FY2022 <sup>1)</sup>, aiming for drastic

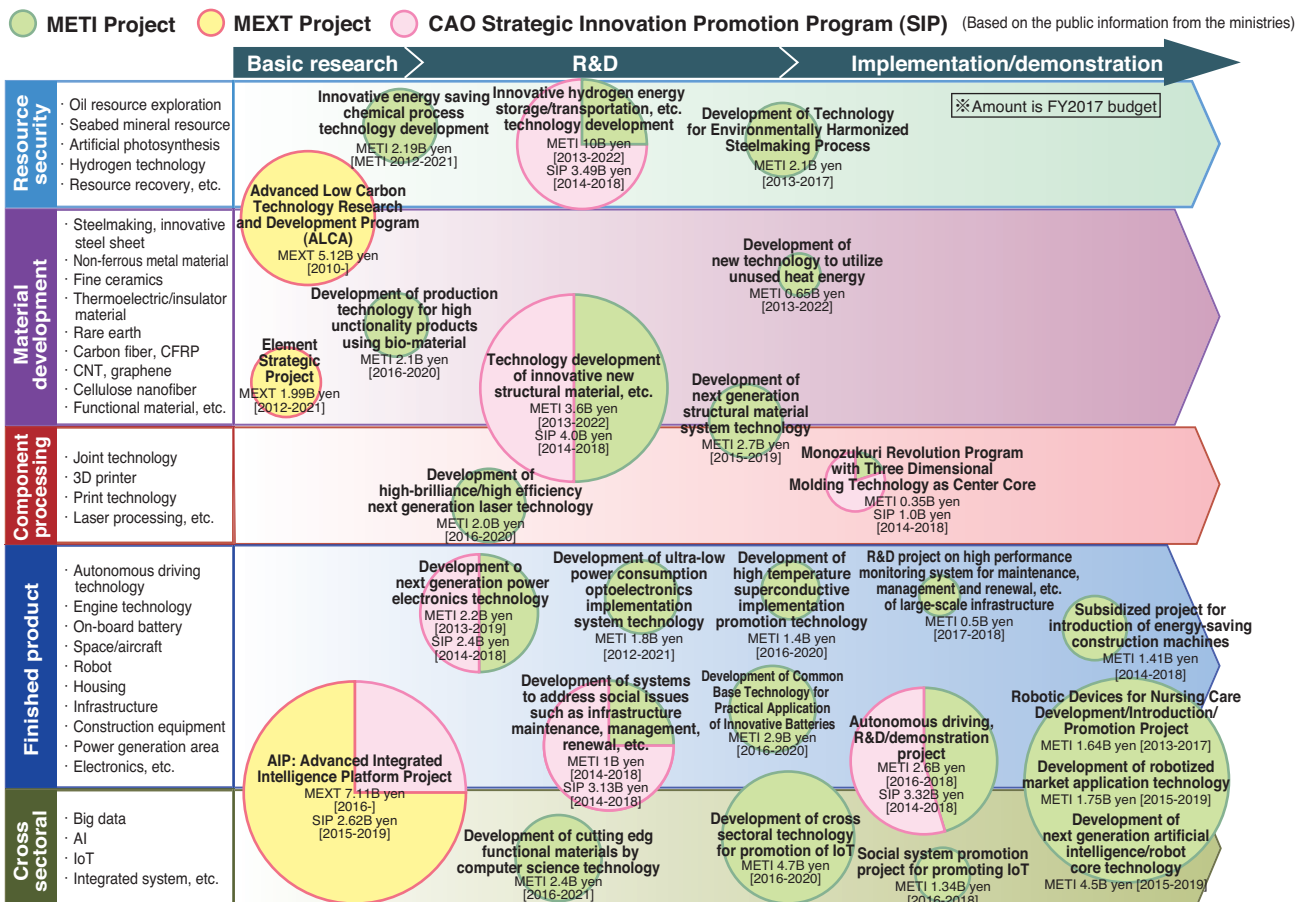


Fig. 1 Overview of R&D projects of our country in manufacturing industry field based on public information of ministry

weight reduction (50% reduction in case of vehicle bodies) and a reduction in CO<sub>2</sub> emissions of 3.738million tons/year in FY2030.

For electrification, METI is promoting projects for developing base technology for implementation of innovative batteries<sup>1)</sup>. This project accelerates R&D for innovative batteries including advanced analytical technology as international competition with Chinese and Korean manufacturers intensifies in the on-board battery market (Fig. 2). The durability/safety and high energy density, which are both required for on-board batteries, are in a trade-off relationship. The plan includes development of new materials that can achieve both requirements at a high level, as well as batteries with energy density five times higher (500Wh/kg) than the current lithium-ion batteries, including verification of no practical issues for on-board application in durability and safety by means of large trial cells of 5Ah with an overall aim to implement the on-board innovative batteries by FY 2030. Details will be described later in Chapter 4.

In the area of autonomous driving, an R&D/demonstration project for the autonomous driving system is underway. METI is conducting development of technologies and arrangement of business

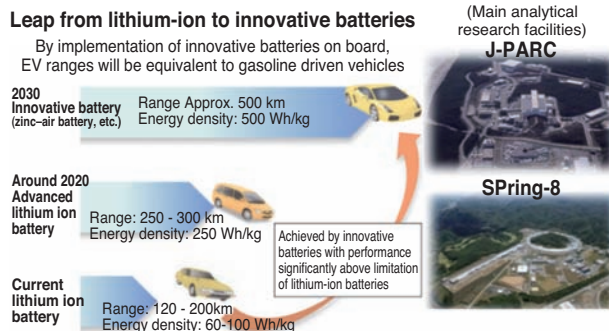


Fig. 2 Research & development initiative for scientific innovation of new generation batteries

environments required for social implementation of advanced autonomous driving systems shown in Fig. 3 (controlled autonomous driving, truck platooning, etc.) through demonstration projects including public roads<sup>1)</sup>. This project aims to establish truck platooning technology and achieve over 10% of energy saving per vehicle by FY2030. In addition, the Cabinet Office is promoting projects focusing on four fields, namely, R&D through large demonstration tests, business development/business model build-up, regional expansion/partnership among industry/ academia/

government and international partnership/standardization activities (Fig. 4)<sup>2)</sup>. R&D is progressing so that the implementation of a system to utilize traffic signal and traffic congestion information (SAE Level 4) is achieved by 2025, using look-ahead information from Intelligent Transportation System (ITS). Details will be described later in Chapter 5.

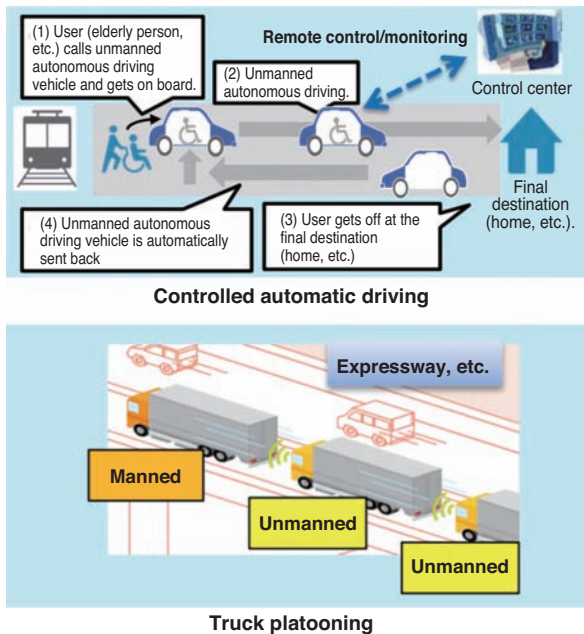


Fig. 3 Image of verification for advanced autonomous driving system

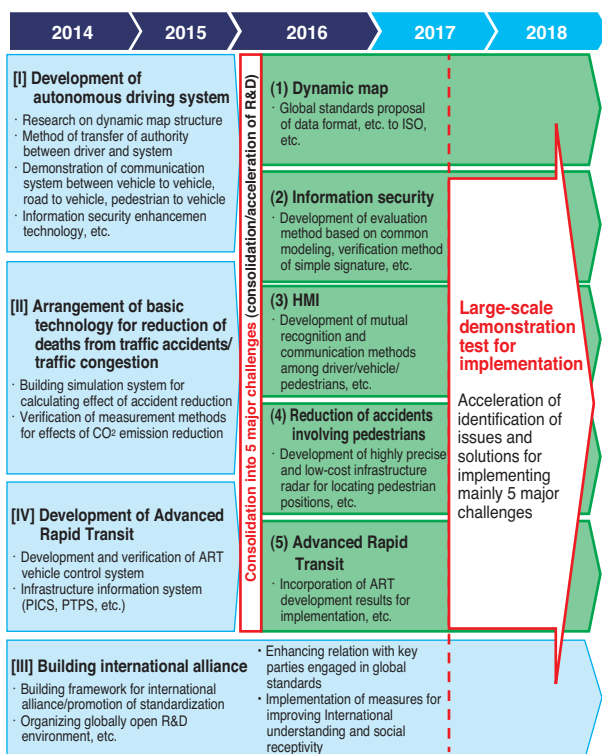


Fig. 4 Progress schedule of SIP-adus automated driving for universal services

### 3. Challenges around next-generation automobiles and market forecast

#### 3.1 Challenges facing the automotive industry

The challenges surrounding the automotive industry, such as restrictions due to environment/energy related issues and the requirement for addressing the aging society will continue to increase. According to "Automotive Industry Strategy 2014," the challenges that the automotive industry in Japan will face in the next 10 to 20 years are as follows<sup>3)</sup>:

##### (1) Environmental/energy restrictions

From the perspective of global environment problems, the regulation on fuel efficiency and emission control will be stricter both from the program and technology aspects.

From the energy security viewpoint, initiatives for reduction of oil dependence including automobiles will accelerate.

##### (2) Increase in population/GDP per capita

The global population will increase to 8.1 billion by 2025. Then the growth rate of global population will reduce, except in Africa, and the population will remain at the same level or start decreasing by 2050.

The middle class in emerging countries will grow due to increases in population and economic growth with GDP per capita approaching that of developed countries after 2025.

##### (3) Aging society

Aging in developed countries and emerging countries will advance by 2025 and 2035, respectively. Global aging, except in Africa and India, will advance by 2050 resulting in reduced numbers of operating vehicles and increased traffic accidents if no appropriate measures are taken.

##### (4) Urban overpopulation and regional depopulation

The total global urban population will increase to 4.5 billion in 2025, 5.3 billion in 2035 and 6.3 billion in 2050. With this urbanization, the social problems caused by automobiles will become serious issues and urban infrastructure/traffic systems will become an important topic to be addressed.

After 2025, as depopulation takes place in regional areas, the need for automobiles may increase.

##### (5) Emergence of new values

Customers with diverse and new values (digital native, borderless, ageless, etc.) will grow to become the main automobile sales target.

The population born after the 1990s will exceed the majority in 2035 (31% in 2025 and 70% in 2050).

### 3.2 Prediction of adoption rate of the next generation vehicles

Fig. 5 shows the vehicle sales forecast in major countries and regions<sup>3)</sup>. It is estimated that global sales will exceed 100 million vehicles in 2025 along with the growth of population and economic development in emerging countries and the market size will reach approx. 250 trillion yen. As the overseas automotive markets grow rapidly along with population growth and income increase, the population in Japan will decrease, which may lead to a significant impact on the automotive industry in terms of the shrinkage of the domestic market and shortage of labor.

While adoption of electric vehicles is an important solution to the environment and energy restriction, the internal combustion engine vehicles have strong cost competitiveness and demand will grow, with their own technology innovation, particularly in emerging markets where motorization takes place. Therefore, a strategy with global market trends in mind is required. In order for our automotive industry to be able to expand its global market share and explore new markets, it is important to build the market environment with no barriers so that optimal investment and trade can be realized.

The increased adoption of next generation vehicles is an important challenge for the automotive industrial policy from the standpoint of increased energy security, to better address the environmental demand and enhanced competitiveness of the automotive industry. "Japan Revitalization Strategy Rev. 2015," aims to increase the ratio of next generation vehicles in new car sales to 50-70% by 2030." Among next generation vehicles, EVs, PHVs and FCVs have high impact on CO<sub>2</sub> emissions reduction, as well as offering new added value such as using the emergency power source in case of disasters; therefore, the government is also supporting their

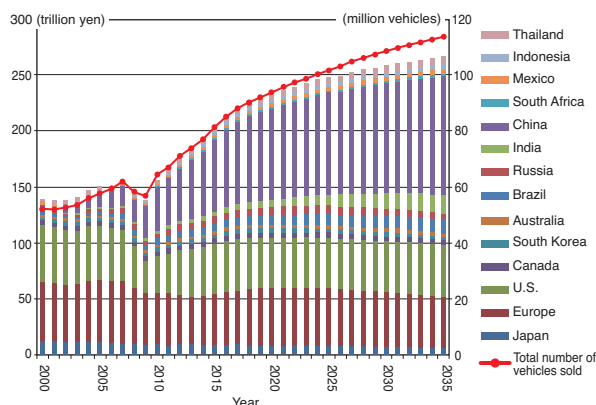


Fig. 5 Prospection of sales total for automobiles by major countries and area

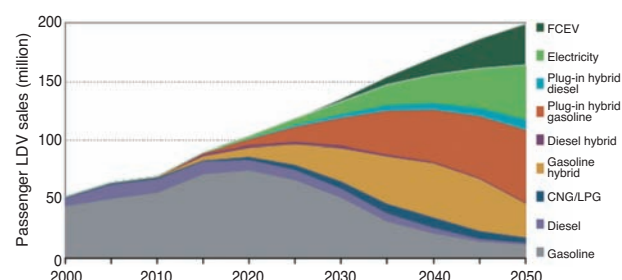
adoption. Table 1 shows the adoption targets of passenger cars by vehicle type published by the government<sup>4)</sup>. The target aimed for EVs and PHVs by 2030 is up to 30%. This target is extremely aggressive even when compared with the scenario laid out by the International Energy Agency (IEA), which is focused on mitigation of global warming.

Fig. 6 shows the forecast of global vehicle sales by IEA. IEA released their forecasts based on several scenarios in Energy Technology Perspectives announced in 2012. In the 2DS improved scenario (Fig. 6) where EVs and PHVs will be most adopted, it is estimated that the market shares of HEVs/PHVs and EVs will be approx. 28% and 4%, respectively in 2025, and approx. 52% and 11%, respectively in 2035. The governments in major countries have also set adoption targets of EVs/PHVs in a magnitude of millions of vehicles and are actively promoting various incentive programs such as support of charging station infrastructure build-out (subsidies), support for development/facility investment for automotive/battery industries, etc.

If Japan has to aim for early development of advanced market for EVs/PHVs while actively taking measures to mitigate global warming, it is desirable to set the target level similar to the 2DS scenario based on the targets shared in the Paris Agreement. Based on the above, the EV/PHV Roadmap Study Committee<sup>4)</sup> is studying the target setting and potential programs for achieving 1 million (max.) vehicles by 2020 on the premise of the efforts over and beyond those in the past by both public and private sectors and the maximum possible outcome.

Table 1 Government target of motorization

	2015 (Actual)	2030 (Target)
Conventional Vehicles	73.5%	30~50%
Next Generation Vehicles	26.5%	50~70%
Hybrid Vehicles (HVs)	22.2%	30~40%
Electric Vehicles (EVs)	0.27%	20~30%
Plug-in Hybrid Vehicles (PHVs)	0.34%	
Fuel Cell Vehicles (FCVs)	0.01%	~3%
Clean Diesel Vehicles (CDVs)	3.6%	5~10%



Source : IEA/ETP (Energy Technology Perspectives) 2012

Fig. 6 Prospection of number of vehicle purchases in the world

## 4. Challenges of on-board batteries

### 4.1 Trends and challenges of R&D for batteries

EVs and PHVs, which run highly efficiently with electric power and can be charged from external power sources including renewable energy, are key low-carbon technology and their growth rate is determined by the technology innovation of the on-board batteries.

Fig. 7 shows the secondary battery technology roadmap developed by NEDO<sup>5)</sup>. It shows the direction of technology development with energy density and output density per unit weight, cost and life as benchmarks. The batteries are classified by use, such as "Output density focused secondary battery" for HEVs and PHVs with LIB, and "Energy density focused secondary battery" for EVs. The target values for battery cost, energy density and output density vary significantly depending on what to consider, such as cells, modules or packs. From the standpoint of comparing materials/batteries, it is desirable to consider cells; therefore, this published information is based on the cells.

One of the major challenges for automotive

manufacturers in pursuing extension of electric-only driving range is the cost of batteries. It takes up the major part of the cost difference with gasoline powered vehicles, restricting driving range. Vigorous R&D must be promoted for the ultimate solution of range extension. METI has been promoting "Advanced Technology Development of Lithium-Ion Battery Application/Implementation Project" (FY2012-2016) aiming for advancing functionality of lithium-ion batteries, which are the current mainstream batteries, based on the roadmap in Fig. 7. It is said that the energy density of lithium-ion batteries is approaching the industry limit. Therefore, "Innovative Battery Advanced Technology Basic Research Project" (FY2009-2015) was conducted to advance R&D of innovative batteries to significantly improve the performance beyond the current lithium-ion battery limit. This project is succeeded by a 5-year project from FY2016 (Fig. 2) to establish advanced analysis technology and basis technology for on-board batteries. Fig. 8 shows the technology map of innovative batteries by NEDO<sup>5)</sup>. There is no clear definition of innovative batteries; however, it shows the relation between the capacity density and

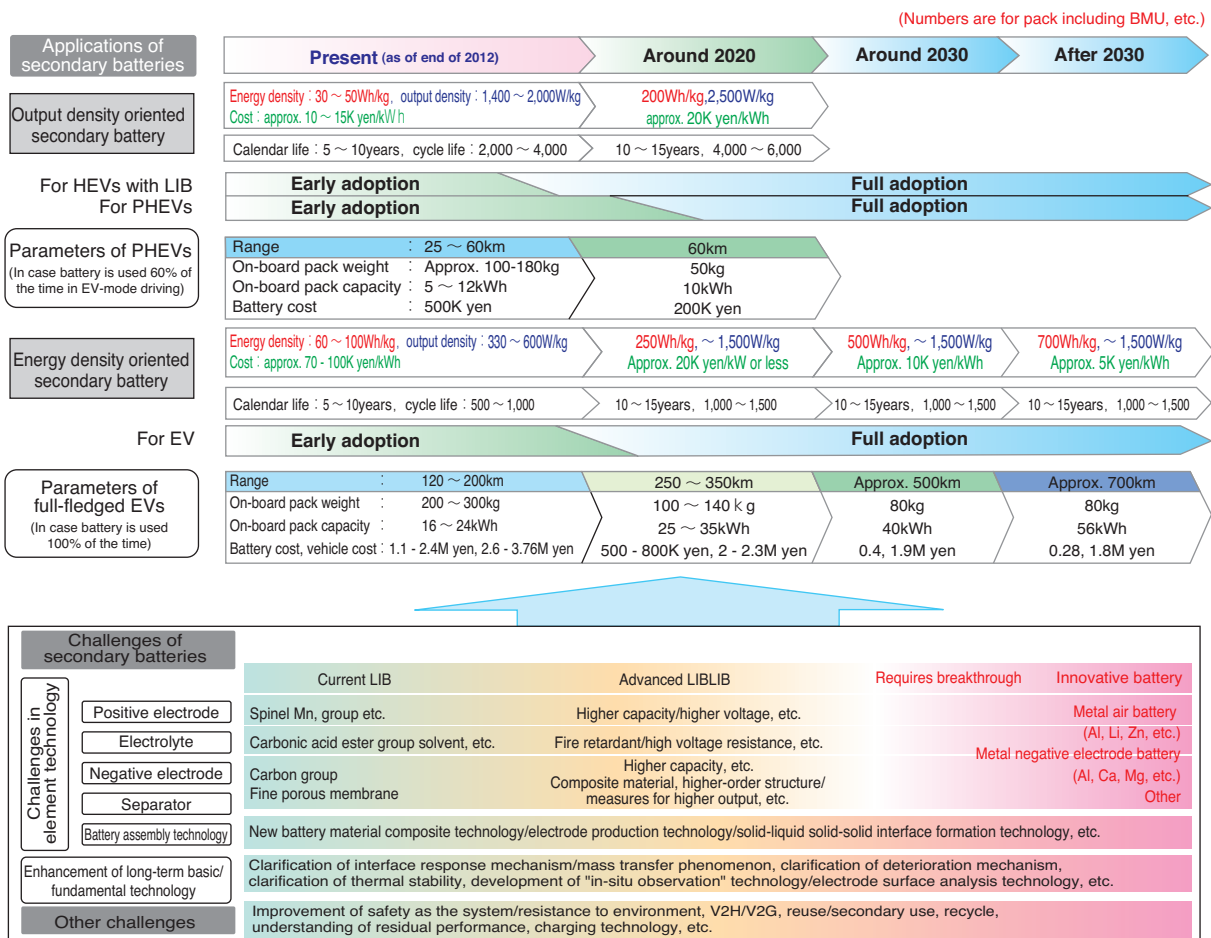
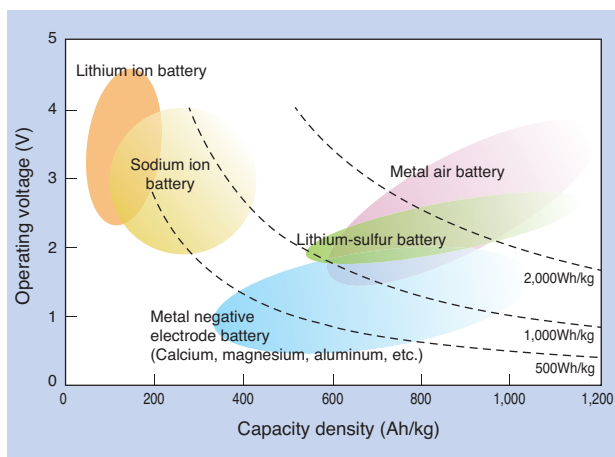


Fig. 7 NEDO Roadmap of secondary battery for automobiles



**Fig. 8** Technology map for new generation batteries (Relation between capacitance density and voltage)

operating voltage of the battery systems which have potential to achieve the high performance required by around 2030 that the current battery system cannot achieve. Examples are metal-air batteries, lithium-sulfur batteries and metal anode batteries. These innovative battery systems are being considered to be adopted for two usages (automotive and stationary) similar to the current battery systems and gradually replace the latter.

However, each of these batteries has many technology challenges. According to NEDO TSC Foresight<sup>6)</sup>, there is an issue of irreversibility of discharge products on the anode metal for metal-air batteries which cause significant capacity degradation when charge-discharge cycles are repeated. For lithium-sulfur batteries, elution of polysulfide ion, which is produced by charge-discharge cycles when organic electrolytes are used, is known to cause reduction of charge-discharge efficiency and shorter life. Metal anode batteries also have issues of irreversibility of electrolyte elution at anode metal, similar to metal-air batteries and lithium-sulfur batteries. As R&D for various innovative batteries is actively pursued globally for superior future battery candidates, it is necessary for Japan, to further accelerate R&D in government/academia/industry for keeping and enhancing our competitiveness in the automotive/battery industry.

**4.2 Use of V2X functionality**

One of the characteristics of EVs is the ability to store power supplied from external sources to large capacity batteries. Vehicles with the ability to supply power externally can provide power to homes and facilities via chargers with discharging capability. Especially, the system which can provide power to homes and buildings (V2X power supply) from EVs is currently gaining attention.

V2H (Vehicle to Home) shown in Fig. 9 indicates

that it can be used for shifting power peak, backup during blackout, utilizing night power, etc. by connecting EVs to homes and office buildings. V2G (Vehicle to Grid) aims for reduction of tribo-electric facilities of the entire smart grid, by using on-board batteries of EVs parked during the night and holidays by connecting them to the power grid of the concerned region. In April 2014, "Charging-Discharging System Guideline for Electric Vehicles" was developed to ensure electric safety and compatibility between the vehicles and connecting devices for V2H which supplies power to buildings and V2L (Vehicle to Load) which directly supplies power to electric devices. In August 2015, Japan Electrical Safety & Environment Technology Laboratory started "Certification of Power Conditioner for V2H for Grid Interconnection (Certification of Protective Devices, etc. for Grid-Interface for Electric Vehicles, etc. On-board Batteries (for serial connection))" and adoption of V2X power supply is being promoted by both the public and private sectors. Grid interconnection type that optimally combines power from solar photovoltaic electricity generation and power from batteries of EVs and PHVs is also to be introduced to the market and its adoption is expected.

It is pointed out that the output fluctuation of renewable energy depending on the time of the day and seasonal/weather conditions is one of the barriers for adoption of renewable energy. If EVs do not hold enough power in their on-board batteries at the time the users want to use them, the traveling range will be insufficient and the convenience of using the vehicles will be lost. Therefore, high energy density, low cost and high storage capacity of on-board batteries are unavoidable challenges.

In the Great East Japan Earthquake, automobiles were used as emergency power sources and for heating until energy infrastructure was recovered. EVs/PHVs are able to supply power to the equivalent of a few days of consumption for average homes; therefore, it is desirable to actively utilize this value,

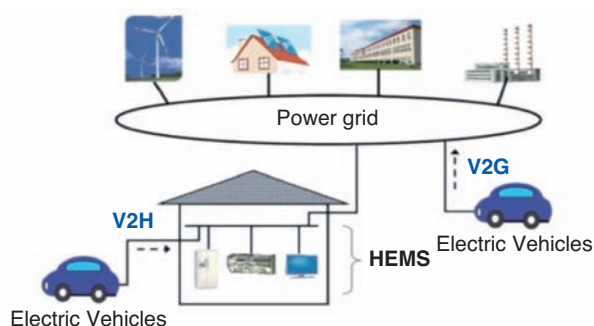


**Fig. 9** V2G, V2H (NEDO, 2015)

including as measures against disasters. However, just mentioning readiness for disasters alone does not convey the message of specific advantages to the users; therefore, it is necessary to clarify specific advantages to the users and communities, and convey the information in order to accelerate their adoption.

In Japan, Agency for Natural Resources and Energy has been leading the "Next Generation Energy/Social System Demonstration Projects" for demonstration of V2H and demand response technology. As we move forward, initiatives for feeding back the results of technology demonstration through to implementation into the real world are required based on the adoption rate of EVs/PHVs and renewable energy, as well as the restructuring trend of the power systems.

## 5. Current status and policy concerns for autonomous driving

### 5.1 Trend of autonomous driving

In Japan, the 10th Traffic Safety Basic Plan (March, 2016) stated "reducing deaths from traffic accidents to 2,500 or less and realizing the world's safest road traffic" as the national objective. In 2016, deaths from traffic accidents decreased, the first time in two years, to 3,904; however, significant efforts are required to achieve the national objective. Especially, traffic accidents at intersections and those involving pedestrians, bicycles and motor bikes are major issues requiring a comprehensive approach including improvement of traffic environment and awareness of pedestrians, not only automobiles.

Autonomous driving levels and the definition of autonomous running system/driving system to realize autonomous driving can be found in SAE J 2016 determined by the U.S. SAE International in September, 2016. The summary of definition is shown in Table 2<sup>2)</sup>. In any level, the driver can always intervene in the system control.

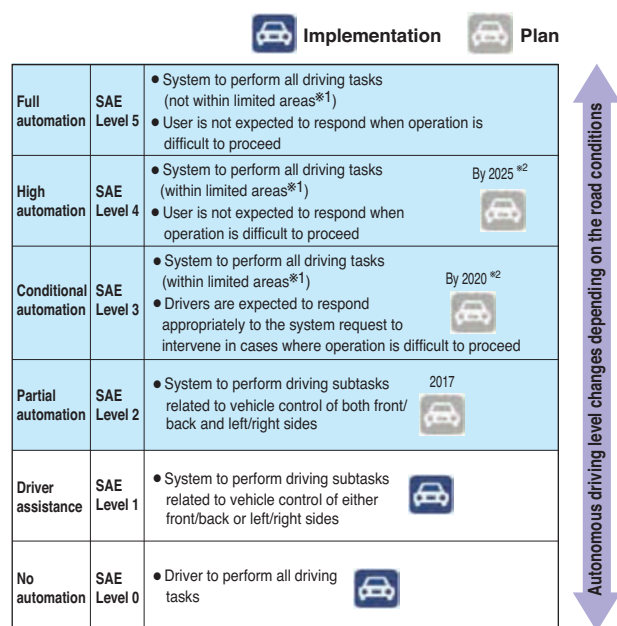
Fig. 10 shows the expected timeframe for realizing autonomous driving systems<sup>2)</sup>. It is expected that the system for SAE level 3 will be achieved by 2020 and SAE level 4 by 2025, as the expected timeframe for market introduction.

The new industries related to autonomous driving are broad. Significant market expansion can be expected around the digital infrastructure industry, such as on-board sensors (cameras, radars, etc.), as well as the information communication industry such as on-board radio devices, street-side radio communication equipment, mobile communication devices, etc. In addition, the implementation and adoption of autonomous driving systems will drive the

Table 2 Definition of driving automation level

Level	Overview	Subject for monitoring and addressing safe driving
<b>Driver to perform all or partial driving tasks</b>		
SAE level 0 No automation	● Driver to perform all driving tasks	Driver
SAE level 1 Driver assistance	● System to perform driving subtasks related to vehicle control of either front/back or left/right sides	Driver
SAE level 2 Partial automation	● System to perform driving subtasks related to vehicle control of both front/back and left/right sides	Driver
<b>Autonomous driving system to perform all driving tasks</b>		
SAE level 3 Conditional automation	● System to perform all driving tasks (within limited area*) ● Drivers are expected to respond appropriately to the system request to intervene in cases where operation is difficult to proceed	System (Driver when operation is difficult to proceed)
SAE level 4 High automation	● System to perform all driving tasks (within limited areas**) ● Users are not expected to respond when operation is difficult to proceed	System
SAE level 5 Full automation	● System to perform all driving tasks (not within limited areas**) ● User is not expected to respond when operation is difficult to proceed	System

\*"Area" is not limited to the geographical area but includes environmental, traffic, speed and time conditions, as well.



\*1 "Area" is not limited to the geographical area, but includes environmental, traffic, speed and time conditions, as well.

\*2 Set as the timeframe for the government to aim so market introduction by the private companies can be achieved.

Fig. 10 Target of automated driving system

emergence of new industries such as technology for the generation of highly precise 3D maps, organizing and operating information in diverse areas other than autonomous driving systems, highly precise location information services, etc.

### 5.2 Challenges and initiatives of autonomous driving

For achieving the national objective of reducing deaths from traffic accidents, it is important to develop and implement/promote driving assistance systems

and autonomous driving systems, deepen the data analysis and simulation technology of deaths from traffic accidents and develop technology to predict and verify the effects of safety policy. It is also necessary to promote technology development in the area of coordination so that the SAE level 4 system can be marketed by around 2025. Furthermore, challenges include the implementation of next generation transportation systems that contribute to our next generation in view of the 2020 Tokyo Olympic/Paralympic Games and having the development of Tokyo and aging society in mind, as well as social acceptance and regulatory consideration toward implementation.

In view of these points, "autonomous driving system" in the Cabinet Office's SIP (Strategic Innovation Promotion Program) sets the following 5 items of autonomous driving as the focused initiative for FY2017<sup>2)</sup>.

- (1) Dynamic map (map information integrating information on the road structure and traveling course environment in addition to conventional map information for generating the route in the autonomous driving system),
- (2) HMI (Human Machine Interface),
- (3) Information security, (move to next line)
- (4) Reduction of accidents involving pedestrians,
- (5) Advanced Rapid Transit

**Fig. 11** shows the categories of R&D themes<sup>2)</sup>.

While the automotive industry conducts autonomous system, etc. in competitive areas, SIP promotes development and implementation of basic technology and cooperative areas (related to cooperative systems) which require initiatives based on partnership between the public and private sectors.

SIP also promotes R&D around large-scale demonstration tests. The plan includes a large-scale and continuous demonstration test along expressways spanning 300 km from Joban Expressway-Metropolitan Expressway-Tomei Expressway to New Tomei Expressway and surface roads around Odaiba from FY2017 until the end of FY2018.

In addition, verification of the dynamic map, mentioned in the above (1), will be conducted for its implementation in the large-scale demonstration test for verifying specification/accuracy of static high-precision map data and data generation/update/distribution systems.

Regarding (2) HMI, evaluation method will be established for proposed standardization and data of driver conditions on test courses and public roads will be collected and stored.

Regarding (3) Information Security, black box tests are conducted to verify anti-hacking performance using vehicles from the participating manufacturers.

Regarding (4) Reduction of accidents involving pedestrians, application with improvement of positional accuracy and maps will be developed from the results obtained until FY2016 and the effect of pedestrian-vehicle communication technology will be validated on public roads toward reduction of accidents involving pedestrians.

Regarding (5) Advanced Rapid Transit, a specific proposal will be made including demonstration tests on public roads for development of control technology for ART (Advanced Rapid Transit system) vehicles and realization of ART Information Center concept which works together with the dynamic map.

In addition to the above promotion of R&D through large-scale demonstration tests, business

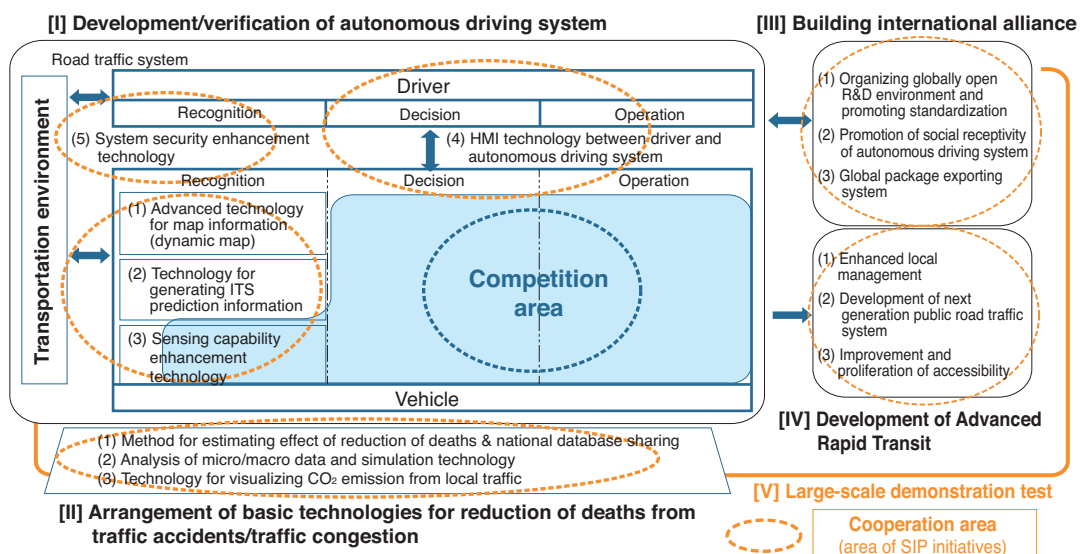


**Fig. 11** R&D theme of SIP-adus automated driving for universal services

development/business model build-up, regional expansion/partnership among industry/academia/government and international partnership/standardization activities are also important. The value that Japan can obtain from playing the leading role is socially and industrially very large and should serve as a global contribution.

## 6. Strategy of mobility area in the New Industrial Structure Vision

### 6.1 Society 5.0 and Connected Industries

As the fourth industrial revolution by disruptive innovation such as IoT, big data and artificial intelligence (AI) is underway, it is indispensable for the public and private sectors to share the vision and work strategically on what the economic and social impact of these developments are and what actions Japan has to take. Under this recognition, METI formed "New Industrial Structure Committee" (Chair: Motoshige Ito, Professor at Tokyo University) under Industrial Structure Council to develop vision that the public and private sectors can share and study the actions that the public and private sectors are required to take, and compiled and published the vision titled "New Industrial Structure Vision: Japan as a future-oriented country solving global challenges on an individual basis" in May 2017<sup>7)</sup>. The following is an overview of this vision :

In this Vision, it is expected to see new products/ services and a productivity revolution which will unfold potential demand by social implementation of the fourth industry revolution technology (IoT, big data, AI, robots, etc.) which is considered to be the major key for realizing Society 5.0 (ultra smart society) depicted in Fig. 12<sup>7)</sup>. Among them, a new concept, "Connected Industries" is proposed. It is a concept of industry

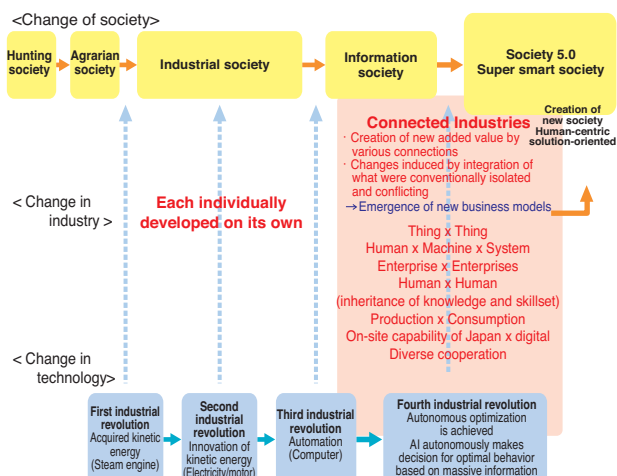


Fig. 12 Connected industries aimed for Society 5.0

society where various people, organizations, machines, technologies and states are connected to achieve Society 5.0, and create new added value and solve social issues. The promotion of Connected Industries is expected to encourage creation of value and technology inheritance over the generations in the areas of "creating and maximizing added value", which is Japan's manufacturing industry's challenge, and "maintaining and improving strong manufacturing work sites" where shortage of labor is surfacing, by connecting various industries, organizations, people, things, technologies and data.

As an example, Fig. 13 shows common basic technology such as AI and innovative products/services by connected technologies and available data<sup>7)</sup>. By utilizing technology innovation such as AI and data, it will be possible to address "social/structural demands = customers' real needs." It is desirable to realize rich society for each individual by taking advantage of new technology/data that leads to solution of global challenges and Japan's economic growth.

With the progress of the social implementation of the fourth industry revolution technology, a new industrial structure shift as depicted in Fig. 14 can be considered<sup>7)</sup> by lowering the barriers among various industries. With this, it is possible that a move to create a new service platform that swallows completely different industries may expand.

Technology	Related data	Related data Innovative products/services
Drive control technology	Accident data, Camera information data	Mobility service by unmanned autonomous driving Unmanned autonomous driving vehicles, etc.
Production control technology	Accident/ Near-miss incident data	Safety/productivity improvement by early detection of anomalies/symptoms, Advanced insurance/ratings, etc.
Bio-informatics	Bio data	Drug discovery, Functional food, Advanced material manufacturing, Bioenergy, etc.
Genome editing		
Drug development technology	Technology related to nursing care Health/medical data	Nursing care data Individualized medication Nursing care plan for self-dependent, etc.
Energy demand Facility control technology	Customer data	Energy demand response, Watching service
FinTech	Procurement/ logistic data, financial market data	Credit based on transaction/payment data, Asset management advice service enhancement, etc.

Fig. 13 Common fundamental technology, Industrial core technology and data

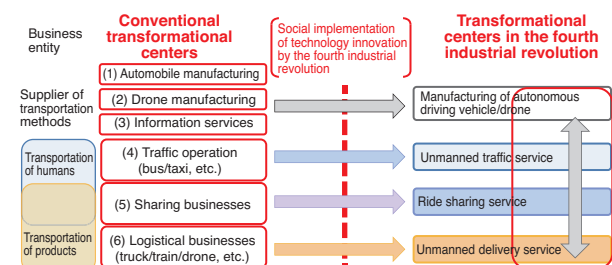


Fig. 14 New transformation of industrial structure in Industry 4.0

### 6.2 Strategy area "mobility"

Industrial Structure Vision organizes strengths and opportunities that Japan should leverage in the following three points:

- Accumulation of diverse and valuable "real data" (potential for creating new values from the real data by leveraging the ability to carefully learn from the facts ongoing at user sites and market)
- Strength in "things" (ability to quickly adopt advanced technology and renovate "things" and potential to achieve new integration of hardware and software)
- Early appearance and magnitude of new social challenges (potential to discover solutions to make people happy and deploy them globally, earlier than anywhere else)

From the above points, it is determined that the following four areas are strategic areas for Japan to take:

(1) "Mobility", (2) Supply-chain, (3) Healthcare, (4) Living. Perspectives in the New Industrial Structure Vision are described in the following:

### 6.3 Challenges of mobility of people and products

The goals for the 2030s include "safe mobility (reduction of traffic accidents)," "resolution for mobility impaired individuals" and "effective use of commuting time" for mobility of people, "resolution of imbalance of labor supply/demand in industries such as logistics," "reduction of re-deliveries in the courier industry," "Expansion of coverage for emergency response during disasters" and "Improvement of logistics for living necessities on remote islands" for mobility of products, and "mitigation of CO<sub>2</sub> emissions in the transportation sector" for both people and products. It is possible that several social and structural challenges regarding "mobility" can be solved domestically and overseas by leveraging innovative technology and use of data.

On the other hand, the following potential risks may surface:

#### (1) Security risk

Risk of accidents for passengers, surrounding people and objects if autonomous vehicles and drones are maliciously hacked and become uncontrollable.

#### (2) System risk (resonance of erroneous information)

Risk of paralyzed traffic systems and accidents when autonomous vehicles share and amplify erroneous information through the network.

#### (3) Risk of labor/employment/social security

Requirement for newly acquired skills and labor conditions due to the changes in the industrial structure. A risk that the labor/employment/social security systems cannot adapt to these changes.

#### (4) Risk of social acceptance

If significant accidents involving people occur before autonomous vehicles and drones are accepted into society, psychology of refusal and avoidance may become dominant. There is a risk of it not being implemented, even when technically feasible, because of this social refusal.

As mentioned above, various risks can be anticipated in each layer of mobility means, system network, employment/labor and social acceptance as technology advances. The New Industrial Structure Vision considers measures against them and incorporates them into the roadmap.

### 6.4 Roadmap for "mobility of people"

Fig. 15 shows the direction of "mobility of people." <sup>7)</sup>

This is a conceptual diagram of providing safe and diverse mobility services by autonomous mobility means. In order to achieve autonomous driving, it is important to realize "recognition" and "decisions" for ensuring safety, in particular, by combining software such as algorithms and hardware such as sensor devices. Fig. 16 shows the strengths and weaknesses of Japan in critical technology for "mobility of people." <sup>7)</sup> Since the importance of semiconductors will increase

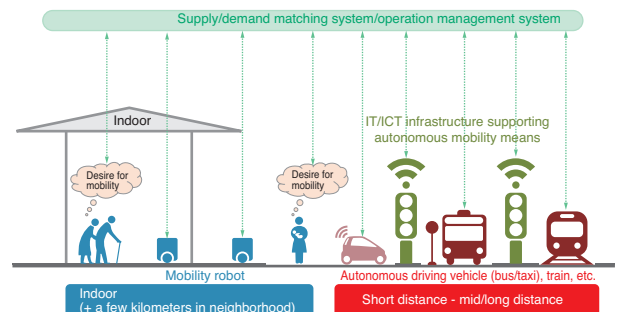


Fig. 15 Future trend of transportation of human

Element technology	Strength/weakness	Competition status
<b>(1) Recognition</b> Sensor devices serving as "eyes"	Millimeter waves (detection of objects (barriers))	△ Europe: 56%, U.S.: 34%, <b>Japan: 10%</b>
	Camera (identification of objects (barriers))	△ Israel's Mobileye exhibits overwhelming presence and fierce competition, such as acquisition announcement by U.S. Intel
	Laser radar (detection of drivable terrain)	△ European suppliers account for the majority of market share and presence of Japanese suppliers is limited
<b>(2) Decision</b> "Brain" to determine driving routes and driving operation	Vehicles themselves (Source of drive data, which is the key for algorithm development)	* Prominent companies are emerging in Japan, as well, however, the number is larger in Europe and U.S.
<b>(3) Operation</b> Mechanism serving as "hands"	Electronically controlled braking system (longitudinal control)	× Europe: 63%, U.S.: 22%, <b>Japan: 9%</b>
	Electric power steering (lateral control)	○ <b>Japan: 55%</b> , Europe: 41%, U.S.: 3%
<b>(4) Semiconductors</b> Platform supporting information processing	On-board semiconductors	△ On-board microcomputers: Europe: 35%, <b>Japan: 33%</b> , U.S.: 8% * U.S. for the leader in semiconductors for AI

Fig. 16 Advantage and weakness of Japan in automated driving technology

as the platform for supporting information processing, technology development for realizing ultra-high efficiency AI processing, such as, on-board semiconductors as a common platform for "recognition" will also be important.

Fig. 17 shows the roadmap calculated back from the target for "mobility of people" reviewed in the New Industrial Structure Vision 7).

It is arranged by categorizing the programs into (i) Autonomous mobility means (edge), (ii) Platform system/infrastructure and (iii) Business environment/rules in the short term (- 2018), mid-term (- 2020) and long term (2020 -). In addition to technology development depicted in Fig. 17, institutional reforms need to be accelerated in order to solve the challenges in the mobility area.

(i) Autonomous edge, (ii) System/infrastructure, (iii) Business/environment rules

	Short term (- 2018)	Mid-term (- 2020)	Long term (2020 -)	
<b>Target</b>		<b>Achievement of mobility service by unmanned autonomous driving in specified regions</b>	<b>Expansion of service area/marketing of unmanned autonomous driving</b>	
<b>Initiatives</b>	i	○ Demonstration test of autonomous driving in 10 model areas	○ Realization of the Tokyo Olympic/Paralympic project	○ Adoption of unmanned autonomous driving (expansion of private businesses), global standardization of safety standards, etc.
		○ Support of technology development for AI semiconductors, etc. which will become the common platform for "recognition" and "decisions" (realize with unmanned autonomous driving as the target)		
		○ Strategic utilization of driving video data, accident data, etc		
	ii	○ Development of 3D precise mapping of expressways	○ Global standardization of expressway platform maps and international deployment	○ Deployment of platform maps for prefectural roads and local roads
		○ Large-scale demonstration of dynamic map	○ Deployment of platform maps for main national roads and regional roads	
		○ Selection of required communication infrastructure	○ Deployment of required communication infrastructure	
		○ Development of action plan for ensuring on-board security		
	iii	○ Study regulatory direction of overall government policy	○ Philosophy for the rules in Road Traffic Law, etc./ Clarification of responsibilities including insurance coverage	
		○ Study framework for international treaty		
		○ Development of guidelines for remote operation (1 to N)		

Fig. 17 Roadmap of transportation of human

6.5 Roadmap of "mobility of products"

Fig. 18 shows the direction of "mobility of products." 7)

It is a conceptual diagram of providing advanced logistical services integrating diversified transportation modes seamlessly from land to air. Fig. 19 shows the roadmap calculated back from the target for "mobility of products." 7) In order to achieve truck platooning/ autonomous driving trucks, it is required to conduct demonstration tests of truck platooning with succeeding unmanned vehicles (on expressways, etc.), develop technology for optimal configuration and management of truck platooning, develop business environment for operation rules and infrastructure, etc. Regarding logistics by drones, it is required to develop technology that allows drone operation out of sight, development of navigation and collision avoidance technologies, certification of individual units and licensing of operators.

(i) Autonomous edge, (ii) System/infrastructure, (iii) Business/environment rules

Timeframe	Short term (- 2018)	Mid-term (- 2020)	Long term (2020 -)
<b>Target</b>		<b>Realize truck platooning with unmanned succeeding trucks on expressways</b>	<b>Business development of truck platooning with unmanned succeeding trucks on expressways</b>
<b>Initiatives (Truck platooning)</b>	i	○ Demonstration tests with succeeding manned trucks toward unmanned truck platooning on New Tomei Expressway	○ Expansion of distance and drivable range of truck platooning on expressways (between Tokyo and Osaka, etc.)
	ii	○ Demonstration tests with succeeding unmanned truck platooning on New Tomei Expressway	
	iii	○ Organize requirements for, perform trial and review based on trial results of cargo transportation by passenger vehicles	
<b>Target</b>	<b>Perform merchandise delivery by drones, out of sight in areas with no population</b>		<b>Deployment of merchandise delivery by drones, out of sight in areas with population including urban areas</b>
<b>Initiatives (Drone)</b>	i	○ Technology development and performance evaluation criteria development for navigation management and collision avoidance leveraging Fukushima Robot Test Field	○ Advanced and intelligent navigation management system and collision avoidance technology
	ii	○ Establish navigation management system and collision avoidance technology to be used for drone logistics	○ Full-fledged social implementation of navigation management
	iii	○ Promotion of drone utilization by public and semi-public demands for inspection of critical/aged infrastructure	○ Acquisition of global service market with global standardization
<b>Target</b>	<b>Requirements for out-of-sight flight, etc. (standards for the units and operators) are reviewed and used for revision of Examination procedures in accordance with the Aviation Law in early FY2018</b>	<b>Requirements for flight above third party, etc. (standards for the units, operators and organizations) are reviewed and used for establishing regulations</b>	<b>Rules for navigation management</b> ○ Qualification system for operators and navigation managers ○ System for certification, identification and registration of units ○ Revision of Examination procedures for flights above third parties in accordance with the Aviation Law

Fig. 19 Roadmap of transportation of things

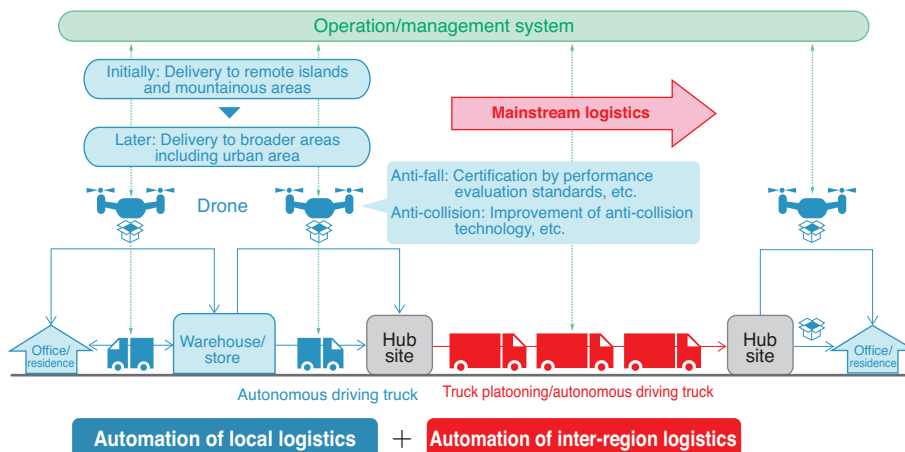


Fig. 18 Future trend of transportation of things

## 7. Conclusion

An overview of large-scale projects of technology development in the manufacturing industry around automation has been provided together with challenges surrounding next generation vehicles and market forecasts, as well as trends and challenges of on-board batteries/autonomous driving. In addition, a brief description of the study status and roadmap of mobility area of New Industrial Vision was provided. Although there are many challenges for vehicle electrification and autonomous driving, I believe that it is important for Japan to accelerate creation of new added values by integrating wisdom and efforts of industry/academia/government, leveraging our strengths, namely, high "technology" and advanced "worksite capabilities" toward a new solution-oriented industry society.

I would like to express gratitude to the members of Ministry of Economy, Trade and Industry, Cabinet Office and NEDO for their assistance in writing this article.

## References

- 1) Website of Ministry of Economy, Trade and Industry
- 2) Cabinet Office SIP Autonomous Driving System R&D Plan (2017)
- 3) Automotive Industry Strategy 2014, Automobile Division, Manufacturing Industries Bureau, METI (2014)
- 4) EV/PHV Roadmap Investigative Committee Report (2016)
- 5) NEDO Secondary Battery Technology Development Roadmap 2013 (2013)
- 6) NEDO TSC Foresight, vol.5, (2015).
- 7) New Industrial Structure Vision, New Industrial Structure Committee, METI (2017)

### <Author biography>

#### Tetsusei KURASHIKI

Associate Professor, Department of Management of Industry and Technology,  
Graduate School of Engineering at Osaka University, Doctor (Engineering)

March, 1997	Doctor Course Completed, Manufacturing Processing Department, Division of Engineering, Osaka University Graduate School
April, 1997 - March, 2004	Research Assistant, Graduate School of Engineering, Osaka University
April, 2004 - April, 2014	Associate Professor, Department of Management of Industry and Technology, Graduate School of Engineering at Osaka University
(May, 2011 - November, 2011	Visiting Professor, Catholic University of Leuven, Belgium)
May, 2014 - September, 2016	Manufacturing Industries Technology Strategy Office, Manufacturing Industries Bureau, METI
October, 2016 - present	Associate Professor, Department of Management of Industry and Technology, Graduate School of Engineering at Osaka University

#### [Major]

Composite material engineering, reliability engineering, numerical simulation, functional creative design, risk management

#### [Academic society and committee affiliations]

Representative, The Society of Materials Science, Japan; Councilor, Advisory Committee Member, The Textile Machinery Society of Japan; Representative, Japan Society for Composite Materials; Chief Manager, Impact/damage assessment subcommittee, No. 180 Committee, Science Council of Japan, and others

## NTN Approach toward the Electrification and Autonomous Driving



Koji KAMETAKA

130 years have passed since the automobile with the internal combustion engine appeared on the market and it's a convenient transportation, on the other hand, (1) the effect on carbon dioxide emission on global warming, and (2) economic loss caused by heavy traffics and human damage caused by the accident. For the former, strengthen the regulation of carbon dioxide emissions and automobile companies are launched the small engine with supercharger, diesel engine, hybrid vehicle (HEV / PHEV), electric vehicle (EV) etc. on the market. They are also promoting the

electrification and high efficiency of auxiliary machinery products for lower fuel consumption. For the latter, it is in the direction to obligate driving assistance such as automatic braking, and automobile companies are also moving on to introducing autonomous driving technology on the market.

In order to contribute to these trends, NTN also developed a new electric motor / actuator. I introduce NTN's efforts for electrification and autonomous driving including existing units and module products.

### 1. Introduction

As mentioned in the abstract, automobiles are being forced to change at an unprecedented pace.

Environmental requirements, in particular, are serious, as various countries are planning to enforce very strict CO<sub>2</sub> emission regulations in 2020 or thereafter.

Automotive manufacturers which do not comply with these regulations may face significant penalties. In addition, since battery prices are still high, the adoption rate of electric vehicles is expected to be slow and many research companies are predicting that vehicles with internal combustion engines will remain at over 50%, even in 2050. Therefore, automotive manufacturers are working on improvement of thermal efficiency (currently at around 40% in the best-case scenario) together with development of electric vehicles (EVs).

Regulation is particularly strict in Europe, enforcing average CO<sub>2</sub> emissions per company of 95 g/km in 2021. This means a fuel efficiency improvement of 38% compared to FY2008 levels is required; therefore, automotive manufacturers are working hard for development of next generation vehicles such as hybrid vehicles (HEVs/PHEVs) with reduced CO<sub>2</sub> emissions and better fuel efficiency, electric vehicles (EVs) and fuel cell vehicles (FCVs) which do not emit CO<sub>2</sub> at all, and their adoption over conventional fossil fuel (gasoline/diesel) engine vehicles.

Automotive components are also becoming more electrified, including the adoption of 48V for improvement in fuel efficiency.

The critical challenges for the upcoming improvement of fuel efficiency include electrification and development of system/module products. In this article, NTN's initiatives that contribute to the automotive electrification and autonomous driving are introduced.

### 2. Development of electric motors and actuators, and examples of application

NTN has developed an "electric motor actuator" series, with indispensable high versatility for by-wire control which is expected to be widely used for driving and control of vehicles.

Recently, autonomous driving and further improvement of fuel efficiency are required in the automotive industry, which is leading to vehicle electrification including by-wire control for supporting adoption and expansion of various systems for driving and control.

In consideration of these market trends, NTN has developed the "Electric motor and actuator" series by combining its core technologies of bearings and ball screws, design technology of motors and electronic control technology for vehicle control. By achieving standardization of components and specifications, and

\*Managing Executive Officer, Motorized Module Product Corporate General Manager

creating a line-up of different types and sizes, individual design is no longer required and development turnaround time can be reduced.

The developed products can be adapted to various on-board applications; however, they can also be applied, not only to automotive, but also to much broader areas. NTN is aiming for early volume production of these series, promoting global sales for vehicle on-board applications, then expand into other devices using actuators.

The line-up includes "parallel shaft type B II (Fig. 1)," "coaxial hollow shaft type B III (Fig. 2) (Table 1)" and brushless DC motor, SP Series, to meet the requirements of the applications.

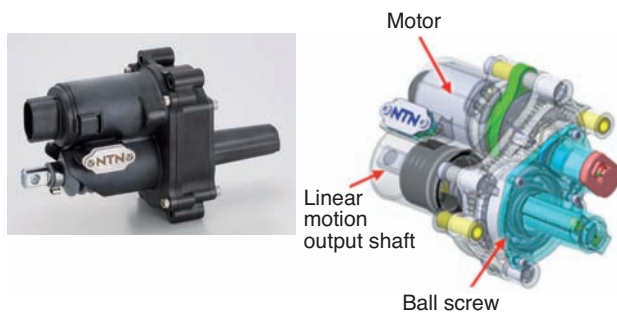


Fig. 1 Picture and structure of B II series

Table 1 Type of electric motor and actuator

Type	Features
1 Parallel shaft type (BII)	<ul style="list-style-type: none"> <li>● Lightweight by adopting resin housing</li> <li>● Reverse input rotation prevention unit can be installed and be applied to parking brakes, etc.</li> <li>● Add-on reducer unit which can be applied for large propulsion</li> <li>● Embedded non-contact linear position sensor</li> </ul>
2 Coaxial type (BIII)	<ul style="list-style-type: none"> <li>● Compact design by adoption of coaxial type</li> <li>● Optimal size, torque and output by polymerization composition of magnet and core</li> <li>● Standardization of magnet and coil which are the main components of motors</li> <li>● Embedded non-contact linear position sensor</li> </ul>



Fig. 2 Picture and structure of B III series

## 2.1. Application example of electric motors and actuators

### 1) Electric variable valve timing unit

An example of application for improved fuel efficiency in internal combustion engines is the cam phaser, which realizes the Atkinson cycle by making the phases of the crank shaft and cam shaft variable.

It was difficult to achieve precise control with the conventional hydraulic mechanism. Electrification can be applied to the electric variable valve timing unit (Fig. 3) to realize this. The unit not only realizes precise control but also contributes to light-weightedness due to the electric motor and actuator.

### 2) Electric EGR valve unit

Another example of improved fuel efficiency in internal combustion engines, which is similar to <sup>1)</sup> is the electric EGR valve unit (Fig. 4) which provides a mechanism for improving fuel efficiency by cooling off and recirculating exhaust gas. It can contribute to controllability, weight reduction and reduction of valves size.

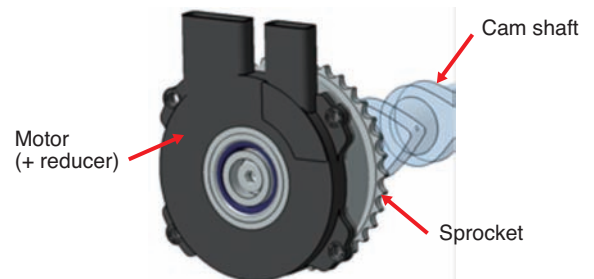


Fig. 3 Electric variable valve timing unit

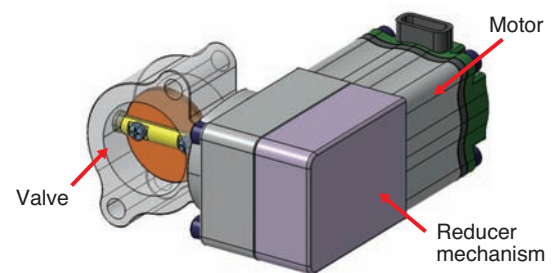
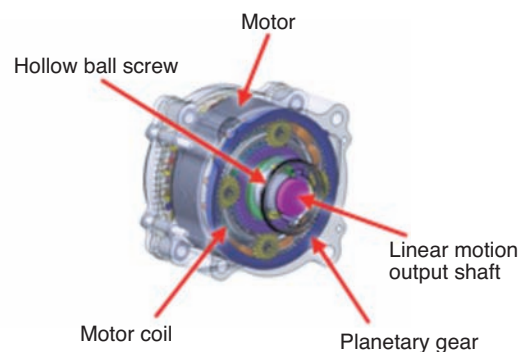


Fig. 4 Electric EGR valve unit



### 3. Other initiatives for autonomous driving and electrification

#### 1) Auto tensioner unit with variable damper mechanism for ISG(Integrated Starter Generator)

We have developed an auto tensioner unit with a variable damper mechanism for ISG (Fig. 5) to be used in engines with auto start/stop features.

Vehicles with auto start/stop mechanisms which automatically stop the engine when the vehicles stop at traffic lights, etc., are increasing to improve fuel efficiency. The auto start/stop mechanism detects the driver's starting operation to restart the engine, and "ISG method," in which the generator (power generator) also works as the starter (ignition motor), is the mainstream method for restarting. However, the conventional auto tensioner with ISG method which adjusts the tension of accessory belt had to be set either to ensure belt tension required for restarting engine from auto-stop state, or to keep low belt tension to improve fuel efficiency in normal driving.

The "auto tensioner unit with the variable damper mechanism for ISG" allows optimal setting of the tensioner automatically depending on the engine status, achieving both stability at restart of the engine and fuel saving while driving.

It is a hydraulic auto tensioner with improved internal design where the oil path is altered from the conventional oil path to one with less path resistance, and the path is automatically switched depending on the direction of force transmitted from the accessory belt. With this mechanism, relatively low tension is given while driving to improve fuel efficiency and instantaneous high tension is achieved when restarting the engine.

In addition, this unit has common components with NTN's conventional products without a switching mechanism, ensuring compatibility when replacing the units.

The belt drive ISG method does not require significant design change for the accessory layout

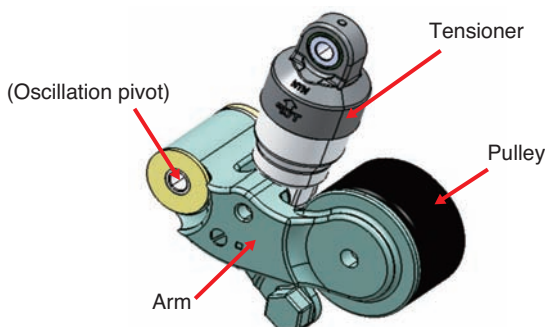


Fig. 5 Auto tensioner unit with variable damper mechanism for ISG

from conventional engines and allows a fast and quiet engine restart. Therefore, it is also adopted in Mild Hybrid and its use is expected to be further expanded.

#### 2) Rear-wheel independent steering system

We have developed a "rear-wheel independent steering system" which applies the steer-by-wire steering system technology, allowing electronic control of the steering system (Fig. 6).

The rear-wheel steering for vehicles is a mechanism to stabilize vehicles in high-speed driving and improve cornering ability in mid-low speed driving, and the electric actuator is used to drive rear-wheel steering. The "left-right combined-type", which controls steering with one actuator lacks left-right toe angle control function, and "left-right independent type" which places actuators to the left and right to control steering has a challenge of decreased driving performance due to increase of unsprung weight.

NTN's "rear-wheel independent steering system" allows left-right toe angle control although it is a left-right combined-type, and the actuator is mounted on the vehicle body side. Furthermore, the maximum steering rate of tires is improved to 10 degrees/second (conventionally 6 degrees/second) to improve the response of vehicle behavior in the case of high speed driving and emergency avoidance. By achieving a wider steering range of max.  $\pm 2.5$  degrees for the tire steering angle, the minimum radius of gyration has become smaller, making it easier to park and contributing to future autonomous driving.

By reducing the volume by approx. 60% compared with NTN's conventional product while maintaining the same rigidity, the weight is reduced by approx. 30%, improves ease of mounting on the vehicles. In addition, since the developed product is left-right

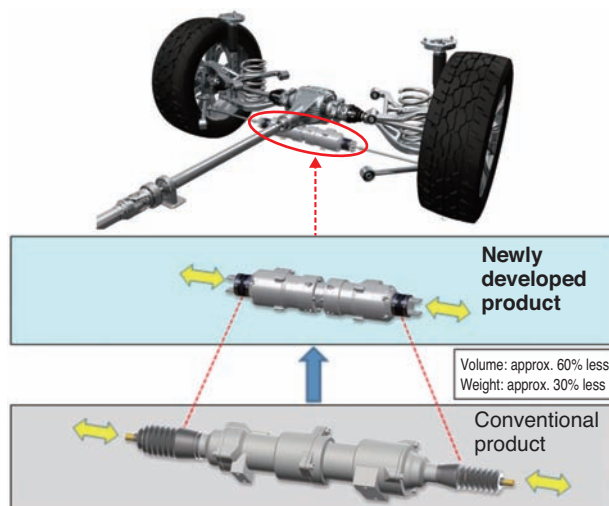


Fig. 6 Rear-wheel independent steering system

combined-type and installed on the vehicle body side, unsprung weight is not increased, resulting in no impact on riding comfort.

### 3) Mechanical clutch unit (MCU) for next-generation steering

NTN developed "mechanical clutch unit (MCU) for next-generation steering (Fig. 7)" to be used in direct adaptive steering developed by Nissan Motor Company (hereafter, "Nissan") and started marketing in 2013.

The conventional steering system transmits the driver's steering operation to the tires through the shaft. On the other hand, the direct adaptive steering transmits the driver's steering operation to the tires through electric signals; therefore, there is no mechanical link between steering and tires that may be affected by road roughness, allowing agile and accurate steering operation.

In addition, direct adaptive steering is equipped with a backup mechanism to mechanically connect the steering wheel and tires in case of function failure detection.



Fig. 7 Mechanical clutch unit for next-generation steering

"Mechanical clutch unit (MCU) for next-generation steering" contributes to achievement of a backup mechanism for direct adaptive steering. Its compact configuration combining the electromagnetic clutch and roller clutch releases the roller clutch when the electromagnetic clutch is electrically driven while direct adaptive steering is functioning, allowing transmission of steering operation to the tires through electric signals. On the other hand, when failure of direct adaptive steering is detected, power to electromagnetic clutch is shut off and the roller clutch is instantaneously engaged so that the steering operation is mechanically transmitted to the tires. It has high reliability in mechanical engagement due to its high-load capacity design.

## 4. Conclusion

For electric vehicles and autonomous driving, motorized modules/system products are indispensable for electrification of steering and control systems. It is an area where NTN's core competence, namely, tribology technology, precise processing technology, precision metering technology and analytics such as simulation can be fully used.

While the automotive industry faces an unprecedented time of changes in meeting challenges such as maintaining/improving environment and improving safety, we would be happy if NTN's technology and products can help meet[ing] these challenges and be contribute to society.

Photo of author



Koji KAMETAKA

Managing Executive Officer  
Corporate General Manager,  
Motorized Module Product  
Headquarters

# Development of Electric Motor, Actuator Series

**Kimihito USHIDA\***  
**Masashi NISHIMURA\***



Action to improve fuel economy by applying various electric devices is accelerated while the fuel efficiency regulation of automobiles progress globally. In addition, the practical use of autonomous driving technology will advance, and it is predicted that by-wire system will be greatly advanced mainly on the function of "running", "turning" and "stopping". Under such a situation, the application of electric actuators that operated for each function with electrification and by-wire has been expanding. In this section, we introduce the electric motor / actuator series developed by NTN.

## 1. Introduction

Global warming has recently become a serious problem. The impact of exhaust gas from automobiles adding to global warming is increasing year by year with the increase of automobiles and vehicles for transportation and distribution. For example, emissions of CO<sub>2</sub> from automobiles account for nearly 20% of total greenhouse gases. Reducing emission gas is challenging. In November 2016 the Paris Agreement, which is a new framework for preventing global warming, took effect. Also initiatives for reduction of greenhouse gases are accelerating in many countries. For automobiles, Europe will adopt the most stringent fuel efficiency regulation of 95g/km of CO<sub>2</sub> emissions by 2021 for passenger cars. The U.S. is setting a goal of 100g/km of CO<sub>2</sub> emissions with 2025 being the last year for compliance for all passenger cars and pickup trucks. Fig. 1 shows fuel efficiency regulations of various countries.

In order to meet these stringent regulations car manufacturers are pursuing the electrification of vehicles. This includes various aspects of fuel efficiency improvement for internal combustion engine vehicles, such as motorizing on-board units which have historically been operated hydraulically for reducing load to engines, in addition to developing EVs and PHEVs.

On the other hand, reducing deaths from traffic accidents is also a major social challenge. In Japan SIP, (Strategic Innovation Promotion Program) headed by the Cabinet Office, is promoting initiatives

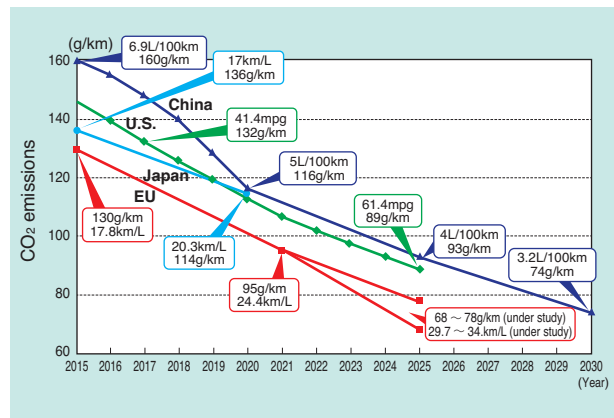


Fig. 1 Fuel consumption regulation <sup>1)</sup>

for development of an autonomous driving system based on the 10th Traffic Safety Basic Program. The goal of SIP is to reduce deaths within 24 hours from traffic accidents to 2,500 or less by 2020. It aims for the practical use of a semi-autonomous driving system (level 3) by 2020 when the Tokyo Olympic/Paralympic games will be held, and commercialization of full autonomous driving system after the latter half of the 2020s.

Fig. 2 shows the definitions of automation levels indicated in the SIP Autonomous Driving System R&D Plan. Auto manufacturers are also working on the development of autonomous driving technology with improved safety and the reduction of traffic accidents. Autonomous technology is using motorized actuators for by-wire control of fundamental functions of automobiles, including run, turn and stop. Motorized actuator technology is becoming critically important.

\*Business Promotion Dept., Motorized Module Product Headquarters

	Implementation	Plan
Full automation	SAE Level 5	<ul style="list-style-type: none"> <li>System performs all driving tasks (not within limited areas*1)</li> <li>User is not expected to respond when an operation is difficult to maneuver</li> </ul>
High automation	SAE Level 4	<ul style="list-style-type: none"> <li>System performs all driving tasks (within limited areas*1)</li> <li>User is not expected to respond when operation is difficult to maneuver</li> </ul> By 2025 *2
Conditional automation	SAE Level 3	<ul style="list-style-type: none"> <li>System performs all driving tasks (within limited areas*1)</li> <li>Drivers are expected to respond appropriately to the system request to intervene in cases where operation is difficult to maneuver</li> </ul> By 2020 *2
Partial automation	SAE Level 2	<ul style="list-style-type: none"> <li>System performs driving subtasks related to vehicle control of both front/back and left/right sides</li> </ul> 2017
Driver assistance	SAE Level 1	<ul style="list-style-type: none"> <li>System performs driving subtasks related to vehicle control of either front/back or left/right sides</li> </ul>
No automation	SAE Level 0	<ul style="list-style-type: none"> <li>Driver performs all driving tasks</li> </ul>

In all of the levels the driver should always be able to intervene in system control. For the semi-autonomous driving system (level 3) and full automation system (level 4), the timeframe has been set as the non-binding target for the government so that the market introduction by private companies can be achieved.

Fig. 2 Automation level of autonomous driving 2)

As mentioned above, electrification of automotive components is expanding while environmental regulations are enhanced and autonomous driving makes progress. In the past, electrification was focused on comfort and convenience, such as power windows, power door locks, power seats and power mirrors. However, electrification is now underway in various components of engine and transmission to achieve lower fuel consumption and increased safety.

Fig. 3 shows main electrification in vehicles.

In consideration of these changes surrounding automobiles, NTN has developed the "Electric motor and actuator" series. This was done by combining its core technology of bearings and ball screws, design technology of motors and electronic control technology for vehicle control, in order to contribute to achieving a secure and safe society by improving fuel efficiency and realizing autonomous driving. This article describes the details of the series.

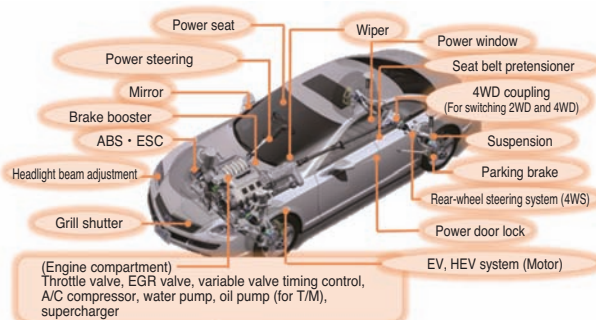


Fig. 3 Electrification of automotive

## 2. Introduction of the electric motor and actuator series

NTN is developing an actuator series to meet requirements of electrification of on-board units. The product line-up includes the following series; parallel shaft type B II Series, coaxial type B III Series and BLDC motor (brushless DC motor) SP Series. The series were designed to address various needs without limiting applications in chassis, engines, and transmission.

The following shows the configuration and features of each series:

### 2.1 B II Series

The B II Series is an electric actuator to reduce motor rotation with respect to the gear pair in the parallel axes and convert rotation to linear motion with a ball screw. This Series is designed to allow optional installation of a reverse input prevention unit. This is used for increasing driving force and keeping the position by adding a planetary reducer unit between the motor and gear pair in the parallel axes. It is also lightweight due to manufacturing the case and gear with resin.

Fig. 4 and 5 show the appearance and structure of B II Series. Fig. 6 shows variations of B II Series and Table 1 shows the typical specifications of the B II Series.



Fig. 4 Appearance of BII series

Table 1 Specification of BII series

Model number	BII 00 (DC motor driven linear motion actuator)
Weight	1.1 kg (not including harness/bracket)
Motor	Stall current 46A
Rated output	20W
Maximum output	100W
Rated thrust	400N
Maximum thrust	1,400N
Response	0.2s / 25mm
Maximum speed	192mm/s
Control method	(Stroke feedback PID position control)

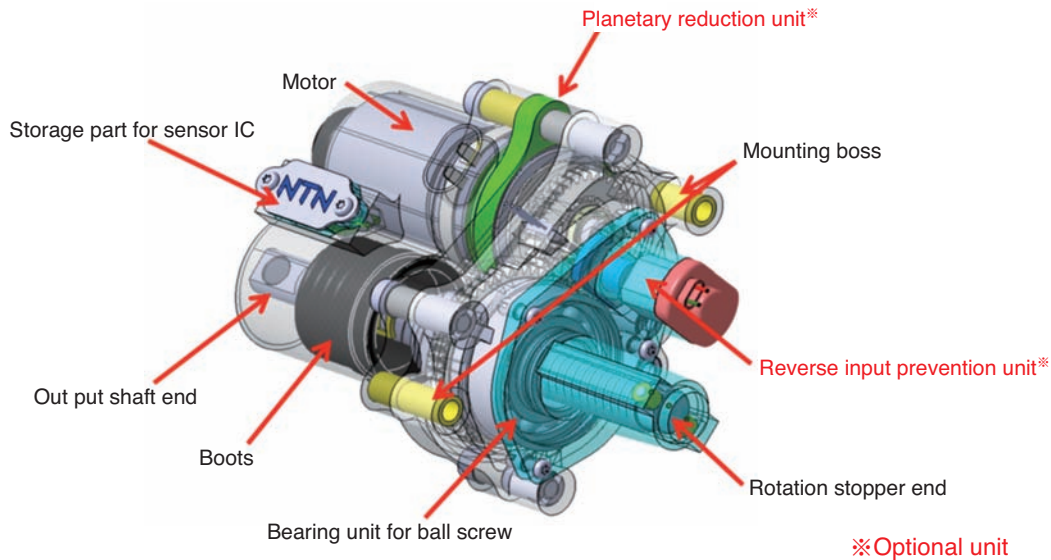


Fig. 5 Structure of BII series

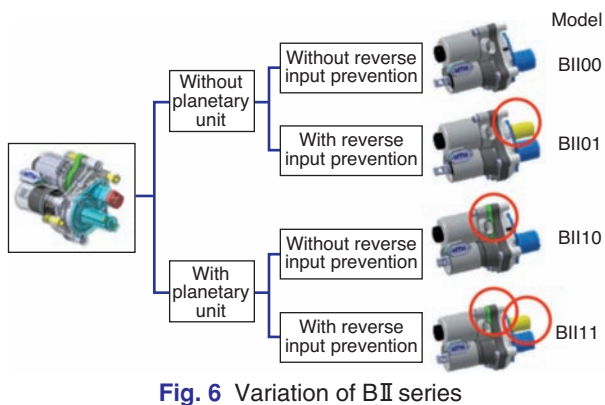


Fig. 6 Variation of BII series

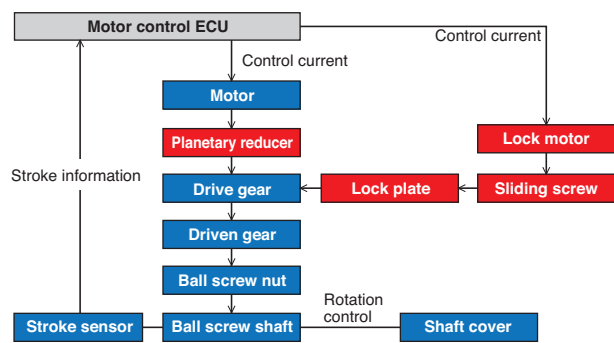


Fig. 7 Block chart of BII series

Fig. 7 shows the operational block chart of B II Series. The motor control ECU supplies control currents to drive the motor, in which torque is amplified (reduced) by the planetary reducer and transmitted from the drive gear to the driven gear. The ball screw nut fixed to the driven gear rotates which drives linear motion of the ball screw shaft, which is restricted from rotating. The travel amount is measured by the stroke sensor and transmitted to ECU.

In the reverse input prevention unit, the rotation of the locking motor is converted to linear motion with the slide screw and the rotation of the gear is regulated by the lock plate installed on the slide screw that is pocket mounted on the drive gear.

## 2.2 B III Series

B III Series is a compact electric actuator combining a high output BLDC motor with the hollow structure, which was developed by NTN, and a ball screw, by placing a linear motion mechanism in the hollow area of the motor. B III Series is best for applications where

it is directly installed in the components. Fig. 8 and 9 show the appearance and structure of B III Series.

Fig. 10 shows the operational block chart of B III Series. The motor control ECU supplies and controls the current that drives motor rotation. In cases where a planetary reducer is attached, the torque will be amplified. The rotational force is transmitted to the



Fig. 8 Appearance of BIII series

screw nut and the ball screw shaft which is restricted from rotating and provides linear motion. The travel amount is measured by the stroke sensor that is integrated in the ball screw shaft and transmitted to ECU.

B III Series is designed with standardized magnetic circuit components such as magnet stator core coil (including bobbins) to create the Series line-up. Specifically, as shown in Fig. 11, B III H, B III N and B III W have the same core diameter with the only difference being thickness. B III L is designed based on B III N with only a change in the number of magnet poles from 12 to 16. In this way, they can adapt to

various applications by changing thickness, expanding diameters or increasing poles for faster rotation or larger torque while maintaining standard components. Table 2 shows the B III Series line-up and Fig. 12 shows the performance curve of B III Series.

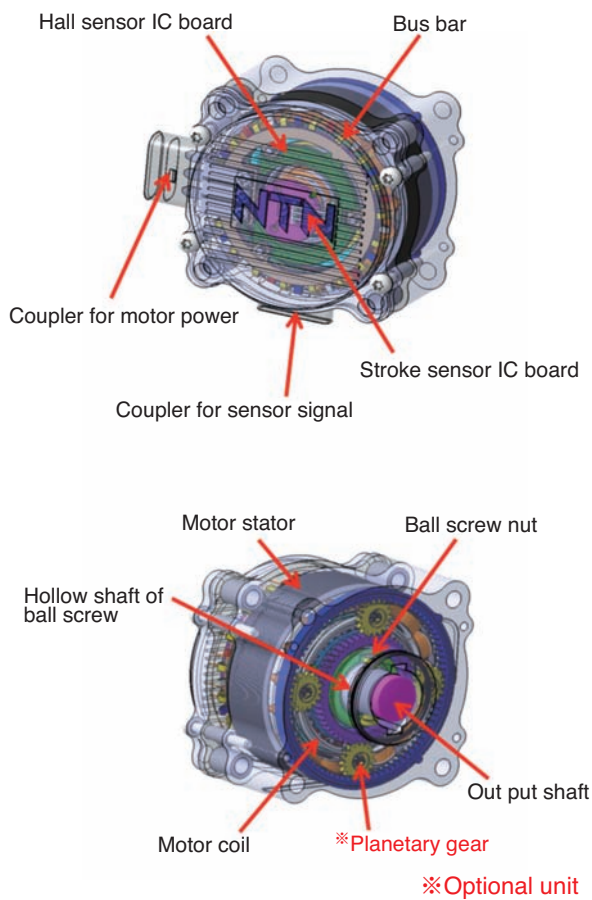


Fig. 9 Structure of B III series

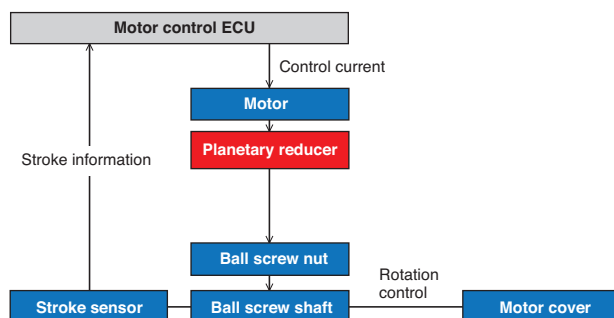


Fig. 10 Block chart of B III series

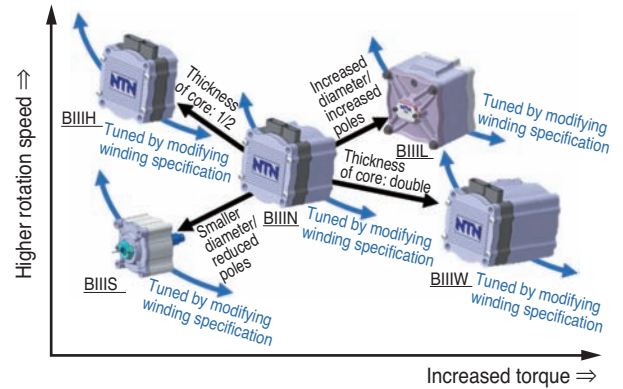


Fig. 11 Concept of B III series

Table 2 B III series line-up

Model number	Outer size (mm)	Linear motion performance			
		Maximum output (W)	Speed at maximum output (mm/s)	Thrust at maximum output (N)	All stroking (mm)
BIIIS	φ61 x 45	140	107	1,300	15
BIIISP	φ61 x 53	130	40	3,300	15
BIIIR	φ70 x 40	145	95	1,500	10
BIIIRP	φ70 x 48	140	36	3,800	10
BIIIN	φ80 x 49	155	48	3,200	10
BIIINP	φ80 x 57	135	18	7,400	10
BIIIH	φ80 x 35	155	96	1,600	10
BIIIW	φ80 x 68	75	20	3,700	30
BIIIM	φ90 x 50	150	40	3,800	10
BIIIMP	φ90 x 58	140	15	9,300	10
BIIIL	□100 x 83	110	31	3,600	40
BIIILP	φ100 x 91	110	12	9,000	40

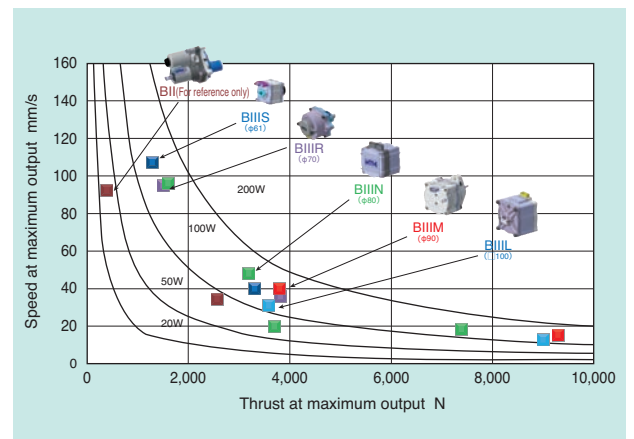


Fig. 12 Performance map of B III series

### 2.3 SP Series

SP Series is a BLDC motor series developed by NTN. It is designed based on the motor of the B III Series, with a hollow motor structure which enables incorporation of a reducer in the hollow space. As a result, it can be applied as a thin and high-torque rotation actuator. Fig. 13 shows the appearance and Fig. 14 shows the performance map of SP Series.



Fig. 13 Appearance of SP motor series

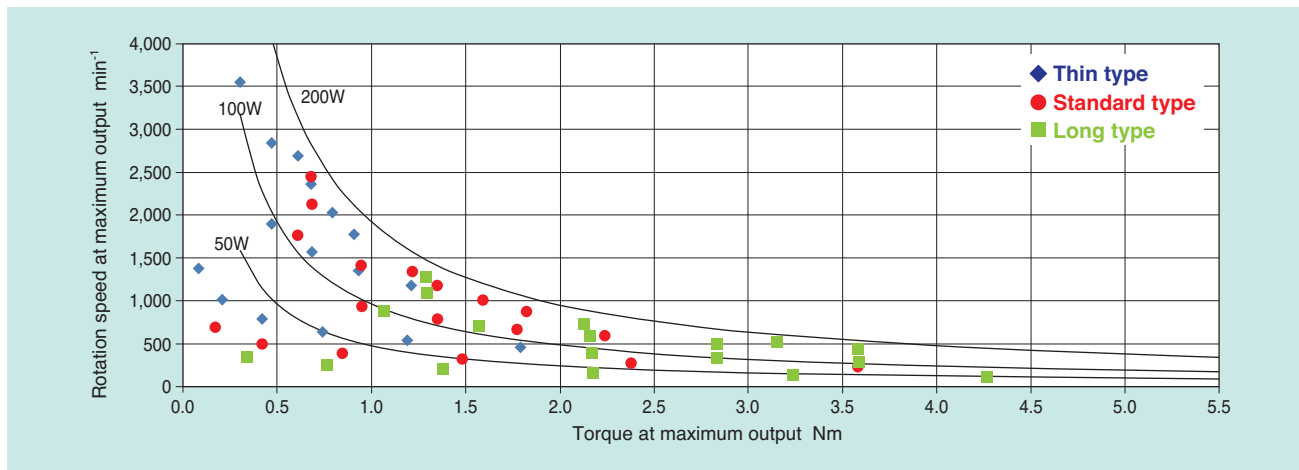


Fig. 14 Performance map of SP motor series

### 3. Performance cases of electric actuator

The following is an evaluation of B III motor performance as a representative case of electric actuator performance.

The motor to be applied to B III actuator has undergone magnetic circuit simulation using magnetic analysis software during the design phase to obtain the optimal shape. Table 3 shows the specifications of the B III motor as a result of simulation.

Verification of motor performance to see if it is the same as the analysis result through individual tests using a prototype revealed that, the target performance was achieved. The motor and the prototype performed at generally matching torques at 40Arms with slightly different rotation speed. Fig. 15 shows an example of simulation with magnetic field analysis software (magnetic flux density vector map) Fig. 16 shows the individual motor measurement results.

Table 3 Specification of motor

Model	BIIN
Number of poles	12
Number of slots	18
Connection method	Star connection
Phase current peak	40Arms
Maximum output*	209 W
Maximum torque*	2.41Nm
Base rotation speed*	740min <sup>-1</sup>
Maximum rotation speed*	2,170min <sup>-1</sup>

\*Normal temperature performance (25°C)

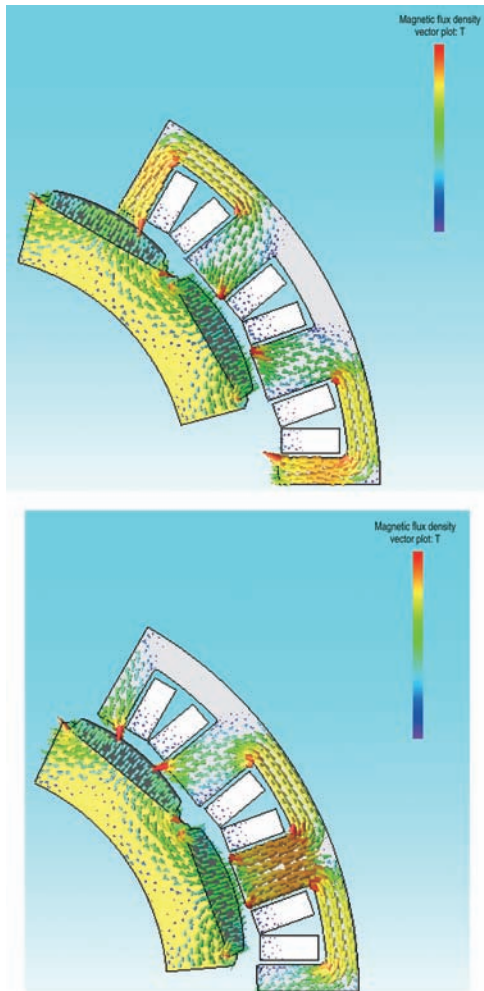


Fig. 15 Vector map of magnetic flux density

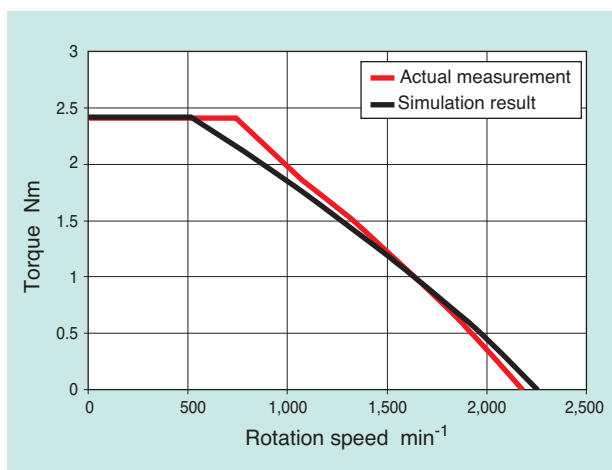


Fig. 16 Torque characteristics of BIII motor (sin-cos sensor control)

## 4. Possible applications of electric actuators

The following describes possible applications for NTN's electric actuator.

### 4.1 Transmission/electric shift selector

With AT and CVT, the shift lever is connected to the transmission with linkage for shift selection. This shift selection can be electrified by applying a B II actuator to this part. When shift selection is electrified the degree of freedom for placing the shift lever is increased, enabling replacement of the shift lever with buttons and dials. This also amplifies the degree of freedom for design and layout around the driver's seat. It can also be used as an actuator for clutch shifting for DCT (Dual Clutch Transmission), which is recently expanding in Europe.

Fig. 17 shows an example of a B II actuator applied to the transmission (CVT).

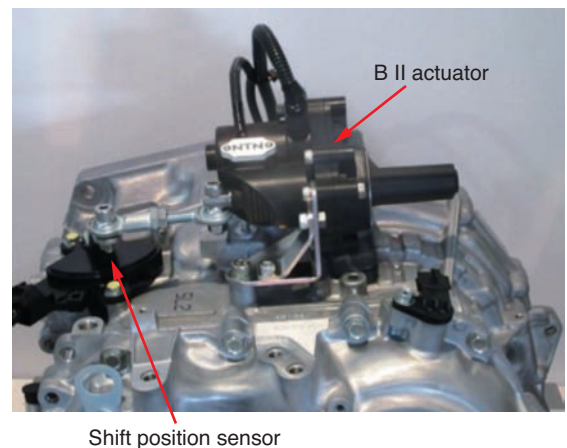
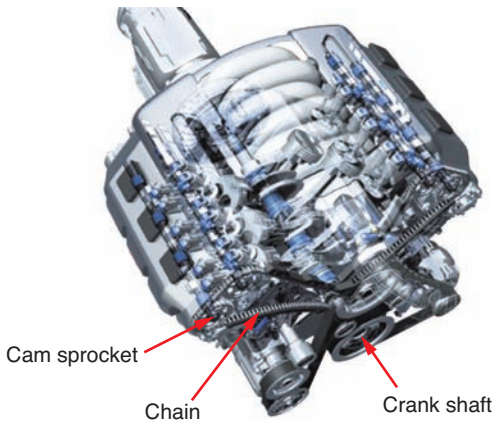


Fig. 17 Shift actuator

※The above picture is shown only as an example of application. It does not indicate that it is provided to any specific auto manufacturer at the present time.

### 4.2 Electric variable valve timing unit

With OHC engines intake/exhaust valves are operated by a rotating cam shaft, which is driven by a cam sprocket installed at the end of the cam shaft, which is driven by crank shaft rotation via a chain (Fig. 18). The variable valve timing control mechanism controls the timing for operating intake/exhaust valves by changing phases of these sprocket and cam shafts. This improves fuel efficiency with high expansion ratio cycle accomplished by improvement of intake efficiency by optimizing the intake/exhaust valve overlapping amount (Fig. 19) and late closure of the intake valve, etc.



**Fig. 18** Camshaft driven structure of OHC engine

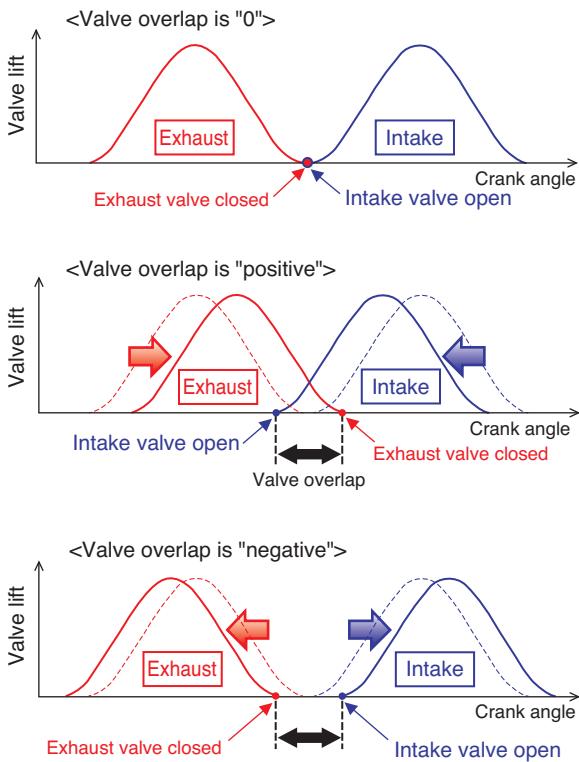


**Fig. 19** Valve overlap<sup>3)</sup>

Currently, this is done by installing a vane in the sprocket and changing the angle of the vane hydraulically to change the cam shaft phase attached to the vane. However, the hydraulic system may not provide sufficiently good operation when cold starting due to high oil viscosity. Therefore, adoption of electric variable valve timing mechanisms is expanding, which control cam shaft phase by motor rotation. The motor and reducer are inserted between the sprocket and cam shaft to improve cold starting. Electrification with motor driven mechanisms allows driving with efficient valve timing that is not affected by the operating temperature and allows the necessary operating angle and operating speed can be obtained.

By placing a reducer in the hollow space of the hollow motor of NTN's B III Series, the electric variable valve timing mechanism can be made thinner, contributing to smaller engine sizes (**Fig. 20**).

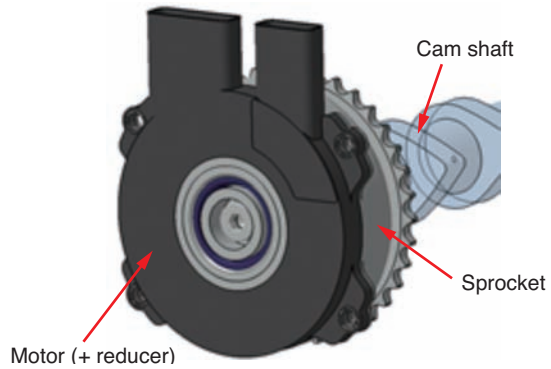


**Fig. 20** Electric variable valve timing unit

### 4.3 Electric oil pump

In general, AV and CVT use multiple wet disk clutches which are hydraulically engaged/disengaged to change gears. An oil pump is also used for operating multiple disk clutches. Conventionally, oil pumps were mainly operated by engine rotation. However, the use of electric oil pumps, which operate without any impact from engine status, is increasing due to introduction of auto start/stop mechanisms. This is required because hydraulically operated oil pumps stop when engine stops. The use of electric oil pumps increases fuel efficiency because they lower load to the engine because engine does not have to operate the oil pump.

When NTN's SP Series higher efficiency motor is applied to this area electric oil pumps can be made smaller (**Fig. 21**).

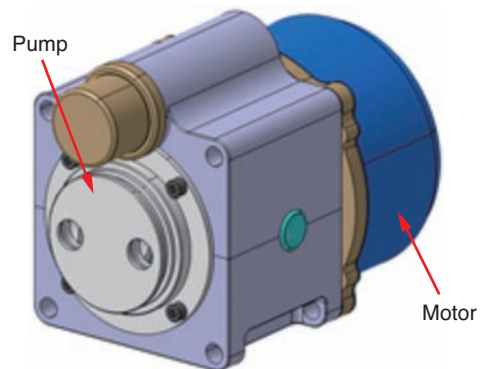


**Fig. 21** Electric oil pump

#### 4.4 Electric hydraulic brake

Currently the brake pedal force of service brake assist is supplied with a booster device that leverages negative pressure produced with engine intake. However, since EVs, where no engine exists, and PHEVs and HVs, where engines do not run all the time, cannot leverage engine negative pressure, electric motors and linear motion mechanisms are used to operate brake hydraulic cylinders for braking.

The use of a B III Series actuator, which incorporates a ball screw into NTN's hollow motor, contributes to the compact size of the electric hydraulic brake system (Fig. 22).

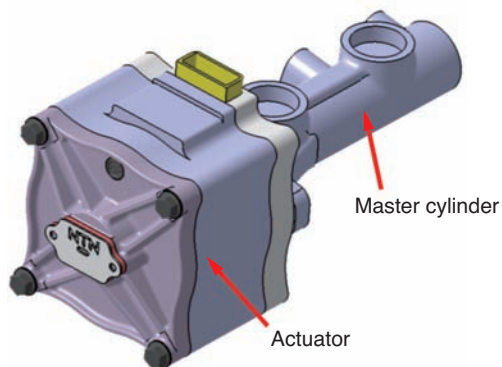


Fig. 22 Electric hydraulic brake unit

## 5. Conclusion

NTN is engaged in the development of various electric actuators and strives to contribute to the development of automobiles and a secure and safe society by "smoothly" connecting and moving every part in vehicles.

### References

- 1) Nikkei Business Publications, Inc., "Environment and Safety toward 2030", Nikkei Automotive, Issue No. 43, March, 2016.
- 2) Cabinet Office SIP Autonomous Driving System R&D Plan (2017)
- 3) Nikkei Business Publications, Inc., "Mechanism basics briefing 1: Variable valve timing mechanism" Nikkei Automotive Technology, Issue No. 105, July, 2014.

#### Photo of authors

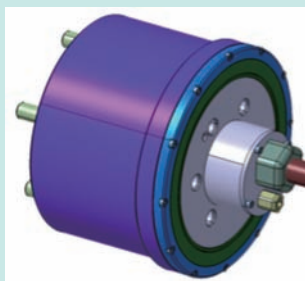


Kimihito USHIDA  
Business Promotion Dept.,  
Motorized Module Product  
Headquarters



Masashi NISHIMURA  
Business Promotion Dept.,  
Motorized Module Product  
Headquarters

# Hub Module with Motor and Generator Function



Kentaro NISHIKAWA\*  
Yasuyuki FUJITA\*

Yuuji YADA\*  
Mitsuo KAWAMURA\*  
Hiroki YABUTA\*

As the regulation on fuel consumption and CO<sub>2</sub> emissions being strengthened, practical application of 48 V mild hybrid systems is expanding mainly in Europe. The NTN is developing a HUB module that combines a Hub bearing and a Motor Generator in order to contribute to further fuel economy improvement in combination with the existing 48 V system.

## 1. Introduction

Reduction of greenhouse gas emissions, mainly CO<sub>2</sub>, as one of the causes of global warming, is a global challenge. In the automotive industry, regulation of CO<sub>2</sub> emissions from automobiles is becoming tougher every year. Europe, in particular, is enhancing regulations such that every auto manufacturer has to keep average CO<sub>2</sub> emissions to 95g/km or less in 2021 and 75 g/km or less in 2025. Fig. 1 shows the trend of fuel efficiency regulations in various countries. These regulations cannot be met with conventional methods such as optimization of internal combustion engines (ICE) and reduction of vehicle weight. Therefore, auto manufacturers are working on development and expansion of next generation vehicles such as hybrid electric vehicles (HEVs), battery-based electric vehicles (BEVs) and fuel cell vehicles (FCVs).

It is considered that the future vehicles will be mainly PHEVs, BEVs and FCVs; however, they have their own challenges such as cost, large battery capacity, stability of power supply in some regions and building infrastructure. Therefore, 48V Mild HEV (48V MHEV) is gaining attention in Europe as a means to meet rapidly approaching regulations. In Japan, strong HEV is the mainstream technology, which is driven by voltage higher than 48V, and there is little trend toward the introduction of MHEV; however, Europe, which has been working on improvement of fuel efficiency by increasing efficiency of ICE, is making progress in development of MHEV as a HEV system

that can be easily incorporated into existing vehicles. There is a forecast that the market share of 48V MHEV will reach 1.5 million or more, equivalent to PHEV by 2025<sup>3)</sup>.

NTN is developing eHUB which is the HUB module with motor and generator for 48V MHEV, based on our hub bearings (HUB), which has the leading global share, applying our technology gained from development of in-wheel motors (IWM)<sup>4)</sup> and electric module products<sup>5)</sup>. In this paper, the product concept, target specification and development status of eHUB is introduced.

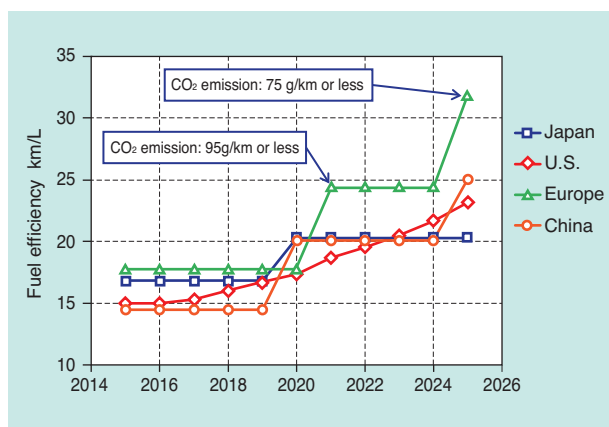


Fig. 1 Fuel consumption targets of each country (Conversion from CO<sub>2</sub> emission targets)<sup>1), 2)</sup>

\*New Product Development R&D Center

## 2. 48V MHEV and vehicle function

### 2.1 48V MHEV

So far, various types of electric vehicles, from 12V MHEVs to BEVs, have been introduced. Electric vehicles are adopting higher voltage, as higher motor output and larger power capacity increases the CO<sub>2</sub> emission reduction effect; however, it also brings higher costs for safety measures and manufacturing process. The characteristics of 48V MHEVs lie midway between strong HEVs and 12V MHEVs, allowing simple measure of safety standards by using a power supply of DC 60V or less.

### 2.2 Position of motor installation and vehicle function

Position of motor/generator (M/G) installation in HEVs can be categorized into P0, P1, P2, P3 and P4 as shown in Fig. 2. In addition, the so-called IWM configuration, which places M/G around the wheels is tentatively defined as P5 in this article.

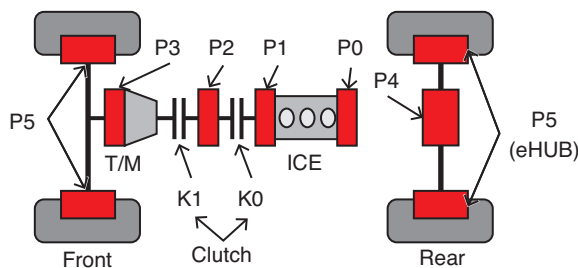


Fig. 2 Mounting position of hybrid system

Their characteristics are shown in Table 1. The functions which can be achieved are different depending on the installation positions. P0, P1 and P2 which can be directly connected to ICE do not require a starter motor that allows auto start/stop functionality. P2 and P3 which can be isolated from ICE by the clutch K0 and P4 and P5 which operate drive shafts can regenerate significant energy in deceleration, in

Table 1 Vehicle characteristics for each mounting position of hybrid system

Item	P0	P1	P2	P3	P4	P5
Regenerative charging	○	○	○	○	○	○
Auto start/stop	○	○	○	×	×	×
Starting torque assistance	○	○	○	○	○	○
Accelerating torque assistance	○	○	○	○	○	○
EV starting + creeping	×	×	○	○	○	○
EV coasting	×	×	○	○	○	○
All wheel drive	×	×	×	×	○	○
Torque vectoring	×	×	×	×	○	○

addition to possibility of EV driving by installing higher power output. Furthermore, P4 and P5 can realize all-wheel driving and torque vectoring since they can drive the vehicle independent from ICE. P5 can further drive left and right wheels independently, allowing finer vehicle control. By combining these functions, even higher functionality can be accomplished. For example, by combining P2 and P3 with P4 and P5, the driving range of EV mode or all-wheel driving in EV mode can be realized.

Different installation position significantly affects not only the functions, but also installation cost and space. P0, which can replace existing alternators, can be installed with little change in the surrounding structure, thus requires low implementation costs. P1, P2 and P3 require increased costs as surrounding components of ICE and transmission (T/M) must be significantly changed. P4 results in smaller cargo space. On the other hand, since P5 places M/G within wheels, there is no space limitation.

## 3. Product concept

### 3.1. Structure

The developed product eHUB integrates stator of M/G into HUB outer ring to rotate the hub ring and M/G rotor as one unit with the rotation sensor inside M/G. It is installed at the P5 position of B and C segment vehicles providing driving assistance to ICE, which is the main driving source, and regenerative braking for deceleration. It has achieved small form factor by limiting output power.

As shown in Fig. 3, it can be installed inside the brake disk and between the brake disk and body. This architecture allows for installation similar to conventional HUB, without requiring major design change.

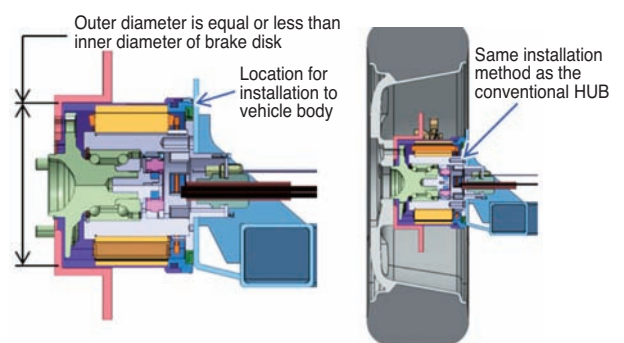


Fig. 3 Mounting position of HUB module

### 3.2 Function

eHUB is installed on the driven wheels independent from the main drive source which allows individual driving/regenerating; therefore, drive assistance and regenerative braking can be controlled depending on the driving conditions. While driving, the driven wheels generate assisting driving force to reduce energy consumption of the main drive source. While braking, the regenerative brake turns the braking energy that is released with conventional brakes as heat, into reusable electric energy.

Fig. 4 shows the eHUB module configuration. eHUB system consists of HUB module which integrates HUB and M/G into a unit, on the left and right wheels, and motor controller which operates M/G.

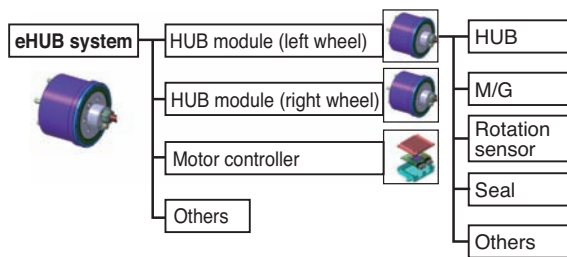


Fig. 4 eHUB system component

### 3.3 Target specification

eHUB assumes installation on the rear wheels, which are the driven wheels of 48V MHEV, based on the front wheel drive vehicle. An example of a vehicle system with eHUB installed is shown in Fig. 5.

M/G is integrated in the P0 position of Fig. 5 (a). The excess energy from regenerative brake by M/G installed on P0 is used by eHUB to contribute to the fuel efficiency.

In another example of P0 + P2 combination depicted in Fig. 5 (b), further high functionality can be achieved such as improvement of vehicle maneuverability in addition to fuel efficiency, such as electric only all-wheel driving while isolating the engine and deceleration with regenerative braking only.

Table 2 shows the target values of vehicle system functions for the combination of the existing 48V MHEV system vehicles and eHUB. The largest target for development was set at reduction of CO<sub>2</sub> emissions and improvement effects of fuel efficiency. eHUB drives at maximum torque for acceleration assistance and EV start + creep and at rated torque for engine off-coasting. Table 3 shows eHUB target specification to realize these functional improvements. The effect of improvements in functionality by eHUB changes depend on the vehicle style and performance.

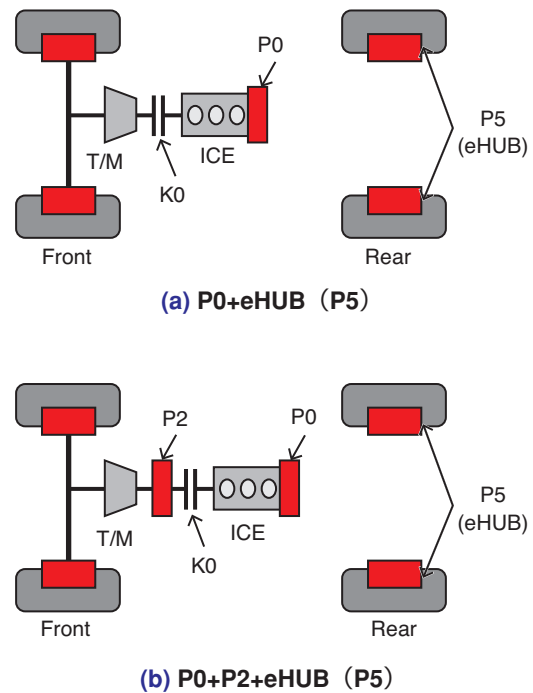


Fig. 5 Examples of eHUB system configuration

Table 2 Target values of existing 48V MHEV system with eHUB

Vehicle system functions	System target values
Reduction ratio of CO <sub>2</sub> emission	25%
Fuel efficiency improvement ratio	25%
Braking method	4-wheel regenerative braking (non-hydraulic)
EV starting + creeping	Continuous for 10s or more
Engine off-coasting	Operated in 50 - 130km/h
Traction control (TCS)	Start assist
	Acceleration assist
	Attitude control

Table 3 Target specification of eHUB (per 1 wheel)

Item	Unit	Values
Maximum output	kW	10
Maximum operation frequency	min <sup>-1</sup>	2,600
Maximum torque	Nm	60
Rated torque	Nm	20
Outer Diameter	mm	φ160 or less

## 4. Development status

### 4.1 HUB module

**Fig. 6** shows the structure of the prototype HUB module and **Table 4** shows the specifications. It was designed with the maximum torque of 60Nm, rated torque of 20Nm as a target and containing the outer most diameter of the HUB module to be within the brake disk. Since it offsets approx. 50mm toward the axial direction compared with the existing HUB, some modifications to the body will be required. Upcoming challenges include lightweight and compactness by higher torque density and optimal design of HUB module. The prototype aims for maximum output of 10kW. This was set to enable maximum rotational speed required for achieving the maximum driving speed of the existing vehicle. The current prototype has a maximum output of 5kW; however, output of 10kW is achievable by changing internal specifications of the motor.

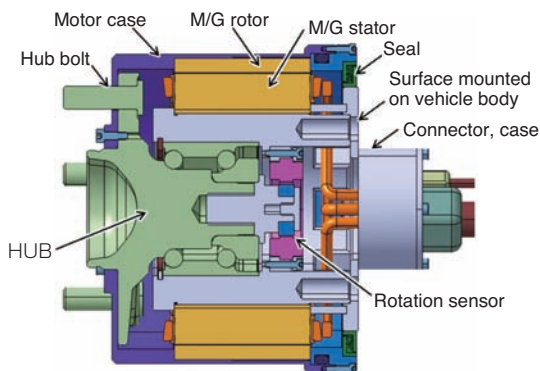


**Fig. 6** HUB module

**Table 4** Prototype specification

Item	Unit	Values	
Maximum output	kW	10	5
Maximum operation frequency	min <sup>-1</sup>	2,600	1,200
Maximum torque	Nm	60	60
Rated torque	Nm	20	25
Outer Diameter	mm	φ159	
Width	mm	115	
Weight	kg	13	

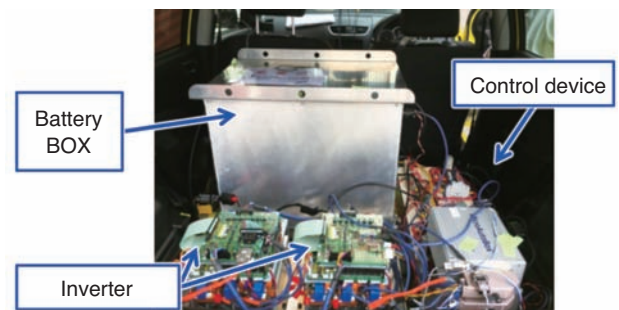
### 4.2 Test vehicle

A test vehicle was created by installing eHUB on a front-wheel drive vehicle in segment B. **Fig. 7** shows the installation in the test vehicle. **Fig. 7 (a)** shows installation of the HUB module on the vehicle. As mentioned earlier, it offsets on the axial direction compared to the existing HUB, and the installation part of the body and the brake disk are modified. **Fig. 7 (b)** shows the control system and battery installed in the vehicle compartment. The control system and battery are installed in the rear seat and cargo space of the vehicle. The control unit, Micro Auto Box II (made by dSPACE) was adopted for the motor controller, hybrid controller and instrumentation system. For batteries and inverters, commercially available units were adopted. No dedicated electronic control unit (ECU) was made, but rather a general-purpose unit was used to create an environment of RCP (Rapid Prototype Control) to prioritize the evaluation of HUB module.

In addition, in the test vehicle, no modifications were made to ECU; therefore, ICE and eHUB are independently controlled.



**(a)** Setting of HUB module



**(b)** Control system and battery set in the test vehicle

**Fig. 7** Setting eHUB in the test vehicle

### 4.3 Vehicle evaluation

Table 5 shows the vehicle evaluation items. The impact on vehicle maneuverability is also evaluated, in addition to the impact of fuel efficiency. The following shows results of impact on fuel efficiency and traction control among the evaluation items:

Table 5 Evaluation point of vehicle test

Test item	Alternative characteristics test
Fuel efficiency improvement effect	Fuel efficiency at constant speed driving
	Fuel economy mode driving
	EV starting + creeping
Acceleration assist	Passing acceleration
Traction control [Start assist]	Stop→start
	Low friction road start
Yaw traction control [Vehicle attitude stability]	Low friction road straight running (corrective steering)
	Steady state circular turning
	Low friction road turning
Direct yaw control [Turning (steering ability)]	Slalom
	Double lane change

#### 4.3.1 Fuel efficiency improvement effect

For the mode running fuel consumption test, WLTC (Worldwide harmonized Lightduty Test Cycle) mode was adopted. In WLTC mode, as shown in Fig. 8, fuel efficiency is measured in 4 segments, namely, Low (urban area), Middle (suburban area), High (Expressway) and Ex-High (extra high speed). In Japan, since extra high-speed driving is not frequent, 3 segments, namely, low, middle and high are evaluated and in Europe, all segments, including Ex-High, are evaluated for fuel efficiency. The standard method for WLTC mode testing is "cold start" in which test starts with the vehicle engine in cold state; however, in order to evaluate efficiency under many conditions, we have used "hot start" with a warmed-up engine.

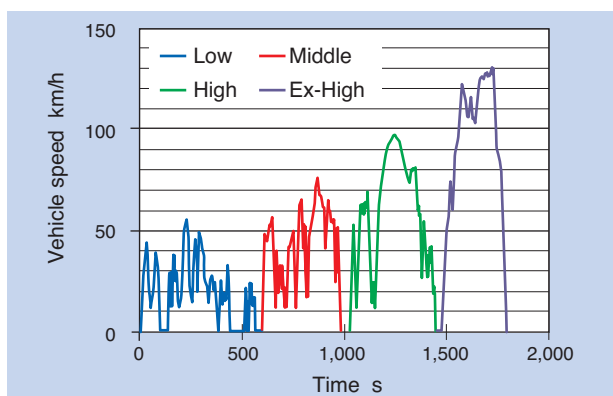


Fig. 8 Driving test result on WLTC mode

Excluding vehicles with external charging capability such as PHEVs and BEVs, the variation of battery state of charge (SOC) before and after the fuel efficiency test must be as close as possible to zero. In this test, we have explored conditions to make higher improvements in fuel efficiency and low SOC variation by changing the control method for driving eHUB and regenerative timing.

The relation between fuel efficiency improvement and SOC variation when the control conditions of eHUB were changed is shown in Fig. 9. As SOC variation becomes negative, fuel efficiency tends to further improve. Fig. 10 shows an enlarged view of ±1% range in SOC variation. Fig. 11 shows changes in fuel consumption and SOC under the condition that improvement on fuel efficiency is high and change of SOC is the lowest (condition A in Fig. 10) and Table 6 shows fuel efficiency of each segment and fuel efficiency with or without the Ex-High segment. Overall fuel efficiency was improved by 3% regardless of the Ex-High segment.

From the above, further improvement of fuel efficiency can be expected by optimizing energy management, reducing weight and increasing efficiency of eHUB.

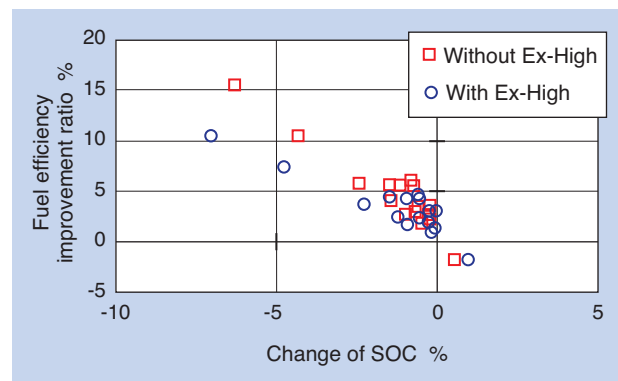


Fig. 9 Driving test result on WLTC mode

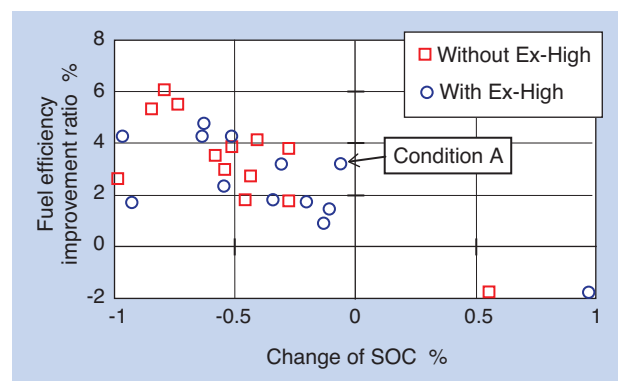


Fig. 10 Driving test result on WLTC mode (Enlarged view)

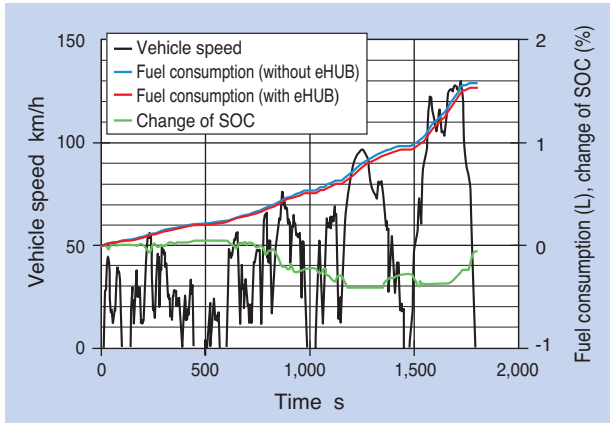


Fig. 11 Driving test result on WLTC mode (condition A)

Table 6 Section and fuel efficiency (condition A)

		Fuel efficiency improvement ratio (%)	Change of SOC (%)
Each segment	Low	3.40	0.05
	Middle	4.74	-0.27
	High	3.40	-0.06
	Ex-Hi	2.30	0.22
Without Ex-High		3.81	-0.28
With Ex-High		3.22	-0.06

In order to reduce fuel consumption, EV mode driving is effective under creep conditions such as traffic jams and parking. Assuming a system of P0 + eHUB under Section 3.3, we verified possibility of starting and driving under 10 km/h with eHUB only. We have confirmed that driving with eHUB only was possible for approx. 180 seconds by starting in EV mode on a flat ordinary road with asphalt, even if the required driving torque changes depend on the vehicle weight, road surface conditions, wind and slope.

### 4.3.2 Traction control

In order to confirm its contribution to vehicle stability, we verified straight-running ability on the road with different friction coefficients for left and right tires at the road contact area. As shown in Fig. 12, the straight-running test was conducted with a locked steering angle on the road surface with a low friction coefficient on the right side, measuring the deviation from the target running line as the yaw angle. The test was conducted under three running conditions as shown in Table 7. Fig. 13 shows the test results. We could confirm that, by driving eHUB with stability control, vehicle deviation from the straight line was reduced, improving straight line running.

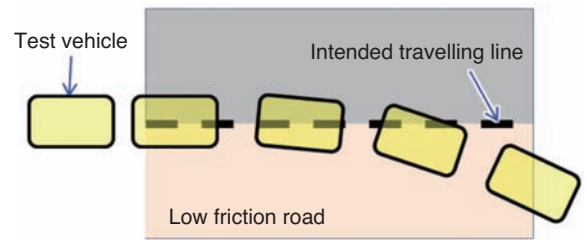


Fig. 12 Driving method of low friction road

Table 7 The condition of low friction road

Yaw angle control	Left wheel	Right wheel
Stability control	Braking	Driving
No control	—	—
Unstability control	Driving	Braking

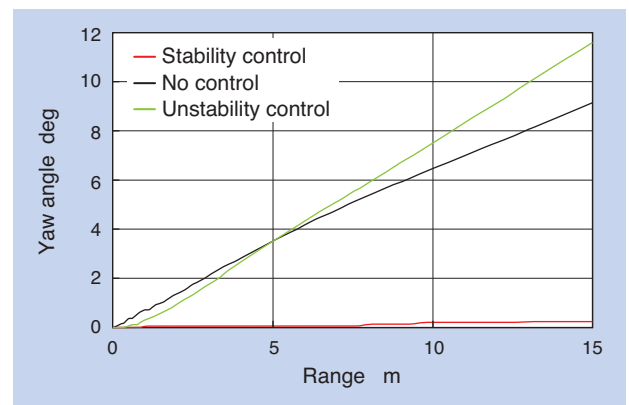


Fig. 13 Test result on low friction road

## 5. Conclusion

In this paper, development status of HUB module with motor/generator functions was introduced, which can improve fuel efficiency and driving performance of vehicles with 48V MHEV system, and with minor changes to the vehicles. We tested the prototype eHUB system on a test vehicle and obtained the following results:

- In WLTC mode, eHUB assistance is effective for reducing fuel consumption
- EV starting + creeping can be maintained for over 180 seconds
- Straight line running ability is improved on low friction roads

We will not only continue to improve eHUB, but also study the effect of fuel efficiency improvement when combined with the existing 48V MHEV and energy management for commercialization.

## References

- 1) Complete analysis of HEV and EV related markets, 2017, Fuji Keizai, 30, 37.
- 2) Fourin Monthly Report on Global Automotive Technology Research No. 34 (2), (2017), FOURIN, Inc.
- 3) Complete analysis of HEV and EV related markets, 2017, Fuji Keizai, 5.
- 4) NTN TECHNICAL REVIEW No 79, (2011) 22-28.
- 5) NTN home page  
[http://www.ntn.co.jp/japan/news/new\\_products/news201600042.html](http://www.ntn.co.jp/japan/news/new_products/news201600042.html)

## Photo of authors

---



**Kentaro NISHIKAWA**  
New Product Development  
R&D Center



**Yuuji YADA**  
New Product Development  
R&D Center



**Yasuyuki FUJITA**  
New Product Development  
R&D Center



**Mitsuo KAWAMURA**  
New Product Development  
R&D Center



**Hiroki YABUTA**  
New Product Development  
R&D Center

# Influence of Vehicle Body Motion on the Effects of G-Vectoring Control



Yuta SUZUKI\*  
Weipeng CHENG\*  
Shuichi KOSAKA\*\*

G-Vectoring control (GVC) which controls longitudinal acceleration in coordination with lateral motion has been installed in an experimental vehicle that can adjust the anti-dive mechanism. Only the pitch motion characteristics of the vehicle body were changed during lane changes, and the vehicle planar motion characteristics itself are kept unchanged. Drivers' steering model parameters during lane change for

the vehicle with/without GVC are identified. Then, the handling quality evaluations by the drivers are compared and analyzed by using the driver parameters identified and the influence of the vehicle body motion on GVC effect is investigated. It is found as a result of the study that the nose-dive pitch motion caused by the control is important for GVC to be effective in improving the vehicle handling quality.

Note) "G-Vectoring" is a registered mark of Hitachi Automotive Systems, Ltd.

## 1. Introduction

Recently electric vehicles have been gaining in popularity. Due to this increase in popularity there is a focus on accurate and responsive motor-driven controls, which can lead to higher energy efficiency than gasoline engines, which can lead to an elimination of emission gases. Among other items, in-wheel motors are able to further improve the accuracy and responsiveness of independent driving and braking control. This is due to the fact that the in-wheel motor sends the driving and braking control directly to the wheels.

In this paper, steering characteristics that a driver feels are objectively and quantitatively evaluated by comparing the cases when GVC is applied and not applied. What GVC is, is when longitudinal acceleration in connection with lateral motion of full-drive-by-wire vehicles that have in-wheel motors installed on all four wheels is applied<sup>1)</sup>. The test vehicle can only change its pitch motion by changing its suspension geometry and without changing its roll rigidity. That is, even when the vehicle motion on a plane surface is the same, the vehicle attitude in a 3D view can be changed. Leveraging this characteristic, the steering characteristics that a driver feels were

objectively and quantitatively evaluated in cases when dynamic coupling of roll motion and pitch motion may have occurred or not<sup>2), 3)</sup>. This dynamic coupling when both a roll motion and pitch motion occur is a diagonal motion; hereafter known as diagonal roll

The above is the result of joint research with the Kanagawa Institute of Technology.

## 2. G-Vectoring Control

In this chapter, GVC is outlined. In the research thus far, Emeritus Professor Abe, Professor Yamakado etc. of Kanagawa Institute of Technology have proposed the formula shown in (1) as the basic control guideline for coupling longitudinal motion depending on lateral motion. This is known as "G-Vectoring Control (GVC)", meaning integrated control of longitudinal and lateral *G* vectors.

$$G_{XC} = -\text{sgn}(G_y \cdot \dot{G}_x) \frac{C_{xy}}{1+T_s} |\dot{G}_y| \dots\dots\dots (1)$$

Where,  $G_{XC}$  is the acceleration command for longitudinal acceleration of the vehicle,  $C_{xy}$  is the control gain,  $G_y$  is lateral acceleration of the vehicle and  $\dot{G}_y$  is the lateral jerk information which is the first-order derivative of vehicle lateral acceleration. This

\*Engineering Dept. Natural Energy Products Division

\*\*Advanced Technology R&D Center

control algorithm was derived from careful observation of driving maneuvers by expert drivers performing J turns. As you can see from the formula, it is a very simple algorithm, just multiplying the gain  $C_{xy}$  to the absolute value of lateral jerk information  $y$ .

As shown in Fig.1, GVC accelerates/decelerates according to vehicle lateral jerk information to smoothly change the direction of combined acceleration  $G$ . In this research, GVC of "only deceleration" at the bottom of Fig.1 was set as an evaluation object, while "no control (no GVC)" was also evaluated for comparison.

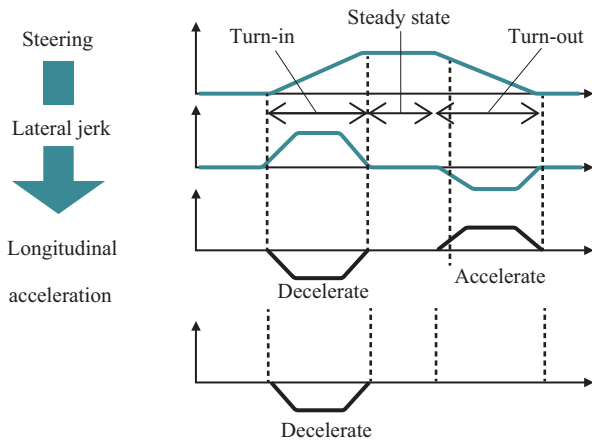


Fig. 1 Schematic concept of GVC algorithm

### 3. Test vehicle

#### 3.1 Vehicle parameters

The following is the description of the test vehicle. The test vehicle shown in Fig. 2 has in-wheel motors in all of its wheels and a steer-by-wire unit for the front and rear; therefore, it provides 4-wheel independent drive and 4-wheel independent steering.

This vehicle is equipped with 2 GNSS sensors on the roof and a gyro sensor under the seat so that it can sense highly accurate positional information and angular velocity to complement each other.

The steering angle is detected by a magnetic encoder installed on the steering wheel. The inverter installed at the front and rear of the vehicle provides power to the motors in the wheels to generate torque and detect rotational speed of the motors. Table 1 shows vehicle parameters.



Fig. 2 Experimental vehicle

Table 1 Vehicle parameters

Name	Symbol	Values
Weight	m	709 [kg]
Wheel base	l	2.05 [m]
Distance from the front wheel to center of gravity	l <sub>f</sub>	1.012 [m]
Distance from the rear wheel to center of gravity	l <sub>r</sub>	1.038 [m]
Front wheel tread	d <sub>f</sub>	1.415 [m]
Rear wheel tread	d <sub>r</sub>	1.415 [m]
Height of center of gravity	h <sub>s</sub>	0.417 [m]
Yaw inertia moment	h <sub>s</sub>	512 [kg·m <sup>2</sup> ]

#### 3.2 Change of suspension geometry adjustment

The test vehicle can change anti-dive/anti-squat force by adjusting suspension geometry. When a vehicle with double-wishbone suspension is viewed from the side (Fig. 3), the intersection of the virtual lines coming from the upper and lower arms will be the "suspension rotation center." The angle between the line connecting this suspension rotation center and the center of the ground contact of the tire with the ground is called the "anti-dive angle (anti-squat angle)" in this report. When the same driving/braking force is given, the larger this angle, the larger the "anti-lift force" which presses the vehicle down or the "anti-squat force" which lifts the vehicle up."

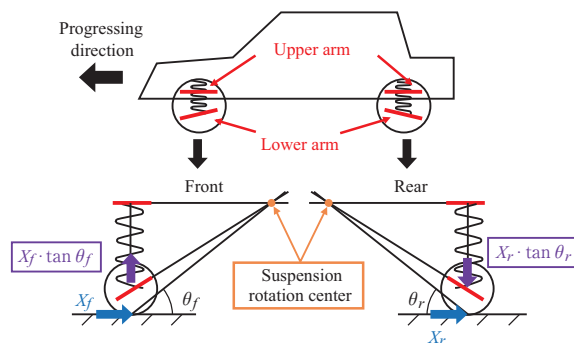


Fig. 3 Anti-dive/anti-squat geometry

The test vehicle shown in Fig. 2 can change the anti-dive angle from 0° to 30° in multiple stages. In this test, braking force is applied to 4 wheels with GVC; therefore, if the anti-dive angle is set larger than 0 degrees, "anti-squat force" is applied to the front wheels and "anti-lift force" is applied to the rear wheels which reduces the pitch motion.

In this paper, the steering characteristics that the drivers feel and the impact of GVC on the vehicle behavior were evaluated, by comparing the case without the reduction of pitch motion by setting the anti-dive angle to 0°, and with the reduction of pitch motion by setting the anti-dive angle to 30°.

### 4. Evaluation method of steering characteristics

#### 4.1. Test course

A single-lane change test was conducted to evaluate driver steering characteristics. The test was conducted in a commonly used single lane change course depicted in Fig. 4. The drivers enter the course at 40 km/h and changed lanes while maintaining a constant speed. The direction of lane change is determined at random immediately before the lane change segment and indicated by turning on the LED installed on the both sides of the windshield.

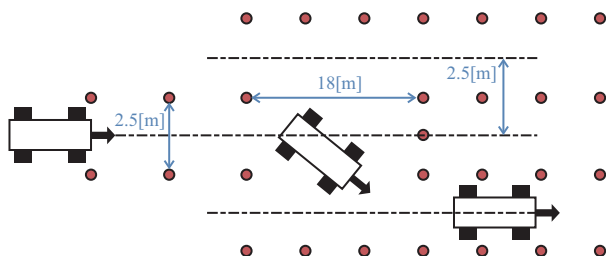


Fig. 4 Single lane-change course

#### 4.2 Evaluation of steering characteristics using a driver model

Subjective evaluation by ordinary drivers tends to be less reliable compared to expert drivers such as test drivers. Therefore, objective and quantitative evaluation of steering characteristics was conducted by using a simple driver model and identifying driver parameters.

The drivers adapt to the change of the vehicles steering characteristics by maneuvering the steering wheel to accomplish predetermined tasks. Therefore, the driver parameters are considered to directly reflect the change of steering characteristics. It should be possible to conduct a quantitative evaluation of (with

or without) GVC by identifying driver parameters from driver behavior (steering wheel maneuvering) and vehicle motion (lateral motion).

Expressing the relation between the steering angle and lateral motion during a single lane change at a constant speed as a transfer function, we obtain equation (2).

$$\frac{\delta}{y_{L0} - (1 + \tau_h s)y} = \frac{h}{1 + \tau_L s} \dots\dots\dots (2)$$

Where,  $\delta$  is the steering angle,  $y$  is the lateral motion and  $y_{L0}$  is the target lateral motion. In addition,  $\tau_L$  is an overall human delay (from the steering command by LED to the time the driver actually starts steering),  $\tau_h$  is the time to focus on the forward view (from the beginning to the end of lane change),  $h$  is the steering gain (relative gain proportional to the magnitude of steering angle), and these three driver parameters were identified.

Describing the details of each parameter,  $h$  and  $\tau_L$  represent driver gain and responsiveness. For example, when the steady gain of vehicle becomes smaller, the driver increases gain  $h$  to create a balance. It can be considered that the driver is controlling the vehicle with confidence when the driver increases  $\tau_L$ . The derivative control action time  $\tau_h$  indicates the drivers derivative control action and should include driver control action predicted by looking ahead.

From past research<sup>4)</sup>, it is known that  $\tau_L$  is strongly related to vehicle steering characteristics indicating that vehicles with large  $\tau_L$  can be driven with confidence, which means the vehicle steering characteristics are good.

The above flow can be expressed in the "human-vehicle system block diagram" shown in Fig 5.

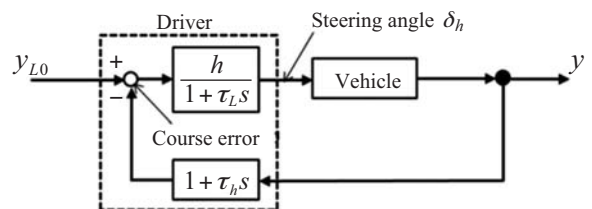


Fig. 5 Simplified driver model

### 4.3 Identification of driver parameters

In this chapter, a method for identifying driver parameters is described. Equation (2) can be converted into equation (3).

$$(1 + \tau_L s)\delta(s) = -h\{(1 + \tau_h s)y(s) - y_{L0}(s)\} \dots \dots (3)$$

$\delta$  and  $y$  of equation (3) are replaced by  $\delta^*$  and  $y^*$ , where,  $\delta^*$  is the time history of human steering maneuvers measured in the single lane change test (steering angle) and  $y^*$  is the vehicle lateral motion during that time. If the human steering model is close to the actual human maneuvering, the left-hand side and right-hand side of equation (3) should be close. To obtain driver parameters  $\tau_L$ ,  $\tau_h$ , and  $h$  to make them close, the performance function indicated in equation (4) is defined.

$$J = \int_0^T \left[ \delta^* + \tau_L \frac{d\delta^*}{dt} + h \left\{ y^* + \tau_h \frac{dy^*}{dt} - y_{L0} \right\} \right]^2 dt \dots \dots (4)$$

By solving equation (5) to minimize this performance function  $J$ , the parameters can be found.

$$\frac{\partial J}{\partial h} = 0, \frac{\partial J}{\partial(\tau_h)} = 0, \frac{\partial J}{\partial \tau_L} = 0 \dots \dots (5)$$

In this research,  $\tau_L$  (overall human delay), from the above parameters, is used as the evaluating parameter.

## 5. Actual vehicle test

### 5.1 Preliminary test

Before evaluating the influence of GVC on the vehicle's pitch motion, the effect of GVC itself was verified in a single lane change test. The anti-dive angle was set to  $0^\circ$  for both the front and rear. The following 5 subjects were chosen (Table 2). All of them were men in their 20s with different driving experience and frequency. The test was conducted by communicating to them that the test can be immediately terminated at their discretion, for example, if they feel uncomfortable during the test.

Fig. 6 shows the comparison of the driver and vehicle motion with or without GVC in the time series data. It can be seen that with GVC, the steering angle is smaller and steering action is slower than without GVC. The yaw rate is also smaller with GVC.

Then the driver parameter  $\tau_L$  was identified. The test results comparing the cases with and without GVC for each subject are shown in Fig. 7.

For all subjects,  $\tau_L$  with GVC is larger than without GVC, which means that the drivers can drive more confidently with GVC.

Table 2 Drivers for the forgoing test

Subjects	Gender	Age	Driving experience	Driving frequency
A	Male	22	4 years	Only weekends
B	Male	21	2 years	Everyday
C	Male	23	4 years	Everyday
D	Male	23	4 years	Only weekends
E	Male	21	3 years	Everyday

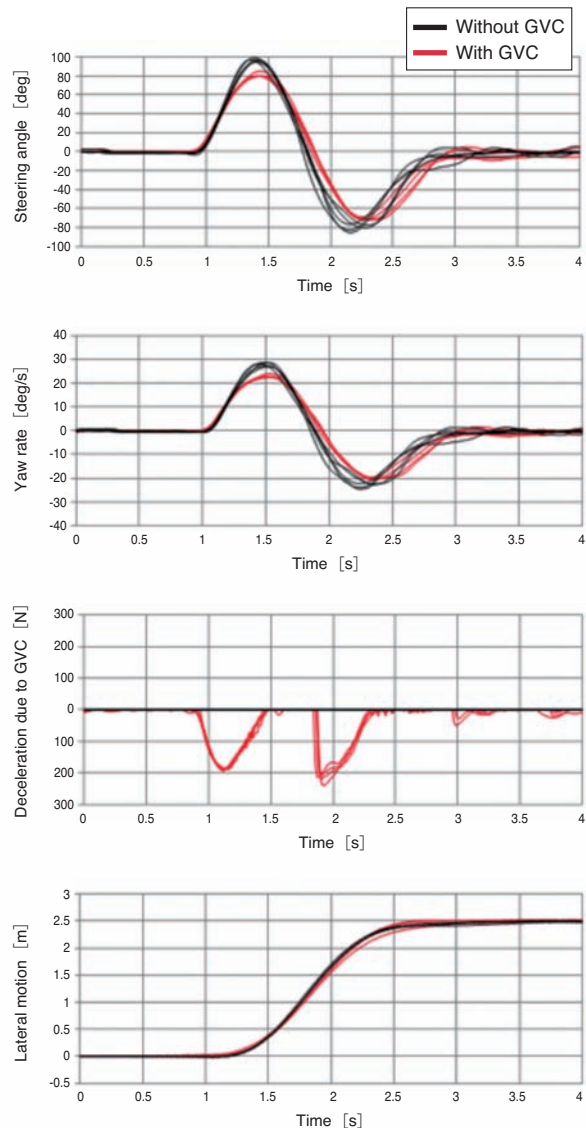


Fig. 6 Driver-vehicle behavior with/without GVC

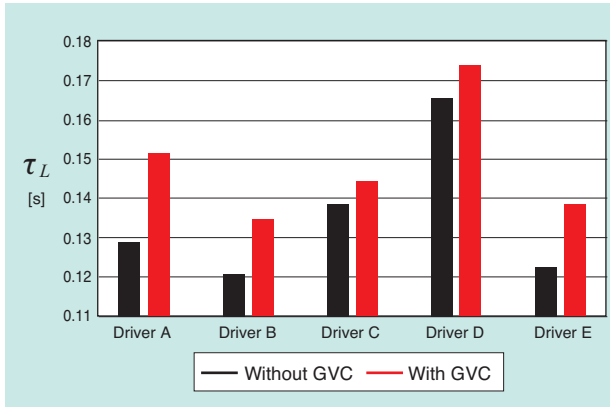


Fig. 7 Effect of GVC on handling quality evaluated by the driver parameter  $\tau_L$

### 5.2 Comparison of cases with and without anti-dive angle (anti-squad angle)

The influence on vehicle pitch motion relative to GVC was evaluated by setting the anti-dive angle to 0° and 30° for both the front and rear. Four subjects shown in Table 3 were chosen.

Fig. 9 and 10 shown on the next page are the graphs that overlay the result data from one of the test subjects.

When the anti-dive angle was set to 0° (Fig. 9), no anti-lift force and anti-squat force was produced by GVC's braking force; therefore, roll motion and diving

pitch motion, namely, diagonal roll was observed. Although longitudinal acceleration by GVC is very small (max. 0.06 m/s<sup>2</sup>), the waveform of the steering angle is more stable with GVC. During this time,  $\tau_L$  was larger with GVC than without GVC for all subjects, the same as during preliminary test (Fig. 8 (a)).

When the anti-dive angle was set to 30° (Fig. 9), anti-lift force and anti-squat force were produced by GVC's braking force; therefore, pitch motion was reduced and no diagonal roll was observed. The waveforms of the steering angle and yaw rate were more unstable than when the anti-dive angle was 0° and there were cases that  $\tau_L$  was larger without GVC than with GVC depending on the subject (Fig. 8 (b)).

From the above, we could confirm that even when the vehicle behavior is the same on a plane, GVC's effect can differ depending on the pitch motion during turns. It is conceivable that diagonal vehicle attitude is important, in addition to vehicle behavior as planar motion, in order to achieve vehicle characteristics for comfortable maneuvering for human drivers.

Table 3 Specifications of research participants

Subjects	Gender	Age	Driving experience	Driving frequency
A	Male	27	9 years	Everyday
B	Male	23	5 years	Only weekends
C	Male	22	4 years	Everyday
D	Male	23	3 years	Only weekends

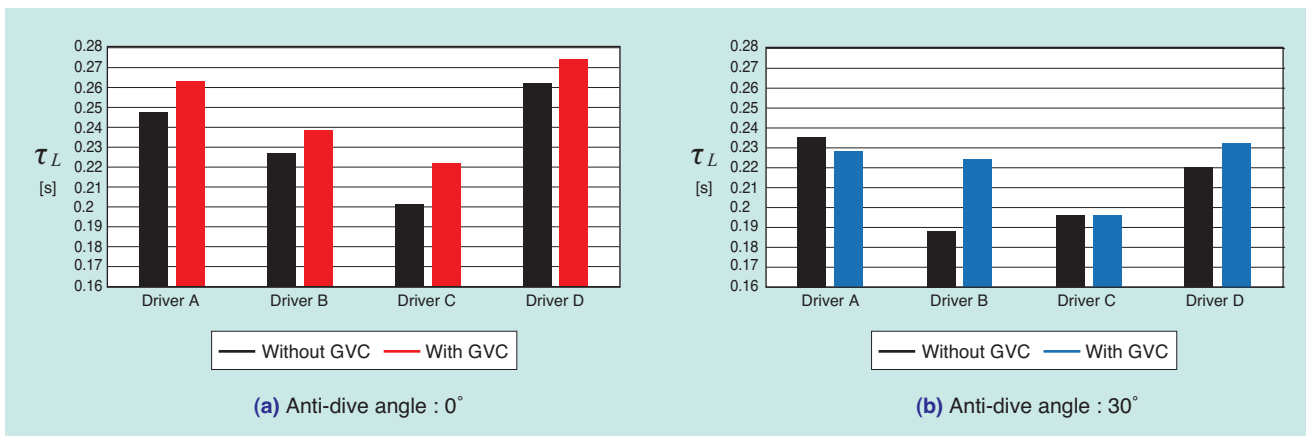


Fig. 8 Effect of anti-dive for driver parameter  $\tau_L$

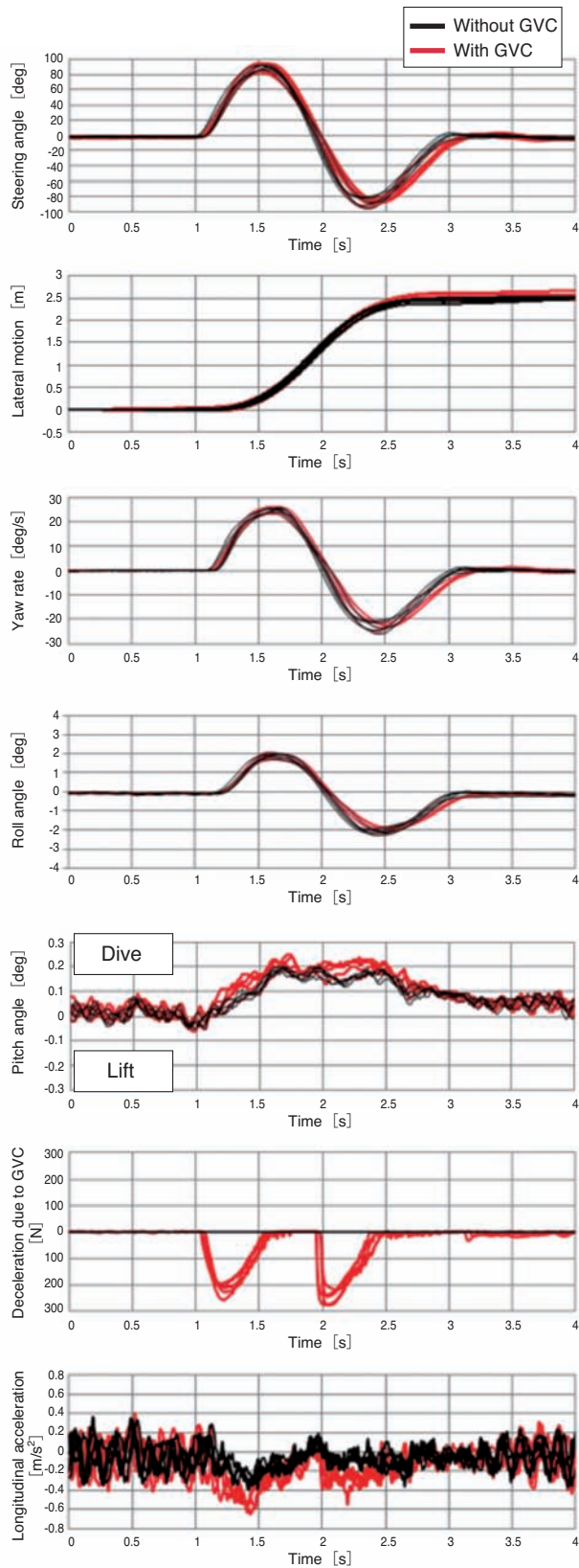


Fig. 9 Driver-vehicle behavior with pitch motion free

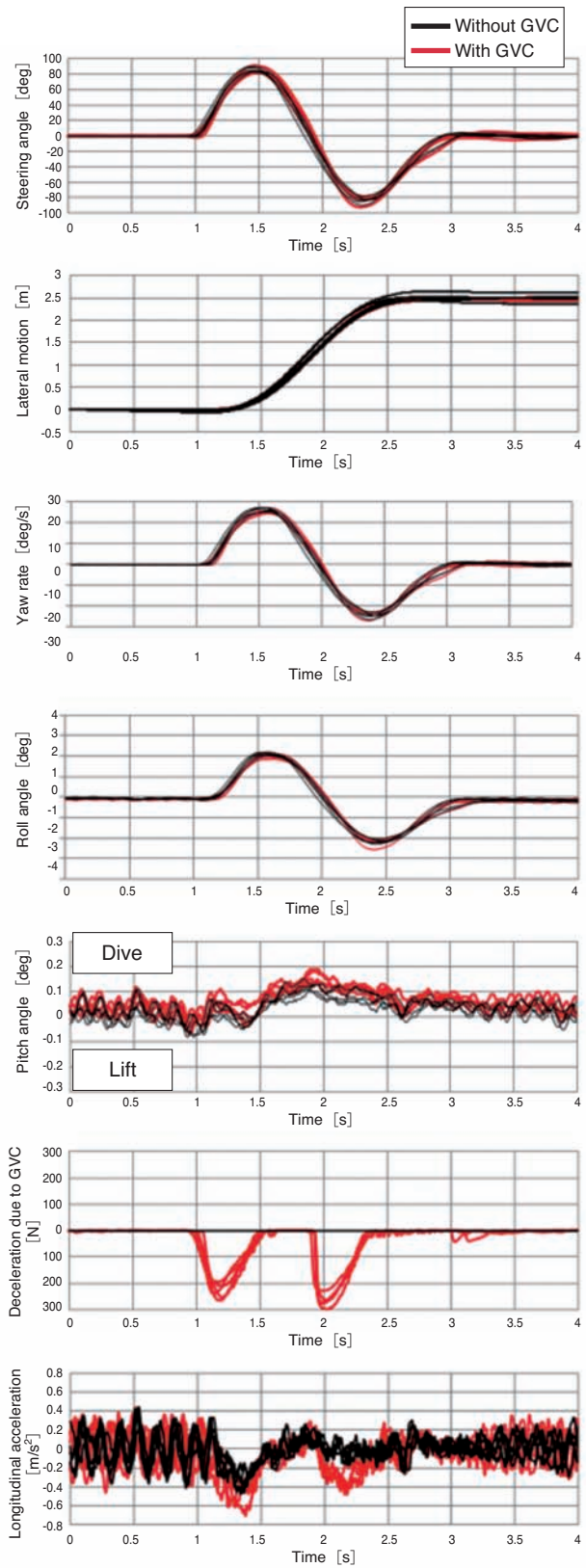


Fig. 10 Driver-vehicle behavior with pitch motion restrained

## 6. Conclusion

It was confirmed that the steering characteristics that drivers feel can be improved by producing longitudinal acceleration with GVC.

When pitch motion was not reduced without changing roll rigidity, all drivers exhibited larger  $\tau_L$  with GVC; however, when pitch motion was reduced, there were drivers with larger  $\tau_L$  without GVC.

It was revealed that the diagonal roll produced by coupling of roll and pitch motion during lane change is required to appropriately obtain the GVC effect.

It is necessary to consider 3D vehicle motion including roll and pitch motion in addition to planar motion, in order to achieve vehicle characteristics for comfortable maneuvering by human drivers.

## References

- 1) Rio Tanaka, Masato Abe et al. "Evaluation of steering characteristics of G-Vectoring Control using in-wheel motor electric vehicles," Proceedings for the Autumn Meeting in 2016, No. 045
- 2) Rio Tanaka, Masato Abe et al. "Influence of vehicle characteristics on G-Vectoring Control," Proceedings for the Spring Meeting in 2017, No. 163
- 3) M.Yamakado, R. Tanaka etc "Influence of vehicle body motion on the effects of G-Vectoring Control" IAVSD 2017 14-18 August
- 4) Shota Abe, Masato Abe et al. "Influence of roll on evaluation of driver steering characteristics," Proceedings for the Spring Meeting in 2015, No. 31-15S

## Photo of authors



Yuta SUZUKI  
Chassis System  
Engineering Department,  
EV Module Headquarters



Weipeng CHENG  
Chassis System  
Engineering Department,  
EV Module Headquarters



Shuichi KOSAKA  
Driveline System  
Engineering Department,  
EV Module Headquarters

# History of Constant Velocity Joints

Shinichi TAKABE\*



In 1963, Constant Velocity Joints (CVJ) have been started production by NTN for the first time in Japan. NTN responded to changes in the automobile industry and worked on the development of CVJ. And CVJ has grown to be the foundation product of NTN. In this article, to celebrate the 100th Anniversary of NTN, I look back on the history of CVJ.

## 1. Introduction

CVJ is a collective term for joints which smoothly transmit power without rotational fluctuation when the input shaft and output shaft rotate at any angle (work angle). Currently, it is commonly used as a driving component for automobiles and industry machines; however, it was originally initiated from the requirements of front wheel drive vehicles and evolved together with the progress of vehicles and industry machines.

The CVT originated when the Rzeppa joint was devised by Rzeppa (Hungary) in the 1930s, then in 1959, the Birfield joint was adopted in European vehicles when front-wheel drive vehicles started making major strides.

In 1963, NTN started manufacturing CVJs for the first time in Japan. Currently, after over a half century, CVJs are being manufactured globally in many sites, totaling 720 million units (CVJs for automobiles as of June, 2017) (refer to Fig. 1).

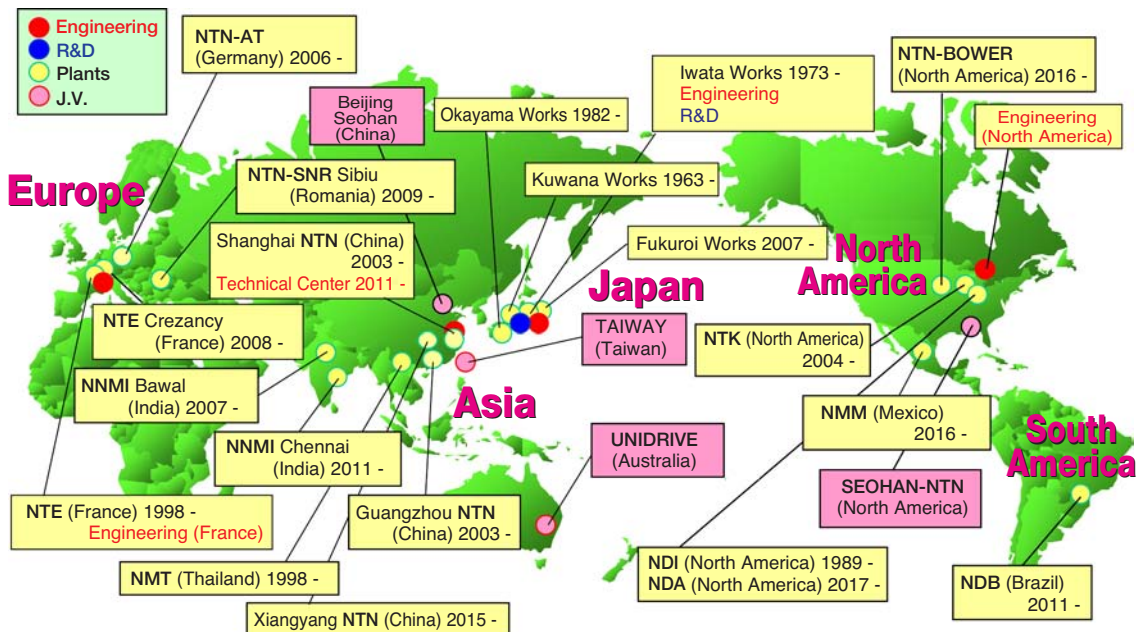


Fig. 1 Manufacturing & engineering location of CVJ

\*Drive Shaft Engineering Department, Automotive Business Headquarters

## 2. Transition of vehicles and history of CVJ

The drive system in automobiles has transitioned with the time and NTN's CVJ has made significant contributions in this transition. **Table 1** reviews the history of CVJ with the transition of vehicles

### 2.1 Before the invention of CVJ (- 1960)

Currently, front-wheel drive vehicles account for the majority in production; however, before 1960, most of the vehicles were rear-wheel drive. With rear-wheel drive vehicles, engine power is transmitted through the propeller shaft into the rear axle. Back then, both rear wheels were directly connected to the shaft as one unit and no independent vertical motion was possible (rigid axle); therefore, the CVJ was not required. The front wheels were used for steering only, without transmitting engine power; therefore, there was no need for CVJs here, either.

### 2.2 Appearance of CVJ (start of 1960s)

Before CVJs were developed, cross joints (Cardan joint) were used for the drive shaft of front wheels of front-wheel drive vehicles and four-wheel drive vehicles. However, it was not constant in velocity and produced vibration and noise with a large work angle; additionally steering stability during cornering was bad. To solve these problems the Tracta joint, Weiss joint, and Double Cardan joint, etc. were developed however, their performance was not sufficient enough for the drive shaft of the front wheels.

Then in 1956, Hardy-Spicer in the UK developed the Birfield joint, which was adopted by Austin Mini of BMC and other front-wheel drive vehicles in Europe in

1959. This produced less vibration and noise and drastically improved steering stability.

In Japan, front-wheel drive vehicles started gaining attention and in 1963, Suzuki Suzulight adopted NTN's ball-fixed joint (BJ) for the first time.

At that time, sliding CVJs, which slide in the axial direction, did not exist. The overall mechanism was realized by BJ- was used on the wheel side, cross joint, which was used on the differential gear side with a smaller work angle and slide spline installed on the shaft, which absorbed the sliding motion in the axial direction.

### 2.3 Market expansion of front-wheel vehicles (1965 -)

NTN developed a double offset joint (DOJ) with the ability to slide on the axial direction to solve the problem of vibration produced by the combination of cross joint and slide spline. The drive shaft combining BJ and DOJ was first adopted in Subaru 1000 by Fuji Heavy Industries Ltd. (currently, Subaru Corporation) in 1965. This structure is the original form of the drive shaft that is still used today (**Fig. 2**).

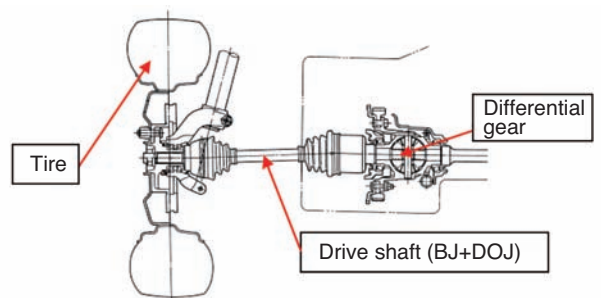


**Fig. 2** Structure of driveshaft

**Table 1** History of NTN CVJ

Decade		1960	1970	1980	1990	2000	2010
Market/vehicle trend			<ul style="list-style-type: none"> <li>●First oil shock</li> <li>●Second oil shock</li> </ul>	<ul style="list-style-type: none"> <li>●Increase of overseas production</li> <li>●Increase of AT vehicles</li> <li>●Increase of 4WD</li> </ul>		<ul style="list-style-type: none"> <li>●Expansion of emerging markets</li> <li>●Enhancement of fuel efficiency regulations</li> </ul>	<ul style="list-style-type: none"> <li>●Introduction of Japanese auto manufacturers</li> <li>●Introduction of HVs and EVs</li> </ul>
Drive shaft	Fixed	●BJ (1963)			●UJ (1988)	●EBJ (1998) ●EUJ (2002)	●VBJ (2010) ●VUJ (2012); CFJ (2012); ●REBJ (2015)
	Sliding	●DOJ (1965)		●TJ (1983) ●DOJ-RPC (1984) ●DOJ-RPCF (1986) ●AC-TJ (1987) ●FTJ (1989)		●SFJ (1997) ●PTJ (2002) ●EDJ (2002) ●ETJ (2002) ●EPTJ (2005)	●REDJ (2015)
Propeller shaft	Fixed					●HEBJ (2005)	
	Sliding			●LJ (1985) ●DOJ-RPCF (1987) ●AC-TJ (1991)	●HLJ (1997)	●HEDJ (2005) ●HETJ (2006)	

In the 1970s, various auto manufacturers introduced front-wheel drive vehicles into the market, which was further accelerated by the second oil crisis in 1978. In the 1980s, the need for quieter vehicles rose as the production of front-wheel drive vehicles increased. With improvements of CVJs, front-wheel drive vehicles expanded into small car segments. Therefore, the need for CVJs increased.

## 2.4 Emergence of IRS vehicles (1976 -)

Rear-drive vehicles transitioned from rigid axle to independent rear suspension (IRS) to improve ride comfort. Since IRS requires each rear wheel to move independently, CVJs were required on the drive shaft. In 1976, Toyota Mark II adopted BJ and DOJ for the first time as an IRS vehicle. Later, adoption of CVJ increased in the propeller shaft of rear-wheel drive vehicles with IRS for reducing vibration.

## 2.5 Expansion of 4-wheel drive vehicles (1980 -)

Originally, 4-wheel drive was limited to off-road vehicles; however, the introduction of Leone 4WD from Fuji Heavy Industries Ltd. (currently, Subaru Corporation) in 1972, and full-time 4WD vehicles from European manufacturers in the 1980s, adoption of 4WD expanded to on-road vehicles. IRS was adopted in the rear wheels of 4WD vehicles, and drive shafts using CVJ on all wheels were required in the mid-1980s.

As the adoption of 4WD expanded to on-road vehicles, reduction of noise and vibration was required, and adoption of sliding CVJs began replacing the combination of cross joint and slide spline on the propeller shaft.

Since the propeller shaft rotates at higher speeds than the drive shaft, cross grooved joints (LJ) were applied because of little backlash and good rotational balance. Then, DOJ to absorb small vibrations, tripod joints (TJ) with small sliding resistance and heat generation, and BJ for fixed CVJ usable at a wider angle than cross joints were all adopted as they were improved for use in the propeller shaft.

Increased usage of CVJs in on-road 4WD vehicles proliferated to off-road 4WD vehicles, too.

## 3. Transition of CVJ technology

As CVJs significantly affect vehicle performance, NTN has been contributing to improvement of vehicle performance through improvement of CVJs.

Around 1980, automatic transmission (AT) started outpacing manual transmission (MT) in Japan. AT vehicles produced vibration while idling due to axial vibration transmitted from the drive shaft to the vehicle

body, caused by the driver pressing the brake pedal while transmission was set at D-range. NTN developed DOJ-RPC and DOJ-RPCF which absorbed small engine vibrations which solved this problem. In addition, NTN started volume production of newly structured sliding type CVJ with smaller sliding resistance, and " (TJ)" in 1983, with wide adoption, particularly with AT vehicles.

Today, TJ type CVJs are used on most AT vehicles.

## 3.1 Low vibration sliding type CVJ (1983 -)

As the automobile evolved, requirements on comfort and quietness also evolved. The following is the history of measures taken for reducing shudder of TJ as an example of vehicle NVH (noise, vibration and harshness).

### (1) TJ (1983 -)

When TJ rotates with a wider angle, periodically, fluctuating slide occurs between the roller and roller groove on the outer ring, producing outer ring axial force (induced thrust). This induced thrust may produce shudder when resonated with the vibration of engine mount during vehicle start and acceleration.

### (2) AC-TJ (1987 -)

Gothic geometry was applied to the cross section of the roller groove of the outer ring to make angular contact with the roller, and induced thrust was induced together with low- $\mu$  urea grease (refer to Fig. 3).

### (3) FTJ (1989 -)

Another roller (free ring) was installed outside the roller so that the free ring always maintains a certain position against the roller groove, and induced thrust was significantly reduced (refer to Fig. 4).

### (4) SFJ (1997 -)

Eliminated the flange on the roller groove of the outer ring prevents an increase of induced thrust when the free ring end of FTJ strikes the flange on the roller groove of the outer ring (refer to Fig. 5).

### (5) PTJ (2002 -)

The journal cross section of the tripod was made into an irregular elliptical shape, and a freely swinging roller cassette was incorporated to be contained within the roller groove of the outer ring. Since the roller cassette smoothly rolls maintaining a certain position on the roller groove of the outer ring, even with a wider angle, lower induced thrust can be always maintained regardless of the work angle (refer to Fig. 6).



Fig. 3 Structure of AC-TJ

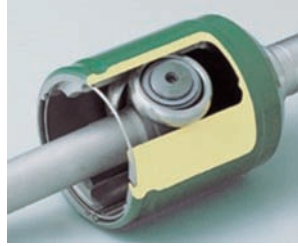


Fig. 4 Structure of FTJ

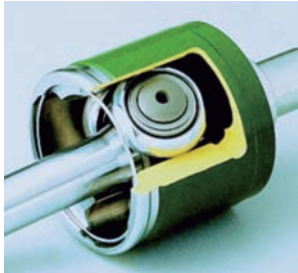


Fig. 5 Structure of SFJ



Fig. 6 Structure of PTJ

**Table 2** Transition of max. angle of fixed CVJ

Max. work angle	Volume production start time	CVJ type
42.5°	1963 -	BJ
44.5°	1980 -	BJ
46.5°	1982 -	BJ
47°	1998 -	EBJ
50°	1988 -	UJ
50°	2012 -	VUJ



Fig. 7 Structure of BJ



Fig. 8 Structure of EBJ



Fig. 9 Structure of UJ



Fig. 10 Structure of VUJ

### 3.2 Larger working angle

#### (1) Fixed type CVJ (1980 -)

The center of the differential gear and the center of the wheels are in different vertical and horizontal positions; therefore, the CVJs on the wheel side and differential gear side would have a specific angle. The CVJ on the wheel side would have a work angle, which is a combination of this angle and the angle created by steering. The turning radius of a vehicle is determined by the maximum work angle of the CVJs. In order to reduce large turning radius due to a longer wheel base and high common angle, CVJs are required to provide a larger work angle.

The maximum work angle of BJ, originally 42.5°, was enlarged to 46.5°, then an undercut free joint (UJ) was developed to increase the angle further to 50°, which was adopted in the Fuji Heavy Industries Ltd. (currently, Subaru Corporation) Legacy. UJ has the same component configuration as BJ, with a straight shape on the end of the ball groove of the outer wheel and inner wheel to provide a larger angle.

In addition, the internal design has evolved with BJ to EBJ (max. work angle: 47°) and UJ to VUJ (max. work angle: 50°) refer to [Table 2](#), [Fig. 7](#) - [Fig. 10](#).

#### (2) Sliding type CVJ (1984 -)

CVJs on the differential gear side are also required to provide a larger angle due to the increased common angle and cope with work angle fluctuation during bump and rebounding vehicle motion. The original maximum work angle was increased from the original 23° to 25° and a 30.5° design was also placed into production.

### 3.3 Lightweight and compactness

#### (1) First phase (1981 -)

In order to adapt to vehicle specifications, CVJ names and sizes were broken down into series in smaller increments.

The manufacturing process of the outer ring was changed to induction hardening using medium carbon steel rather than carburized steel to enhance the strength allowing choice of smaller sizes.

#### (2) Second phase (1992 -)

High strength shafts made of medium carbon boron steel and long operating life urea grease were developed to allow choice of CVJ with an even smaller size than the first phase.

#### (3) Third phase (1998 -)

In order to achieve lighter and smaller units maintaining load carrying capacity equivalent to BJ, EBJ was developed, increasing the number of balls from 6 to 8 by reducing the ball size. This was implemented in the Suzuki Cultus Crescent Wagon in 1998.

Also for sliding type CVJ, EDJ with 8 balls and ETJ with renewed internal design were developed. EPTJ

was also placed into volume production, which is a compact version of PTJ.

On the other hand, on the propeller shaft side, HLJ was developed by making LJ lighter and smaller, and increasing sliding area. Also, HEBJ, HEDJ and HETJ were developed by improving EBJ, EDJ and ETJ for use on the propeller shaft.

### 3.4 Grease and CVJ boots

Originally, lithium soap grease with molybdenum disulphide was used; however, improvement in performance was made since the 1980s by focusing on urea grease for "durability," "low vibration," "high efficiency" and "low heat generation." High performance urea grease with organic molybdenum, etc. was developed and currently in use.

On the other hand, for CVJ boots, chloroprene rubber was used in the past; however, damage occurred due to external wear and deterioration of material. Although some improvements in material and design were made, it was not sufficient for use on fixed-type CVJ for front wheels.

Around 1985, boots made of thermal plasticized polyester elastomer (resin boots) were produced, which drastically increased the life of boots. Today, resin boots are used for almost all fixed-type CVJ, as well as increased use for sliding type CVJ.

### 3.5 High functionality of CVJ (2010 -)

The following is a description of CVJs with higher functionality.

#### (1) Fixed-type CVJ, "VUJ"

The requirements for a larger maximum work angle increased due to the increase of global demand for SUVs. Therefore, VUJ was developed by making UJ lighter and smaller with increased robustness, and placed into volume production in 2012.

#### (2) Next generation high-efficiency fixed type CVJ, "CFJ"<sup>1)</sup>

As higher fuel efficiency is being explored for environmental measures and economy, we have been pursuing improvement of transmission efficiency of CVJs, in addition to reduction of weight for CVJ as another contribution.

EBJ was developed, which reduced torque loss by 20% compared with BJ, and then OFJ was developed, which reduced torque loss by 60% compared to that of EBJ.

CFJ has a structure to alternate inclined ball grooves from the outer ring and inner ring (cross groove) to reduce internal friction for reducing torque loss (refer to Fig. 11).

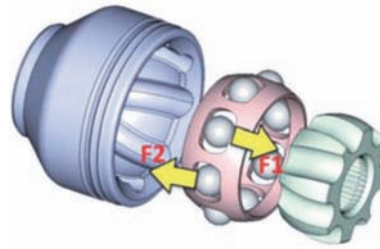


Fig. 11 Structure of CFJ

### (3) Lightweight Rear Drive shaft "R-Series"

CVJ for front wheels is used as CVJ for rear drive shafts. We have developed REBJ and REDJ dedicated to rear wheels for rear-drive vehicles and 4WD pursuing lightweight and compactness. We have succeeded in reducing weight by 30% for the entire drive shaft, including use of the hollow shaft as the intermediate shaft, compared to EBJ and EDJ, which boast the world's highest level of lightweight and compactness as CVJ for front wheels (refer to Fig. 12).



Fig. 12 Structure of light weight driveshaft for rear (REBJ + hollow shaft + REDJ)

### 3.6 High functionality of drive shaft

#### (1) Intermediate shafts with dynamic damper (DD)

Resonance may occur with natural bending frequency of the intermediate shaft of the drive shaft through engine vibration. DDs can be installed on the intermediate shaft as a means to shift the resonance frequency.

Due to improved quietness of vehicles, demand for reducing vibration of the drive shaft has been diversified. Until the 1990s, DDs were used to absorb one resonant frequency (1-mass spec); however, since the latter half of the 1990s, DDs to absorb 2 resonant frequencies (2-mass spec) were applied. Further, during the mid-2000s, dual mode DDs which can solve 2 resonant frequencies with only one mass were applied.

#### (2) Integrated hollow shaft

The drive shaft is required to have high rigidity; however, thicker intermediate shafts for increasing rigidity increase weight. Therefore, hollow intermediate shafts were introduced to reduce weight.

Conventionally, intermediate shafts were made with shaft components for engaging CVJs welded on both ends of the pipe material. Currently, integrated hollow shafts by swaging process have been used for volume production since 2003.

### (3) Isometric drive shaft

The drive shaft of front-wheel drive vehicles has different lengths on the left and right sides because of transmission placement. Taking rigidity balance of the left and right may be limited, even when the thickness of the intermediate shaft is changed. High output vehicles may experience torque steer.

Therefore, outer wheel stem length of the differential side is made differently on the left compared to the right (long shaft and short shaft), and the intermediate shaft is made isometric to match the common angles of both sides. The long shaft outer ring is connected to the differential gear through bearings and brackets, etc.

The long shaft outer ring can be manufactured with integrated cup and stem components, or cup and stem components may be manufactured separately and welded together. The cup components are commonly designed, and the stem components are individually designed, based on the vehicle specification. EBW outer rings with those components welded by electron beam welding (EBW) have been placed in volume production since 2016 (refer to Fig. 13).

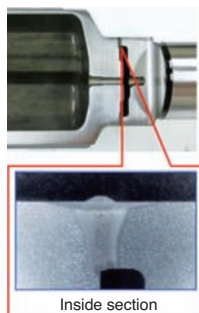


Fig. 13 Combined by electron beam welding

## 4. Future development

HEVs and EVs have emerged as the new drive power; however, diesel engines and gasoline engines are also changing every day. On the other hand, vehicle designs not only widely vary from light vehicles to large passenger cars and SUVs, but also need to meet the requirements of their individual dynamic performance and ride comfort at a high level.

Although power types and vehicle designs vary, drive train structures evolve based on current structures. The drive shaft is indispensable among these, and has an increased role to play.

Performance required to the drive shaft may change depending on the power type and vehicle design; however, the basic elements are "lightweight," "high angle," "high rigidity," "quietness," "high efficiency" and "high speed." NTN strives to address these elements by appropriately forecasting the needs, and pursuing development without delay for continuous evolution.

## 5. Summary

Front-wheel drive vehicles, which were a revolutionary drive system 50 years ago, are driven everywhere in the world today. We are proud that NTN's CVJ has contributed to the development of front-wheel drive vehicles which were not imaginable 100 years ago.

I have reviewed the history of CVJ by taking the opportunity of NTN's 100th anniversary. Imagining the world in 100 years from now, we would like to deliver CVJs with evolution beyond imagination. NTN will continue growing with the history of CVJs in its memory.

## References

- Takeshi Ikeda: History of CVJ Design for Automobiles and Recent Technology NTN TECHNICAL REVIEW No. 70 (2002) 8-17
- 1) Teruaki Fujio: Next generation high efficiency fixed-type constant velocity joint "CFJ" NTN TECHNICAL REVIEW No.81 (2013) 64-67

Photo of author



Shinichi TAKABE  
Drive Shaft Engineering  
Department, Automotive  
Business Headquarters

# History of Axle Unit Bearings for Automobile



Daisuke NAKA\*

Axle unit bearing has been innovated by integrating the surrounding components. This article introduces the transition of bearing type and the latest NTN's technology.

## 1. Introduction

While rolling bearings for general use are standardized by organizations such as ISO and JIS, rolling bearings for supporting vehicle wheels (hereinafter "axle unit bearings") have gone through significant transitions over the years on their types/materials and design specifications.

In addition, as environmental issues have become the focus of the entire automotive industry, size, weight and fuel efficiency of vehicle components are strongly required to improve these environmental concerns<sup>1)</sup>.

In parallel with the development of technologies to address these market requirements, the production/technology centers of NTN's axle unit bearings have expanded globally (Fig. 1), which I would like to review with its history and market needs.

## 2. Market needs

The design specifications of axle unit bearings are diverse based on automotive manufacturer needs (mounting methods, allowable space and bearing size, bearing load carrying capacity, friction, sealing capability, rigidity and strength, etc.). Their historical and current requirements can be categorized as follows:

- a) Ease of assembly
- b) Simplification or elimination of bearing clearance adjustment
- c) Compactness and lightweight and large bearing load carrying capacity
- d) Maintenance-free  
(Particularly, elimination of greasing operation and external seals for sealed bearings)
- e) Reduction of components
- f) Reduction of total cost including bearing units, peripheral components and labor

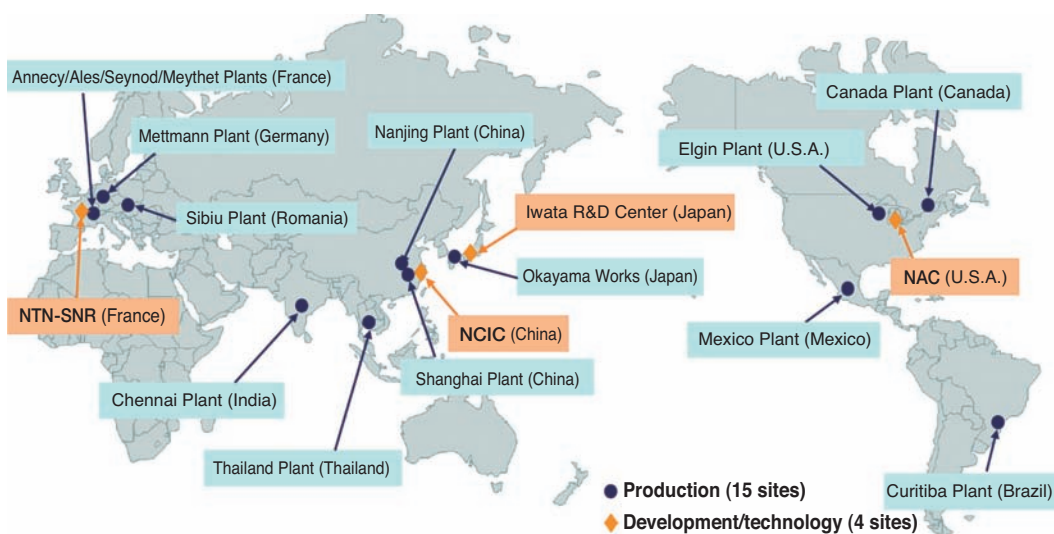


Fig. 1 Axle unit bearing global production and R&D location

\*Automotive Unit Engineering Dept., Automotive Business Headquarters

NTN has been developing and marketing volume production of GEN1, GEN2 and GEN3 successfully for approximately 40 years, responding to the above requirements<sup>2)</sup>.

### 3. Transition of axle unit bearings

#### 3.1 From standard bearings to GEN1

Until the 1970s, standard bearings conforming to the ISO Standard were mainly used for axle unit bearings, placing two deep groove ball bearings or conical rolling bearings on an axle and appropriately selecting spacer rings and nut tightness to adjust the assembly clearance.

This method of using standard bearings had limitations in weight and size; therefore, the market needs for sealed/integrated bearings with potential for a compact and light form factor increased, which provided ease of assembly onto vehicles and did not require clearance adjustment. In the late 1970s, sealed double-row angular contact ball bearings (angular unit) and sealed double-row conical roller bearings (taper unit), called GEN1, were introduced into the market, and are still widely used as the axle unit bearings for passenger cars even in the 21st century. NTN produces GEN1 axle unit bearings in domestic plants, as well as overseas.

#### 3.2 From GEN2 to GEN3

In the 1980s, the requirements for lightweight and compact vehicle components increased. As a result, the peripheral components of axle unit bearings, such

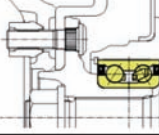
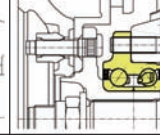
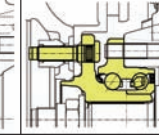
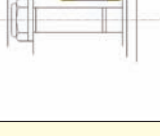
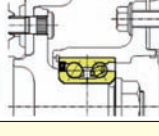
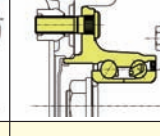
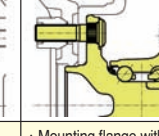
as hub and housing (knuckle) were integrated as a unit, evolving into GEN2 (GEN2 and later products as units are called hub bearings at NTN, among the axle unit bearings). NTN started development of GEN2 hub bearings in 1979 and volume production in 1983, the first being produced in Japan. GEN2 hub bearings required integration of the hub flange and outer ring raceway surface as a unit. This was achieved by applying high frequency heat treatment to the raceways, ensuring rolling fatigue life required for bearings, rotating bending fatigue strength required for hub flanges, and fracture strength for expected large load bearings from the road surface were met. Adoption of GEN2 bearings by the automotive manufacturers increased from the 1980s to 2000s as its advantages are well recognized in the market.

Later, GEN2 evolved into GEN3 by integrating the inner ring, which improved ease of assembly of hub bearings in the vehicle assembly line<sup>1)</sup>.

NTN started volume production of GEN3 in the mid-1980s, the first being produced in Japan. Then, full adoption of GEN3 started in the latter half of the 1990s and its wave rapidly propagated throughout the world up until today.

In this case, GEN3 continued to evolve with superior specifications such as shaft-end tightening to facilitate pre-load control and improving ease of assembly in the vehicle assembly lines, as well as improving reliability by integrating wheel velocity sensors in the anti-lock brake system which prevents damage from pebbles and corrosion from muddy/salty water.

Table 1 Characteristics of NTN axle unit bearings

Generation		Conventional	GEN1	GEN2	GEN3
Volume production start time		- 1970s	From latter half of 1970s	1983 -	From latter half of 1980s
Structure	Drive wheel				
	Driven wheel				
Feature		· Two single row rolling bearings are used	· Two single row rolling bearings are integrated	· Mounting flange with mating component and outer ring are integrated	· Mounting flange with mating component, outer ring and inner ring are integrated · Press fitting of bearings to mating component
Ease of assembly to vehicles		☆	☆☆	☆☆☆	☆☆☆☆
Compactness		☆	☆☆	☆☆☆	☆☆☆☆
Rigidity		☆	☆☆	☆☆☆	☆☆☆☆
Pre-load control		☆	☆☆	☆☆☆	☆☆☆☆
Running torque		☆	☆☆	☆☆☆	☆☆☆☆

Superiority: ☆☆☆☆ > ☆☆☆ > ☆☆☆ > ☆☆☆ > ☆

NTN has been responding to the demand of axle unit bearings from the market based on specific technology accumulated over the years.

Table 1 on the previous page shows the transition and features of NTN's axle unit bearings by generation, including the period when two standard bearings were used before integration.

**3.3 Evolution of raceway material, grease and seals**  
**(1) Raceway material**

NTN used high carbon chromium bearing steel for inner/outer ring raceway materials for GEN1 axle unit bearings. For outer rings and hub rings of GEN2 and GEN3, carbon steel with high frequency heat treatment is used on the raceway, which contribute to increased rolling operating life and forgeability. For inner rings of GEN2 and GEN3, high carbon chromium bearing steel is used, similar to GEN1.

Axle unit bearings use grease lubrication which is easy to handle, contributes to simplified design of sealing device and is most economical. Internal grease for axle unit bearings is required to have the following features:

- (1) Reduction of friction and wear
- (2) Extension of bearing life
- (3) Prevention of corrosion
- (3) Prevention of foreign materials from entering
- (5) Prevention of fretting wear

**(2) Grease**

Table 2 shows features of grease used in NTN's axle unit bearings. NTN originally used highly refined mineral oil as the base oil and urea-based organic compound as thickener. Then, grease with improved anti-corrosion properties was used as the standard product. In addition, grease with improved low-temperature tolerant properties was introduced for volume production by blending additives to prevent fretting wear when used for long-haul freight car transportation in cold regions. Furthermore, with stricter fuel efficiency regulation planned to be implemented by 2021 in Japan, U.S. and Europe, due to the recent increase of fuel cost and environmental issues such as global warming, low-torque specification is required for axle unit bearings. To meet the low torque requirements, NTN has developed low-torque grease by modifying the base oil/kinematic viscosity and consistency. This low torque grease is currently in volume production.

**(3) Seals**

Seals for axle unit bearings are required to have airtightness and low torque properties preventing muddy water from penetrating from the operating environment. Table 3 shows characteristics of seals used in NTN's axle unit bearings. It shows the evolution from 2-lip seal that consist of only radial lips to Hipack seals which improved sealing properties

**Table 2** Characteristics of NTN axle unit greases

		Conventional grease	Standard grease	Grease with improved fretting resistance	Low-torque grease
Performance	Anti-corrosion property	☆	☆☆☆	☆☆☆	☆☆☆
	Fretting resistance	☆☆	☆☆	☆☆☆	☆☆☆
	Torque	☆☆	☆☆	☆☆	☆☆☆

Superiority : ☆☆☆ > ☆☆☆ > ☆☆☆ > ☆

**Table 3** Characteristics of NTN axle unit seals

Format		2-lip seal	Hipack seal		
			1-side lip seal	2-side lip seal	2-side lip seal with magnetic encoder
Cross-section					
Performance	Anti- muddy water properties	☆	☆☆	☆☆☆	
	Grease leakage tolerance	☆☆☆	☆☆☆		
	Torque	☆☆☆	☆☆	☆☆☆	
	Anti-corrosion properties of seal land	☆	☆☆☆		
	Airtightness	☆☆☆	☆☆☆		

Superiority : ☆☆☆ > ☆☆☆ > ☆☆☆ > ☆

against muddy water by adding side lips, as well as significant anti-corrosion properties of the seal land by adding stainless steel slingers. Additionally, it achieved low-torque properties responding to the aforementioned low-torque requirement, by optimizing seal lip sliding surfaces and developing grease dedicated for seal lips. Furthermore, NTN has extended volume production of value-added seals by integrating magnetic encoders, vulcanizing magnetic rubber on the side of the slinger.

**3.4 Next generation hub joint**

After the development of GEN3 for volume production, NTN completed development of the next generation hub bearings, GEN4, integrating constant velocity joints (hereafter "CVJ"). This technology has not been adopted since it requires significant modification to the vehicle assembly lines at the automanufacturers.

Therefore, NTN developed a new joint method for CVJ and hub bearings which can be assembled without changing the assembly lines at the automanufacturers and has achieved a significant reduction in weight. The following is the introduction of Press Connect Spline Hub Joint (PCS-H/J) (Fig. 2).

Conventionally, CVJ and hub bearings are engaged with a spline and tightened with a nut. The spline teeth are generally designed for interference fit with the

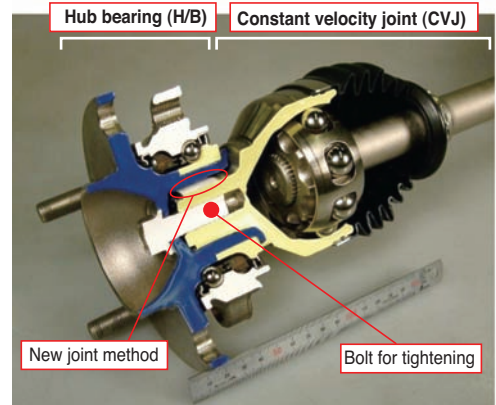


Fig. 2 Structure of PCS-H/J

helix angle to eliminate backlash, which requires long spline fit length ( $L_1$  in Fig. 3 (a)). The new press connect fit method finishes forming the spline by tightening a bolt, which results in a tighter interference fit than the CVJ stem spline on the inner diameter of the hub bearings. This enables the torque to be applied to the entire spline area, resulting in significant reduction of spline fit length ( $L_2$  of Fig. 3 (b)).

Adopting the press connect method, PCS-H/J achieves approx. 65% reduction in CVJ stem length, 12% reduction in weight (max) and no spline fit backlash<sup>3)</sup>.

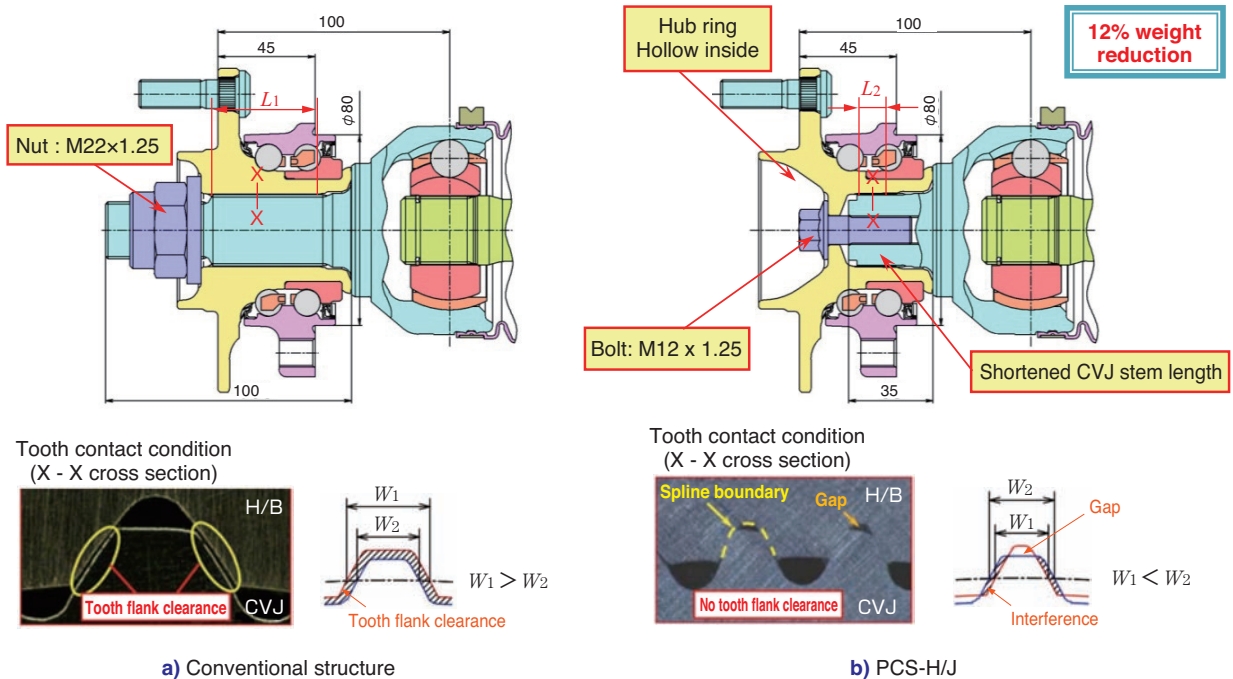


Fig. 3 Example of The Application and Spline Cross Section of PCS-H/J

## 4. Summary

NTN has been leading the evolution of axle unit bearings for approximately 40 years, and through expansion of market share with the merger of **NTN-SNR** in 2008, it has acquired the top share today.

This paper reviewed the history of axle unit bearings on the occasion of the 100th anniversary of **NTN**. This development is the result of efforts of the forerunners which we are very proud of, and we strive to continue this spirit of development while continuing to achieve vehicles with higher functionality and better comfort, setting our eyes on the next 100 years.

## References

- 1) Eiji Funahashi, NTN Technical Review No. 70, 52-57, (2002).
- 2) Masao Kato, Hiroshi Morishita, Kenji Hibi, Kunishige Ootake, NTN Bearing Engineer, NTN Technical Review No. 52, 40-53, (1986).
- 3) Takayuki Norimatsu, Tsutomu Nagata, NTN Technical Review No. 81, 58-63, (2013)

Photo of author

---



Daisuke NAKA

Automotive Unit Engineering Dept.,  
Automotive Business  
Headquarters

## ULTAGE<sup>※1</sup> Tapered Roller Bearing for Automotive Application



**Yasuhito FUJIKAKE\***  
**Takanori ISHIKAWA\***  
**Susumu MIYAIRI\***

NTN has developed the "ULTAGE Tapered Roller Bearing for Automotive Application" that delivers the world's highest standard of high-load capacity and high-speed rotational performance with optimal internal design of bearing.

Tapered roller bearings for automobiles are used in transmission components such as transmissions and differentials, and need to have a high-load capacity to operate conditions that are becoming increasingly harsh in recent years, including the greater loads due to higher power output of automobiles, as well as greater unbalanced loads caused by the lower rigidity due to lightweight housings. The tapered roller bearings also need to provide low torque required for lower fuel consumption and high-efficiency and high-speed rotational performance in low temperature. The developed "ULTAGE Tapered Roller Bearing for Automotive Application" is a new, compact series lineup that has been modified with optimal design technology for the shape of tapered rollers that maximize the rolling operating life as used for the Large Size Tapered Roller Bearing. This design maximizes the potential operating life with minimize of contact surface pressure between the rolling element (rollers) and raceway (inner and outer ring), even when there are high loads or unbalanced loads. It is introduced design and performance of "ULTAGE Tapered Roller Bearing for Automotive Application" contributing to fuel saving.

### 1. Introduction

As global warming and extreme weather associated with the increase of CO<sub>2</sub> emissions are raised as social issues, initiatives for achieving a low carbon society <sup>1)</sup> has become an urgent issue. In line with this social environment, vehicle fuel efficiency standards and regulations for CO<sub>2</sub> emissions are becoming stricter every year in many countries. <sup>2)</sup> This forces vehicle units such as transmissions and differential gears to become smaller and lighter, which increases the need for smaller bearings. As a result, long-life bearings are required, even in more severe operating conditions, such as increased loading on bearings and increased unbalanced load due to the reduction of rigidity in weight-reduced housings.

In response to these requirements, NTN developed crowning optimization technology to maximize the rolling fatigue life with high robustness, by minimizing the rolling contact stress of roller bearings and

applying a special crowning shape (a shape where the-diameter is gradually reduced by a few micrometers toward the end) that suppresses excessive pressure at the end of the contact area (edge load) of the rolling elements <sup>3)</sup>.

NTN announced "Large ULTAGE Tapered Roller Bearing for Industrial Machines" which applies this design technology in 2014 <sup>4)</sup>, and started volume production of a series of standard products with bearing outer diameter of 280 mm or more.

NTN has now developed "ULTAGE Tapered Roller Bearing for Automotive Applications" which applies the improved optimization design technology that maximizes the rolling fatigue life to small tapered roller bearings (with bearing outer diameters of 150 mm or less). In this paper, we will introduce the structure and characteristics of these bearings.

※1 ULTAGE<sup>®</sup> is the name created from the combination of "ultimate," signifying refinement, and "stage," signifying NTN's intention that this series of products be employed in diverse applications, and is the general name for NTN's new generation of bearings that are noted for their industry-leading performance.

## 2. Structure

**Fig. 1** shows the overall structure of the ULTAGE Tapered Roller Bearing for Automotive Applications.

As shown in **Fig. 1**, contact stress is minimized by applying a special crowning shape to the rollers. As a result the temperature rise during bearing operation is reduced by optimizing the sliding contact of the rollers with the inner ring and cage, in turn allowing greater permitted rotational speed. Bearing steel for these applications is adopted which is characterized by improved cleanliness, ease of thermal treatment and global procurement. The specification where the aforementioned internal design optimization and standard quenching are applied is called "standard type." NTN also developed the "high functionality type" which combines NTN's proprietary FA thermal treatment<sup>5)</sup>, as well, for use under severe lubrication conditions such as ingress of hard foreign matter.

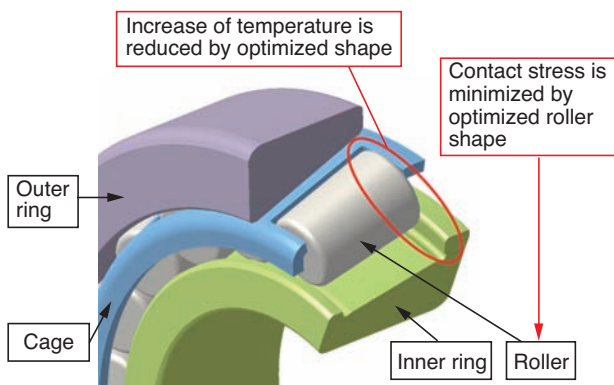


**Fig. 1** Structure of ULTAGE tapered roller bearing for automotive application

## 3. Features

The following list shows the characteristics of ULTAGE Tapered Roller Bearings for Automotive Applications in comparison with conventional tapered roller bearings<sup>6)</sup>.

- (1) High-load capacity at the world's highest level:  
Basic dynamic load rating - 1.3 times
- (2) Long operating life (compared with the basic rating life):  
Standard type - 2.5 times or more  
High-functionality type - 3.8 times or more
- (3) High speed rotational performance at the world's highest level:  
Permitted rotational speed - approx. 10% improvement
- (4) Permitted inclination (magnitude of misalignment):  
Permitted inclination - max. 4 times

**Fig. 2** shows an example of the calculation of contact stress distribution at the axial cross section of the

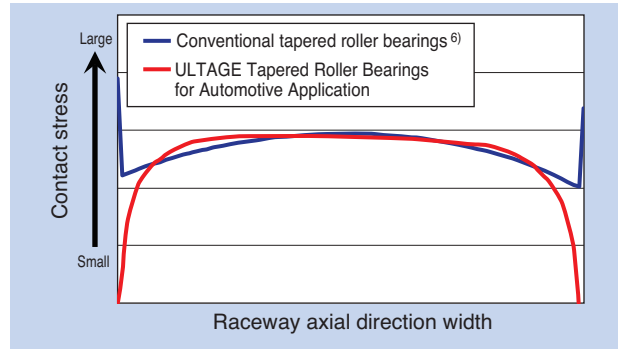


**Fig. 2** Contact stress distribution on raceway

raceway. With ULTAGE Tapered Roller Bearings for Automotive Applications, bearing operating life is improved by suppressing excessive pressure at the edge of the contact area (edge load) and minimizing the overall contact stress distribution by the adoption of special crowning.

### 3.1 The mechanism of long operating life through special crowning

In the development of optimized crowning, minimization of the internal maximum shear stress was explored based on the basic concept of the rolling fatigue life calculation that states "the probability of internal originated delamination increases when internal shearing stress becomes large." Conventionally, the crowning shape is distributed to the inner ring, outer ring and rolling contact surface of the rolling elements due to the restrictions of processing. In that case, roller fatigue life is reduced when distribution of such shear stress and contact stress is misaligned due to the displacement of crowning settings from the behavior of the rollers during bearing operation. In contrast, if the optimized special crowning shape is applied to only the rollers, such shear stress and contact stress are minimized regardless of the behavior of the rollers, maximizing the potential roller fatigue life of the associated bearings.

### 3.2 Special crowning analysis method

A new design method was introduced for the special crowning shape to minimize contact stress. by an optimization algorithm applied to a newly proposed logarithmic function<sup>3)</sup> with 3 newly introduced design parameters, from "misalignment" and "applied load" calculated from the actual operating conditions. With this method, special crowning shapes can be quickly, automatically and easily obtained, which was traditionally complicated in the past. **Fig. 3** shows a case study of running optimization of the special crowning shape when minimization of the max. contact stress is set as the objective function. The results from

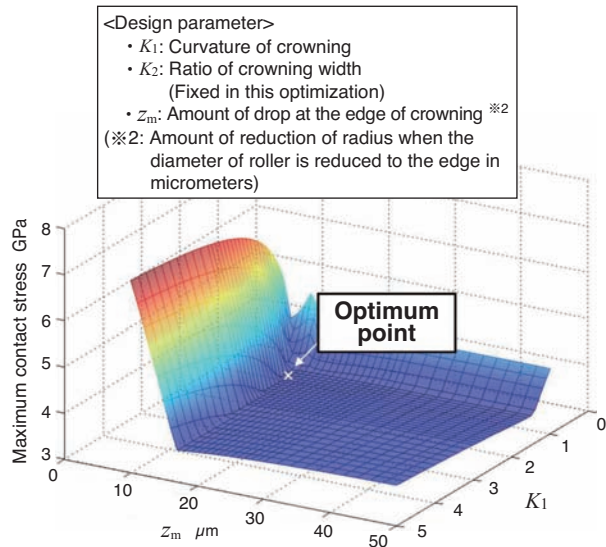


Fig. 3 Optimize by case-study of special crowning shape

different runs for exploring optimized solutions by several combinations of design parameters provide the optimum point to minimize the max. contact stress, as shown in Fig. 3, as well as the tolerance setting considering the range for minimizing the impact of the contact stress.

## 4. Bearing performance

### 4.1 Clean oil lubrication life test under highly misaligned conditions

In order to determine the life level of ULTAGE Tapered Roller Bearing for Automotive Applications, a clean oil life test was conducted under highly misaligned conditions (0.002 rad), which is considered to be the maximum level of misalignment under the operating conditions of vehicles.

<Test conditions>

- Bearing material heat treatment: SUJ2 standard heat treatment
- Load: 26% of basic dynamic load rating
- Misalignment: 0.002rad
- Rotational speed: 4,000min<sup>-1</sup>
- Lubrication: Equivalent to ISO VG100 gear oil
- JIS calculated operating life: 73h ( $a_2$  factor (life adjustment factor for special bearing properties) not considered)

Fig. 4 shows the test results. The result shows that the conventional tapered roller bearings do not satisfy the JIS calculated operating life with 29.4h of 10% life ( $L_{10h}$ ), as the edge originated surface damage progresses under this test condition where edge load is applied. On the other hand, ULTAGE Tapered Roller Bearing for Automotive Application "Standard

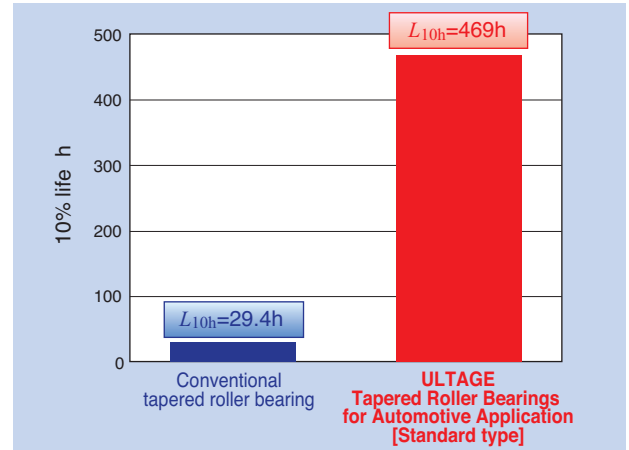


Fig. 4 Clean oil life time test under high misalignment condition

Type" has 469h of  $L_{10h}$ , which is approx. 16 times the conventional tapered roller bearings and 6.5 times the JIS calculated life. This is due to the optimization of the contact stress distribution and adoption of special crowning which eliminated edge loading.

When, for example, "Harris' Equation" <sup>7)</sup> is applied to these ULTAGE bearings with the long-life effect characteristics, even when misalignment increases, the rolling fatigue life under high misalignment (0.002rad or more) does not exceed the permissible contact stress rating and indicates 2.5 times life or more compared to conventional tapered roller bearings. ULTAGE Tapered Roller Bearings for Automotive Applications adopts this theoretical life comparison as the basic rated life comparison. When this is converted to an increase of the basic dynamic load capacity, it is equivalent to 1.3 times.

### 4.2 Life testing with contamination in the lubricant

Life tests under conditions of hard foreign objects in the lubricant were conducted for NTN's conventional long life ECO-top tapered roller bearings (long-life type where carbonitriding treatment is applied to carburized steel) and ULTAGE Tapered Roller Bearings for Automotive Applications .

<Test conditions>

- Bearing material heat treatment
  - (1) ULTAGE: FA thermal treatment on bearing steel
  - (2) ECO-Top: Carbonitriding treatment on carburized steel
- Load: 40% of basic dynamic load rating
- Misalignment: None
- Rotational speed: 3,000min<sup>-1</sup>
- Lubrication: ISO VG56 turbine oil
- Foreign object condition: Hard gas-atomized powder 0.2g/L foreign object under NTN specification
- Calculated operating life: 113.8h ( $a_2$  factor not considered)

Fig. 5 shows the test results. Compared to the conventional long-life type ECO-Top tapered roller bearings' 10% life ( $L_{10h}$ )  $L_{10h}=19.5h$ , ULTAGE Tapered Roller Bearings for Automotive Application [high functionality type] exhibited  $L_{10h}=32.8h$ , approx. 1.7 times longer life, due to nitration of FA heat treatment and improvement of roller fatigue strength through grain refinement.

Here, the  $a_2$  factor of ULTAGE Tapered Roller Bearings for Automotive Applications [high functionality type] is considered. With the life test result of ECO-Top tapered roller bearings as the baseline, foreign object factors of such a test is assumed.

$$\gt 19.5 \text{ (test result } L_{10h}) / [113.8 \text{ (calculated operating life)} \times 2.8 \text{ (} a_2 \text{ factor)}] = 0.0612$$

Using the calculated foreign object factor 0.0612,  $a_2$  factor of ULTAGE Tapered Roller Bearings for Automotive Application [high functionality type] is calculated.

$$\gt 32.8 \text{ (test result } L_{10h}) / [113.8 \text{ (calculated operating life)} \times 2.5 \text{ (ULTAGE life ratio)} \times 0.0612 \text{ (foreign object factor)}] \doteq 1.9$$

From the above result,  $a_2=1.5$  is adopted as a conservative value for the  $a_2$  factor of ULTAGE Tapered Roller Bearings for Automotive Applications [high functionality type].

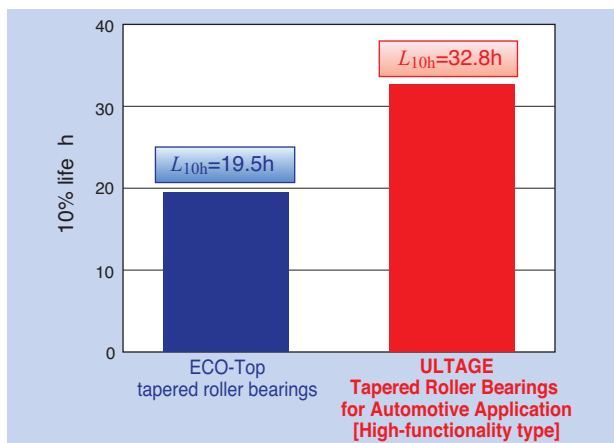


Fig. 5 Life time test under contaminated lubrication condition

### 4.3 Rotational speed verification test.

A temperature rise test was conducted under the permitted rotational speed.

Fig. 6 shows the result of the temperature rise test and Table 1 shows the summary of the test results. The conventional tapered roller bearings showed 95.2°C as the bearing average temperature in the stable temperature range at 10,100min<sup>-1</sup>, which is the permitted rotational speed. ULTAGE Tapered Roller

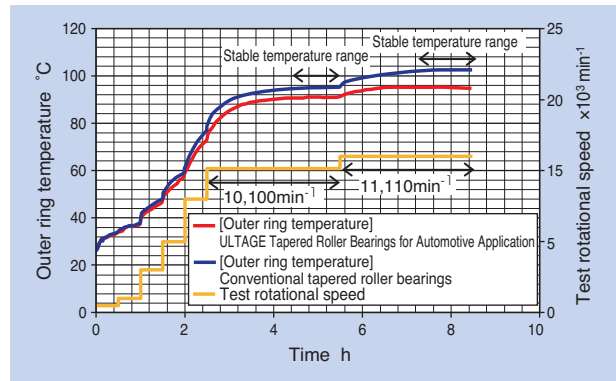


Fig. 6 Temperature rise test

Table 1 Test results in stable region temperature summary

	Rotational speed (min <sup>-1</sup> )	
	10,100	11,110
ULTAGE Tapered Roller Bearings for Automotive Applications	91°C	94.3°C
Conventional tapered roller bearings	95.2°C	102°C

Bearings for Automotive Applications showed 94.3°C as the bearing average temperature in the stable temperature range at 11,110min<sup>-1</sup>, which is 1.1 times the permitted rotational speed, indicating a low rise in temperature compared with conventional tapered roller bearings. Therefore, it is possible to improve the permitted rotational speed of ULTAGE Tapered Roller Bearings for Automotive Applications by 10% compared to conventional products.

<Test conditions>

- Load: 9% of basic dynamic load rating
- Lubrication: ISO VG32 turbine oil

## 5. Compact/lightweight design

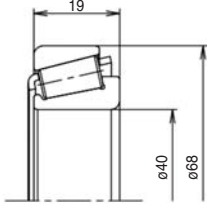
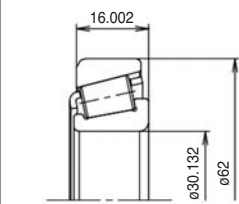
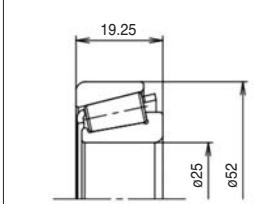
Since ULTAGE Tapered Roller Bearings for Automotive Applications can obtain long operating life by minimizing contact stress, it is possible to achieve a compact/lightweight design of bearings under the same life conditions. In this section, an example of a small/lightweight design study is shown.

The following is an example of a small/lightweight design when ULTAGE specifications are applied to the catalog standard type tapered roller bearings 32008X.

<Study conditions>

- Load condition:
  - Maximum load during driving conditions (equivalent to 1st gear full torque)
- Determination of life:
  - Calculated by JIS calculated operating life using dynamic load ratings

**Table 2** Study example of downsizing and lightweight of applying the ULTAGE tapered roller bearing for automotive application

Specification	Conventional tapered roller bearings	ULTAGE Tapered Roller Bearings for Automotive Application [Standard type]	ULTAGE Tapered Roller Bearings for Automotive Application [High-functionality type]
Model number	32008X	17119/17244	32205R
Bearing size	φ40×φ68×19	φ30.162×φ62×16.002	φ25×φ52×19.25
Bearing weight (compared to conventional product)	0.273kg	0.226kg (17% reduction)	0.181kg (34% reduction)
Basic dynamic load rating $C_r$ (N)	Conventional: : 50,000N	51,500N (Conventional: : 39,000N)	50,000N (Conventional: : 38,000N)
Result of contact stress determination (equivalent to 1 <sup>st</sup> full torque load)	Satisfied the standard [However, edge load occurred]	Satisfied the standard [No edge load occurred]	Satisfied the standard [No edge load occurred]
Life ratio compared to conventional standard	1	1.10	1.90
Cross section diagram			

- Determination of contact stress: Satisfy the NTN standard
- Selection of small/lightweight model number: The most compact model number is selected from the standard catalog series

**Table 2** shows the study results. The ULTAGE Tapered Roller Bearings for Automotive Applications [standard type] can achieve a 17% reduction in weight while the ULTAGE Tapered Roller Bearings for Automotive Application [high functionality type] can achieve a 34% reduction in weight.

In addition, reduced weight was also achieved in other model numbers with different sizes from the above, as follows:

- ULTAGE for Automotive Applications [standard type]: 15% - 30%
- ULTAGE for Automotive Applications [high functionality type]: 30% - 45%

## 6. Conclusion

We believe that the "ULTAGE Tapered Roller Bearing for Automotive Applications," which contributes to a reduced burden on the environment and fuel efficiency, is a new product that will be installed on vehicles worldwide as the standard product, and contribute to a low-carbon society.

Furthermore, NTN also developed new processing technology in line with the new design technology, establishing new technology for "Monozukuri."

NTN will continue to advance technological innovation of tapered roller bearings for automotive applications and contribute to the international community through development of new products.

## References

- 1) Ministry of Environment HP, A Proposal for Low Carbon Energy for Achieving Low Carbon Society, <http://www.env.go.jp/earth/ondanka/rmsuggestion.html>
- 2) Ministry of Environment HP, Global Trend of Environmental Tax on Vehicles, [http://www.env.go.jp/policy/tax/misc\\_jokyo.html](http://www.env.go.jp/policy/tax/misc_jokyo.html)
- 3) Hiroki Fujiwara, Tatsuo Kawase, Logarithmic Profile of Rollers in Roller Bearing and Optimization of the Profile, NTN TECHNICAL REVIEW, No.75 (2007), 140-148.
- 4) NTN Large Tapered Roller Bearings ULTAGE Metric Series, Catalog, CAT. No.3035/J.
- 5) Chikara Ooki, Kikuo Maeda, Hirokazu Nakashima, Improving Rolling Contact Fatigue Life of Bearing Steels Through Grain Refinement, NTN TECHNICAL REVIEW, No.71 (2003), 2-7.
- 6) NTN, Roller Bearings, Overview Catalog, CAT. No. 2202 - VII/J.
- 7) Harris, T. A., Rolling Bearing Analysis, Forth Edition, (2000), pp.728-729, John Wiley & Sons.

## Photo of authors



Yasuhito FUJIKAKE  
Automotive Bearing Engineering Dept., Automotive Business Headquarters



Takanori ISHIKAWA  
Automotive Bearing Engineering Dept., Automotive Business Headquarters



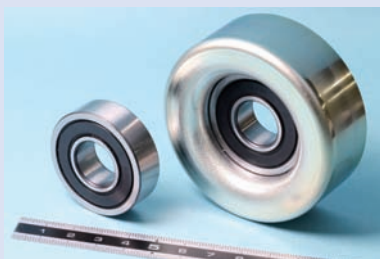
Susumu MIYAIRI  
Automotive Bearing Engineering Dept., Automotive Business Headquarters

## High Speed Rotation Ball Bearing for Pulley

Hayato KAWAGUCHI\*

Shouhei FUKAMA\*

Masaharu INOUE\*\*



Layout of auxiliary belt becomes complicated by engine downsizing, and high speed rotation performance of pulley bearings accompanying miniaturization of pulley diameter is required.

NTN has developed “High Speed Rotation Ball Bearing for Pulley” capable of handling 20,000min<sup>-1</sup> at outer ring rotation (by #6203).

This article introduces the feature and performance of the High Speed Rotation Ball Bearing for Pulley.

### 1. Introduction

Due to a recent increase of small engines and ISG-mounted vehicles focused on downsizing technology, layout of engine auxiliary system has become complex with greater restrictions on placement of auxiliary belts and bearings for pulleys. Degree of freedom for placement layout increases by reducing pulley diameters; however, that forces the bearings for pulleys to rotate at higher speeds.

In addition, requirements for improving comfort and reliability of automobiles are demanding bearings for pulleys to acquire higher functionality such as measures against hooting noises when running cold and protection against brittle flaking, as well as low torque properties<sup>1)</sup>.

High Speed Rotation Ball Bearings for Pulleys are capable of enduring up to 20,000 rotations (outer wheel rotation) per minute by suppressing a rise in heat by optimizing the cage, seal, inner/outer rings, balls and grease.

At the same time, they achieved retaining and improving measures against hooting noises when running cold, protection against brittle flaking and low torque properties.

This developed product is introduced in the following:

### 2. Characteristics

The following are the characteristics of the High Speed Rotation Ball Bearings for Pulleys:

High speed:

permitted rotational speed of 20,000min<sup>-1</sup>  
(in rotation with outer ring size of 6203)

Hooting noise when running cold:

no noise at -40°C

Protection against brittle flaking:

equivalent to the conventional product  
(under NTN test conditions)

Running torque:

10% reduction  
(compared to NTN conventional product)

Durability against high temperature:

equivalent to the conventional product  
(under NTN test conditions)

### 3. Structure and performance

#### 3.1 High speed

Fig. 1 shows issues associated with high speed rotation of bearings for pulleys.

In high speed rotation, cages can deform due to centrifugal force causing friction with steel balls and outer rings which produces heat. In addition, as the bearings for pulleys are used for outer ring rotation,

\*Automotive Bearing Engineering Dept., Automotive Business Headquarters

\*\*Application Engineering Dept., Automotive Business Headquarters

<b>Deformation of cage</b>	Cage deforms due to centrifugal force, causing friction with steel balls and outer rings which produces heat
<b>Deformation of seal lip</b>	Seal lips deform due to centrifugal force and seal reaction force changes→heat generation or sealing property loss
<b>Shortage of grease supply</b>	Shortage of grease supply due to centrifugal force causes heat generation, seizure and reduction of bearing life
<b>Increase in rolling resistance</b>	Rolling resistance increases due to high speed rotation, causing heat generation, seizure and reduction of bearing life

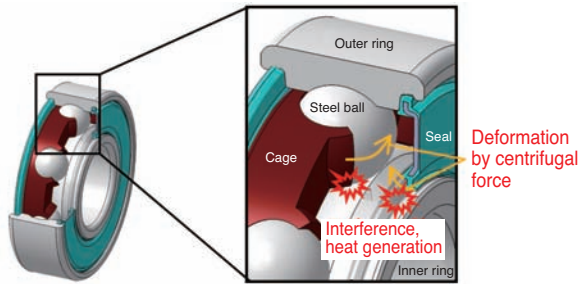


Fig. 1 Issues of bearing at high speed rotation

centrifugal force is also applied to the seal lips, causing heating or damage to seal properties due to a change of seal reaction force. Furthermore, seizure or bearing life reduction may be caused by shortage of grease supply and increased rolling friction.

Due to these issues, the permitted rotational speed of bearings for pulley was conventionally around 15,000min<sup>-1</sup>.

### 3.2. Design objectives of developed product

The cage, seal, inner/outer rings and steel balls of the High Speed Rotation Ball Bearings for Pulleys (hereafter "developed product") are made to endure high speed rotation.

#### 3.2.1 Cage

For the shape of cage of the developed product, resin cage developed for Grease Lubrication Type High Speed Deep Groove Ball Bearings for EVs and HEVs<sup>2)</sup> was adopted.

Fig. 2 shows the comparison with the conventional resin cages.

The following 3 points were improved to reduce deformation during high-speed rotation.

- (1) Thicker pocket bottom  
→ improvement of cage rigidity
- (2) Reduction of material between cage pockets  
→ reduction of centrifugal force
- (3) Adoption of high strength material  
→ improvement of cage rigidity

The results of centrifugal analysis of the cages are shown in Fig. 3 and 4.

The rotation speed conditions for the conventional resin cages were 15,000min<sup>-1</sup>, and were set to 20,000min<sup>-1</sup> for the High Speed Rotation Ball Bearings for Pulleys. We confirmed that the deformation from the centrifugal force of the resin cage for high-speed rotation, which underwent severer rotational speed conditions, was reduced by approx. 30% compared to the conventional product at the edges A and B (Fig. 4) of the cage where the friction with the outer ring and steel ball is suspected.

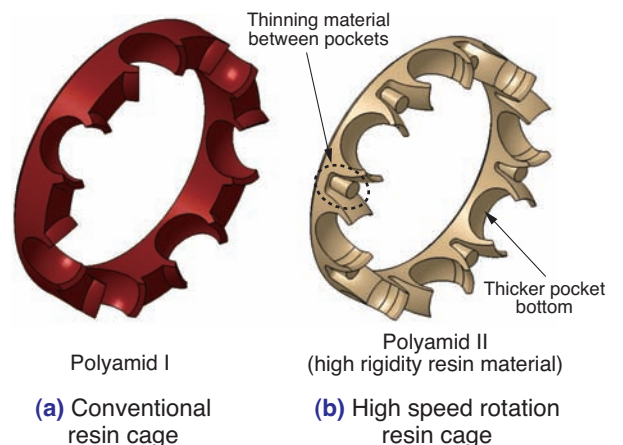


Fig. 2 Cage shape (Comparison of current and developed)

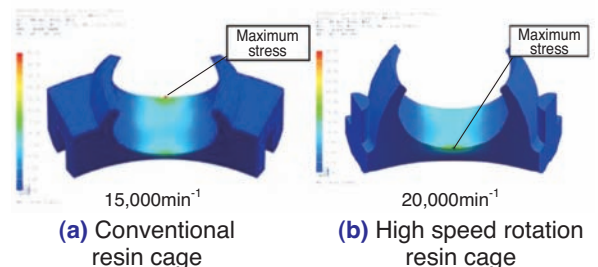


Fig. 3 Cage centrifugal analysis (Comparison of current and developed)

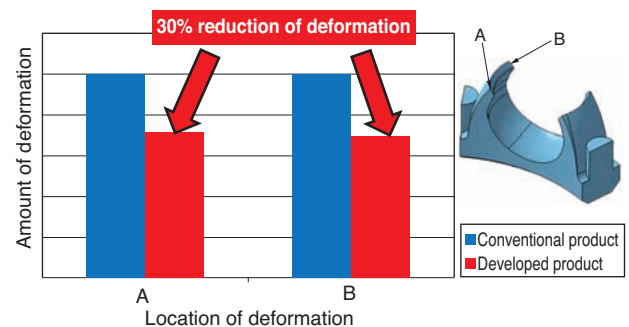


Fig. 4 Deformation amount of current and developed

### 3.2.2 Seal

Fig. 5 shows an overview of NTN's standard bearing seal for pulley.

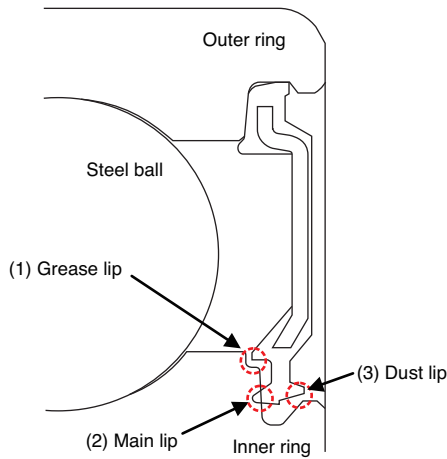


Fig. 5 NTN standard bearing seal for pulley

The standard bearing seal for pulley consists of 3 lips.

#### (1) Grease lip

→ Penetration of grease to the area around the main lip is reduced by the labyrinth structure with the inner seal groove to prevent grease leakage

#### (2) Main lip

→ Prevention of grease leakage and penetration of water/dust, as well as low torque are ensured, maintaining interference even with centrifugal force due to rotation of the outer ring

#### (3) Dust lip

→ Penetration of foreign objects from outside is reduced by the labyrinth structure with the inner seal groove  
Even when penetration occurs, they can be ejected by the tapered shape of the dust lip

For the shape of the developed seal, the center of gravity of the seal lip and thickness of the waist section of the lip are optimized to minimize variation of reaction force in the high-speed rotation range for reducing heat and to keep low torque. The result of analysis of the seal reaction force is shown in Fig. 6 and 7.

With the conventional products, seal reaction force tends to decrease when rotational speed increases regardless of the initial seal interference, and heat generation due to seal interference becomes unstable even at a high rotational speed range around 20,000min<sup>-1</sup>, because of large variance of seal reaction force.

On the other hand, with the developed products,

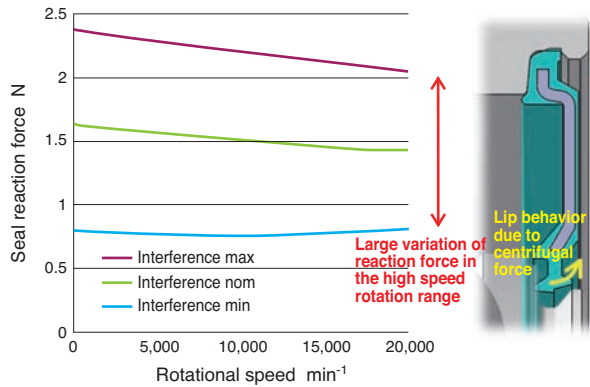


Fig. 6 Seal centrifugal force analysis (Current)

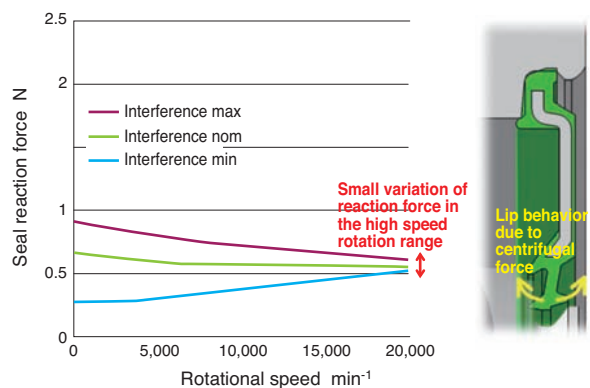


Fig. 7 Seal centrifugal force analysis (Developed)

variance of seal reaction force is small, which reduces heat generation at high rotational speed range even with different initial seal interference, as the center of gravity of seal lips is optimized.

Seal interference and torque (calculated value) of the conventional and developed products are shown in Fig. 8 and 9.

The seal interference of the developed product is increased to improve the seal lip followability. On the other hand, lip rigidity is reduced, which achieved low torque and low heat generation by optimizing the thickness of the waist section of the seal lip.

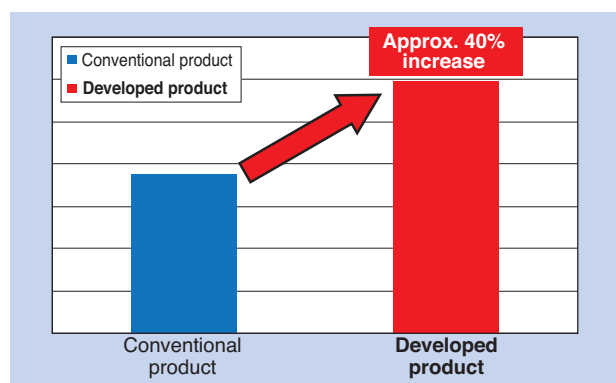


Fig. 8 Seal calculation interference (Comparison of current and developed)

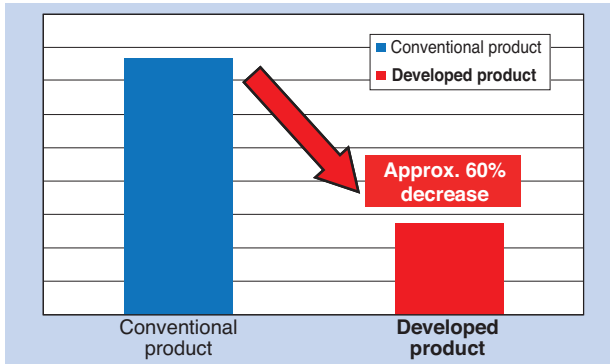


Fig. 9 Seal calculation torque (Comparison of current and developed)

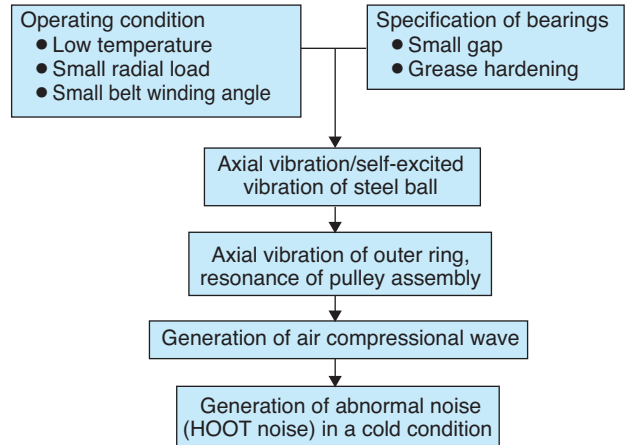


Fig. 10 Generation mechanism of hoot noise

### 3.2.3 Bearing internal specification

Bearing internal specification of the developed product was set to maintain load carrying capacity compared to the conventional product, and to decrease PCD and reduce heat generation by revising steel ball size.

Table 1 shows the bearing internal specification.

Table 1 Internal specification comparison of current and developed

Specification	Conventional bearings	Developed bearings
Key dimensions (mm) * inner diameter x outer diameter x width	φ17×φ40×12	←
Size and number of steel balls	9/32in × 7	17/64in × 8
Basic dynamic load rating (N)	9,600	9,500
Basic static load rating (N)	4,600	4,700

### 3.3 Other requirements of bearings for pulleys and their measures

#### 3.3.1 Hooting noise when running cold

Hooting noise when running cold is a high pitch tone, like a whistle generated when running in low temperatures, known to be generated for a few seconds from the bearings for pulleys when an engine starts.

Fig. 10 shows the presumed mechanism of the hooting noise. Since a decrease of grease consistency in low temperatures is assumed to be the cause of the hooting noise, newly developed grease with improved low temperature fluidity was adopted for the developed product.

Table 2 shows a comparison of the grease characteristics for the conventional product and developed product.

The developed grease lowered the fluid point in low temperatures with softer consistency. This achieved 100% pass rate of hooting noise (no hooting noise) when running cold at -40°C from 70% of the conventional products under the NTN measurement conditions.

Table 2 Grease characteristics comparison

Item	Conventional grease (1)	Conventional grease (2)	Developed grease
Base oil	Ester + PAO	Ester	Ester + PAO
Thickener	Urea	Urea	Urea
Base oil fluid point (°C)	-42.5	-42.5	-50 or less
Worked penetration	270	280	286

#### 3.3.2 Protection against brittle flaking

Brittle flaking is a singular flaking including microstructural change which is observed in the bearings used for accessories of automotive engines and occasionally in the bearings for pulleys, as well.

Fig. 11 shows the presumed mechanism of the brittle flaking<sup>1) 3)</sup>.

The developed product suppresses slipping of steel balls and penetration of hydrogen by adjusting grease additives and thermal treatment of inner/outer rings to ensure protection against brittle flaking equivalent to the conventional products.

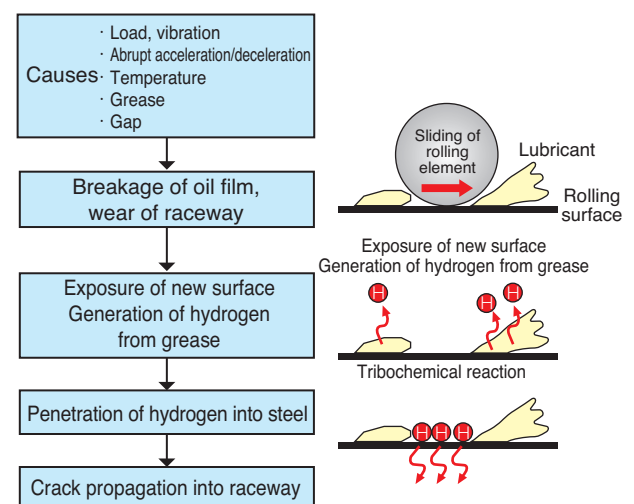


Fig. 11 Generation mechanism of brittle flaking

### 3.4. Evaluation results of developed product

#### 3.4.1 Test of elevation in temperature

Elevation of temperature due to an increase in rotational speed was confirmed in the test. The test conditions are shown in **Table 3**, appearance of tester is shown in **Fig. 12** and the test results are shown in **Fig. 13**, respectively.

Elevation of temperature of the developed product at 20,000min<sup>-1</sup> was less than that of the conventional product at 15,000min<sup>-1</sup>. The developed product achieved a permitted rotational speed of 20,000min<sup>-1</sup>.

**Table 3** Test condition

Bearing size	6203
Radial load (N)	960
Belt winding angle (°)	180
Atmosphere temperature (°C)	100

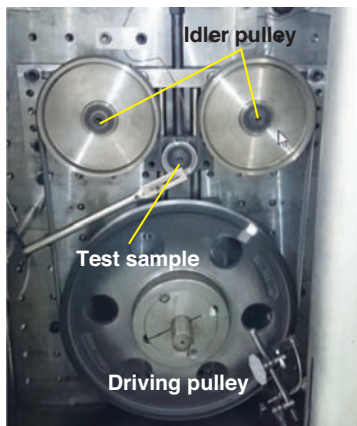


**Fig. 12** Temperature rising tester

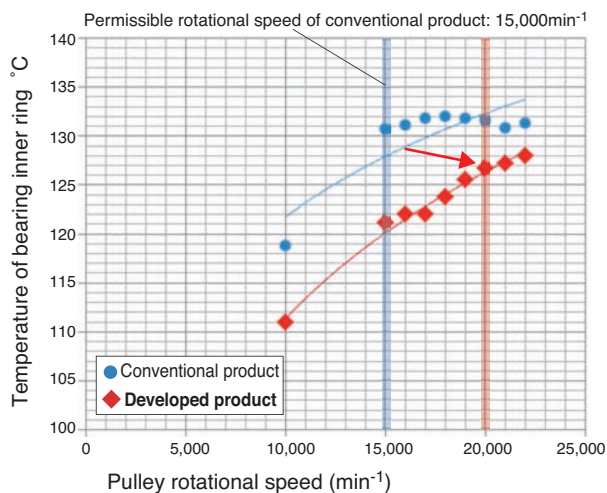


**Fig. 13** Temperature rising test result

#### 3.4.2 High speed durability test

Durability at the rotational speed of 20,000min<sup>-1</sup> was confirmed. The test conditions are shown in **Table 4** and the appearance of the test product after the test is shown in **Fig. 14**.

The durability equivalent to the conventional product was confirmed after 400 hours of operating time without flaking, seizure, damage or abnormal noise.

**Table 4** Test condition

Bearing size	6203
Radial load (N)	960
Belt winding angle (°)	180
Pulley rotational speed (min <sup>-1</sup> )	20,000
Atmosphere temperature (°C)	80
Operating time (h)	400



**Fig. 14** Appearance of after test sample

#### 3.4.3 Running torque

Torque reduction effects were confirmed in the low temperature torque test. The test conditions are shown in **Table 5** and the test results in **Fig. 15**.

The low temperature torque of the developed product was confirmed to be approx. 15% lower than the conventional product.

**Table 5** Test condition

Bearing size	6203
Radial load (N)	No-load (only the weight of test jig)
Inner ring rotational speed (min <sup>-1</sup> )	0→12,000 (60s sweep)
Outer ring temperature (°C)	-40

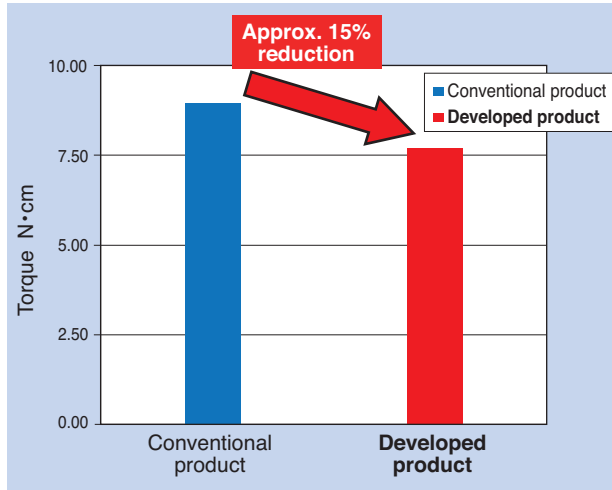


Fig. 15 Torque measurement results at low temperature

## References

- 1) Takayuki Kawamura, Hidenobu Mikami, Development of Long Life Grease 'NA103A' for Automotive Components, NTN TECHNICAL REVIEW, No. 75, (2007).
- 2) Masahiko Satoda, Goro Nakao, Grease Lubricated High-speed Deep Groove Ball Bearing for EV and HEV Motor, NTN TECHNICAL REVIEW No. 83 (2015).
- 3) Seiichi Nozaki, Koushirou Fujimoto, Kenji Tamada, Brittle Flaking on Bearings for Electrical Instruments and Auxiliary Devices and Life Extension of these Bearings NTN TECHNICAL REVIEW No.61 (1992).

## 4. Conclusion

In this paper, we have introduced the High Speed Rotation Ball Bearings for Pulleys. This developed product achieved outer ring rotational speed of 20,000min<sup>-1</sup> with the size of 6203, and met the requirements of bearings for pulleys (measures against hooting noises when running cold, protection against brittle flaking and low torque properties), simultaneously, by optimizing design of the cage, seal, grease and bearing internal specifications.

The developed product is expected to contribute to downsizing and fuel efficiency of engines and will be actively marketed. We are poised to promote development of new products to meet the requirements of ongoing improvement of functionality.

Photo of authors



Hayato KAWAGUCHI  
Automotive Bearing  
Engineering Dept.,  
Automotive Business  
Headquarters



Shouhei FUKAMA  
Automotive Bearing  
Engineering Dept.,  
Automotive Business  
Headquarters



Masaharu INOUE  
Application  
Engineering Dept.,  
Automotive Business  
Headquarters

# Ultra Low Friction Sealed Ball Bearing for Transmission



Katsuaki SASAKI\*  
Takahiro WAKUDA\*  
Tomohiro SUGAI\*\*

Along with fuel-saving of automobiles, demands for lightweight, compact and low torque are increasing. In this report, we will introduce characteristics and performance of developed products with both low torque and long life of sealed ball bearing for transmission to utilize tribology technology.

## 1. Introduction

In order to mitigate life reduction under severe bearing operating conditions, where hard foreign objects such as gear wear particles are suspended in transmission lubricating oil, we have been improving the tolerance of our bearings for foreign objects by adopting contact seals and applying special heat treatment to special bearing material (open product) in order to mitigate life reduction under severe bearing operating conditions. However, bearings with contact seals work against the trend of increasing fuel savings<sup>1)</sup>, since they have increased bearing rotating torque due to the seal sliding friction. In addition, special heat treatment has a disadvantage of increased cost. NTN has developed a new mechanism for ball bearings with seals to achieve a significant reduction in running torque, while maintaining life equivalent to the bearings with special heat treatment, by leveraging tribology technology. The following is a description of such bearings.

## 2. Characteristics

The following are the characteristics of the developed product:

- 80% reduction of running torque (compared to bearings with contact seals)
- 5 times or more of bearing life (compared to open products)
- Support of high seal circumferential speed (50m/s or more)
- Prevention of harmful foreign objects from entering

## 3. Structure and performance

### 3.1. Design methods of developed product

Optimization of the following was the focus of reducing friction of contact seals:

- Seal contact pressure
- Surface roughness
- Rubber hardness

In addition to the above, we have focused on a seal shape with which the wedge film effect increases. With this change, friction of the seal lip contact of the developed product during rotation was in the hydrodynamic lubrication range in the Stribeck curve (Fig. 1), as opposed to the case of the conventional contact seal, where the friction of the seal lip contact usually stays in the boundary/partial film lubrication. This allows a drastic reduction of torque.

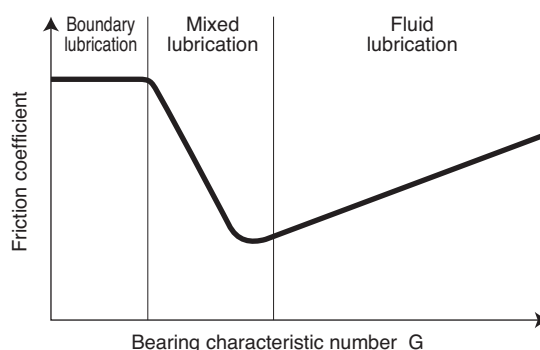


Fig. 1 Stribeck curve

\*Automotive Bearing Engineering Dept., Automotive Business Headquarters

\*\*Advanced Technical Research Center

### 3.2 Objective of seal design

When multiple arc-shaped micro convexes are placed evenly on the sliding surface of the seal lip (Fig. 2), a wedge film effect develops (Fig. 3) in an oil lubricated environment, like that of transmissions, which leads to the friction coefficient being in the hydrodynamic lubrication range during rotation.

For the shape of the micro convexes, the optimized shape drawn from our analysis "Fluid Lubrication Analysis (Soft EHL Analysis) considering rubber-like elasticity" (Fig. 4) was adopted. This achieved both low torque and long operating life.

Fig. 5 shows an example of FEM analysis of the developed product under the conditions in Table 1. Fig. 6 shows the minimum film thickness obtained from this analysis. It was verified that the minimum film thickness in the temperature range of Fig. 6 is in the hydrodynamics lubrication range of the Stribeck curve (Fig. 1).

Table 1 Analysis condition

Rotational speed (min <sup>-1</sup> )	1,500
Lubricating oil	CVTF
Bearing temperature (°C)	-40~120

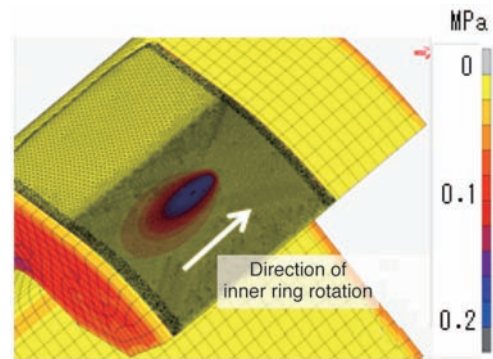


Fig. 5 Calculation result of oil film pressure distribution

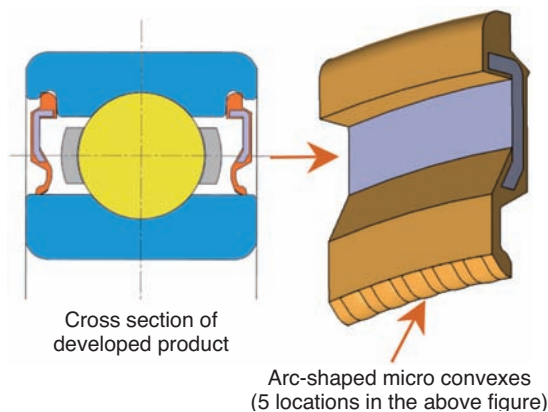


Fig. 2 Developed seal

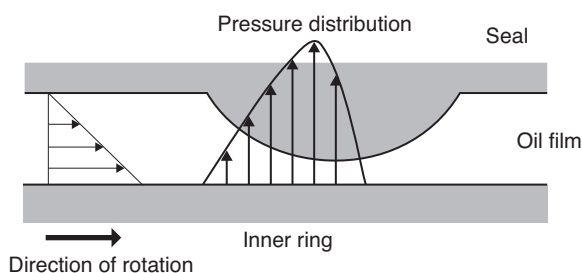


Fig. 3 Wedge film effect

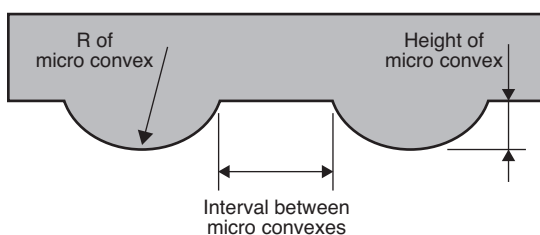


Fig. 4 Setting of micro convex

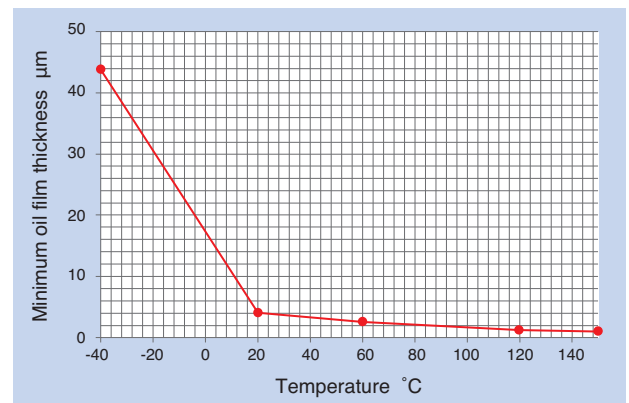


Fig. 6 Temperature and oil film thickness

### 3.3. Evaluation of developed product

An evaluation was conducted using test bearings equivalent to the product with the representative model number 6010, which is the support bearing for CVT vehicles with high market share.

#### 3.3.1 Running torque

##### (1) Bearing temperature and running torque

Running torque was measured with varied bearing temperatures. The test conditions are shown in Table 2 and measurement results in Fig. 7.

The developed product achieved 80% reduction of torque (compared to the bearing with conventional

Table 2 Test condition

Radial load	0.05C
Rotational speed (min <sup>-1</sup> )	1,500
Lubricating oil	CVTF
Bearing temperature (°C)	35~120

contact seals) and low torque equivalent to bearings with non-contact seals.

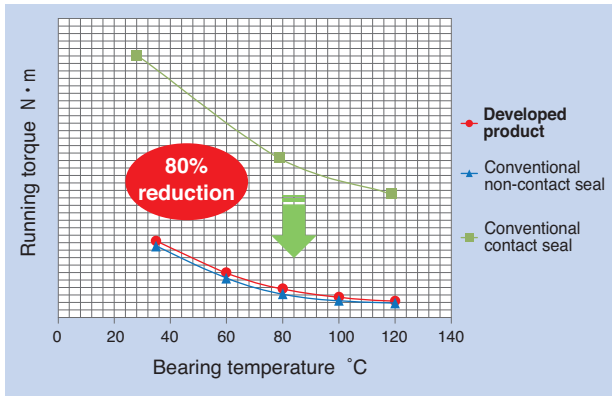


Fig. 7 Bearing temperature and rotation torque

**(2) Interference and running torque**

Running torque was measured with varied interferences. The test conditions are shown in Table 3 and measurement results in Fig. 8.

The developed product exhibited little change in torque, regardless of interference, due to wedge film effects.

Table 3 Test condition

Radial load	0.04C
Rotational speed (min <sup>-1</sup> )	1,500
Lubricating oil	CVTF
Bearing temperature (°C)	40, 80, 120

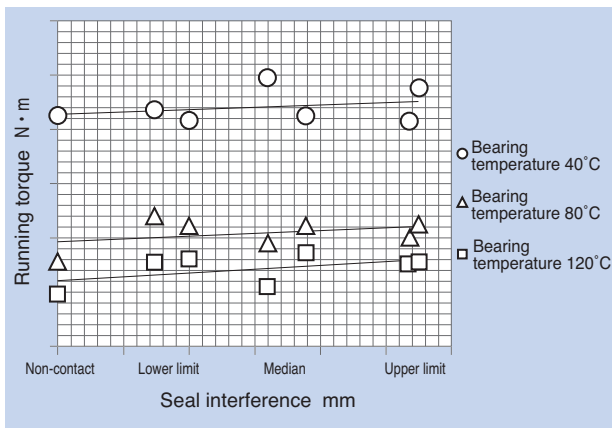


Fig. 8 Interference and rotation torque

**(3) Rotational speed and running torque**

Running torque was measured with varied rotational speeds. The test conditions are shown in Table 4 and measurement results in Fig. 9.

The developed product achieved 60-80% reduction of torque (compared to the bearing with conventional contact seals).

Table 4 Test condition

Radial load	0.05C
Rotational speed (min <sup>-1</sup> )	500–6,000
Lubricating oil	CVTF
Bearing temperature (°C)	80

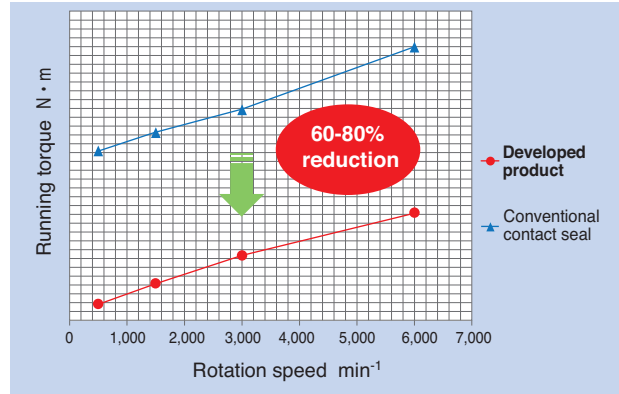


Fig. 9 Rotation speed and torque

**(4) Running torque assuming oil splash by gears**

Running torque was measured assuming oil splash conditions. The test conditions are shown in Table 5 and measurement results in Fig. 10.

The developed product mitigated excessive oil penetration due to the micro gap effect between the micro convex shapes, resulting in stable torque transition. On the other hand, the open product exhibited an increase of torque as oil stirring resistance increased due to oil splash.

Table 5 Test condition

Axial load	0.09C
Rotational speed (min <sup>-1</sup> )	5,000
Lubricating oil	300ml of turbine oil VG32 was injected
Bearing temperature (°C)	Natural rise in temperature

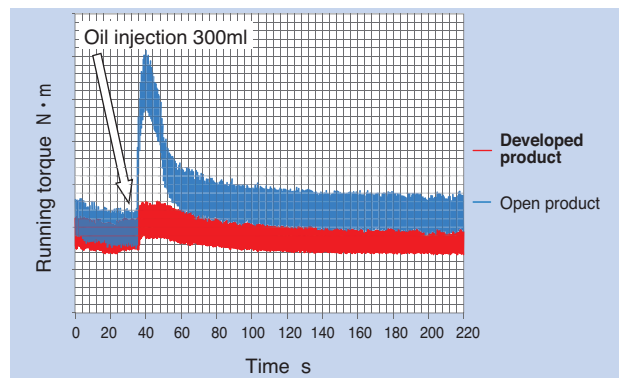


Fig. 10 Rotational torque under oil splash lubrication

### 3.3.2 Life/durability test

#### (1) Life test under contaminated lubrication

The effect on bearing life under contaminated lubrication was verified for with the developed product. The test conditions are shown in **Table 6** and measurement results in **Fig. 11** <sup>2)</sup> and **12**.

The developed product suppressed penetration of harmful foreign objects into the bearings through the microconvex effect exhibited. No flaking in any samples was found, even after suspending the test at 10 times the calculated operating life. Compared with the open products in terms of  $L_{10}$  life, the developed product achieved bearing life of 5 times or more. In addition, no significant rubber wear of the micro convexes was observed, maintaining low torque properties.

**Table 6** Test condition

Radial load	0.33C
Rotational speed (min <sup>-1</sup> )	2,000
Misalignment	2/1,000rad
Lubricating oil	CVTF immersion lubrication of shaft center
Bearing temperature (°C)	120
Condition of foreign objects 0.15 g/L	Steel beads up to 50µm 97wt% 50 to 100µm 3wt%

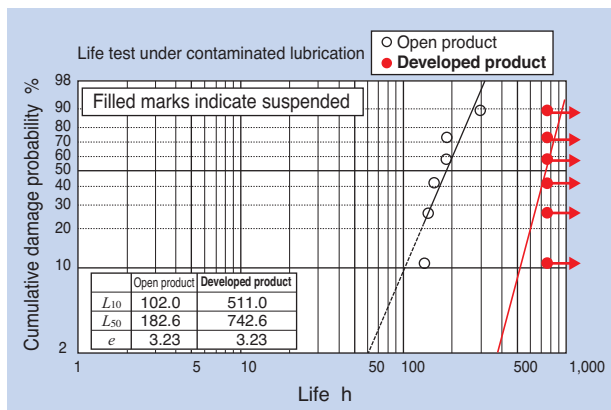


**Fig. 11** Bearing life under contaminated lubrication

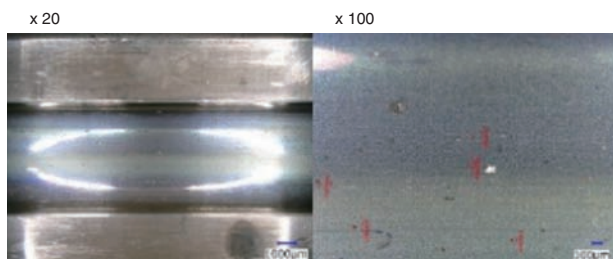


**Fig. 12** Appearance of inner ring surface after test

#### (2) Verification test under lubrication with a large amount of different foreign objects

Tolerance against foreign objects was verified under lubrication with irregular foreign objects with different particle diameters using a vertical type tester. The test conditions are shown in **Table 7** and measurement results in **Fig. 13**.

It was verified that the developed product mitigated penetration of foreign objects into the bearings due to the microconvex effect, even under lubrication with harder foreign objects than assumed. In addition, the penetrated foreign objects were similar in particle diameter and quantity to those in the bearings after the life test under contaminated lubrication shown in (1).

**Table 7** Test condition

Axial load	0.05C
Rotational speed (min <sup>-1</sup> )	3,000
Lubricating oil	Turbine oil VG10
Bearing temperature (°C)	Natural rise in temperature
Condition of foreign objects 1.0g/L	Steel beads up to 50µm 40wt% 50 to 100µm 30wt% 100 to 180µm 30wt%
Operating time (h)	6

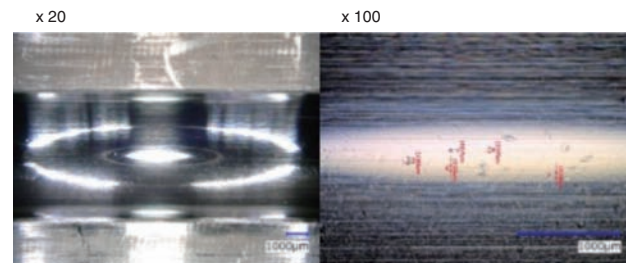


**Fig. 13** Appearance of inner ring surface after test

#### (3) Durability test under high seal circumferential speed

A durability test under high seal circumferential speed was conducted. The test conditions are shown in **Table 8** and measurement results in **Fig. 14**.

The developed product underwent the test until it was suspended without any abnormal rise in temperature. In addition, no significant rubber wear of the micro convexes was observed, maintaining low torque properties.

**Table 8** Test condition

Radial load	0.05C
Circumferential speed (m/s)	50
Lubricating oil	CVTF 7°C × 100ml Forced oil supply, immersion lubrication of shaft center
Bearing temperature (°C)	Natural rise in temperature
Operating time (h)	30

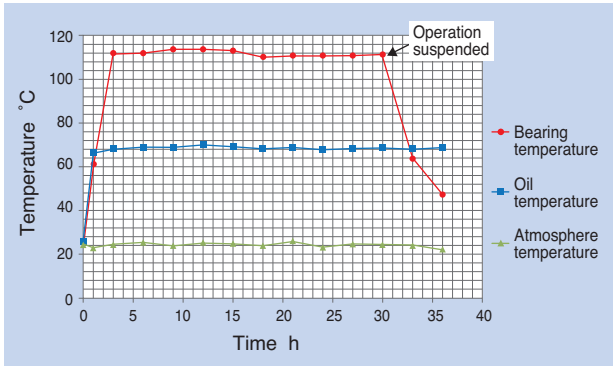


Fig. 14 Seal high peripheral speed endurance

**(4) Durability test with sudden acceleration/ deceleration under lubrication**

A durability test with sudden acceleration/deceleration under lubrication was conducted. Table 9 shows the test conditions.

The developed product underwent the test until it was suspended without any abnormal rise in temperature or significant wear of micro convexes, maintaining low torque properties. It was also verified by soft EHL analysis that an oil film was formed between the seal and inner ring at around 30-50rpm, entering the hydrodynamic lubrication range.

Table 9 Test condition

Radial load	0.05C
Circumferential speed (m/s)	Alternately between 0 and 50 2s rising, 2s falling
Lubricating oil	CVTF 70°C x 100ml Forced oil supply, immersion lubrication of shaft center
Bearing temperature (°C)	Natural rise in temperature
Operating time (h)	2.5

**3.3.3 Oil flow rate**

The oil flow rate of lubricating oil through the bearing was measured. The test conditions are shown in Table 10 and measurement results in Fig. 15.

It was verified that the developed product had approx. 8 times more flow rate than the conventional contact seal due to the micro gaps between micro convexes of the seal lip.

With these properties, it can achieve an appropriate supply of lubricating oil to the bearings, even with poor lubrication.

Table 10 Test condition

Axial load	0.05C
Rotational speed (min <sup>-1</sup> )	5,000
Lubricating oil	Turbine oil VG10
Bearing temperature (°C)	Natural rise in temperature
Operating time (s)	Measured time until 100ml of oil flow went through

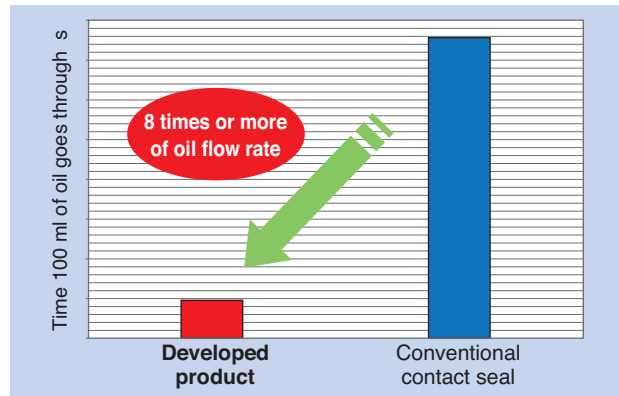


Fig. 15 Oil through time

**4. Conclusion**

In this paper, we have introduced the technology of Ultra-low Friction Sealed Ball Bearings for transmissions. This developed product achieves high functionality and can be produced without new investment in machines or equipment. We plan to actively market this as the main product of NTN's ball bearings for transmissions.

**References**

- 1) Ministry of Environment HP, Global Trend of Environmental Tax on Vehicles, [http://www.env.go.jp/policy/tax/misc\\_jokyo.html](http://www.env.go.jp/policy/tax/misc_jokyo.html)
- 2) Takumi Fujita, Strategy of Rolling Contact Fatigue Life Testing and Interpretation of Life Data, NTN TECHNICAL REVIEW No. 84 (2016)

Photo of authors



Katsuaki SASAKI  
Automotive Bearing Engineering Dept.,  
Automotive Business Headquarters

Takahiro WAKUDA  
Automotive Bearing Engineering Dept.,  
Automotive Business Headquarters

Tomohiro SUGAI  
Advanced Technical Research Center

## Low Friction Hub Bearing



Makoto SEKI\*

The fuel efficiency regulations has been strengthening, therefore the good fuel efficiency is one of the important requirement from the field. Based on this background, NTN has been developing the low friction hub bearing continuously.

The hub bearing applicable to such around 50% low friction requirement is introduced in this report.

### 1. Introduction

Recent initiatives to promote hybrid and electric vehicles over conventional vehicles, which use engines as their source of power, are being actively pursued. Hybrid vehicles combine engines and electric motors to power the vehicle, while electric vehicles use electric motors. Global increase in fuel costs and environmental issues, including global warming, are some of the factors behind this initiative. Reduction of energy required by vehicles is the focus with plans for strict fuel efficiency regulations by 2021 in Japan, U.S., and Europe. Automotive companies are competing every day to continually introducing new technology into the global market.

NTN, which has a large market share in passenger car hub bearings, is proposing various technology to achieve higher fuel efficiency <sup>1), 2)</sup>.

In this article NTN will introduce low friction hub bearings which achieve a torque reduction of approximately 50% by enhancing grease and seals.

### 2. Initiative for low friction properties

Fig. 1 shows a structural example of a generation 3 hub bearings.

Friction of hub bearings can be divided into rolling resistance of bearings and sliding resistance of seals, approximately 50% each. As shown in Fig. 2, various types of friction reduction technology have been developed. These include optimization of bearing specifications and use of resin as cage material for

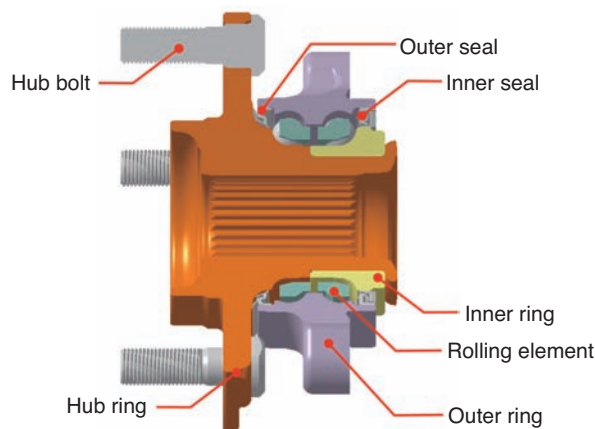


Fig. 1 Structure example of generation 3 hub bearing

reduction of rolling resistance. For reduction of sliding resistance, low friction seal rubber material has been developed and seal structure and interference have been optimized.

This article focuses on new bearing internal grease for further reduction of friction from rolling resistance by reexamining base oil, kinematic viscosity, and consistency, etc. Friction at the seals from sliding resistance was also further reduced by development of new grease for application to the seal lips. By reexamining seal structure, lip contact surface was optimized and contact of the seal lips was reduced.

\*Automotive Unit Engineering Dept., Automotive Business Headquarters

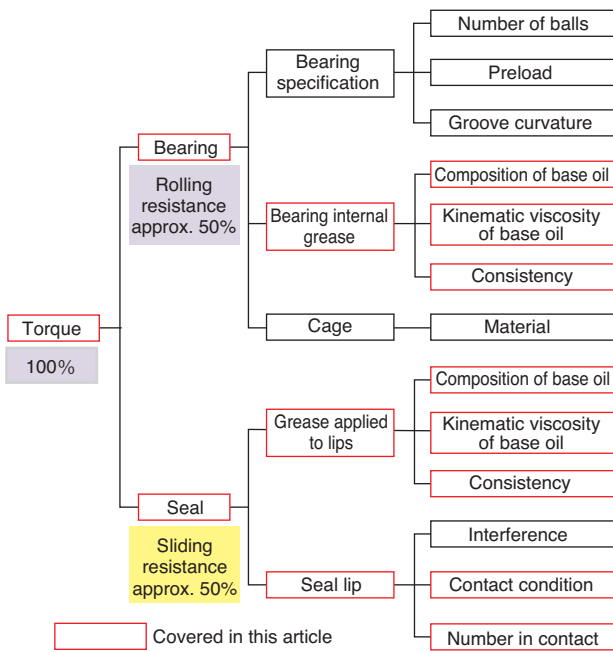


Fig. 2 Influence factor of bearing friction

2.1 Reduction of rolling resistance

2.1.1 Functional requirements and specifications of developed grease

In addition to low friction properties, the following functions are required for hub bearing internal grease.

- (1) Long life without shortage of oil film and seizure under the load, temperature and speed conditions of hub bearings
- (2) Excellent fretting resistance in low temperatures
- (3) Sufficient anti-corrosion and leakage prevention properties
- (4) Protection against penetration of foreign objects

Based on the above functional requirements, the specifications of the newly developed grease were determined as follows:

For reduction of torque, reducing kinematic viscosity of grease base oil and softening grease are general methods to suppress stirring resistance; however, it may cause bearing flaking and grease leakage by oil film shortage. Especially, in high temperatures, reduction of kinematic viscosity of base oil becomes significant; therefore, the possibility of flaking may increase.

Therefore, as shown in Table 1, in order to solve poor lubrication conditions in high temperatures while pursuing low friction, which is a contradictory condition, at the same time base oil with high viscosity index was applied. The kinematic viscosity of base oil was designed to be reduced to room temperature or lower, yet maintained at the level equivalent to the conventional product in high temperatures. In addition,

thickener was optimized to further reduce stirring resistance as well.

Furthermore, in order to reduce fretting wear due to vibration during long-haul transportation, base oil with a low pour point and anti-wear agent were blended to improve fretting properties in low temperatures.

Table 1 Concept of grease property

Grease properties	Comparison with conventional product
Base oil	Application of base oil with high viscosity index Application of base oil with low pour point
Kinematic viscosity of base oil	Low to room temperature: reduced High temperature: equivalent to conventional product
Thickener	Optimized
Additives	Application of anti-wear agent

2.1.2 Evaluation test

Running torque test of hub bearings with the developed grease was conducted without seals.

The results are shown in Fig. 3. With a torque reduction rate of 24% compared to the conventional product, the reduction of rolling viscosity resistance with low viscosity properties of the bearing internal grease was verified.

In addition, the reliability evaluation test shown in Table 2 was conducted to verify the required functions. The bearings with the developed grease met the development objectives in all the test items, satisfying the functional requirements for bearing internal grease.

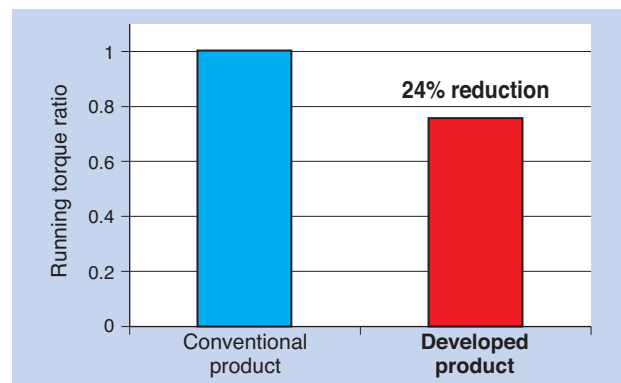


Fig. 3 Rotation torque test (room temp.)

Table 2 Bearing grease reliability evaluation test

Test item	Result
Bearing life during vehicle turning*1	3 times or more than the rated life
Seizure properties during high-speed rotation*2	No seizure on bearing raceway surface
Low temperature fretting*3	78% reduction of wear amount (compared to conventional product)

\*1 Turning load: 0.6G load condition

\*2 Rotational speed condition of vehicle velocity of 200km/h

\*3 Micro dynamic wear test under a -20°C environment

## 2.2 Reduction of sliding resistance

### 2.2.1 Functional requirements and specification of developed seals

Fig. 4 shows a structural example of the outer seal and inner seal adopted in generation 3 hub bearings. The outer seal shown in Fig. 4 (a) is a standard 3-lip seal type. The inner seal shown in Fig. 4 (b) is a Hypack type design of cassette type with the slinger with stainless steel based sliding material integrated in the unit. Since 50% of the friction of hub bearings comes from the sliding resistance, improvement in this aspect was pursued, while maintaining tolerance against muddy water and air-tightness.

In this development, low friction was achieved by optimization of seal lip contact (sliding) surface, development of grease dedicated for seal lip application, and reduction of number of seal lip contacts by optimizing the peripheral structure, compared to the conventional product.

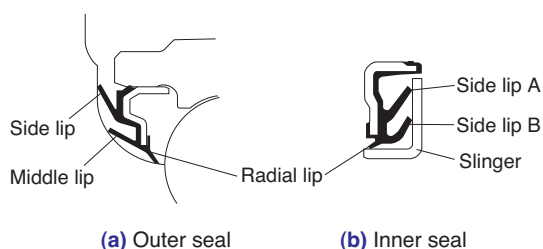


Fig. 4 Structure example of seal

### 2.2.2 Optimization of seal lip contact

The conventional seal lip contact surface has even contact to the circumference of the mating material, with no irregularities on the surface. On the other hand, the developed product has micro irregularities on the sliding surface or seal lip surface (Fig. 5). These irregularities reduce the contact area with the mating material and form sufficient oil film on the contact surface since the recessed area can retain

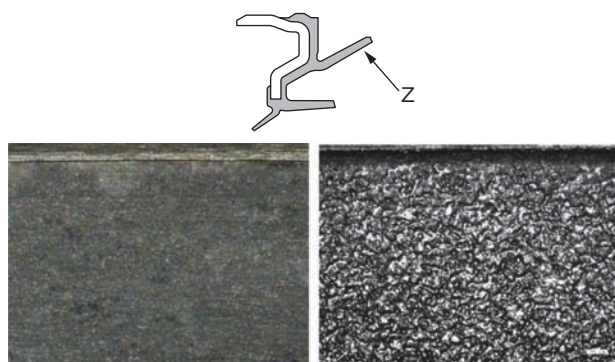


Fig. 5 Seal lip surface (the enlargement from Z)

grease. The roughness of the seal surface was determined in the range that produces friction reduction effects and does not undermine tolerance against muddy water and air-tightness.

### 2.2.3 Grease dedicated to seals

In general, grease applied to the tip of seal lips is the same as the grease injected inside the bearings to avoid adverse effects when mixed with each other. However, we have developed grease dedicated to seals specially formulated for the requirements of seals to reduce friction.

In the development of grease dedicated to seals, the following two points were considered under the assumption of securing the basic seal performance.

Reduce sliding resistance by decreasing kinematic viscosity of base oil.

Avoid any adverse effects to the function of the bearings, even when mixed with internal grease.

### 2.2.4 Reduction of number of seal lip contacts

In general, a seal has a structure to possess 3 lips in contact in order to secure required tolerance against muddy water; however, we reduced the number of lips in contact to achieve lower friction.

Fig. 6 shows an example of seal structures of the developed product. Deterioration of tolerance against muddy water due to reduction of number of lip contacts was avoided by placing a labyrinth structure on the outside and by arranging the seal shape.

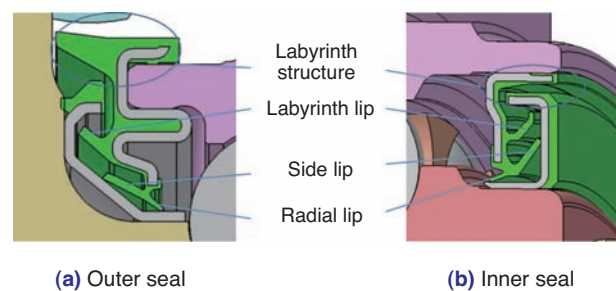


Fig. 6 Structure example of developed seal

### 2.2.5 Evaluation test

Running torque test was conducted with the individual seal. The results are shown in Fig. 7.

The developed product showed approximately 70% torque reduction compared to the conventional product by optimization of seal lip contact surface, and reduction of number of contacts and application of grease dedicated to seals. A significant reduction of seal sliding resistance in rotation was achieved.

In addition, a reliability evaluation test against NTN specifications shown in Table 3 was conducted to verify the required functions. Although the reduction of number of lips may have caused deterioration of tolerance against muddy water, penetration of muddy water into the contact lip area was reduced by setting a labyrinth structure. The developed product achieved equivalent tolerance against muddy water as the conventional product.

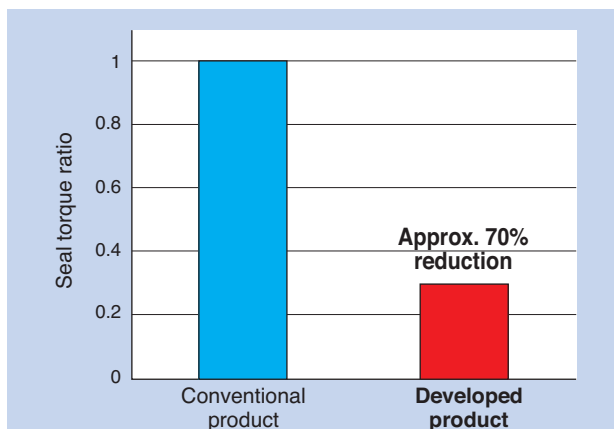


Fig. 7 Rotation torque test (room temp.)

Table 3 Low-friction seal reliability evaluation test

Test item	Result
Property against muddy water*1	Equivalent to conventional product
Airtightness*2	Equivalent to conventional product
Heat resistance*3	Equivalent to conventional product

\*1 NTN test for tolerance against muddy water  
 \*2 NTN test for rotational airtightness  
 \*3 Use of dumbbell piece; 120°C x 1,000 h grease immersion

### 3. Performance of low friction hub bearings

Fig. 8 shows the friction performance of hub bearings combining the developed bearing internal grease and low friction seal. Approximately 50% reduction of friction was achieved with the entire hub bearings by reducing rolling resistance and sliding resistance of the outer/inner seals.

Fig. 9 shows the performance evaluation chart for key functional requirement items of hub bearings.

The developed product achieved equal or better performance compared to the conventional product in all required aspects. Particularly, as the fretting resistance in low temperature has improved, the developed bearings can be considered for use in more severe environmental conditions.

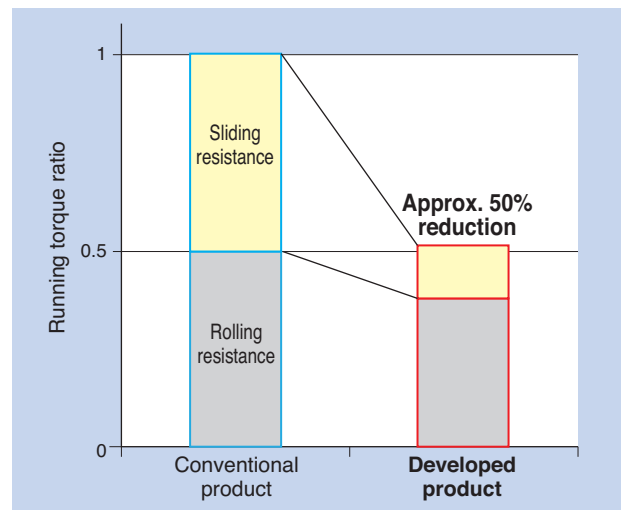


Fig. 8 Friction performance of the hub bearing

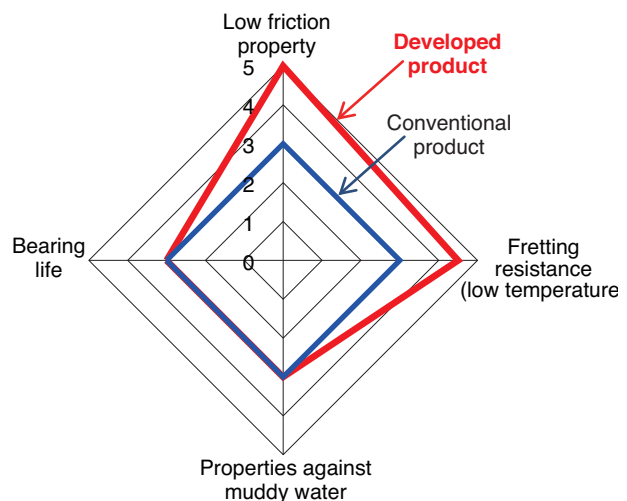


Fig. 9 Performance evaluation chart

## 4. Summary

In order to meet the requirement of improved fuel efficiency, we have commercialized hub bearings with lower friction and reliability equivalent to conventional products by developing bearing internal grease and low friction seals for hub bearings. The bearing internal grease has already been adopted by some auto-manufacturers.

We are poised to continue our efforts for lower friction and higher reliability and contribute to society by developing products that meet global needs.

## References

- 1) Haruo Nagatani, Tsuyoshi Niwa, Application of Topology Optimization and Shape Optimization for Development of Hub-Bearing Lightening, NTN TECHNICAL REVIEW No.73, (2005) 14-19.
- 2) Kiyotake Shibata, Takayuki Norimatsu, Technical trends and development products of axle bearings, NTN TECHNICAL REVIEW No. 75 (2007) 29-35.

Photo of author

---



Makoto SEKI  
Automotive Unit  
Engineering Dept.,  
Automotive Business  
Headquarters

## Chain Tensioner for Motorcycle Engine



Kouichi ONIMARU\*

NTN has developed the hydraulic auto tensioner of timing belt drive and timing chain drive unit for engine camshaft drive application.

Since 2004, NTN has started to supply timing chain tensioner for motorcycle engine application.

Today I would like to introduce new technology of auto tensioner to reduce engine noise and increase durability performance.

### 1. Introduction

OHC engines use ribbed belts or chains to transmit rotation of crank shafts to camshafts and synchronize the timing of all these units. The auto tensioners are used to keep adequate tension of these ribbed belts and chains which contribute to longer life and the quietness of engines.

For engines of motorcycles, chains are used more often than ribbed belts for the above synchronization. As such, auto tensioners for chains of motorcycles (hereafter, chain tensioners) are required to meet certain functionality particular to motor cycle engines.

NTN has been developing and commercializing chain tensioners that meet these requirements. This article introduces the structure and characteristics of chain tensioners for motorcycle engines.

### 2. Current situation of chain tensioners for motorcycle engines

#### 2.1 System configuration and required functionality

When a chain is used for the above mentioned synchronization of rotation, the chain is slide guided by a chain lever and chain guide (Fig. 1). The sliding resistance between those slide guides and the chain creates friction loss; therefore, adequate chain tension is critical. When the chain tension is too high, the friction loss becomes larger, resulting in deterioration of fuel efficiency, low output and, at worst, chain rupture.

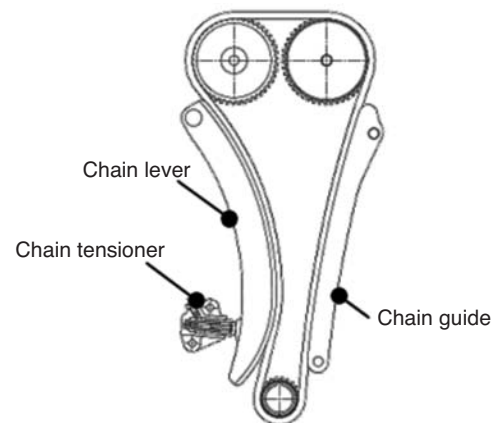


Fig. 1 Layout example

On the contrary, if the chain tension is too low, chain fluttering becomes larger, resulting in larger noise and vibration, as well as wear elongation. Therefore, the optimized design of the chain tensioner, which adjusts chain tension, is critical, requiring optimization of damping force, etc. for each engine.

Usually, there is a time lag between the starting of an engine and when lubricant oil reaches each component.

Chain tensioners with hydraulic damping mechanisms may produce abnormal noise due to chain fluttering after starting the engine until oil is filled into the high pressure chamber. Therefore, a no-back mechanism is required to prevent the chain from being pushed in when the engine stops.

\*Automotive Unit Engineering Dept., Automotive Business Headquarters

In addition, chain tensioners for motor cycles are required to have the following functionality since they are often installed by being inserted from outside of the engine.

**1) Initial setting release mechanism from outside the engine**

A chain tensioner is delivered with the initial setting where the internal component is pushed into the cylinder. The initial setting needs to be released, after the tensioner is installed to the engine, to allow the internal component of the tensioner to be extended until it is in contact with the chain lever. Therefore, a mechanism to release the initial setting (being pushed in) is required either manually from outside or automatically (Fig. 2).

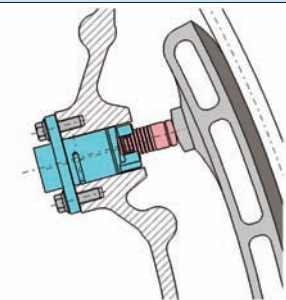
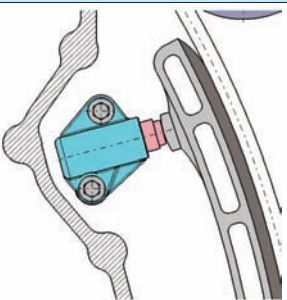
For motorcycles	For four-wheel vehicles
	
Installed from outside of the engine, without requiring removal of the cover, allowing saving of internal space. No manual operation from outside is possible after installation, requiring an automatic release mechanism of the initial setting.	The entire mechanism is installed inside the engine. Installation/removal requires removal of the cover. The initial setting is released by removing the set pin of the tensioner before installing the cover.

Fig. 2 Installation of chain tensioner

**2) Prevention of fallout of internal components**

A mechanism to prevent fallout of internal components into the engine is required in case chain tensioners are removed for maintenance, etc.

**2.2 Chain tensioners of other manufacturers**

Mechanical chain tensioners have been used for motor cycle engines with simple structures of springs and ratchets or damping with friction force of screws.

**3. NTN chain tensioners**

NTN has tackled the following challenges of the chain tensioners.

- (1) Improvement of quietness and reliability
- (2) Compact/lightweight
- (3) Improvement of workability
- (4) Stability of hydraulic damping force

**3.1 Improvement of quietness and reliability**

There are two types of structures to achieve a no-back mechanism regarding quietness and reliability. These structures are introduced in this paper.

**1) Buttress thread type chain tensioner**

The no-back mechanism (Fig. 3) utilizing a buttress thread with NTN proprietary technology makes it possible to reduce chain fluttering. This is even possible with no oil supply to the chain tensioner immediately after the engine starts and when no damping force exists from oil hydraulics (Fig. 4 and 7).

The buttress threads enable the no-back mechanism, regardless of the position of the tensioner tip when the engine stops; significantly contributing to quietness of the engine when it starts.

In addition, the frictional force of the buttress threads also work as a part of the damping force during normal operation, and not only when the engine starts (Table 1). In recent years, the load on

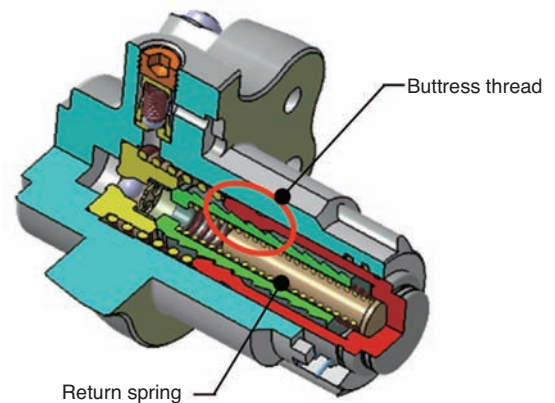


Fig. 3 Buttress thread type chain tensioner

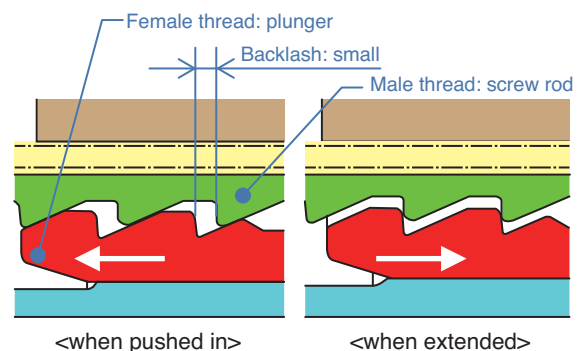


Fig. 4 Operation of buttress thread

Table 1 Functions of each no-back mechanism

No-back mechanism	Damping function	No-back mechanism
Buttress threads	Hydraulic + screw friction	Stepless
Register ring	Hydraulic	Stepped

the chain tensioners immediately after starting the engine increases due to the increase in driving torque of cam shafts, higher power output of engines, and downsizing of oil pumps. In response to these trends, NTN is marketing products with increased load capability while maintaining the conventional functionality of tensioners by reexamining the buttress thread specifications.

**2) Register ring type chain tensioner**

NTN is also marketing chain tensioners with simplified buttress thread functions with a structure that allows a stepped no-back mechanism using the grooves of the plunger outer perimeter and the register ring (freed on the extended direction by the grooves of the plunger outer perimeter and latched on the return direction). As opposed to other products with ratchet structure for the stepped no-back mechanism in the market, NTN products are characterized by the compact design by utilizing elasticity of the ring placed concentrically with the chain tensioner plunger (Fig. 5).

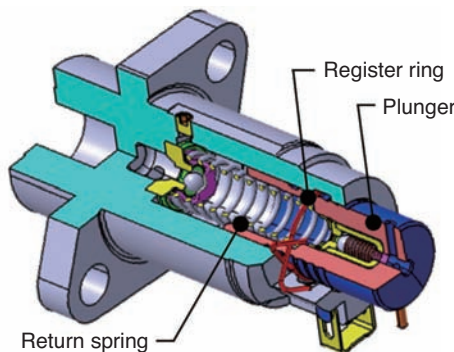


**Fig. 5** Ring type chain tensioner

The traveling line of the chain (plunger position of the tensioner) can vary depending on the temperature and rotational speed. With the register ring type no-back mechanism, the backlash amount until the no-back mechanism starts functioning needs to be set so that the axial movement of the plunger can follow the variation of the traveling line of the chain. Caution to this point is particularly needed for the motorcycle engines which allow high-speed rotation range, and therefore, produce significant variations of rotational speed (Fig. 6).

The register ring also prevents the plunger to fall out from the cylinder when it is completely extended, an important role for motor cycle engines from a maintenance standpoint, for which installation is often accomplished from outside the engines.

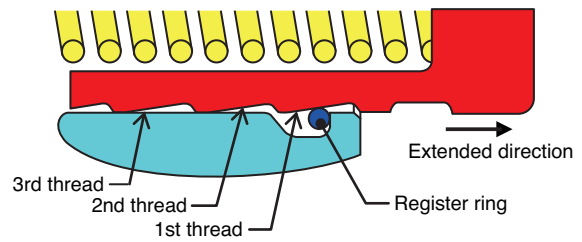


**Fig. 6** Structure of ring type

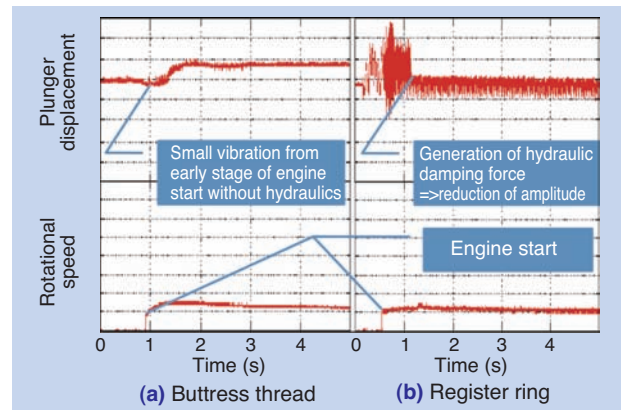
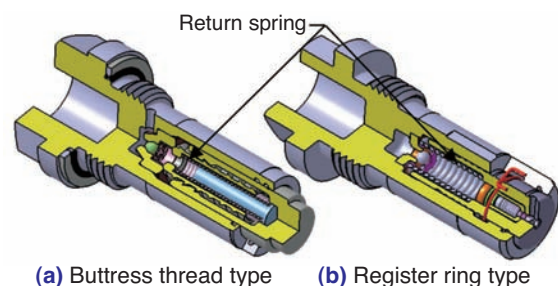


**Fig. 7** Engine startup characteristic of each no-back mechanism

**3.2 Compact/lightweight**

NTN has long been working on lightweight chain tensioners by adopting cylinders made of aluminum; however, we developed even lighter and more compact chain tensioners which can be directly installed on the engine with threads (self-mount type chain tensioners,) and started marketing them in 2010 (Fig. 8). This product comes with male threads on the cylinder outer perimeter which can be screwed into the female threads on the engine for installation. Therefore, bolts and washers for installation of the conventional products are no longer required, contributing to space saving, reduced weight and labor for installation on the engines. This product is particularly effective for motor cycle engines because they have limited space in the engine, and chain tensioners are often installed from outside the engine. In addition, this product can be used both for the aforementioned buttress thread type and register ring type.



**(a)** Buttress thread type **(b)** Register ring type

**Fig. 8** Self-mount type chain tensioner

### 3.3 Workability

#### 1) Automatic release of initial setting

For engines of four-wheel vehicles, the release of the initial setting after installation of chain tensioners is accomplished by removing the set pin of the chain tensioner and then installing the front cover (Fig. 9).

However, motorcycle engines do not have working space for removing the set pin after installation; therefore, an easy and secure releasing mechanism is required. NTN addresses these challenges by adopting the mechanism shown in Fig. 10.

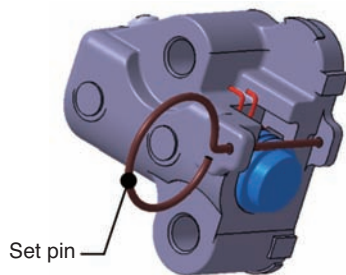


Fig. 9 Chain tensioner for automotive engines

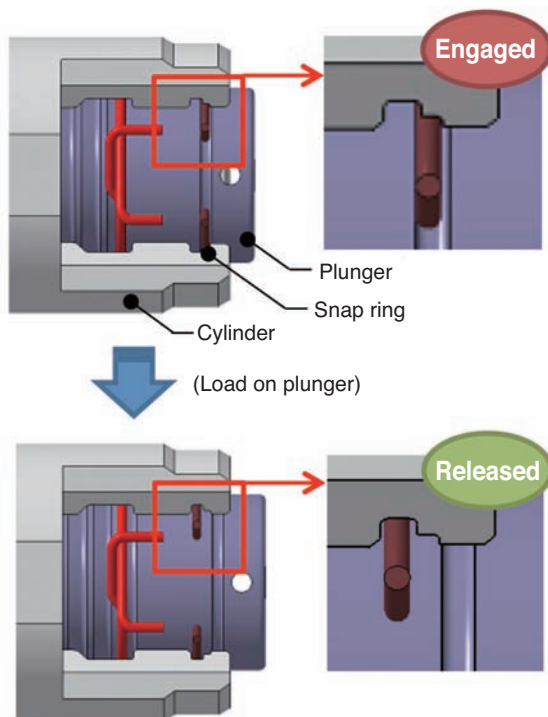


Fig. 10 Release mechanism of initial setting

#### (Initial setting status)

- The snap ring is shrunk and set into the grooves on the plunger outer perimeter and cylinder inner perimeter.
- The plunger is pushed in the extended direction by the internal return spring (Fig. 8) and kept in the initial setting position.

#### (Releasing initial setting)

- With the load applied to the plunger, the snap ring moves in the axial direction along with the groove of the plunger as they move in the pushed-in direction.
- As the snap ring moves toward the cylinder groove on the larger diameter side, the snap ring is expanded.
- When the snap ring is expanded, it cannot prevent the plunger from being extended, releasing the initial setting.

#### (Reapplying initial setting)

- After the chain tensioner is removed from the engine for maintenance, etc., the initial setting can be reset with the snap ring in place by pushing the plunger to the initial setting position.

This structure allows automatic release of the initial setting by applying load with engine cranking, which causes displacement after the chain tensioner is installed onto the engine.

#### 2) Prevention of fallout of internal components

With the register ring type chain tensioner, the register ring works as a prevention mechanism against fallout of the internal components. However, since the said component does not exist with the buttress thread type, another snap ring shown in Fig. 11 is provided separately from the snap ring for initial setting.

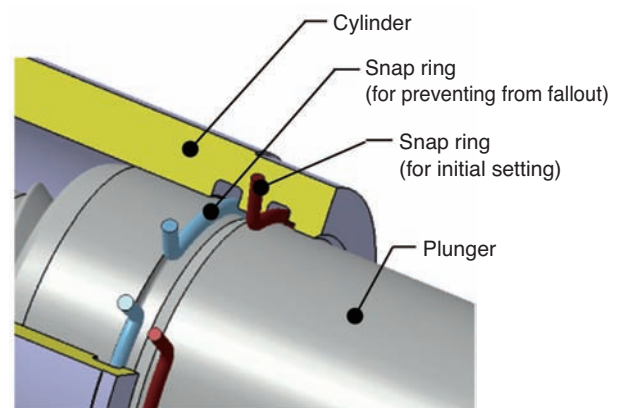


Fig. 11 Prevention mechanism of parts falling off

### 3.4 Stability of hydraulic damping force

#### 1) Relief valve setting

For higher power output, motorcycle engines have higher permitted rotational speed than four-wheel vehicles. It is necessary for the hydraulic damping mechanism to restrain the chain tension because of the tendency of excessive damping force in the higher rotational speed range. By controlling leak gaps with the conventional simple hydraulic damping mechanism, it is difficult to optimize the damping force in the lower and higher rotational speed ranges. NTN addressed these challenges by integrating a compact relief valve in the chain tensioner (Fig. 12). The open valve pressure of a relief valve can be changed with the internal spring setting, allowing adjustments for damping force appropriate to different engines. This mechanism supports engines with higher permitted rotational speed such as large and sports type motorcycles; therefore, NTN chain tensioners are often adopted.

Fig. 13 and 14 show the verification results of relief valve effects. The tuning of damping force was conducted under conditions of 100°C/200 Hz.

Compared to the case when damping force is adjusted only by the leak gap (Fig. 13), adding a relief valve produces stable damping force against variation of oil temperatures and frequency (=engine rotational speed) (Fig. 14).

The comparison of the characteristics in the actual test is shown in Fig. 15. Reduction of load in the higher rotation range can be expected with the relief valve setting.

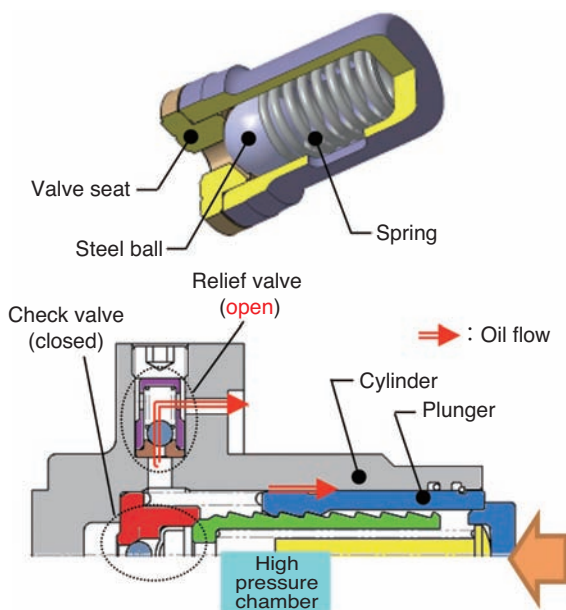


Fig. 12 Relief valve structure and oil flow

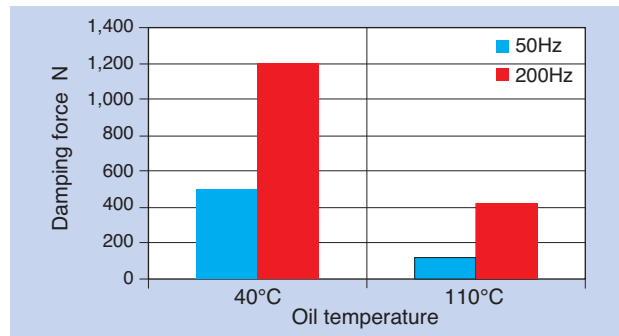


Fig. 13 Adjust with leak clearance (without relief valve)

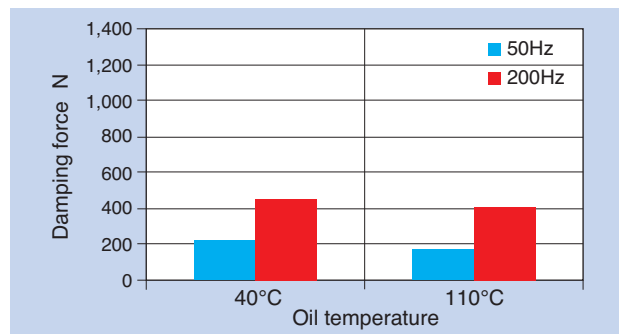


Fig. 14 Adjust with relief valve

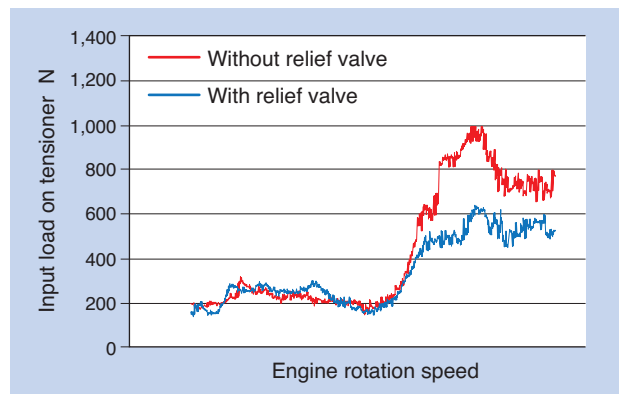
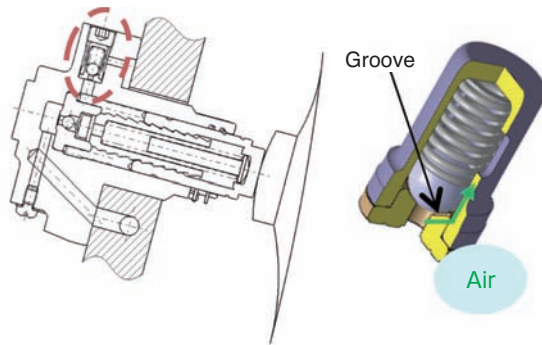


Fig. 15 Comparison of characteristics with or without relief valve

#### 2) Bleed mechanism setting

Hydraulic chain tensioners cannot satisfy the function if air is present in the oil pressure chamber. Therefore, NTN has adopted various bleeding mechanisms so that they can be added to the best location depending on usage (Fig. 16 and 17).



**Fig. 16** Added bleed mechanism to relief valve

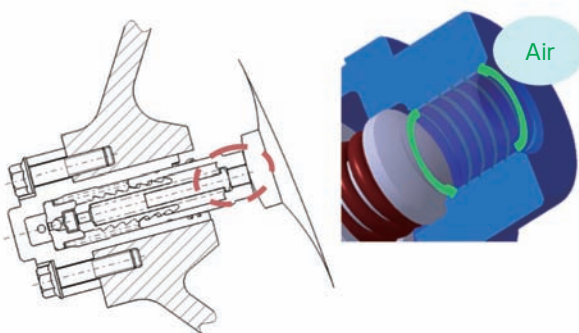


**Fig. 17** Added bleed mechanism to leak adjustment part

## 4. Conclusion

We have been developing chain tensioners for motorcycle engines, particularly for higher power output and sport vehicles, to satisfy requirements for functionality and reliability. Going forward, it is expected that the requirements for chain tensioners will be diversified, even for motorcycles possessing environmental concerns.

NTN will continue to address these requirements while developing chain tensioners for applications to broader vehicle types.

## References

- Yoshiaki Ryouno, et al.: The Engine Part Technical Trends and New Products for Engines, NTN TECHNICAL REVIEW, 75 (2007) 62-71.  
 Seiji Sato: Technology Trends of Auto Tensioner, NTN TECHNICAL REVIEW, 79 (2001) 83-89

Photo of author



**Kouichi ONIMARU**  
 Automotive Unit  
 Engineering Dept.,  
 Automotive Business  
 Headquarters

# Light Weight Drive Shaft for FR vehicle “R series”

Tomoshige KOBAYASHI\*



For the purpose of improving environmental performance, weight reduction is also required in the rear wheel drive system which is often adopted for luxury cars.

In this paper, I introduce the features and performance of "Light weight drive shaft for FR vehicle" developed for rear wheel drive car.

## 1. Introduction

For the driveshaft of front-wheel drive (FF) vehicles, a fixed type constant velocity joint (CVJ), which can take a wider work angle on the tire side and a sliding type CVJ, which can slide in the axial direction on the engine side, are used.

On the other hand, rear-wheel drive (FR) vehicles have a fixed axle (rigid axle that linearly connects both wheels) suspension and an independent suspension which allows each wheel on the same axle to independently move vertically, depending on the road conditions.

Independent suspension systems require a drive shaft, since each axle is independent; however, it is widely adopted by luxury cars as it offers superior comfort and driving maneuverability.

Recently, luxury cars are also facing stricter regulation of CO<sub>2</sub> emissions, and therefore, reduced weight and compactness are required for drive shafts of rear-drive vehicles in order to improve fuel efficiency. NTN has developed "Lightweight Drive Shaft for FR Vehicles" to meet these requirements.

## 2. Structure and characteristics of the developed product

In the past, NTN applied CVJ of the common design for both FR vehicles and FF vehicles. However, the drive shafts for rear-drive vehicles do not require the wide work angle for steering, and the CVJs for the tire side are only required to follow the vertical suspension movement. By focusing on this fact, NTN has developed a light and compact drive shaft for rear-drive vehicles with a reduced maximum work angle, dedicated to the rear-drive vehicles that can contribute to reduced weight and improved fuel efficiency.

The developed drive shaft consists of (1) newly designed light/compact fixed CVJ, (2) sliding CVJ, (3) hollow shaft with reduced material that connects the former two CVJs, and (4) compact boots with reduced grease amount, achieving approximately 30% reduction of weight compared to the conventional product.

Configuration of the newly developed Lightweight Rear Drive shaft "R-Series" is shown in Fig. 1.

The specification of the developed product and the weight reduction ratio compared with the conventional product is shown in Table 1. Note that the weight calculation excludes the stem section\* from the

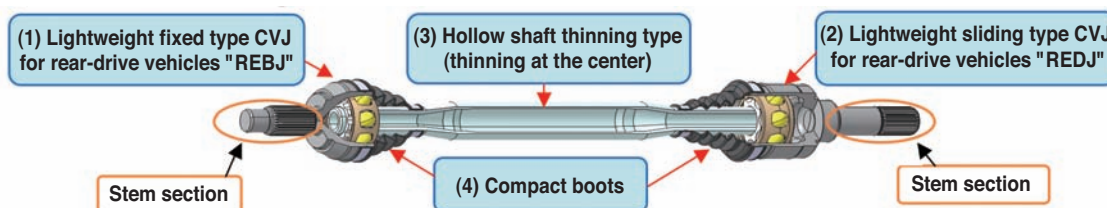


Fig. 1 Light weight drive shaft for FR vehicle “R series”

\*Drive Shaft Engineering Department, Automotive Business Headquarters

Table 1 R series mass reduction rate

Developed product (R-Series)	Conventional product	Weight reduction ratio	
Fixed type CVJ (REBJ)	EBJ	▲28%	Drive shaft assembly ▲30%
Sliding type CVJ (REDJ)	EDJ	▲13%	
Hollow shaft	Solid shaft	▲53%	
Compact boots and injected grease dedicated for rear-drive vehicles	Boots and injected grease for front CVJ	▲36%	

configuration shown in Fig. 1, since the installation mechanism varies depending on user specifications.

\*Stem section: shaft for engagement used for mounting the body

### 3. Lightweight fixed type CVJ for rear-drive vehicles "REBJ"

The maximum work angle of the fixed type CVJ for FF vehicles is set at 47 - 50 degrees to cope with the vertical movement of suspension and steering angle.

On the other hand, the fixed type CVJ for FR vehicles can be set at 19 degrees or less working angle, in most cases considering the practical use, as it only needs to follow the vertical movement of the suspension.

In the past, the fixed type CVJ for FR vehicles had specifications common with the fixed type CVJ used for FF vehicles. However, we have explored light/compact design by optimizing the functions by 19 degrees or less.

The required functions are shown below:

- (1) Strength: equivalent to the conventional product with a max work angle of 19 degrees or less
- (2) Durability: equivalent to the conventional product
- (3) NVH performance: equivalent to the conventional product

#### 3.1 Characteristics

Table 2 shows the comparison of the developed product "Lightweight fixed type CVJ for rear-drive vehicles (REBJ)" and the conventional product "EBJ".

In this article, we focus on the newly designed fixed type CVJ (REBJ) and the sliding type CVJ (REDJ), as well as the compact boots that reduced the injected grease amount.

The following shows the focused design area reexamined due to the change of the maximum work angle from 47 degrees to 19 degrees or less.

##### (1) Length in axial direction

The required ball groove length can be reduced as the ball movement range becomes smaller due to the reduced maximum work angle (Fig. 2).

Therefore, the length of various components in the axial direction can be reduced compared to the

Table 2 Comparison of REBJ and EBJ

Item	Developed product REBJ95	Conventional product EBJ95
Max. work angle (deg)	19	47
Outer diameter (mm)	φ80.8	φ83.6
Ball diameter (mm)	φ15.081	φ15.081
Weight (kg)	1.016 Ratio compared to conventional product: -28%	1.401
SUB-ASSY		

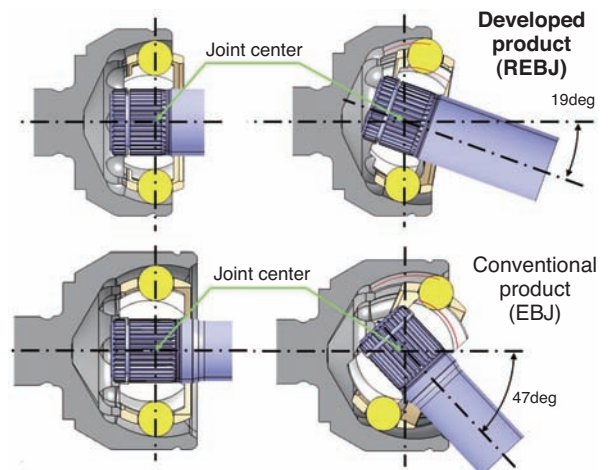


Fig. 2 Comparison of Ball groove length (red line)

conventional product (Fig. 3).

In addition, the assembly method was improved because of compact components.

The conventional product (EBJ) requires space for incorporating the cage at the bottom of the outer ring cup (L2) so that the cage can be installed at 90 degrees relative to the outer ring (Fig. 4).

On the other hand, the developed product (REBJ) has a small undercut at the cup end of the outer ring;

therefore, the cage can be incorporated horizontally, requiring less space at the bottom of the outer ring cup (L1).

The bottom of the outer ring cup only requires minimum space to incline the cage to the angle required for incorporating the ball (Fig. 5).

As described, the difference of the assembly method also contributes to the reduction of weight and size.

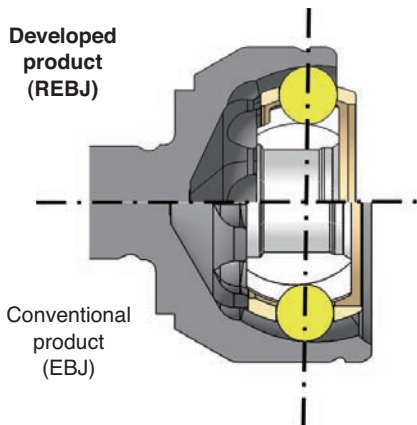


Fig. 3 Comparison of axial length

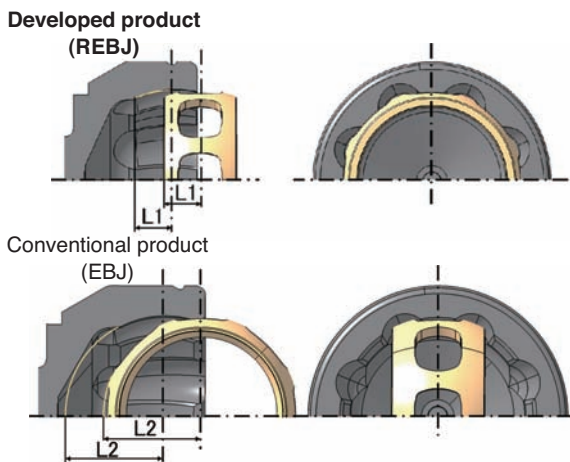


Fig. 4 Cage built-in method

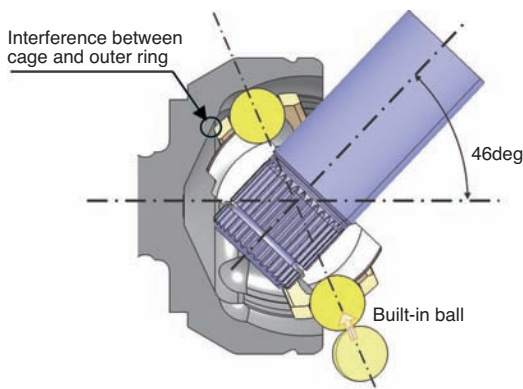


Fig. 5 Built in ball

**(2) Dimension of outer diameter**

As the max. work angle becomes smaller, input load to various components are also reduced, allowing less material required for those components (Fig. 6).

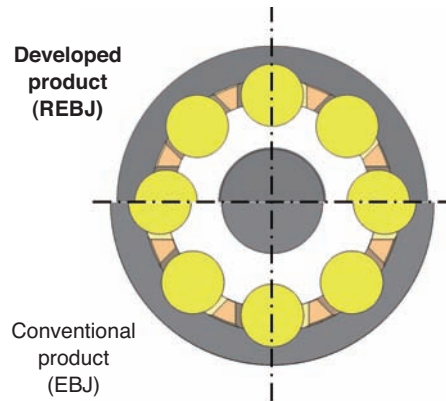


Fig. 6 Comparison of Outer dia.

**3.2 Functional evaluation**

Fig. 7 shows results from static torsional tests of the developed product REBJ and the conventional product EBJ (n=2 each). The light and compact REBJ has the equivalent strength of EBJ.

Fig. 8 shows the results from the durability test. Durability of the developed product REBJ sufficiently achieved the development objectives, together with the conventional product.

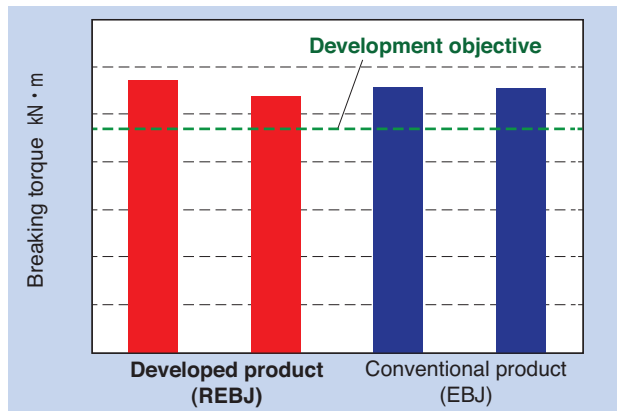


Fig. 7 Results of static torsional strength test

CVJ	No	Damage table/inspection time (h)		
		100	230	350
REBJ95	1	○	○	○
	2	○	○	○
	3	○	○	○
	4	○	○	○
EBJ95	1	○	○	○
	2	○	○	○
	3	○	○	○
	4	○	○	○

○ : No error    △ : Slight error    × : Significant error  
 - - - : Development objective

Fig. 8 Results of durability test

#### 4. Lightweight sliding type CVJ for rear-drive vehicles "REDJ"

There are various types of sliding type CVJs, which are used paired with fixed CVJs. For luxury FR vehicles, cross groove type and double offset type are more preferred than triport type, as they require minimum backlash in all drive systems.

EDJs used by NTN for FR vehicles are light and compact; however, the maximum work angle is 25 degrees, and they were used for both FF and FR vehicles, similar to the fixed type CVJ.

Therefore, we explored development of further reduction in weight and size, also for the sliding type CVJ, by optimizing the functions for a work angle of 19 degrees or less.

The required functions are described below, similar to the fixed type CVJ.

- (1) Strength: equivalent to the conventional product with a max work angle of 19 degrees or less
- (2) Durability: equivalent to the conventional product
- (3) NVH performance: equivalent to the conventional product

#### 4.1 Characteristics

Table 3 shows the comparison of the developed product "Lightweight sliding type CVJ for rear-drive vehicles (REDJ)" and the conventional product "EDJ".

Table 3 Comparison of REDJ and EDJ

Item	Developed product REBJ95	Conventional product EBJ95
Max. work angle (deg)	19	25
Outer diameter (mm)	φ79	φ82
Ball diameter (mm)	φ15.875	φ15.875
Weight (kg)	1.124 Ratio compared to conventional product: -13%	1.294
SUB-ASSY		

\*Sliding length: 40 mm

The following shows the focused design areas which were reexamined due to the change in the maximum work angle from 25 degrees to 19 degrees.

#### (1) Length in axial direction

The required ball groove length can be reduced as the ball movement range decreases due to the reduced maximum work angle (Fig. 9).

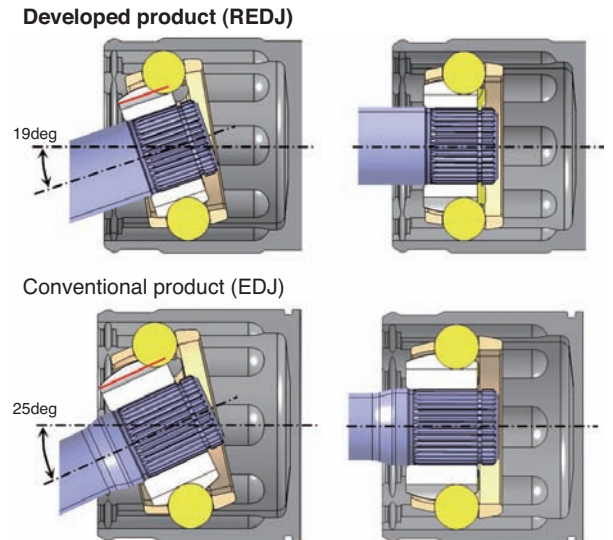


Fig. 9 Comparison of Ball groove length (red line)

As the axial length (width) of the inner ring/cage is reduced, the outer ring cup length can also be reduced ( $L1 < L2$ ), achieving compactness (Fig. 10).

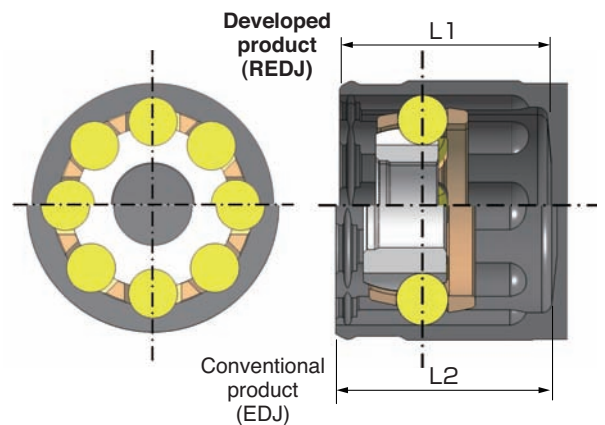


Fig. 10 Comparison of Outer dia. and axial length

**(2) Dimensions of outer diameter**

Similar to the fixed type CVJ (REBJ), as the max. work angle is reduced, input load to various components are also reduced, allowing less material required for those components (Fig. 10).

Furthermore, as the max work angle is reduced, the moving range of the ball within the cage window is reduced, which shortens the length of the cage window, as well as the angle of the cage outer diameter tapered area.

Therefore, the cross-section of the cage pillar increases, enhancing the cage strength, which makes it possible to downsize the radial direction (Fig. 11).

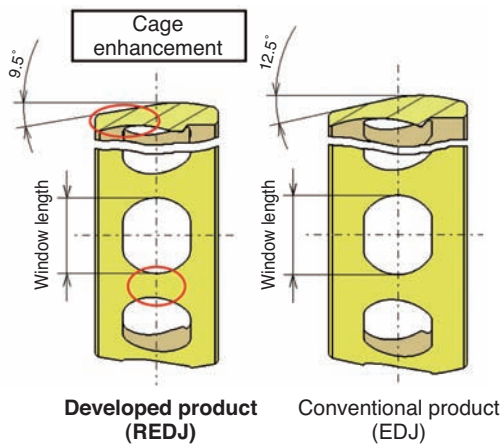


Fig. 11 Comparison of REDJ cage and EDJ cage

The detailed dimensions of each component are determined by optimization through FEM stress analysis and evaluation test for validating suitability.

Fig. 12 shows an example of FEM stress analysis of the cage. The developed product (REDJ) shows the same level of stress balance as the conventional product, while achieving compact size.

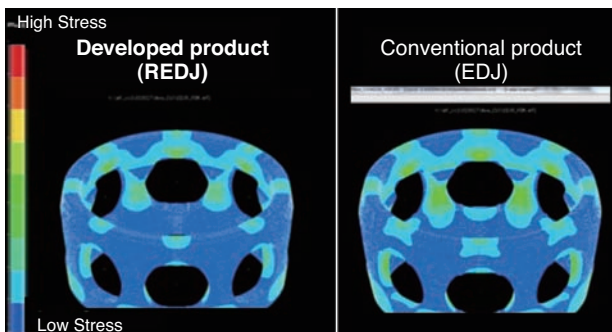


Fig. 12 FEM analysis of REDJ cage

**4.2 Functional evaluation**

Fig. 13 shows results from static torsional tests of the developed product REDJ and the conventional product EDJ (n=2 each).

The light and compact REDJ has strength equivalent to or better than the conventional product EDJ.

Fig. 14 shows the results from the durability test.

The developed product REDJ has durability equivalent to or better than the conventional product EDJ.

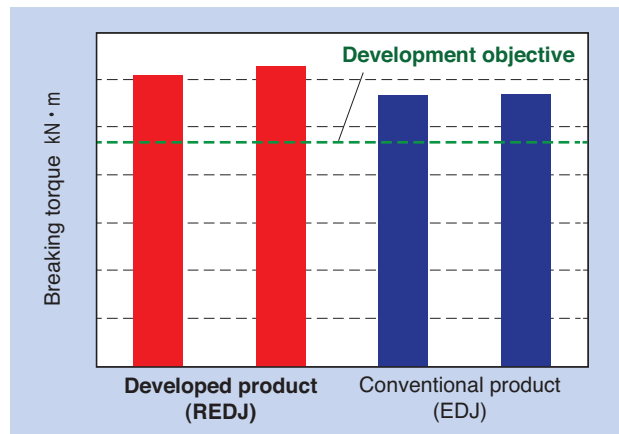


Fig. 13 Results of static torsional strength test

CVJ	No	Damage table/inspection time (h)		
		100	230	350
REDJ95	1	○	○	○
	2	○	○	○
	3	○	○	○
	4	○	○	○
EDJ95	1	○	○	○
	2	○	○	○
	3	○	○	○
	4	○	○	○

○ : Continued operation allowed  
 × : Continued operation not allowed  
 - - - : Development objective

Fig. 14 Results of durability test

### 5. Boots

As the max work angle is reduced, the boots can also be light and compact, which allow for a reduced amount of injected grease, as the capacity is reduced (Fig. 15).

Table 4 shows the comparison of weight of the boots and the injected grease for the fixed type CVJ and sliding type CVJ.

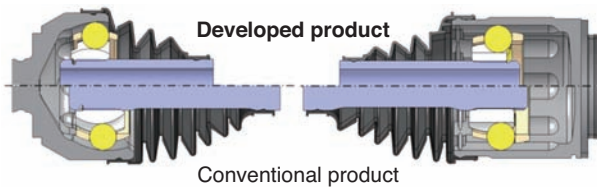


Fig. 15 Miniaturization of boots

Table 4 Mass of boots and grease

Item	Developed product (REBJ+REDJ)	Conventional product (EBJ+EDJ)
Weight of boots (g)	62	120
Weight of grease (g)	151	215

### 6. Conclusion

In this article, characteristics and performance of the Lightweight Rear Drive shaft "R-Series" development for rear-wheel drive vehicles are presented.

Table 5 is a summary of the performance of the developed products compared with general drive shafts for rear-wheel drive vehicles. It shows that the developed products, which achieved significant reduction of weight while maintaining basic performance, are generally the most superior drive shafts.

Table 5 Comparison of performance according to drive shaft

	Fixed type + sliding type		Sliding type + sliding type
	Developed product "R-Series"	BJ type + TJ type	LJ type + LJ type
Weight	★★★	★★	★★
Strength	★★★	★★	★★
Durability life	★★★	★★	★★
NVH	★★	★★	★★
Transmissibility	★★★	★★	★★

Superiority : ★★★ > ★★

Recently, as requirements for improvement of environmental performance also increases for luxury cars, which often adopt rear-wheel drives, this developed product, which achieved significant weight reduction is believed to meet the current needs.

### References

Hiroshi Tone, Kenji Terada, Masamichi Nakamura  
 Summary of E Series, High Efficiency Constant Velocity Joints,  
 NTN TECHNICAL REVIEW No.70 (2002) 18-23  
 Shin Tomogami  
 Technical Trend and Development Products of Constant Velocity Universal Joint  
 NTN TECHNICAL REVIEW No.75 (2007) 10-15

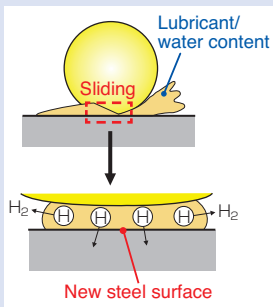
Photo of author



Tomoshige KOBAYASHI  
 Automotive Business  
 Headquarters  
 Driveshaft Engineering  
 Department

# Effects of Lubricant on Hydrogen-Related Rolling Contact Fatigue Life Improvement

Takayuki KAWAMURA\*



In rolling bearings used under severe conditions such as automotive electrical instruments and auxiliary device, an early bearing damage is occurred and accompanied by unique white microstructures below the raceway subsurface. The main cause is thought to be the result of hydrogen embrittlement. One of the possible mechanisms of this flaking failure is due to metal contact between the steel surfaces, i.e. exposing active fresh metal surfaces, by which the lubricants decompose. Subsequently, hydrogen is generated and penetrates into steels. This report introduces the outline of NTN's hypothesis concerning about the hydrogen-related failure mechanism and in addition, countermeasure by lubricant.

## 1. Introduction

In the latter half of the 1980s and the beginning of the 1990s, the drive belts for automotive engine accessories and auxiliary devices were changed from standard V-belts to serpentine belts. During the transformation to serpentine belts, early flaking was observed on the fixed bearing raceway of the engine accessory bearings and caught the industry's attention<sup>1)</sup>. Even if this flaking appears to be small, widespread cracks with white microstructural change extend deep through the circumferential cross section, which is a peculiar phenomenon that is not observed with conventional fatigue failures (Fig. 1).

Several hypotheses have been proposed based on experimental verifications in order to pinpoint the cause of this peculiar flaking<sup>2-5)</sup>. The current leading idea is hydrogen embrittlement, which is what NTN also claims to be the cause of the flaking<sup>6-8)</sup>.

Today, failure due to flaking is decreasing in the market mainly due to improvement of grease to prevent flaking<sup>9)</sup>. However, since this peculiar flaking is still observed in applications such as bearings for CVT and wind turbines bearings in addition to engine accessories<sup>6)</sup>,<sup>10)</sup>, clarification of the detailed mechanism of the flaking development and more effective counter-measures are being investigated.

Presented in this article are hypotheses of the mechanism of the peculiar flaking development and

evidence with the most economically favorable solution using lubricant technology among all possibilities, from materials to lubrication.

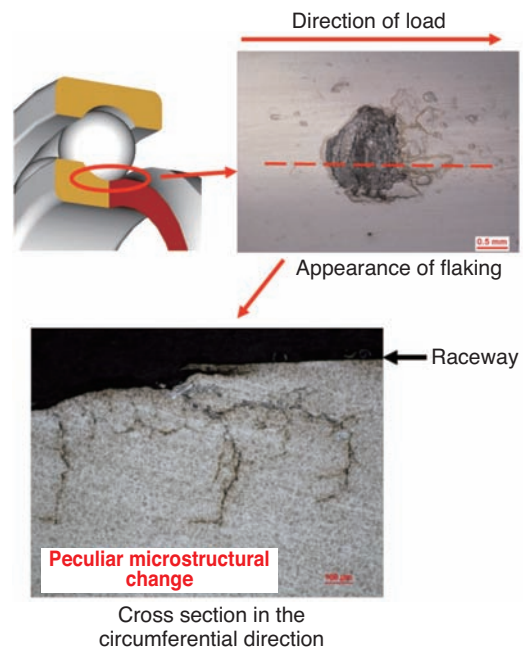


Fig. 1 Appearance of peculiar flaking failure and its circumferential cross-section

\*Advanced Technical Research Center

## 2. Characteristics of peculiar flaking and its relation with hydrogen embrittlement

### 2.1 Characteristics of peculiar flaking

Table 1 shows a comparison of conditions leading to the conventional fatigue microstructural change and peculiar flaking with widespread white microstructural change under severe operating conditions. This table implies that the peculiar flaking is significantly affected by environmental factors such as hydrogen rather than operating stress.

Table 1 Difference of occurrence condition between peculiar and conventional flaking failure

	Peculiar flaking	Conventional flaking
Operating load/stress	Small	Large
Loading cycle	Less frequent	More frequent
Impact of lubricant	Large	Small

### 2.2 Reproduction of the deterioration of fatigue strength and peculiar flaking with advanced addition of hydrogen<sup>11)</sup>

Reproduction of reduced life and microstructural change with hydrogen was explored using test pieces with hydrogen added in advance by the process of cathodic charge. Fig. 2 shows the evaluation results of the ultrasonic wave fatigue test, which allows for a high-speed load for reducing dispersion of hydrogen under testing. The test pieces charged with hydrogen significantly reduced fatigue strength compared to the test pieces without hydrogen. The larger the hydrogen content, the larger the reduction of fatigue strength.

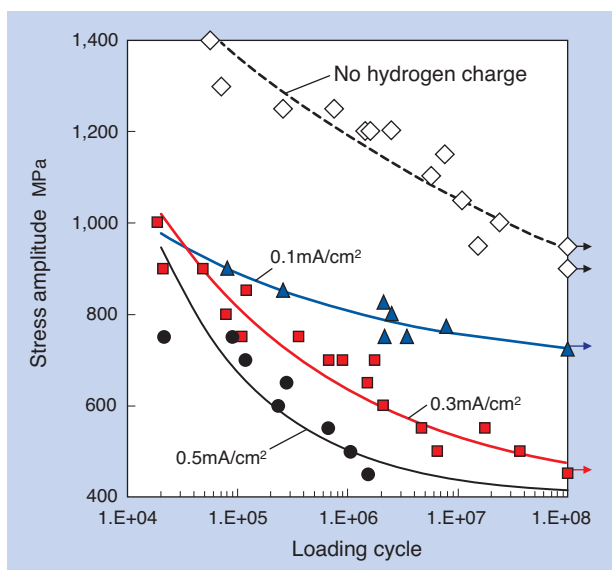


Fig. 2 Effects of hydrogen charge on stress amplitude at ultrasonic fatigue testing

Also, as shown in Fig. 3, in the two-cylinder rolling contact fatigue test after the hydrogen charge, early cracking occurred under the influence of hydrogen. When the injected hydrogen was significant, peculiar white microstructural change similar to Fig. 1 appeared.

Based on these results, it is revealed that the fatigue strength is reduced, and peculiar widespread flaking with white microstructural change occurs from hydrogen embrittlement when the hydrogen penetrates into the bearing steel. Therefore, we consider this as hydrogen embrittlement flaking.

From the above, the mechanism of the hydrogen embrittlement flaking that NTN considers is shown in Fig. 4. To verify this hypothesis, it is necessary to demonstrate the possibility of hydrogen penetration into the steel in an actual operating environment.

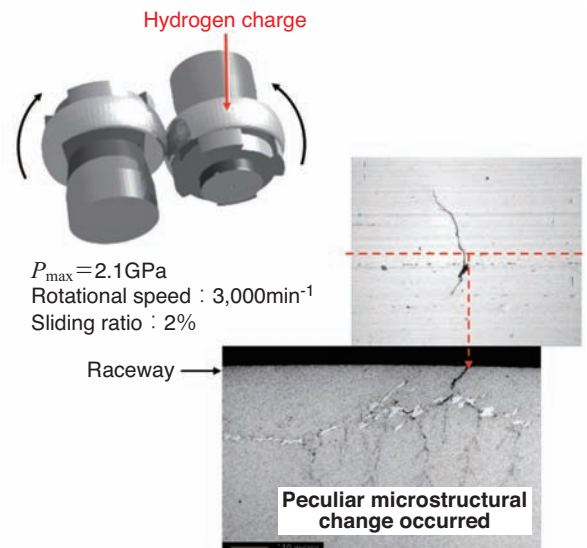


Fig. 3 Photographs of surface cracks and their circumferential cross sections after two cylinder rolling contact fatigue test with hydrogen charge

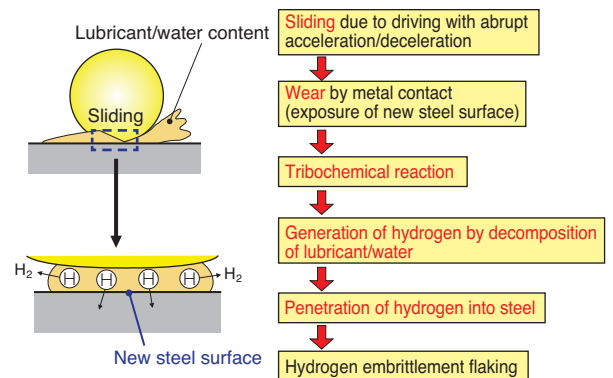


Fig. 4 Hydrogen embrittlement flaking failure mechanism

### 3. Verification of generation/ penetration of hydrogen

The source of hydrogen can be a lubricant that contains hydrocarbon and water content in the atmosphere. Also, possible driving forces of generation of hydrogen from lubricant and water includes (1) sliding and vibration from abrupt acceleration/deceleration while driving, (2) electrical effects from electric currents and statics, and (3) from severe environments under which rolling bearings are used<sup>12)</sup>.

Presented below are the results from the investigation of effects of sliding on generation of hydrogen and penetration into the steel.

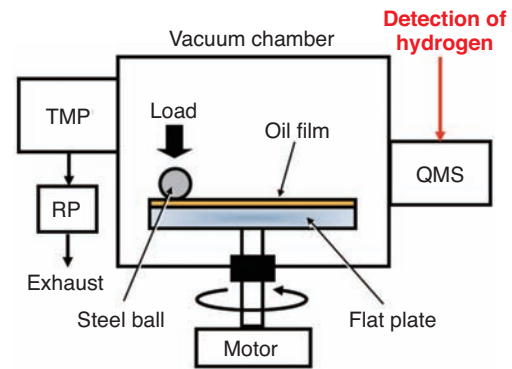
#### 3.1 Verification of generation of hydrogen through sliding<sup>13)</sup>

In order to verify generation of hydrogen through sliding, a sliding test of ball-on-disk was conducted in a vacuum. Fig. 5 shows the results of hydrogen detection. It shows the change of generated hydrogen (red line) and the friction coefficient (blue line) when sliding-stopping is repeated three times. If we define the amount of hydrogen generation as the increase in area of hydrogen ion current during sliding, the amount of hydrogen generation is increasing as sliding increases while the friction coefficient remains almost constant. It is also revealed that hydrogen is not generated immediately after the start of the first test, but rather is generated immediately after the start of the second and third tests.

From these results, the following phenomenon is deduced:

- (1) Usual bearing raceway surfaces are covered with an inactive oxide film<sup>14)</sup>. Friction from the initial sliding removes the oxide film, exposing an active steel surface. Because of that, hydrogen is generated in the mechanism shown in Fig. 4.
- (2) Since the test is conducted in a vacuum, the amount of oxygen in the atmosphere is scarce. The steel surface, once exposed, is only recovered with a very thin oxide film that is easily removed in the next sliding cycle.
- (3) By repeating the sliding cycle, the friction surface gradually becomes rougher making it easier to expose a new steel surface. This result of this is an increase in the amount of generated hydrogen.

Therefore, if friction heat is considered to be equivalent to the friction coefficient because of the constant load, generation of hydrogen is considered to be affected by exposure of the new steel surface rather than friction heat.



Test piece	Steel grade/flat plate
Material	SUS440C
$P_{\max}$	1.0GPa
Slide velocity	207mm/s
Vacuum level	$10^{-5}$ Pa

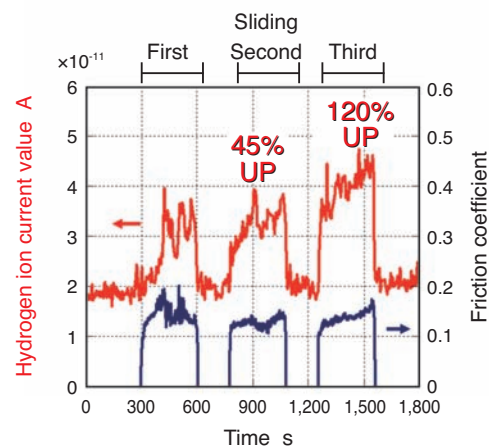


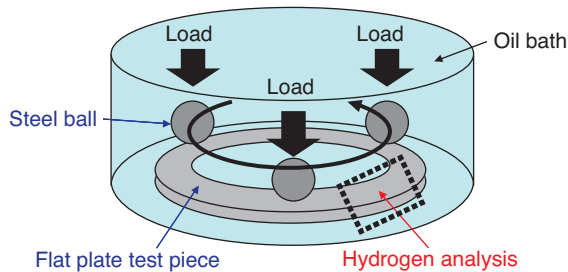
Fig. 5 Coefficient of friction vs. hydrogen generation from lubricant during sliding test in vacuum

#### 3.2 Verification of penetration of hydrogen through sliding<sup>13), 15)</sup>

In order to verify penetration of hydrogen into steel through sliding, a sliding test of 3-balls-on-disk was conducted in an oil bath similar to the actual environment, using 5 different types of test oil. Fig. 6 shows the result of hydrogen detection. The tendency that was observed was that the amount of hydrogen penetrated into steel increased as friction increased.

In addition, in order to verify the impact of water content in the atmosphere, an abrasive wear test was conducted under controlled humidity. This revealed that the water content in the atmosphere works as the supply source of hydrogen, increasing the amount of hydrogen penetrated into steel as the volumetric humidity (water content in the atmosphere) increases (Fig. 7).

These results imply that lubricant and water content are decomposed by a tribochemical reaction<sup>16)</sup> on the steel surface that was newly exposed due to metal contact, including sliding, generating hydrogen which penetrated into the steel.



Test piece	Steel grade/flat plate
Material	SUJ2
$P_{max}$	3.0GPa
Slide velocity	300mm/s
Time	20h
Oil temperature	100°C

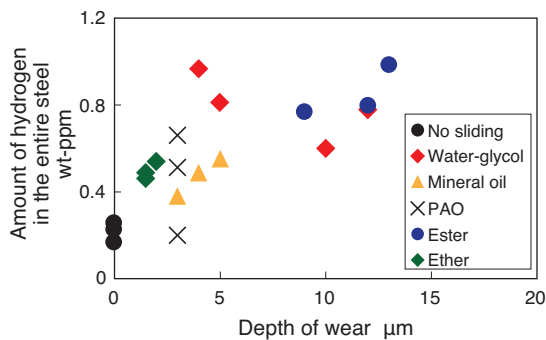


Fig. 6 Wear depth vs. amount of penetrated hydrogen after sliding test in oil

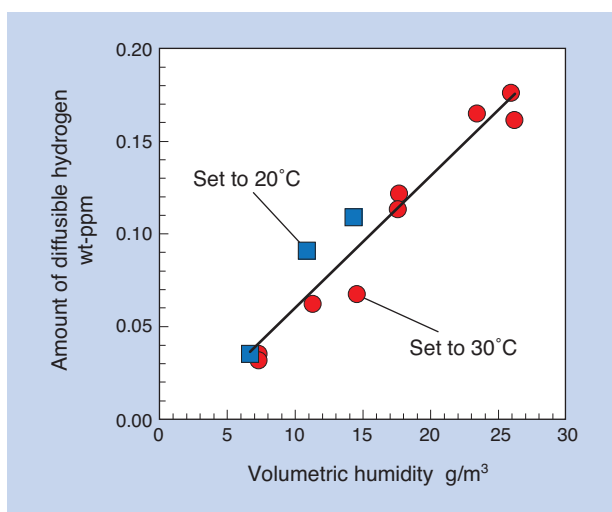


Fig. 7 Absolute humidity vs. amount of penetrated hydrogen under an abrasive wear condition

#### 4. Preventative measures against generation and penetration of hydrogen from lubricants

The process of the effects of lubricant in the above verification of the hydrogen embrittlement flaking mechanism is "wear due to metal contact" and "tribochemical reaction". Therefore, with the addition of "anti-wear agent (action: reduction of wear under high-speed sliding)" and "corrosion inhibitor (action: formation of oxide film on the steel surface)" are considered to be effective as preventative measures. The effect of addition of these agents was confirmed in the verification test of suppressing hydrogen penetration from sliding and in the reproducibility test using the actual bearings.

##### 4.1 Verification of suppressing penetration of hydrogen from sliding<sup>13)</sup>

Fig. 8 shows the result of hydrogen detection in the sliding test with anti-wear agent (organic zinc + organomolybdenum) or corrosion inhibitor (peroxomolybdate + tungstate) added to water-glycol fluid for verifying the effect of the additives for suppressing penetration of hydrogen due to sliding.

It was revealed that the amount of hydrogen in the steel was low when any additive was used compared to the fluid without additives and, in particular, peroxomolybdate was effective for suppressing hydrogen penetration.

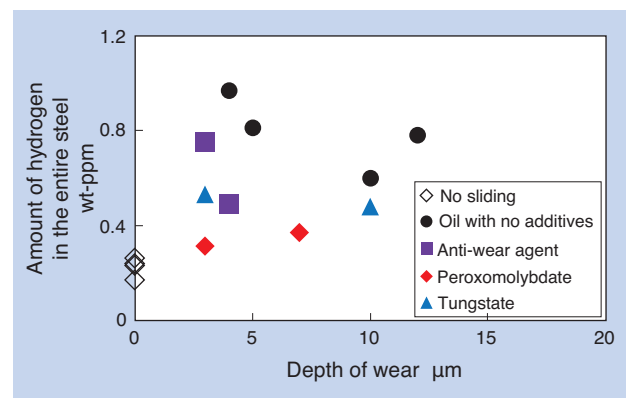


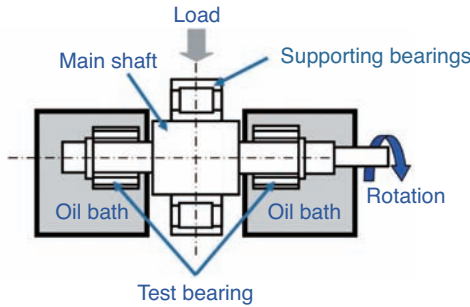
Fig. 8 Effect of additive on prevention of hydrogen penetration after sliding test in oil

##### 4.2 Verification of reproducibility test using actual bearings<sup>17)</sup>

The effect of the prevention of hydrogen embrittlement flaking with an anti-wear agent (organic zinc + organomolybdenum) and corrosion inhibitor (peroxomolybdate + tungstate), which had suppressed the amount hydrogen penetration into the steel, was

evaluated under oil lubrication. **Fig. 9** shows the Weibull distribution of flaking life. It was verified that all the failed bearings were caused by hydrogen embrittlement flaking. The lubricant with peroxomolybdate and the anti-wear agent, , showed longer life, especially with peroxomolybdate proving to be especially effective.

In addition, **Fig. 10** shows the analysis of oxygen on the inner ring surface in the depth direction after a test using XPS (X-ray photoelectron spectroscopy). It



Base oil	Water-glycol fluid (32mm <sup>2</sup> /s@40°C)
Test bearing	Needle roller bearing
$P_{max}$	2.61GPa
Oil temperature	100°C
Driving pattern	Abrupt acceleration/deceleration* (500↔300min <sup>-1</sup> )

\* Repeating acceleration: 1s ⇒ constant speed: 1s ⇒ deceleration: 1s

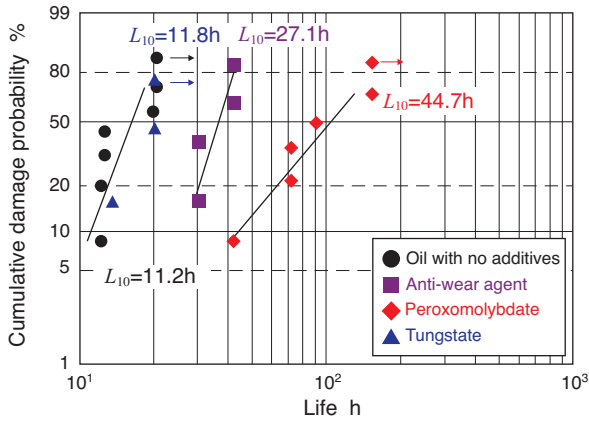


**Fig. 9** Weibull distributions of hydrogen-related rolling contact fatigue life

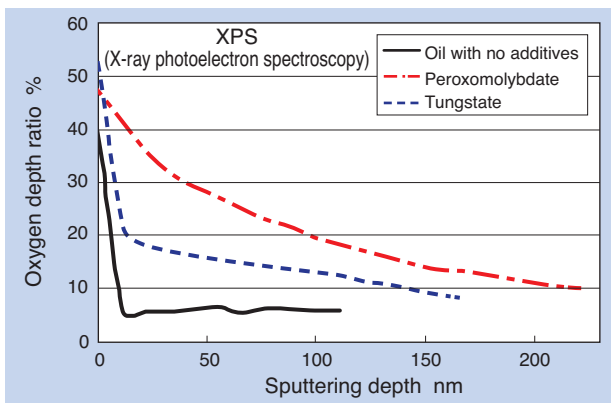


**Fig. 10** Oxygen depth profile on worn portion of inner ring raceway

shows that peroxomolybdate, among corrosion inhibitors, forms a thick oxide film.

From the above, we believe that peroxomolybdate suppresses the exposure of the steel surface and generation/penetration of hydrogen as well as achieving long life by reducing wear and forming a thick oxide film, as shown in **Fig. 11**.

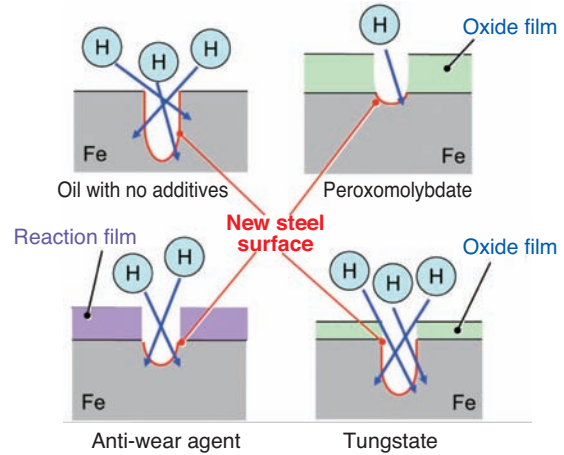


**Fig. 11** Mechanism of tested additive action

### 5. Application of effective additives to grease<sup>9)</sup>

In order to verify the effects of peroxomolybdate in the grease, an accelerated reproducibility test was conducted using grease lubricated ball bearings with anti-wear agent (organic zinc + organomolybdenum) or corrosion inhibitor (peroxomolybdate) added to the base grease. **Fig. 12** shows the Weibull distribution of flaking life. It was verified that all the failed bearings were caused by hydrogen embrittlement flaking. It was revealed that the grease with peroxomolybdate suppressed hydrogen embrittlement flaking similar to oil lubrication.

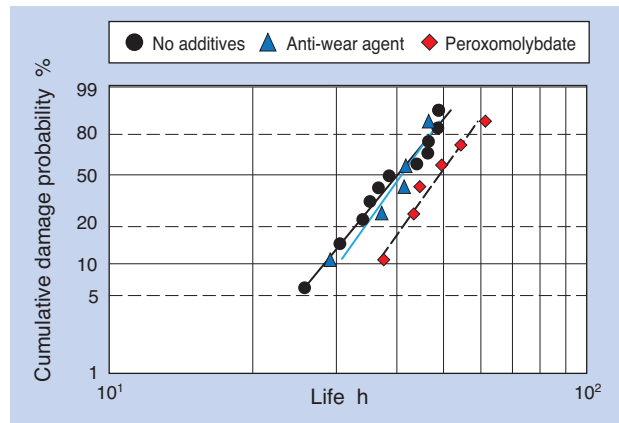


**Fig. 12** Weibull distributions of hydrogen-related rolling contact fatigue life under grease lubrication

NTN developed its proprietary grease by leveraging this technology and uses it widely for many applications in preventing hydrogen embrittlement flaking.

## 6. Conclusion

In this article, the mechanism of hydrogen embrittlement flaking and the technology for preventing it are discussed. Due to the increased requirements on energy efficiency from the viewpoint of environment protection, rolling bearings tend to be lubricated under the conditions of a thin oil film, which may induce metal contact (from use of base oil with low viscosity). Therefore, the demand for a lubricant with appropriate measures is increasing. Going forward, it is expected that the requirement for development of a lubricant with refined design in chemical composition and characteristics for each application will increase.

In addition, we consider that comprehensive clarification of hydrogen embrittlement flaking will be critical, not only from material or lubricant standpoints, but also by quantitatively linking the operating conditions of rolling bearings and event probability.

## References

- 1) Seiichi Nozaki, Koushirou Fujimoto, Kenji Tamada: Brittle Flaking on Bearings for Electrical Instruments and Auxiliary Devices and Life Extension of these Bearings NTN TECHNICAL REVIEW No.61 (1992) 36.
- 2) Kenji Tamada, Kikuo Maeda, Noriyuki Tsusima: A New Type of Microstructural Change in Bearings for Electrical Instruments and Auxiliary Devices of Automotive Engines, NTN Technical Review, 61 (1992) 29.
- 3) K. Tamada, H. Tanaka : Occurrence of Brittle Flaking on Bearings used for Automotive Electrical Instruments and Auxiliary Devices, Wear, 199 (1996) 245.
- 4) Yasuo Murakami, Hiromichi Takemura, Michiharu Naka, Takashi Ogawa, Tatsunobu Momono, Akira Iwamoto, Shigeru Ishihara: Study on Fatigue Mechanism of Bearings for Automotive Alternators, NSK Technical Journal, 656 (1993) 1.
- 5) Masamichi Shibata, Masao Goto, Noriyasu Oguma, Tsuyoshi Mikami: A New Type of Microstructural Change Due to Rolling Contact Fatigue on Bearings for the Engine Auxiliary Devices, Koyo Engineering Journal, 150 (1996) 16.
- 6) Nobuo Kino, Takeshi Yamamoto, Keizo Otani, Noriko Uchiyama: Analysis of Short Life Flaking due to Hydrogen Embrittlement, Transactions of the Japan Society of Mechanical Engineers (Series A) 70, 696 (2004) 54.
- 7) H. Uyama, H. Yamada, H. Hidaka, N. Mitamura : The Effects of Hydrogen on Microstructural Change and Surface Originated Flaking in Rolling Contact Fatigue, Tribology Online, 6, 2 (2011) 123.
- 8) Toshiya Kinami: Effects of Hydrogen on Rolling Contact Fatigue Phenomena due to Hydrogen Embrittlement, Denkiisei, 84, 1 (2013) 55.
- 9) Takayuki Kawamura, Hidenobu Mikami: Development of Long Life Grease 'NA103A' for Automotive Components, NTN TECHNICAL REVIEW, No. 75 (2007) 116.
- 10) M. H. EVANS : White Structure Flaking (WSF) in Wind Turbine Gearbox Bearings: Effects of Butterflies and White Etching Cracks (WECs), Material Science and Technology, 28, 1 (2012) 3.
- 11) Hiroshi Hamada, Yukio Matsubara: The Influence of Hydrogen on Tension-Compression and Rolling Contact Fatigue Properties of Bearing Steel, NTN Technical Review, 74 (2006) 50.
- 12) Hideyuki Uyama: Effects of Hydrogen in Rolling Bearings, Tribologist 60, 10 (2015) 658.
- 13) M. Kohara, T. Kawamura, M. Egami : Study on Mechanism of Hydrogen Generation from Lubricants, Tribology Transactions, 49 (2006) 53.
- 14) Yuji Yamamoto, Motohiro Kaneta: Tribology (2nd Ed.) Ohmsha (2010) 11.
- 15) Motohiro Ito: The Influence of the Humidity and Quantity of Hydrogen into Steel under the Abrasive Wear, NTN Technical Review, 82 (2014) 88.
- 16) Shigeyuki Mori, Hidetaka Nanao: Surface Chemistry in Microtribology, Journal of the Surface Science Society of Japan, 19, 6 (1998) 379.
- 17) M. Itoh, T. Kawamura, H. Mikami : Effects of Additives on Hydrogen-Related Rolling Contact Fatigue Life Improvement, International Tribology Conference, Tokyo (2015) 748.

Photo of author

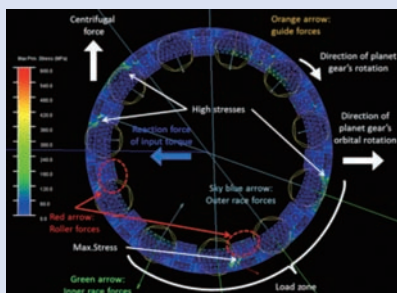


Takayuki KAWAMURA

Advanced Technical  
Research Center

# Relationship between Cage Stress and Degree of Freedom of motion in Dynamic Analysis for Needle Roller Bearings

Naoto SHIBUTANI\*  
Tomoya SAKAGUCHI\*



In dynamic analysis considering elastic deformation of cage, it requires a long time to calculate cage stress. To shorten calculation time, a two-dimensional analysis was conducted whose degrees of freedom of motion were restricted to three. However, an influence of the restricted degrees of freedom in this analysis was not clarified.

In this paper, the influence of the restricted degrees of freedom on cage stress and its generating mechanism are discussed by calculating both two-dimensional and three-dimensional analysis for needle roller bearings in planetary gears.

## 1. Introduction

Generally, a rolling bearing consists of an inner ring, outer ring, multiple rolling elements and a cage. The main role of the cage is to place the rolling elements an equal distance apart. If the number of rolling elements is increased in order to increase the load carrying capacity of the bearing, the bars of pockets in the cage become too thin, increasing the risk of damage to the cage itself. Therefore, the bearing needs to be designed to predict the stress applied on the cage. Since measuring stress applied to the rotating cage is not easy, prediction using dynamic analysis is an effective method.

A bearing application where a large load is applied to the cage is the support portion of the planet gear in the planetary transmission. The reason why a large load is applied is because the centrifugal acceleration from the planetary motion is always applied to the bearings.

Suzuki et al. <sup>1)</sup> reported factors that generate thrust force and running torque due to roller skew by dynamic analysis, including 3D behavior on needle roller bearings under planetary motion. However, stress on the cage is not considered as the cage is assumed to be a rigid body.

Sakaguchi et al. <sup>2)</sup> calculated stress on the cage by dynamic analysis of the bearings taking into consideration elastic deformation of the cage. They also explored 2-dimension dynamic analysis, considering only 3-degrees of freedom on the radial plane wave for the bearings at the support area of the

planet gear in the planetary transmission, for calculating the stress on the cage <sup>3)</sup>.

2-dimensional analysis of 3-degrees of freedom provides a shorter calculation time compared with 3-dimensional analysis of 6-degrees of freedom; however, skew of raceway, rollers and cage cannot be considered. In addition, the impact of the difference of these degrees of freedom on the dynamic analysis of the cage stress is not clear.

In this paper, we conduct 2-dimensional and 3-dimensional dynamic analysis, considering the cage as an elastic body against the bearings at the planet gear support and clarify their differences. Together, we examine the reason why the stress on the cage is created when autorotation speed, revolution speed and input torque of the planet gear are changed.

## 2. Dynamic analysis model

As shown in Fig. 1 <sup>3)</sup>, various loads act on the planet gear, which is the subject of this analysis of the planetary transmission. These loads determine the load on the needle roller bearings which support the planet gear. In this paper, we study the impact of the degrees of freedom of the motion when the stress on the cage of these bearings is obtained by dynamic analysis. The dynamic analyses are conducted by 2-dimensional analysis taking into consideration motion of only 3-degrees of freedom on the radial plane, and 3-dimensional analysis taking into consideration motion of 6-degrees of freedom.

\*CAE Engineering Dept., Automotive Business Headquarters

The calculation method of 2-dimensional analysis is the same as the existing report<sup>3)</sup>, introducing the following 5 assumptions for simplification of the analysis model. As a result, Fig. 1 can be simplified as Fig. 2.

- (1) The center of the inner ring raceway which is fixed to the carrier moves on the circular orbit around the carrier center at a constant speed. That is, the carrier autorotates at a constant speed with its center at a fixed position.
- (2) The outer ring has degrees of freedom of 2 - translation motion on the radial plane and autorotates at a constant speed.
- (3) The roller and the cage have degrees of freedom of 2 - translation motion and 1-rotation motion on the radial plane.
- (4) The centrifugal force of the planet gear itself is only supported by the bearings.
- (5) The radial force components of the sun gear and ring gear to the planet gear are assumed to be balanced. Therefore, only the force generated by the input torque of the transmission acts on the direction of the planet gear revolution (Fig. 2).

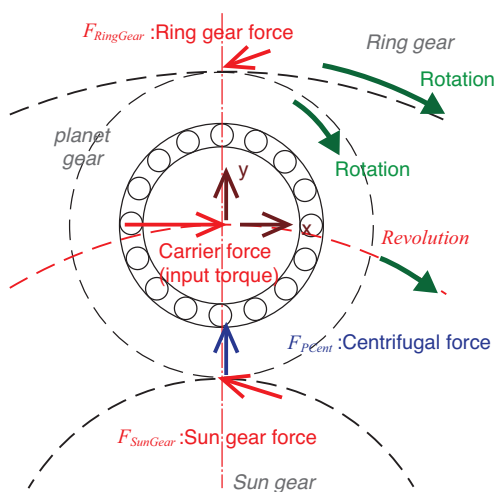


Fig. 1 Actual forces and motions on a planet gear<sup>3)</sup>

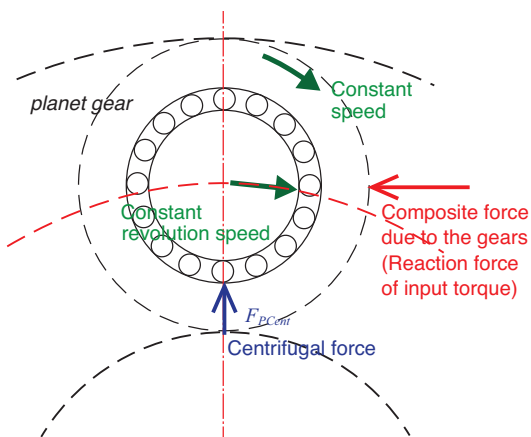


Fig. 2 Analyzed forces and motions on a planet gear<sup>3)</sup>

On the other hand, key assumptions of 3-dimensional dynamic analysis are as follows:

- (1) Motion of the inner ring and outer ring is the same as the 2-dimensional analysis.
- (2) The roller and cage have 6 degrees of freedom for the motion.
- (3) The outer ring has a flange face in contact with the cage.
- (4) The cage can be in contact with the roller, outer ring raceway and outer ring flange face.
- (5) Assumptions (4) and (5) in the 2-dimensional analysis also apply to the 3-dimensional analysis.

In the contact calculation of the roller and cage in the 2-dimensional analysis, as shown in Fig. 3, the force acting on the cage is applied to both ends of the lines set on the bar of the cage, and the lines set according to the interference amount of the roller.

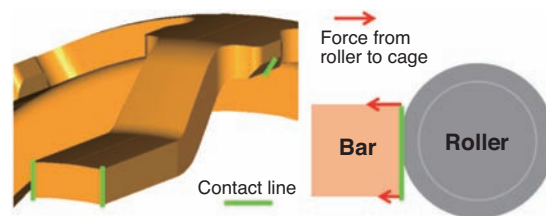


Fig. 3 Contact calculation method between roller and cage in two-dimensional analysis

On the other hand, in the contact calculation of the roller and cage in the 3-dimensional analysis, as shown in Fig. 4, many nodes are placed on the cage pocket surface which is in contact with the rollers, and the forces that act on these nodes are calculated.

In addition to these assumptions, the calculation methods for the contact area between the rollers and raceway, and between the cage and raceway are the same as the existing reports<sup>1), 3)</sup>. These analyses mentioned above consider all apparent forces (centrifugal force, inertia force, etc.).

Hereinafter, 2-dimensional analysis is referred to as "2D analysis", and 3-dimensional analysis as "3D analysis."

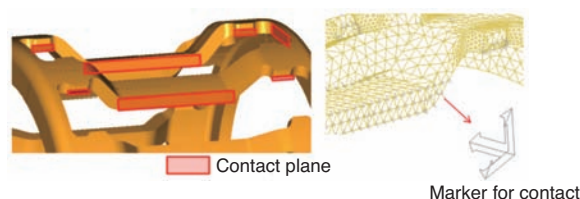


Fig. 4 Contact calculation method between roller and cage in three-dimensional analysis

### 3. Subject of analysis

The specifications of the planetary transmission mechanism and needle roller bearing, which are the subject of analysis, are shown in **Table 1**. The cage is the steel cage of the outer ring guided type (NTN's "KMJ-S" type). The operating conditions listed in the table are the standard conditions of this analysis. In addition, the input torque into the planetary transmission mechanism assumes that it applies to the carrier.

**Table 1** Specifications of needle roller bearing and planetary gear system

Planetary mechanism	Pitch circle diameter of sun gear (mm)	95.3
	Pitch circle diameter of planet gear (mm)	28.7
	Pitch circle diameter of ring gear (mm)	152.7
	Weight of planet gear (kg)	0.05
Bearing specifications	Outer ring raceway diameter (mm)	19.85
	Inner ring raceway diameter (mm)	13.85
	Roller diameter (mm)	2.997
	Roller effective length (mm)	13.8
	Number of rollers	11
Operating conditions	Revolution speed of planet gear $N_c$ , $\text{min}^{-1}$	5,000
	Autorotation speed of planet gear $N_p$ , $\text{min}^{-1}$	17,000
	Load acted on each bearing from the input torque (N)	300
	Lubricating oil	Mineral oil ISO VG100
	Typical temperature of lubricating oil ( $^{\circ}\text{C}$ )	100

### 4. Calculation results of cage stress

#### 4.1 Impact of autorotation speed of planet gear

**Fig. 5** shows the cage stress by 2D and 3D analyses when the revolution speed of the planet gear is fixed to  $5,000\text{min}^{-1}$  and the autorotation speed of the planet gear is changed from  $11,000\text{min}^{-1}$  to  $53,000\text{min}^{-1}$ . The vertical axis of the figure indicates a dimensionless number with the maximum principal stress divided by the fatigue strength of the material (dimensionless maximum principal stress). Even if the cage stress from the 2D analysis is slightly higher than 3D analysis, the difference between those analyses is small and the stress increases as the autorotation speed increases.

In the calculation of force acting on the bar of the cage in 2D analysis, as shown in **Fig. 3**, since the load evaluation point is placed on the cross section of the bar center in the axial direction, the load evaluation point is far from the base of the bar of the pocket compared with the case of 3D analysis. As the cage stress increases at the base of the bar, the cage stress in 2D analysis is calculated higher than 3D

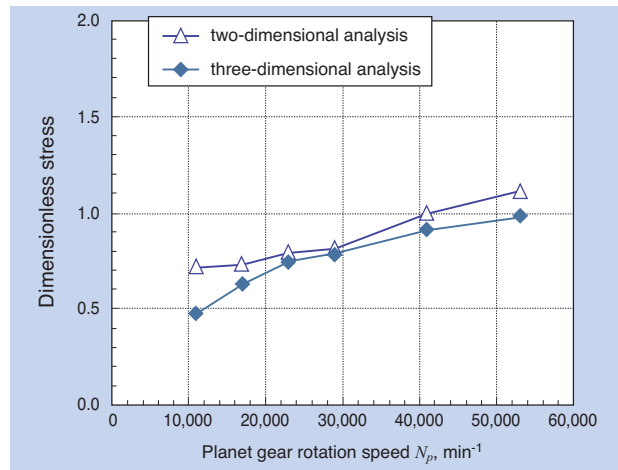


**Fig. 5** Cage stress with various rotation speeds of planet gear (orbital rotation speeds of planet gear  $N_c=5,000\text{min}^{-1}$ )

analysis. This is assumed to be the reason why the cage stress in 2D analysis is slightly higher than 3D analysis.

#### 4.2 Impact of revolution speed of planet gear

**Fig. 6** shows the dimensionless maximum principal stress of the cage when the autorotation speed of the planet gear is fixed to  $17,000\text{min}^{-1}$  and the revolution speed of the planet gear is changed from  $2,500\text{min}^{-1}$  to  $20,000\text{min}^{-1}$ . Even if the cage stress from the 2D analysis is slightly higher than 3D analysis, the difference between those analyses is small and the stress increases as the revolution speed increases. This change of stress is nearly proportional to the squares of revolution speed.

Comparing **Fig. 5** and **6**, the impact of revolution speed of the planet gear on the cage stress is larger than the autorotation speed of the planet gear.

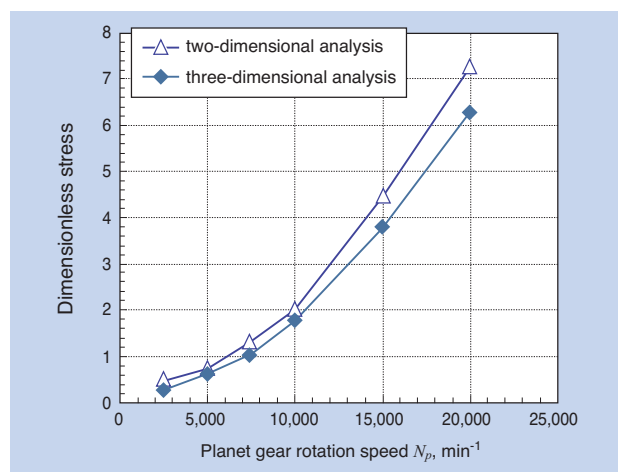


**Fig. 6** Cage stress with various orbital rotation speeds of planet gear (rotation speeds of planet gear  $N_p=17,000\text{min}^{-1}$ )

### 4.3 Impact of input torque

**Fig. 7** shows the dimensionless maximum principal stress of the cage when the revolution speed of the planet gear is fixed to  $5,000\text{min}^{-1}$ , the autorotation speed of the planet gear is fixed to  $17,000\text{min}^{-1}$ , and the load that acts on each bearing by input torque is changed from  $0\text{N}$  to  $1,200\text{N}$ . In 2D analysis, the maximum principal stress changed according to the load, but in 3D analysis the change is small. The reason for this will be interpreted later.

In the above calculation, the calculation time required for 2D analysis was  $1/10 - 1/30$  of 3D analysis, considerably shorter than 3D analysis.

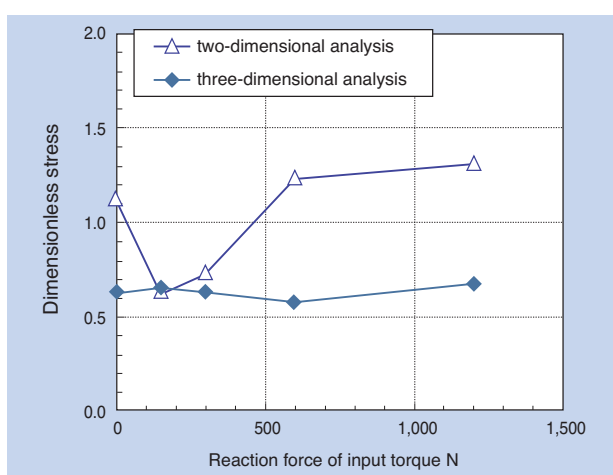


**Fig. 7** Relationship between reaction force of input torque and cage stress (rotation speeds of planet gear  $N_p=17,000\text{min}^{-1}$ , orbital rotation speeds of planet gear  $N_c=5,000\text{min}^{-1}$ )

## 5. Cause of cage stress

**Fig. 8** shows the calculation result at the instance when the principal stress of the cage became the maximum, when the revolution speed of the planet gear is at  $5,000\text{min}^{-1}$  in 2D analysis. The bearings revolve toward the right and the outer ring autorotates clockwise. The center of rotation of the carrier is at the bottom of the figure and the centrifugal force acts upward. Due to the centrifugal force of the planet gear and the input torque of right rotation, four rollers at around the 5 o'clock position (indicates the position within the bearing compared to a clock) support the bearing load. The maximum principal stress occurred at the second pocket from the exit of the load zone. Other locations where relatively high stress occurred were within the load zone and the pockets at 9 and 10 o'clock. On the other hand, **Fig. 9** shows the calculation result at the instance when the cage stress became the maximum, when the revolution speed was at  $5,000\text{min}^{-1}$  in 3D analysis.

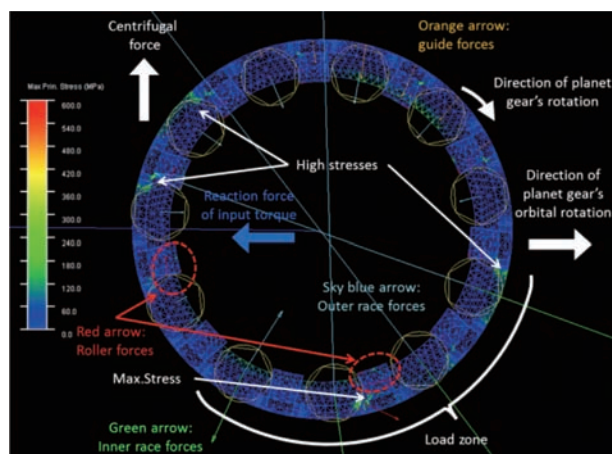


**Fig. 8** Result in two-dimensional analysis when the maximum cage stress occurs at the planet gear orbital speed of  $5,000\text{min}^{-1}$

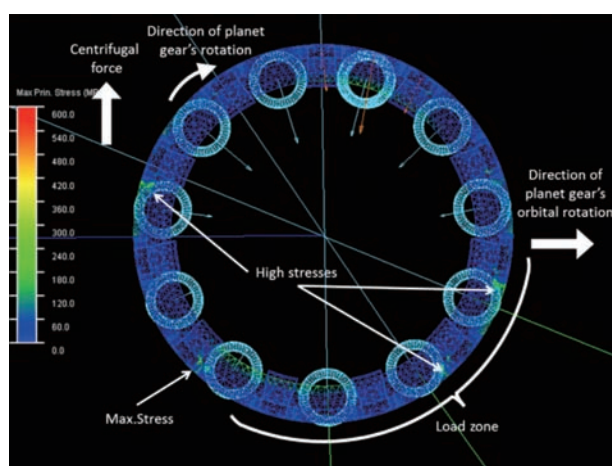


**Fig. 9** Result in three-dimensional analysis when the maximum cage stress occurs at the planet gear orbital speed of  $5,000\text{min}^{-1}$

The maximum principal stress occurred with the pocket at the exit of the load zone, different from 2D analysis. Relatively high stress was also observed in the load zone and with the pocket at 9 o'clock. Compared to 2D analysis, even if the location of the pocket with the maximum principal stress was different, the location where relatively high cage stress occurred, including the maximum principal stress, were the same.

In these calculation results, the principal forces that act on the cage are categorized into 5 items, as shown in **Fig. 10**.

- (1)  $F_{Rfc}$ : Force that acts on the front bar of the cage pocket from the rollers, mainly by the centrifugal force of the rollers
- (2)  $F_{Rrc}$ : Force that acts on the rear bar of the cage pocket from the rollers, mainly by the centrifugal force of the rollers
- (3)  $F_{Ri}$ : Force that acts on the cage from the rollers in the load zone
- (4)  $F_{Fg}$ : Friction force that acts on the cage from the

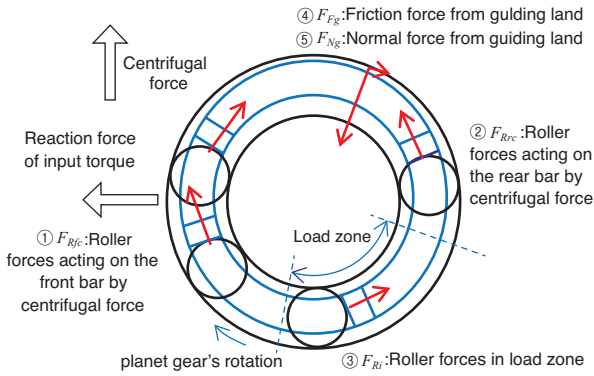


Fig. 10 Principal forces acting on cage

outer ring guideway

(5)  $F_{Ng}$  Normal force that acts on the cage from the outer ring guideway

In Fig. 8 and 9, either  $F_{Rfc}$  or  $F_{Rrc}$  occurred at almost all of the pockets out of the load zone. Since the center position of the cage and the rotation speed can be considered mostly constant, the forces and moments that act on the cage can be considered as balanced. Therefore,  $F_{Ri}$  should be balanced with the moments of  $F_{Rfc}$ ,  $F_{Rrc}$  and  $F_{Fg}$  on the cage.

Based on this kind of dynamic characteristics, the mechanism that the maximum principal stress occurs can be explained as follows:

- At the exit of the load zone, the roller is accelerated by the centrifugal force colliding to the front (in the direction of revolution) bar of the cage pocket. At that time,  $F_{Rfc}$  surges.
- With the collision, autorotation of the cage increases; however, since the rollers in the non-load zone can move freely, change of  $F_{Rrc}$  is small.
- Since the rollers within the load zone cannot move freely as they are caught in the raceways, the accelerated cage and rollers collide, and the cage decelerates. That is,  $F_{Ri}$  surges as it offsets the moment of  $F_{Rfc}$

As a result, as the rollers out of the load zone collide to the cage,  $F_{Rfc}$  and  $F_{Ri}$  surge and the stress of the pocket receiving these forces increases.

Next, Fig. 11 and 12 show the calculation results at the instance when the cage stress became the maximum, when the revolution speed was at  $15,000\text{min}^{-1}$  in 2D and 3D analyses. Compared with the case of revolution speed of  $5,000\text{min}^{-1}$ , the following is observed:

- As the centrifugal force of the rollers is large, the cage stress is also high at 6 times.
- As the centrifugal force of the planet gear is also large, the load zone is wider and the center of the load zone becomes closer to 6 o'clock.

- The maximum principal stress of the cage occurs outside the load zone in both 2D and 3D analyses. It can be explained that in 2D and 3D analyses of revolution speed of  $5,000\text{min}^{-1}$ , the collision of rollers and the cage caused an increase of  $F_{Rfc}$  and  $F_{Ri}$ , to generate high cage stress, and at  $15,000\text{min}^{-1}$ , the centrifugal force due to high revolution speed increased the impact of  $F_{Rfc}$  and  $F_{Rrc}$ , generating the maximum principal stress in the non-load zones of both 2D and 3D analyses.

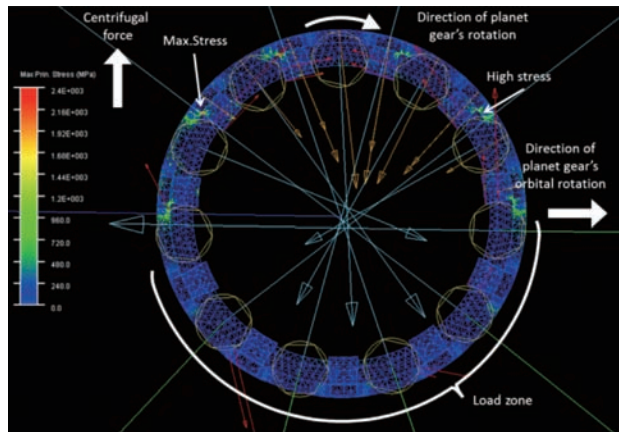


Fig. 11 Result in two-dimensional analysis when the maximum cage stress occurs at the planet gear orbital rotation speed of  $15,000\text{min}^{-1}$

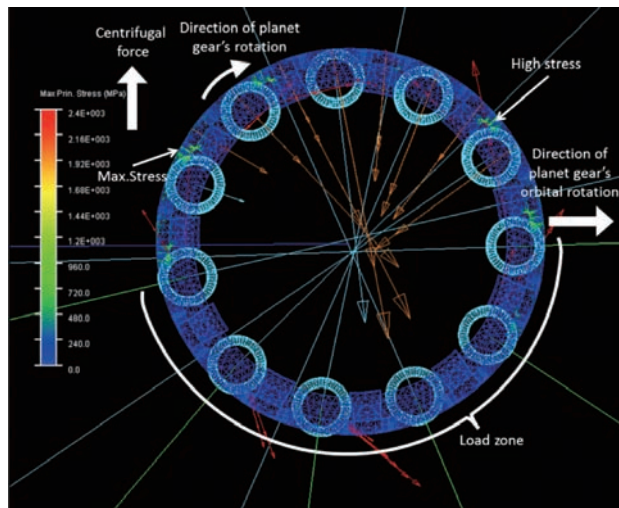


Fig. 12 Result in three-dimensional analysis when the maximum cage stress occurs at the planet gear orbital rotation speed of  $15,000\text{min}^{-1}$

## 6. Comparison of 2D and 3D analyses

In this chapter, we examine the difference in tendency of stress change in 2D and 3D analyses when the input torque described in 4.3 is changed.

First, we discuss the impact of change of the input torque and the reason why this caused the cage stress change in 2D analysis.

**Fig. 13 a)** is the status of forces that act on the load zone and cage,  $F_{Rfc}$ ,  $F_{Rrc}$  and  $F_{Ri}$ , when the input torque is small. When the input torque increases, as shown in **Fig. 13 b)**, the load zone moves to the right side, which causes the non-load zone to move as well. As a result, the difference between  $F_{Rfc}$  and  $F_{Rrc}$  increases, which causes an increase of  $F_{Ri}$  for balancing the moments of the cage. Since the collision force of the roller exiting the load zone to the bar of the cage pocket depends on acceleration of the roller from the centrifugal force, as shown in **Fig. 14**, the angle at the exit of the load zone plays an important role, indicating that the collision force becomes larger when the input torque is smaller.

As the force applied to the cage changes, the cage stress in 2D analysis changed as shown in **Fig. 7 4)**.

Next, the reason why the cage stress did not change in 3D analysis when the input torque changed is discussed in detail.

The forces that act on the cage from the roller at the instance when the maximum principal stress occurred in 2D and 3D analyses are shown in **Fig. 15**, and **16**

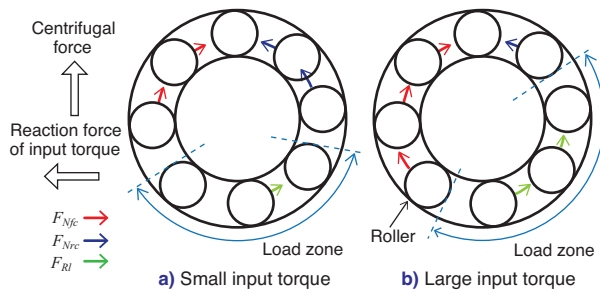


**Fig. 13** Load zone and principal forces acting on cage under large and small reaction forces of input torques

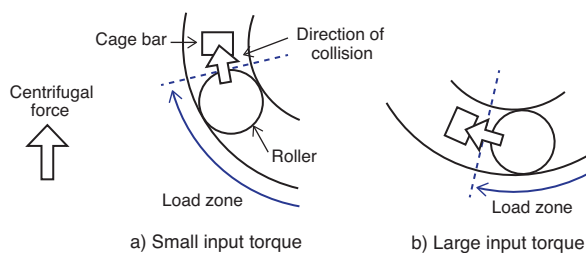


**Fig. 14** Location of load zone and acceleration of roller by centrifugal force under large and small reaction forces of input torques

respectively, under the conditions that revolution speed of the planet gear is  $5,000\text{min}^{-1}$ , autorotation speed is  $17,000\text{min}^{-1}$ , and the load applied to each bearing from the input torque is 300N. The characteristics of 3D analysis when the force that acts on the cage is calculated is that the distribution in the axial direction is considered, as shown in **Fig. 16**. In this calculation of forces, skew of the rollers is considered as well.

The total forces that act on the cage from the rollers in **Fig. 15**, and **16**, are summarized as 61N in 2D analysis and 31N in 3D analysis. It is considered that the difference comes from the skew of rollers as described in the following.

**Fig. 17**, shows an image of the rollers colliding into the cage in 2D and 3D analyses. In 2D analysis, the roller does not skew, even when the roller and the bar of the cage collide. On the other hand, in 3D analysis where skew of the rollers is considered, the rotation in the direction of the skew also changes, not only translational motion when the roller collides to the bar of the cage pocket. Since it is rare that the peaks of each motion occur at the same time, the normal force of collision is distributed on the time axis. That is, by considering the rotational motion the time that the roller and the bar of the cage are in contact is extended. As a result, the maximum value observed during collision in 3D analysis becomes smaller than 2D analysis.

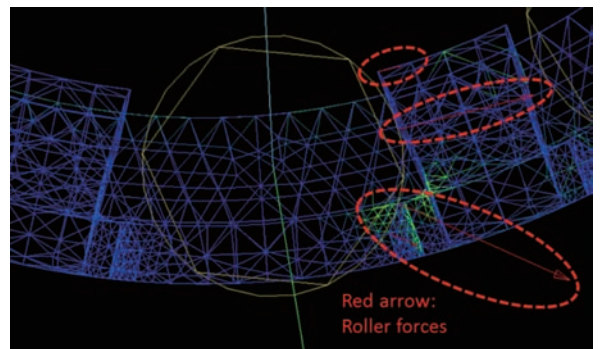


**Fig. 15** Roller force on cage when the maximum cage stress occurs in two-dimensional analysis

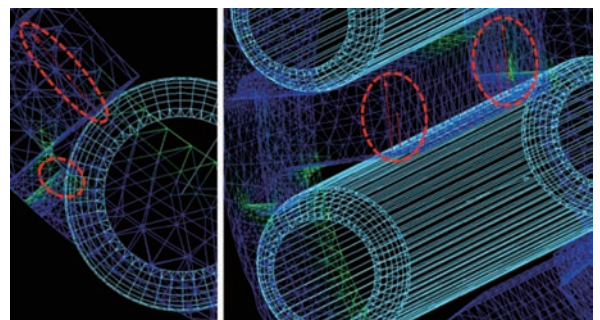


**Fig. 16** Roller force on cage when the maximum cage stress occurs in three-dimensional analysis

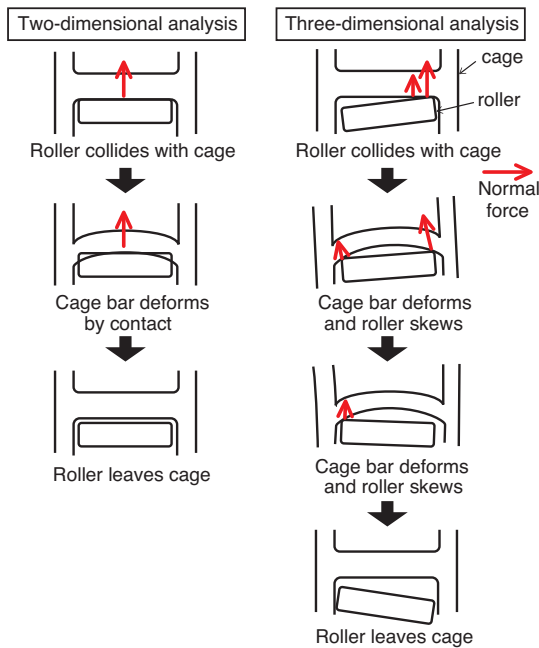


**Fig. 17** Difference in collision between roller and cage in two-dimensional and three-dimensional analysis

This is the reason why the change of the cage stress was small when the input torque was changed in 3D analysis.

In addition, although the roller which the centrifugal force acts on remains in contact with the cage for a relatively longer time, there does not appear to be a collision. Contact of the rollers in the non-load zone and the cage are not collision-like either. Under these situations, even with or without the consideration of rotational motion on the skew direction, the time of contact should remain almost the same. The reason why the 3D analysis result was similar to 2D analysis in **Fig. 5** and **6** is because the cage stress was dominated by the phenomenon of the relatively long contact time, as mentioned above.

## 7. Summary

For the needle roller bearings under planetary motion, 2D and 3D dynamic analyses were conducted, taking into consideration elastic deformation of the cage and the impact that degrees of freedom of motion has on the cage stress was examined.

As a result, when autorotation and revolution speed of the planet gear was changed, the trend that the stress increases as the rotational speed increases was verified in both the 2D and 3D analyses. On the other hand, when the input torque was changed, stress change due to the change in the load zone was observed in 2D analysis, but little change in cage

stress was observed in 3D analysis. That is because in 3D analysis, as skew of rollers is considered, the force when the rollers collide into the cage is distributed and the maximum value is reduced.

With the above study, it can be determined that in 2D analysis the impact force of collision tends to be overestimated and the cage stress is calculated on the high side. If 2D analysis, which can be done in a relatively short time, is conducted first to study cage strength then the cage may be efficiently designed on the safe side.

One point to note, in this analysis the damping effect of lubricant which exists inside the bearings is ignored. Therefore, the actual collision force should be smaller than the values obtained in this calculation; however, their magnitude is unknown and remain a technical challenge for the future.

## 8. Conclusion

Recently, a shorter time to market is required in design and development of automotive components. On the other hand, the importance of analyses is increasing. Therefore, we would like to promote an efficient product development by fully grasping the characteristics of analysis assumptions in order to quickly deliver the analysis results.

## References

- 1) Atsushi Suzuki: Dynamic Analysis of Needle Roller Bearings on Torque Loss, Transactions of the Japan Society of Mechanical Engineers Series C, Vol. 79 No. 801, (2013) 1386-1395.
- 2) Sakaguchi, T., et al : Dynamic Analysis of Cage Stress in Tapered Roller Bearings, Proc. ASIATRIB 2006 Kanazawa, Japan, (2006) 649-650.
- 3) Tomoya Sakaguchi: Dynamic Analysis for Needle Roller Bearings Under Planetary Motion, NTN Technical Review No. 75, (2007) 94.
- 4) Naoto Shibutani: Dynamic Analysis for Needle Roller Bearings Under Planetary Motion, Journal of Society of Automotive Engineers of Japan, Vol.71, No.9 (2017) 97-101.

## Photo of authors



Naoto SHIBUTANI  
CAE Engineering Dept.,  
Automotive Business  
Headquarters



Tomoya SAKAGUCHI  
CAE Engineering Dept.,  
Automotive Business  
Headquarters

# Proposal of Low Fuel Consumption and High Functionality of Composite Material Products for Automobile



Kayo SAKAI\* Tomonori YAMASHITA\*\*  
Hajime ASADA\*\* Takuya ISHII\*\*\*

We manufacture and sell composite material products molded from resin and metal powder. These products are used in a wide variety of fields because of their high degree of freedom in shape and their ability to impart various functions. In this paper, we introduce composite material products that contribute to low fuel consumption and high performance of automobiles.

## 1. Introduction

NTN is manufacturing composite material products using resin and metal powder as raw materials and combining our own proprietary design at the affiliated companies shown in Fig. 1. The composite material products are used in broad fields as the composition of resin, metal powder, and additives are changed according to operating conditions. In addition, since they are formed with molding, they have a high degree of freedom for shaping, which provides good volume production properties for products with complex shapes. NTN is manufacturing and distributing oil retaining bearings and plastic bearings containing hydrodynamic BEARPHITE, machine parts (such as sliding parts), gears and cams, magnetic products (such as magnetic sensors), and reactors for broad industries (such as automotive and industrial machinery).

In this article we introduce composite material products that contribute to fuel efficiency and high functionality for automotive applications.

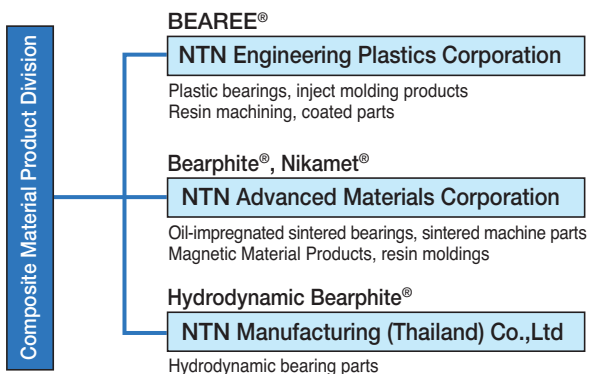


Fig. 1 Composite material products of NTN group

## 2. Seal rings for transmissions

Several resin based seal rings, with outer diameters from 15 to 60mm, are used in automobile transmissions. Seal rings are required to have low torque and low oil leak characteristics for fuel efficiency. NTN has developed a low torque seal ring<sup>1)</sup> made of PEEK (polyetheretherketone) with a 60% reduction in torque by providing a V-shaped lubrication groove on the side of the seal ring (Fig. 2), low oil leakage equivalent to the conventional grooveless product, and started volume production.

However, as regulations on the fuel efficiency of vehicles continues to become more strict, even lower torque is required. With the developed product incorporating an optimized V-shape lubrication groove in low torque seal rings, we achieved an additional 10 - 15% lower torque.

Seal rings are installed between the relative moving shaft and housing in the hydraulic circuit of the transmission. They seal oil and maintain pressure within the hydraulic circuit, pressed against both the housing inner diameter and the side wall of the shaft groove with hydraulic pressure in a sliding motion (Fig. 3). The contact area between the seal ring and

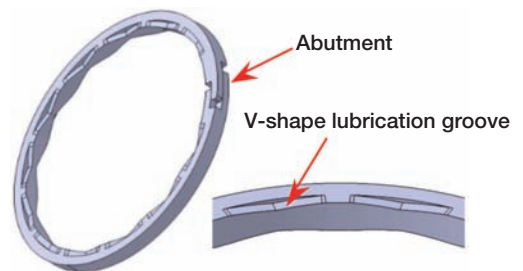


Fig. 2 Low torque seal ring

\*New Material Development Dept. Composite Material Product Division

\*\*Composite Material Engineering Dept. Composite Material Product Division

\*\*\*Engineering Dept. NTN Engineering Plastics Corporation

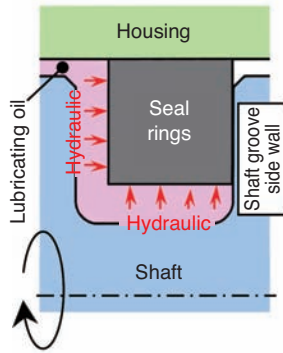


Fig. 3 Operating state of seal ring

side wall of the shaft groove is smaller than the contact area between the seal ring and housing inner surface; therefore, when the housing or shaft rotates, the seal ring side and side wall of the shaft groove slide due to lower sliding resistance. Therefore, providing lubrication grooves on the side of seal rings is effective for torque reduction and manufacturers are working on the design of their shapes.

NTN's low torque seal ring reduces torque as the edges of the V-shaped lubrication groove are under high pressure due to hydrodynamic effects. As the groove is symmetric, the seal ring can be installed on the shaft without concerns regarding direction.

Table 1 shows the conventional and developed low torque seal rings and Fig. 4 shows the dependency of torque on oil hydraulics.

The developed low torque seal ring showed a 10 - 15% torque reduction from the conventional product.

An increasing number of V-shaped lubrication grooves is a factor in lower torque because of elevated hydrodynamic effects; however, it can be a factor in increasing torque as the sliding area between grooves increases as well. Therefore, optimization of the number of lubrication grooves, as well as optimization of width and length in the circumferential direction were investigated for the developed product.

Table 1 Test seal rings

Test seal rings		Shape of side lubrication groove
Low torque seal ring (conventional product)	V-shaped 12	
Low torque seal ring (developed product)	V-shaped 24	

Seal ring dimensions: outer diameter 45mm, thickness 2mm, width 2.4mm

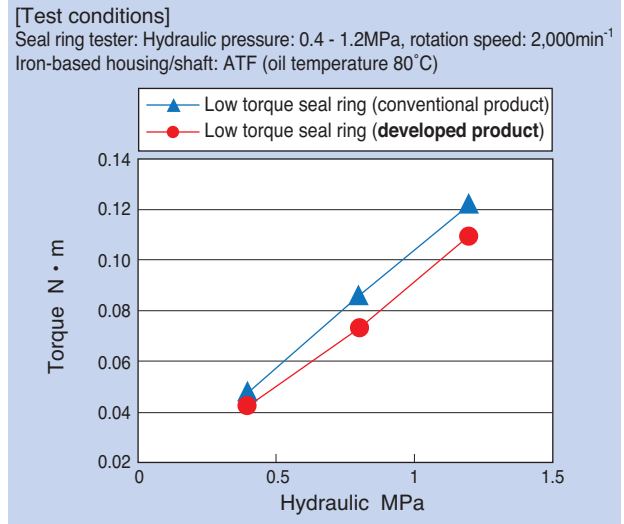


Fig. 4 Torque versus oil pressure

pumps was 20.8 million units and is expected to grow to 34.75 million units in 2020 and 54.7 million units in 2025.

Fig. 5 shows the typical configuration of electric water pumps. The rotor (which integrates the impeller, magnet and sliding bearing) is contained in the pump chamber and the stator is placed facing the magnet. The rotor is supported by the shaft via sliding bearings. The magnetic field is generated by energizing the stator which rotates the rotor, and the impeller transports the coolant water out of the pump chamber.

### 3. Plastic sliding bearings for electric water pump

Electric water pumps are being installed on internal combustion engine, hybrid, and electric vehicles, with the trend of electrification and improved fuel efficiency of vehicles. They have the advantage of arbitrarily controlling flow as they are battery powered, and are used for cooling engines, inverters, and motors, as well as for heating the cabins. BEAREE AS5704 sliding bearings<sup>2)</sup>, which use polyphenylenesulfide (PPS) blended with special filler, are adopted in these electric water pumps, contributing to energy saving.

The global market volume in 2015 of electric water

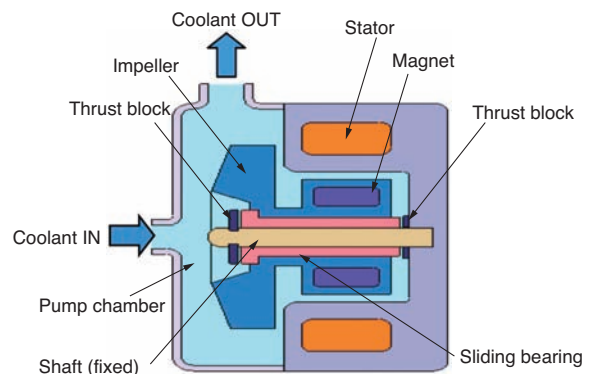


Fig. 5 Structure of electric water pump

When the rotor operates, radial and axial loads are generated in the inner diameter of the sliding bearing and the shaft, as well as the ends of the sliding bearings and thrust block slide.

For electric water pumps, carbon sliding bearings have been traditionally used. The carbon sliding bearings are tolerant to corrosion from the coolant and single-piece forming with the impeller is also possible; however, the degree of freedom for shaping is low and costs are high as they are made by machining from the molded material.

The plastic sliding bearings made of PPS are superior in self-lubricity, chemical resistance, and are made by injection molding, which brings a high degree of freedom for design, including shaping and low cost. It is possible to easily form lubrication grooves on the inner diameter and at the ends of the bearings, as well as the structure for retaining the bearings with the impeller on the outer diameter of the bearings (D-cut, protrusion, etc.) by injection molding, making it possible to form a single-piece with the impeller without machining.

The sliding bearings are required to have low-wear properties, long operating life, and not damage/wear the mating components in the coolant. Therefore, BEAREE AS5704 sliding bearings shown in Fig. 6 were adopted. The following is a list of features for these bearings.

**[Features]**

- (1) Wear amount in the coolant water is 1/5 or less than the universal PPS sliding bearings.
- (2) Low damage/wear properties for mating materials such as stainless steel.
- (3) High degree of freedom for design due to injection molding.
- (4) Usable in antifreeze, acidic, and alkaline fluid.

Fig. 7 shows the comparison of specific wear amount and dynamic friction coefficient of BEAREE AS5704 and the bearings of PPS blended with glass fiber, carbon fiber and PTFE. The specific wear amount of BEAREE AS5704 is small compared to other PPS bearings, at 1/5 or less of PPS+carbon fiber bearings. In addition, the friction coefficient of BEAREE AS5704 bearings is the lowest and stable.



Fig. 6 Plastic sliding bearings for electric water pump

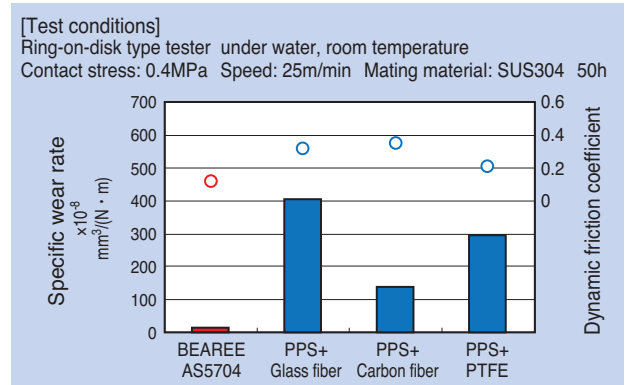


Fig. 7 Relation between PPS bearing materials and sliding property

**4. Bearings for power windows and fan motors**

Oil-impregnated sintered bearings are widely used in automotive and industrial machinery applications, and the materials are broadly categorized into bronze-based, iron-based, and bronze-iron-based. For applications where high sliding properties are required for the bearings, such as automotive electrical components for power windows, fan motors, copiers, and laser printers, bronze-based materials are the most appropriate. However, due to the recent increase in copper prices, NTN developed Bearphite CL<sup>3)</sup> as a new material to replace the bronze-based material by reducing the use of copper.

Bearphite CL is characterized by showing the same or higher maximum permissible PV value when compared to bronze-based material and the same or higher wear resistance when compared to bronze-iron based material, all while reducing the use of copper by using unique copper powder.

A thin copper film is formed on the surface by using a unique copper powder, which contributes to superior sliding properties. Inexpensive iron powder is used inside, which exhibits superior wear resistance compared to a bronze-based material. The cross section of the bearings is shown in Fig. 8. The upper side of the figure is the bearing bore diameter on which a thin layer of copper is formed, and iron powder is found inside.

Table 2 shows the chemical composition of Bearphite CL. The copper content in the mixture is about 20%; however, copper is exposed on the inner diameter surface at about 60% or more.

Fig. 9 shows the results of measurement of permissible PV value for Bearphite CL.

From this result, it is revealed that Bearphite CL shows a friction coefficient equivalent to bronze-based material from the low PV value range, and maintains a low friction coefficient up to the high PV value range.

Therefore, it can be used in a broad *PV* value range.

The evaluation of wear resistance was conducted by measuring the dimensions of the bearing bore diameter (wear amount) before and after the operation test. The evaluation results are shown in **Fig. 10**.

The wear amount of the developed product is less than the bronze-based and bronze-iron based products, which shows that the developed product has excellent wear resistance.

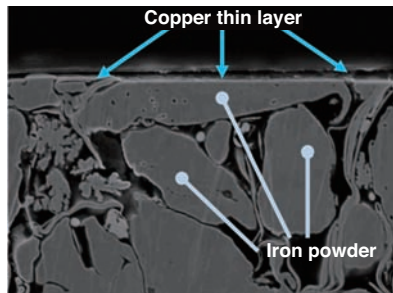


**Fig. 8** Section of BEARPHITE CL

**Table 2** Chemical components of BEARPHITE CL

Developed product	Chemical composition wt%			
	Cu	Sn	C	Fe
	15~22	0.5~2.5	0.5~2.5	Remainder

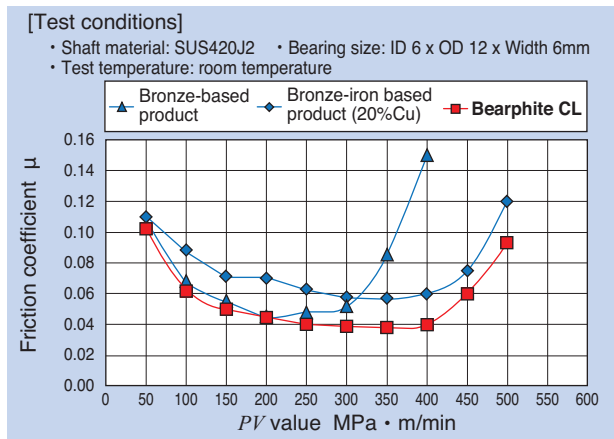


**Fig. 9** Limit *PV* value of BEARPHITE CL

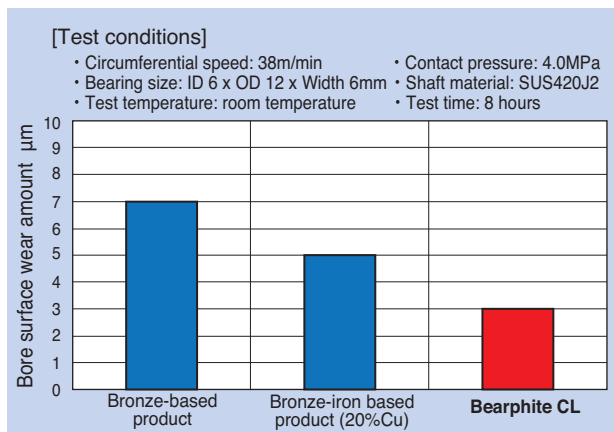


**Fig. 10** Abrasion resistance of BEARPHITE CL

## 5. Sliding bearings for AFS and EGR

Within a high temperature environment, lubricant can evaporate due to the heat which presents a risk of contamination; therefore, lubricants such as grease cannot be used in the sliding section. NTN is developing self-lubricating sintering sliding material<sup>4)</sup> by adding a significant amount of graphite, which is a solid lubricant for improving lubricity.

The self-lubricating sintered sliding material will be used for AFS (Adaptive Front-Lighting System) (**Fig. 11**), which becomes very hot due to the heat of the head lamp, and bearings for valves of EGR (Exhaust Gas Recirculation) units which are exposed to hot emission gases.



**Fig. 11** Self-lubricating sliding material (For AFS)

When a significant amount of graphite is added, the fluidity of the material powder is reduced due to the low bulk density of graphite. This limits the shapes and dimensions that can be molded. In addition, even when the shapes can be molded, the molding cycle may be delayed, resulting in relatively high costs. The developed self-lubricating sintering sliding material has a high degree of freedom for shaping and productivity, even with the significant addition of graphite. This is done by increasing the fluidity of specially treated graphite powder. This developed product has superior low friction properties and wear resistance, even in environments where lubricants such as grease cannot be used.

### [Features]

- (1) Superior friction/wear properties in dry environments
- (2) High degree of freedom for shaping is due to special graphite

**Table 3** shows the chemical composition of the developed product. More than double the amount of graphite is added when compared to the typical bronze-based material.

The friction/wear test conditions of the self-lubricating sintering sliding material are shown in **Table 4**, and the test results are shown in **Table 5**. The friction coefficient of the self-lubricating sintering bearings was approx. half that of typical bronze-based materials without oil impregnation. In addition, the

wear resistance was improved by approx. 40 times when compared to the typical bronze-based material.

**Table 3** Chemical components

Material	Chemical composition %		
	Cu	Sn	C
Typical bronze-based material	Remainder	7~11	1~2
Developed material	Remainder	7~11	4~7

**Table 4** Test conditions for friction and wear property

	(1) Friction test	(2) Wear test
Load (N)	98	15
Rotational speed (min <sup>-1</sup> )	1,000	450
Test sample dimensions (mm) (inner diameter × outer diameter × width)	φ6×φ12×6	φ6×φ12×6
Mating material	SUJ2	SUS420J2
Test time (min)	90	60
Lubrication condition	No oil impregnation (dry)	No oil impregnation (dry)

**Table 5** Specific wear rate and friction coefficient

	Developed material	Typical bronze-based material
Friction coefficient	0.2~0.3	0.45
Specific wear rate m <sup>3</sup> / (N·m) × 10 <sup>-12</sup>	0.08	3.56

## 6. Low-profile reactor

As part of the recent trend of electrification of automotive components, many power supply devices such as converters and inverters are now installed in vehicles. Reactors are used to regulate voltage among these power supply devices. In order to make the power supply devices smaller, the use of high frequency power is increasing. There are also increased requirements for reactors to provide stable and low-loss performance through the higher frequency range.

A reactor consists of a core made of soft magnetic material and wires wound around the core called a coil. When a current is supplied to the coil, a magnetic force is generated in the core. Reactors are capable of converting the current in the coil into a magnetic force and accumulating it in the core. They can then reconvert the accumulated magnetic force to electric current and release it from the coil. Reactors are used to step the voltage up or down in the power supply circuit by leveraging this conversion capability. As an example of a reactor, NTN's pot-shaped hybrid reactor (hereafter, pot-shaped conventional product) is shown in Fig. 12.

Reactor performance degrades as the current increases. The characteristics indicating the level of

current to which the performance can be maintained are called superimposition characteristics. This is considered to be a particularly important index. Generally in order to improve the superimposition characteristics, a gap is created in the core; however, the magnetic force leaked from the gap causes the increase of performance loss and heat generation. NTN's hybrid product improves superimposition characteristics without creating a gap by combining core components with different properties.

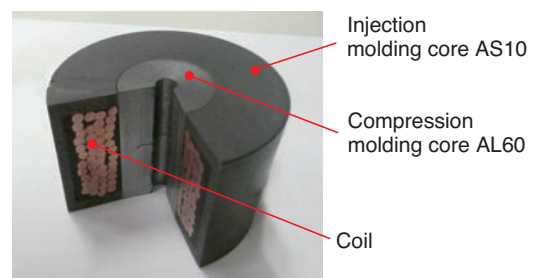
The widely used toroidal type is a reactor made of a ring-shaped core with coils. To improve the DC superimposition characteristics, a gap with an air layer is required, which raises concerns of leakage flux. For cooling, coils can be directly cooled, but the entire reactor must be resin sealed for cooling the core.

Fig. 13 shows the newly developed EEP-type hybrid reactor. The EEP-type reactor has a big opening for drawing wires compared to the pot-shaped reactor.

In addition to the superior superimposition characteristics of the gapless core of the pot-shaped conventional product<sup>4)</sup>, the developed product optimized the shape of the core. This is done by changing the cross-section shape closer to a square which can utilize a larger area for reactor mounting for heat dissipation and to lower the profile for shortening the heat dissipation path.

### [Features]

- (1) Excellent superimposition characteristics with gapless core
- (2) Low increase in temperature due to superior heat dissipation
- (3) Low profile



**Fig. 12** Pot type hybrid core

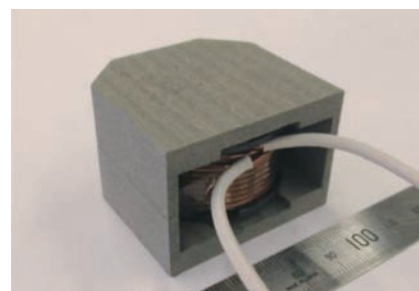


**Fig. 13** EEP type hybrid core

**Table 6** shows a comparison of the developed product, NTN's pot-shaped conventional product, and general toroidal type product.

The analysis results of the developed product and the pot-shaped conventional product are shown in **Table 7** and **Fig. 14**, and the analysis results of heat generation are shown in **Fig. 15**. The heat generation analysis was conducted with an installation surface (bottom part) temperature of 60°C assuming cold plate mounting, and atmospheric temperature of 60°C.

The developed product has similar superimposition characteristics, loss and installation space (width and depth) as the pot-shaped conventional product, with a 22% lower profile. In addition, the generated temperature of the developed product was 117°C (increase of 57°C) compared with the conventional product of 134°C (increase of 70°C), improving heat dissipation performance by approx. 19% by changing the shape of the mounting space and lowering the profile.

**Table 6** Characteristics comparison

	Developed product	Pot-shaped conventional product	Toroidal
Heat dissipation performance	◎	○	△
Leakage flux	○	○	△
Height of component	◎	○	◎

◎: Excellent ○: Good △: Fair

**Table 7** Iron loss and copper loss by magnetic field analysis

	Developed product	Conventional product
Dimensions (mm)	W46×D44×H32	φ42×H41
Iron loss**	3.1	3.4
Copper loss**	13.1	13.3

\*\*With sinusoidal wave current of ripple rate 30% superimposed on DC 20A

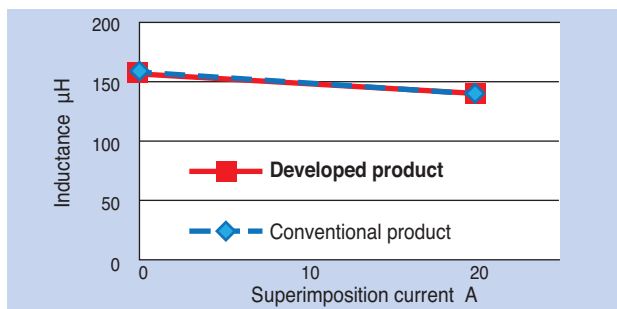


**Fig. 14** DC bias characteristics

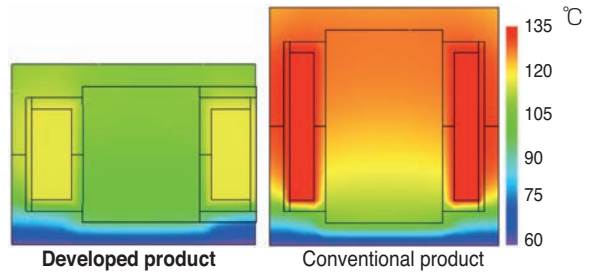


**Fig. 15** Thermal analysis results

## 7. Conclusion

In this article, composite material products are introduced which contribute to fuel efficiency through smaller and lighter form factors and high functionality, such as improvements to sliding properties for automotive applications.

Going forward, as electrification of vehicles and component units advance, more rigorous requirements on these component units, as well as accelerated transition from the conventional components to composite material products, are expected.

NTN strives to contribute to the development of the automotive industry by providing products that match market trends, not only by raising the added value of the components, but also addressing modularizing and unitizing components, including the peripheral structure.

## References.

- 1) Kouzou Kakehi, Takumi Kondou, Takuya Ishii, Masato Yoshino: Development of Low Torque Seal Ring for Automotive Transmission, NTN TECHNICAL REVIEW, No. 81 (2013) 68-73.
- 2) Norio Itoh, Takuya Ishii: Plastic Bearings for Electric Pumps for Next Generation Battery Cells, NTN TECHNICAL REVIEW, No. 77 (2009) 49-53.
- 3) Tomonori Yamashita: Copper-Iron-based Material Equivalent to Bronze-based Material for Sintered, Oil-impregnated Bearings, NTN TECHNICAL REVIEW, No. 82 (2014) 30-33.
- 4) Kayo Sakai, Eiichirou Shimazu, Takahiro Gotou, Hajime Asada, Takuya Ishii: Product Introduction of Composite Material for Automotive, NTN TECHNICAL REVIEW, No.83 (2015) 54-59.

## Photo of authors



Kayo SAKAI  
New Material Development  
Dept. Composite Material  
Product Division



Tomonori YAMASHITA  
Composite Material  
Engineering Dept. Composite  
Material Product Division



Hajime ASADA  
Composite Material  
Engineering Dept. Composite  
Material Product Division



Takuya ISHII  
Engineering Dept.  
NTN Engineering Plastics  
Corporation

## Japan Powder Metallurgy Association Awards 2016 in New Products Category (New Design)

## Hybrid Magnetic Material Reactor Core for Booster

Hajime KATSUURA\*

Shinya AMANO\*

Shouhei SUZUKI\*

Toshihiro TAKAKUSU\*\*

## 1. Introduction

"Development of Hybrid magnetic material reactor core for booster" received the 38th (2016) Industry Award from Japan Powder Metallurgy Association.

Realization of optimized magnetic performance in the large current/high frequency range, and miniaturization with a hybrid structure of an amorphous powder compact and injected amorphous powder was recognized.



Fig. 1 Application example (MRI)

## 2. Structure

Fig. 2 shows the structure of the hybrid magnet material reactor coil core. Miniaturization and high magnetic performance are optimized by a hybrid structure of an amorphous powder compact and injected amorphous powder, and optimized shaping from magnetic field analysis.

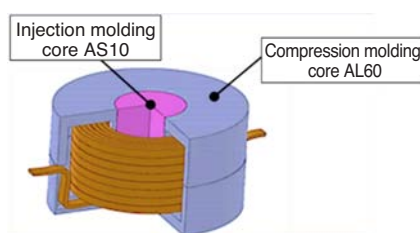


Fig. 2 Structure of Hybrid magnetic material reactor

## 3. Features

The following shows the features of the hybrid magnet material reactor coil core.

- (1) No magnetic saturation compared to the conventional ferrite material
- (2) Reduction of DC superimposition characteristic is less than 1/2, with a large current (300A) compared to the conventional ferrite material
- (3) Loss of high frequency (100kHz) is 1/10 of the conventional Fe-Si material

## 4. Effect

Compared to the conventional materials such as ferrite and Fe-Si based material, the following effects can be obtained to contribute to the miniaturization and performance improvement of the devices:

- (1) 1/8 of volume
- (2) 2.6 times the maximum applied current (100A -> 260A)
- (3) 5 times the circuit operating frequency (10 kHz -> 50 kHz)

## 5. Summary

Since this product achieves properties not possible with single moldings by a hybrid structure of different moldings, development for even broader applications is expected.

## References

Yoshio Oki: Product Introduction and Complex Technology of Resin, Sintered Metal and Magnet for Growth Markets, NTN TECHNICAL REVIEW No. 82 (2014), 12-20

Photo of authors



Hajime KATSUURA  
New Material  
Development Dept.  
Composite Material  
Product Division



Shinya AMANO  
New Material  
Development Dept.  
Composite Material  
Product Division



Shouhei SUZUKI  
New Material  
Development Dept.  
Composite Material  
Product Division



Toshihiro TAKAKUSU  
Mono-Zukuri Center,  
NTN Advanced Materials  
Corporation

\*New Material Development Dept.  
Composite Material Product Division

\*\*Mono-Zukuri Center,  
NTN Advanced Materials Corporation

Japan Powder Metallurgy Association Awards 2016 in New Products Category (New Design)

# Multi Layer BEARPHITE®

Takashi YAMAGUCHI\*

Toshihiko MOURI\*

Kazuki TAKAI\*\*

## 1. Introduction

NTN's development of "Multilayer BEARPHITE®" received the 38th (2016) Industry Award from Japan Powder Metallurgy Association.

Our unique, dual layered, large bushing for construction machinery was highly recognized because of its sliding performance and wear resistance in the inner layer, improved strength and ductility in the outer layer, elimination of the need of CQT (Carburize, Quenching and Tempering) and finish machining.

"Multilayer BEARPHITE®" developed for joints of hydraulic shovels (Fig. 1), etc. was recognized for achieving low friction/wear resistance and high strength with low cost.

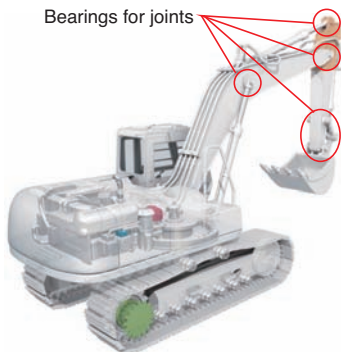


Fig. 1 Application example

## 2. Structure

The structure of multilayer BEARPHITE® is shown in Fig. 2.

This two-layer structure of different materials is made by powder molding instead of press fitting or adhesion.

The inner layer is made of hard ferrous material, adding copper to achieve both low friction and wear resistance. The

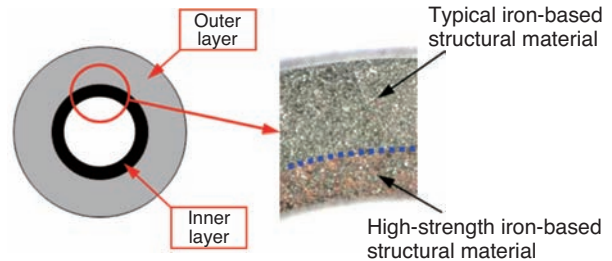


Fig. 2 Structure of the Multi Layer BEARPHITE®

outer layer is made of strong and inexpensive iron-based material, blended with metal possessing a low melting point, achieving the mechanical characteristics equivalent to the conventional products without carburizing and quenching.

## 3. Features

This product achieves a radial crushing strength of 500MPa or more without heat treatment such as quenching. In addition, correction of dimensional distortion by a sizing operation is enabled, eliminating the requirement of machining.

## 4. Summary

This product achieves both low friction/wear resistance and strength by the integrated forming of different materials. We strive to contribute to the market through the development of new products.

## References

- Yosuke SUGAI, Toshihiko MOURI: Multilayer BEARPHITE, NTN TECHNICAL REVIEW 80, (2012) 83-86.
- Toshihiko MOURI, Yoshinori ITOU, Yosuke SUGAI, Eiji YUASA: Award Winning Products, NTN TECHNICAL REVIEW 84, (2016) 115.

## Photo of authors



Takashi YAMAGUCHI  
New Material Development  
Dept. Composite Material  
Product Division



Toshihiko MOURI  
New Material Development  
Dept. Composite Material  
Product Division



Kazuki TAKAI  
Composite Material  
Engineering Dept. Composite  
Material Product Division

\*New Material Development Dept.  
Composite Material Product Division

\*\*Composite Material Engineering Dept.  
Composite Material Product Division

2016 "CHO" MONOZUKURI Innovative Parts and Components Awards,  
Environmental Components Award

Low Torque Seal Ring

Kouzou KAKEHI\* Takuya ISHII\* Yuuki YAMAZOE\* Souichirou YAMAMOTO\* Takumi KONDOU\*\*

1. Introduction

NTN developed low torque seal rings 1) for automotive transmissions (Fig. 1), achieving both low torque and low oil leakage, and started volume production. Recognized for its contribution to high efficiency transmissions and vehicle fuel efficiency by lowering torque, it received the 2016 "CHO" MONOZUKURI Innovative Parts and Components Award, Environmental Component Award sponsored by Nikkan Kogyo Shimbun, Ltd.

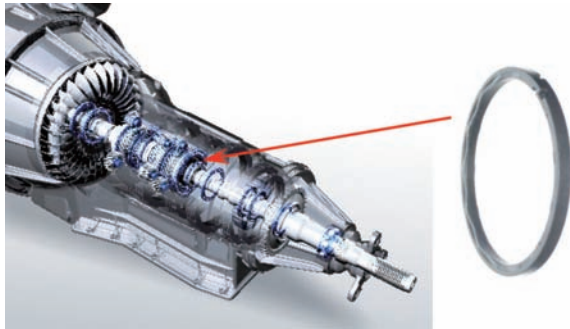


Fig. 1 Automatic transmission

2. Features

Fig. 2 shows the structure of the low torque seal ring. By providing a V-shaped lubrication groove on the side of the conventional PEEK-based seal ring by injection molding, torque was reduced by 60% while maintaining the same low oil leakage as the conventional product (Fig. 3). This is due to the hydrodynamic effect that occurs at the edges of the V-shaped lubrication groove.

The low torque seal ring has the following features compared with the conventional seal ring:

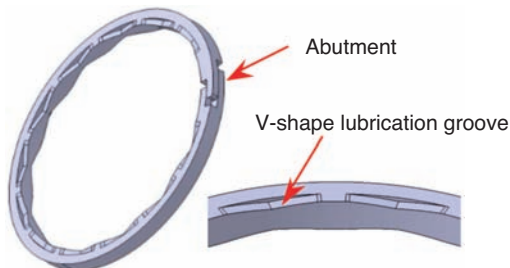


Fig. 2 Shape of low torque seal ring

- (1) 60% lower torque compared to our conventional seal ring
- (2) 1/10 of the wear
- (3) Equivalent low oil leakage properties

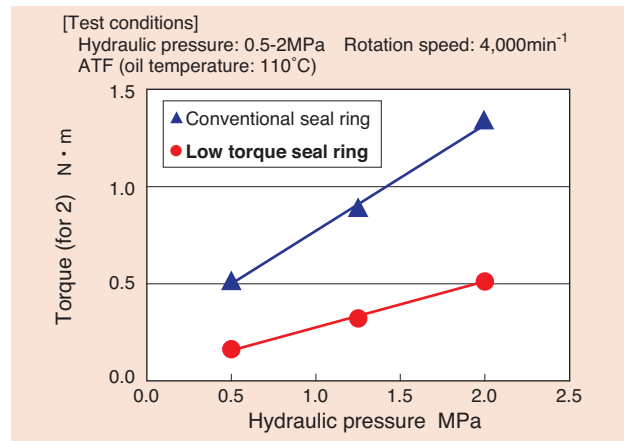


Fig. 3 Torque versus oil pressure

3. Summary

As the regulations on fuel efficiency will be further enhanced, continued reduction of torque will be required. By optimizing the V-shape lubrication groove even further, we have achieved an additional 10 - 15% lower torque. We will explore further reduction of torque to meet the market demand.

References

- Kouzou Kakehi, Takumi Kondou, Takuya Ishii, Masato Yoshino: Development of Low Torque Seal Ring for Automotive Transmission
- NTN TECHNICAL REVIEW No. 81 (2013) 68-73

Photo of author (representative)

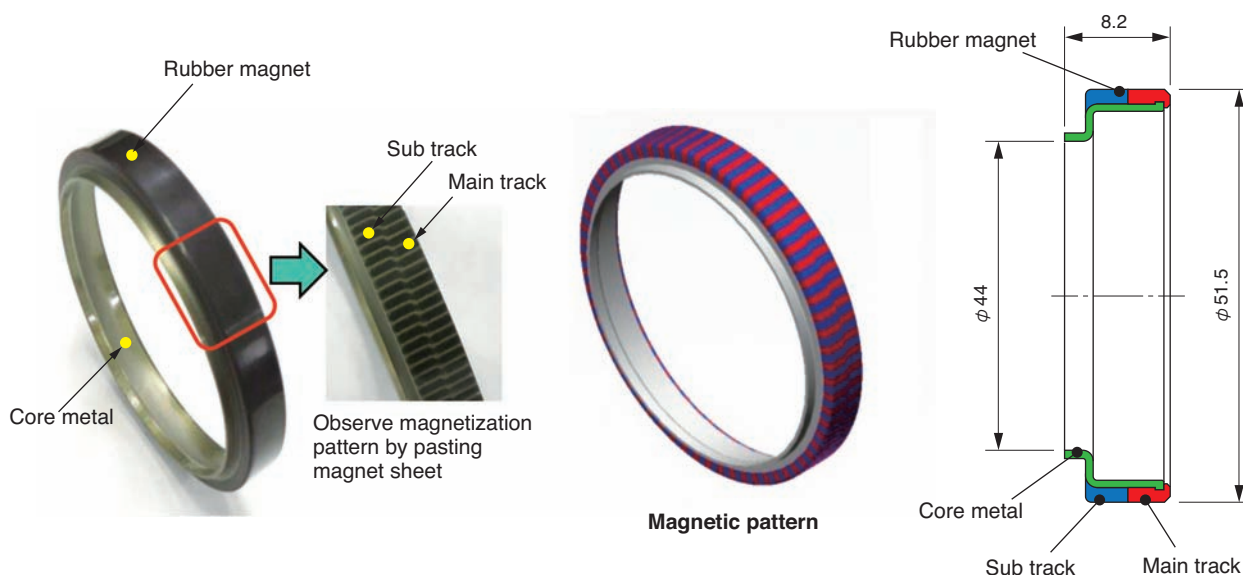


Kouzou KAKEHI  
NTN Engineering Plastics Corporation  
Engineering Dept.

\*Engineering Dept.  
NTN Engineering Plastics Corporation  
\*\*Sales Engineering Dept.  
Composite Material Product Division

# Thin Type High Precision Angle Sensor

**Achieved high precision absolute angle sensing for rotational area of industrial machinery with thin and light components**



## Features

- (1) Easy miniaturization of rotational area and integration of wiring due to its thin and hollow structure
- (2) Low impact on response due to light and small inertia moment
- (3) High precision      Conventional product: angle precision  $\pm 0.2^\circ$   
                                  Developed product: angle precision  $\pm 0.1^\circ$

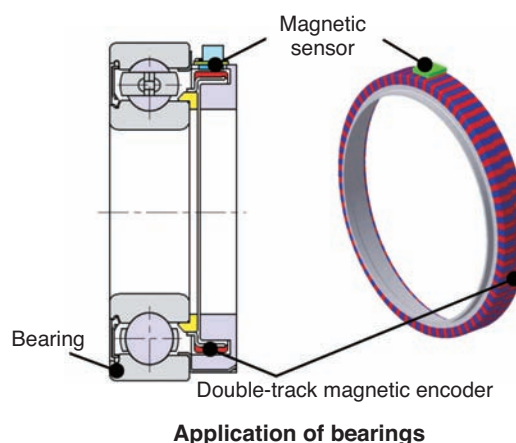
## Structure

High precision magnetization of 2 magnetic tracks with different number of polarized polar pairs (64/63 polar pairs)

Item	Double-track magnetic encoder
Magnet	Rubber magnet
Number of polarized polar bodies	64/63 polar pairs (128 poles/126 poles combining N and S poles)
Size	Outer diameter: $\phi 51.5\text{mm}$ , inner diameter: $\phi 44\text{mm}$ , width: $8.2\text{mm}$
Weight	10.7g
Inertia moment	$6.3 \times 10^{-6} \text{ kg m}^2$
Operating temperature	$-40 \sim +120^\circ\text{C}$

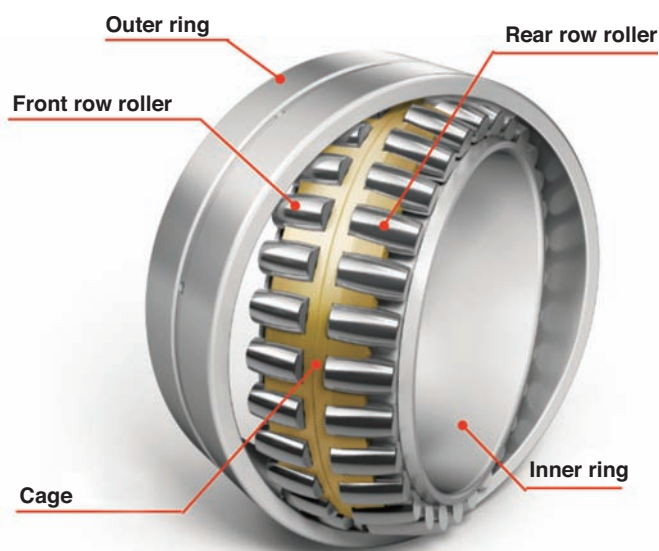
## Applications

- Encoder for detecting robot joint angle
- Encoder for detecting motor rotation angle



# Double row asymmetric self-aligning roller bearings for main shaft of wind turbines

Long life and improved wear-resistance characteristics by double row asymmetrical design of rollers

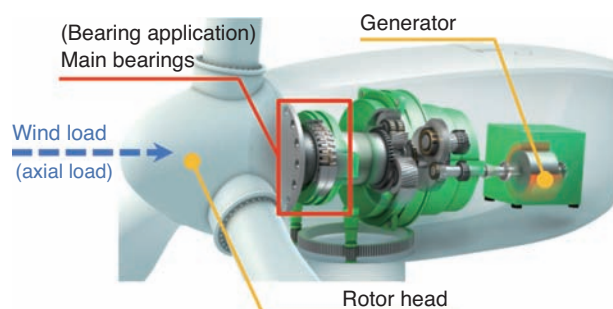


## Features

- (1) **Long life:**  
improvement of approx. 2.5 times of calculated life
- (2) **Wear resistance:**  
improved wear resistance by approx. 30% reduction of PV value
- (3) **Compactness and lightweight:**  
design capability for bearings with life equivalent to that of conventional products, with approx. 10% less bore diameter and approx. 30% less weight

## Applications

### • Main bearings for wind turbines



Internal structure of wind power generator

## Structure

Achieved long life and improved wear resistance properties by efficiently sharing load by front and rear rows in double-row asymmetrical design of rollers

